Multi-Scale Characterization of Bitumen Doped with Sustainable Modifiers

by

Alireza Samieadel

A Dissertation Presented in Partial Fulfillment
of the Requirements for the Degree
Doctor of Philosophy

Approved April 2020 by the
Graduate Supervisory Committee:

Elham H. Fini, Chair
Kamil E. Kaloush
Kristen Parrish
Brajendra Kumar Sharma
Mahour M. Parast

ARIZONA STATE UNIVERSITY

May 2020

ABSTRACT

This research is a comprehensive study of the sustainable modifiers for asphalt binder. It is a common practice to use modifiers to impart certain properties to asphalt binder; however, in order to facilitate the synthesis and design of highly effective sustainable modifiers, it is critical to thoroughly understand their underlying molecular level mechanisms in combination with micro and macro-level behavior. Therefore, this study incorporates a multi-scale approach using computational modeling and laboratory experiments to provide an in-depth understanding of the mechanisms of interaction between selected modifiers and the constituents of asphalt binder, at aged and unaged conditions. This study investigated the effect of paraffinic wax as a modifier for virgin binder in warm-mix asphalt that can reduce the environmental burden of asphalt pavements. The addition of wax was shown to reduce the viscosity of bitumen by reducing the self-interaction of asphaltene molecules and penetrating the existing nano agglomerates of asphaltenes. This study further examined how the interplay of various modifiers affects the modified binder's thermomechanical properties. It was found that the presence of wax-based modifiers has a disrupting effect on the role of polyphosphoric acid that is another modifier of bitumen and its interactions with resin-type molecules.

This study was further extended to using nanozeolite as a mineral carrier for wax to better disperse wax in bitumen and reduce the wax's adverse effects such as physical hardening at low service temperatures and rutting at high service temperatures. This

novel technique showed that using a different method of adding a modifier can help reduce the modifier's unwanted effects. It further showed that nanozeolite could carry wax-based modifiers and release them in bitumen, then acting as a scavenger for acidic compounds in the binder. This, in turn, could promote the resistance of asphalt binder to moisture damage by reducing the quantity of acidic compounds at the interface between the binder and the stone aggregates.

Furthermore, this study shows that iso-paraffin wax can reduce oxidized asphaltene molecules self-interaction and therefore, reduce the viscosity of aged bitumen while cause brittleness at low temperatures.

Additionally, a cradle to gate life-cycle assessment was performed for a new bio-modifier obtained from swine manure. This study showed that by partially replacing the bitumen with bio-binder from swine manure, the carbon footprint of the binder can be reduced by 10% in conjunction with reducing the cost and environmental impact of storing the manure in lagoons.

DEDICATION

This dissertation is dedicated to my parents, Ahmad and Fariba. The two persons who were truly happy when I was happy and truly sad when I was sad. I would not be the person I am today if it wasn't for them.

I also want to dedicate this dissertation to those who advanced science. During this difficult time of the Corona Virus pandemic, we all owe a lot to health workers of the frontline, scientists working day and night to find a cure and all the essential workers.

ACKNOWLEDGMENTS

I want to acknowledge the unlimited support and love I have received from my parents, brothers, and friends during the past few years of my life. It couldn't happen without them.

My infinite gratitude goes to my advisor, Dr. Elham Fini, who believed in me, trusted me, and mentored me, educationally and spiritually, while away from my family thousands of miles. Her patience taught me what it takes to be a teacher. Her calmness showed me what it takes to be a leader. Her hard work showed me what it takes to be successful. I am in her debt for the rest of my life.

I am also thankful to my committee members for their keen observance and high-level technical comments and their serving on my doctoral committee.

I am grateful to Dr. Keith Schimmel for always supporting me.

I am thankful to Drs. Don Seo, Kamil Kaloush, BK Sharma, Albert Hung, and Farideh Pahlavan for their scientific insights.

I appreciate the financial support provided for my research from the National Science Foundation.

I want to thank my friends Daniel Oldham, Bjarke Hogsaa, Shahrzad Hosseinnezhad, Amirul Rajib, and Faisal Kabir for their supports through thick and thin of this journey.

Special thanks to Mahsa Keshavarz, my friend and my partner in crime, for always being there for me.

TABLE OF CONTENTS

Page

LIST OF TABLES

Table Page

Table Page

LIST OF FIGURES

Figure Page

Figure Page

Figure Page

Figure Page

1 INTRODUCTION

1.1 Asphalt History

Known as a good adhesive in the construction sector, bitumen has been used in more than 90 percent of paved roads in the U.S. (Jackson et al. 2011). The volatility in the price of oil has made the price of bitumen unstable. The price of a ton of bitumen in 2007 was $275, which spiked to the all-time high price of $662 in 2008 and went back to $332 in 2018 (Oklahoma department of transportation). On the other hand, innovation in refinery techniques has led to producing more fuels such as gasoline and diesel and less bitumen because of higher profits in the fuel industry (U.S. energy information administration)(Figure1).

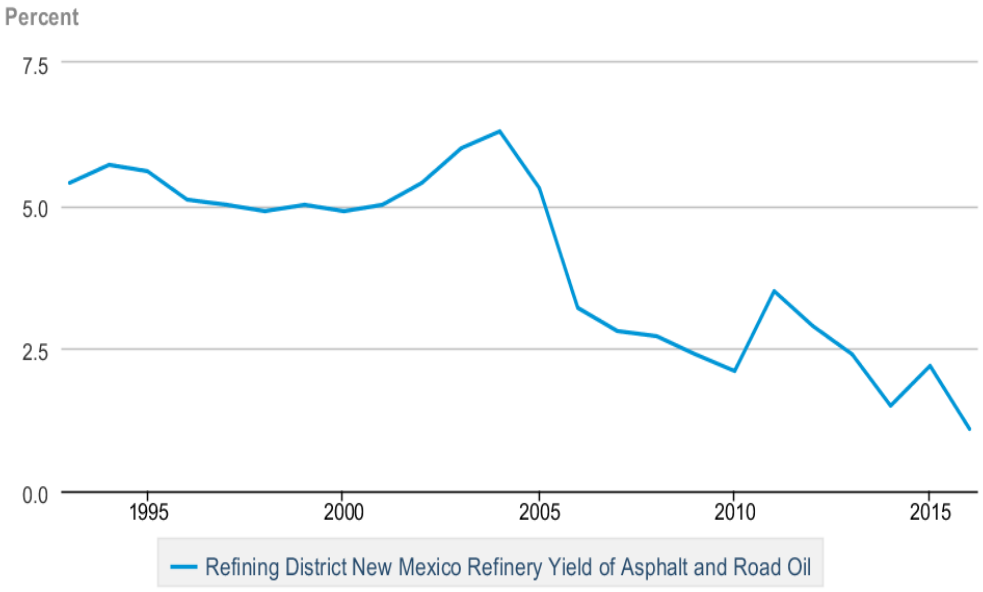

Figure 1.1 Bitumen yield of district New Mexico refinery (U.S. energy information administration)

To overcome the scarcity and price volatility of bitumen, researchers started to find modifiers to better use the remaining supply of bitumen for a longer time or to use the recycled pavements in new pavements. The use of modifiers has received rising attention in the past decade as the need for a better performance bitumen increased. Some asphalt cements require modification in order to meet specifications, which is another reason to use modifiers. Some of the reasons for using modifiers are as follow (Pavement interactive):

- **Increased demand on HMA pavements**. Traffic volume, loads, and tire pressure have increased substantially in recent years, which can cause increased rutting and

cracking. Many modifiers can improve asphalt stiffness at normal service temperatures to increase resistance to rutting while decrease its stiffness at low temperatures to improve its thermal resistance to thermal cracking.

- **Environmental and economic issues**. It is both environmentally and economically sound to recycle waste and industrial byproducts (such as tires, roofing shingles, glass and ash) to gain added benefit. Thus, when they can benefit the final product without creating an environmental liability, they are often used as additives in HMA. The other use is to maintain less environmental impacts, such as reduced emission and energy consumption. It can be done by improving the workability of bitumen to use it at less mixing and compaction temperature.
- **Superpave bitumen specifications**. Superpave bitumen specifications developed in the 1990s require bitumen to meet stiffness requirements at both high and low temperatures. In regions with extreme climatic conditions, this is not possible without bitumen modification.

1.2 Bitumen Additives to Improve Sustainability

1.2.1 Warm mix additives

The inherent benefit of using warm mix asphalt technology is to reduce asphalt viscosity and improve its workability at lower temperatures. Warm mix additives and warm mix technologies have recently gained attention as many countries are starting to practice more sustainable approaches to reduce energy consumption, especially in the

construction sector. Normally asphalt is mixed and compacted at a relatively high temperature of 150 ^{o}C or above, which makes asphalt mixing and compaction an energy consumer industry. To reduce the cost of energy consumption, different warm-mix technologies have been utilized. Some of which are:

- Utilizing organic additives such a low molecular weight wax
- The addition of zeolite to create a foaming effect in the mix
- Introduction of a soft bitumen and hard foamed bitumen during plant production

In this research, we focused on the use of wax in asphalt and how it affects binder mechanical, thermal, and molecular properties.

1.2.2 Rejuvenators

Modifying additives are utilized to rejuvenate recycled asphalt materials to reuse them completely or partially in asphalt mixture designs, which are called rejuvenators. Rejuvenators are products designed to restore original properties of aged (oxidized) bitumen by restoring the original ratio of asphaltenes to maltenes. Many rejuvenators are proprietary, making it difficult to offer a good generic description. However, many rejuvenators contain maltenes because their quantity is reduced by oxidation. Rejuvenators will retard the loss of surface fines and reduce the formation of additional cracks; however, they will also reduce pavement skid resistance for up to 1 year (Departments of the Army and the Air Force 1988).

The main usage of asphalt rejuvenators can be listed as follows (Brownridge 2010):

- Introduce maltenes and saturates (light fractions) to the aged bitumen
- Soften the stiffness of oxidized asphalt pavement and flux the bitumen
- Extend the life expectancy or service life of the pavement

1.2.2.1 Different sources of asphalt rejuvenators

Some rejuvenators are petroleum-based and are obtained from oil refineries. The other source for rejuvenators that recently gained attention is from waste oils such as engine oil or cooking oil (Zaumanis et al. 2013). Another source is bio-modifiers that can be used both as a modifier of virgin bitumen to improve its mechanical performance and workability, and rejuvenator to regain the bitumen properties after aging. Bio-binder from swine manure is one of the modifiers that can enhance the mechanical and rheological properties of both virgin and aged bitumen (You et al. 2011). It also can be used as a partial replacement of bitumen to reduce the demand for petroleum bitumen (Fini et al. 2011).

Straight-chain wax is one of the common parts of modifiers of bitumen, which can be used as a modifier of virgin bitumen (used in warm-mix asphalt technologies) or as a component of rejuvenators. On the other hand, paraffinic wax is also a part of bitumen itself, which is a non-reactive saturate and forms a portion of virgin and aged bitumen. Because of existence of wax in the bulk of bitumen, in the modifiers and in the rejuvenators from different sources, it is necessary to understand its effect on bitumen at different scales.

1.2.3 Other modifiers

Other modifiers that are used in asphalt pavements are as follow:

- Fillers (such as mineral fillers, carbon black)
- Extender (such as sulfur)
- Rubber (such as natural latex, synthetic latex)
- Plastic (such as polyethylene, PVC)
- Fiber (natural and artificial)
- Oxidant and antioxidant
- Antistrips (such as amines and lime)

1.3 Specific Aim of the Research

The goal of this study is to evaluate the effect of modifiers (from a petroleum source or a bio source) on bitumen properties and mechanical characteristics at different scales. Form a macro-scale study, the effect of wax on rheological and mechanical properties of bitumen is of interest. Using conventional tests to characterize the rheology of bitumen before and after doping with paraffinic wax, this research aims at evaluating the effects of paraffinic wax with different concentrations on both virgin and aged bitumen. The tests that have been utilized in this study cover both high and low service temperature characteristics of bitumen. Furthermore, the interplay between wax as a warm mix asphalt additive and an inherent component of bitumen and polyphosphoric acid (as a regularly used modifier of bitumen) needs to be investigated.

From a nanoscale point of view, the interaction of paraffinic wax with bitumen constituents and mostly asphaltene molecules needs to be studied. Asphaltene molecules play an important role in changes of the rheology of bitumen, and because of that, its interactions with other components may result in different changes in bitumen behavior.

Providing a linkage between bitumen rheological and mechanical properties with molecular interactions of its constituents is the unique contribution of this study and will help to understand some of the unknown aspects of bitumen behavior.

Another modifier that was studied is bio binder from swine manure and the viability of its use from a life cycle assessment perspective. The market analysis and industry needs and pains to understand the usefulness of this product is another aspect of this research

1.4 Objectives of This Study

Since the use of modifiers in the asphalt industry has gained much attention in recent years, understanding the effect of modifiers and mechanisms of that effect plays an important role in the design of new, sustainable, and effective modifiers to improve infrastructure quality and resilience. To achieve this goal, understanding the underlying reason of the effect of modifiers on bitumen is important. For this purpose, study the bitumen and modifiers' effect should be done as a multi-scale approach by using experimental studies, rheological analysis, chemical characterization as well as theoretical means such as molecular dynamics.

In pursuant of stated goals for this study, the following objectives are selected to achieve:

- Study the effect of wax as a warm mix asphalt additive on bitumen high, medium, and low service temperatures using experimental methods such as rheology study and chemical characterization. Furthermore, investigation of molecular-level interactions between wax and bitumen constituents can reveal the underlying reason of experimental results.
- Investigation of effect of wax-based modifiers and rejuvenators on aged bitumen mechanical properties, thermal characteristics, and chemical characteristics. Moreover, the molecular interaction between wax and aged bitumen molecules should be studied to explain the experimental results.
- Interplay between wax-based modifier and polyphosphoric acid (PPA) as an elastomer needs to be investigated. This objective helps to understand the synergistic and antagonistic effects of the two modifiers, which help explain some adverse effects that using two or more modifiers can have.
- Proposing a novel method to use a carrier for wax molecules to better disperse the modifier
- Environmental and economic impact assessment of the novel bitumen modifier obtained from swine manure as a sustainable approach towards lower carbon emission.

1.5 Research Approach

To achieve the goals of this research, a multi-scale method was proposed to understand and explain the effect of selected modifiers on bitumen properties. For this

reason, the bitumen samples after modification are evaluated using experimental mechanical tests (such as viscometry, dynamic shear rheometer, bending beam rheometer, and direct tension test). To evaluate the effect of modifier on chemical characterization of bitumen, further experimental studies were conducted (such as use of gel permeation chromatography, Thin-layer chromatography, SARA fractionation of bitumen, X-ray diffraction). The thermal properties of samples are also investigated to determine the effect of modifiers on the thermal response of samples. Thermal properties of samples were evaluated using differential scanning calorimetry and thermogravimetric analysis.

Molecular dynamics simulation is a means to simulate the molecular interactions. In this study this approach is used to explain the underlying mechanisms causing observed material behavior in laboratory experiments and to maintain a more scientific explanation for the effects of a modifier.

To evaluate the merits of the bio modified bitumen and its effects and impacts on environment, life cycle assessment (LCA) approach is a well-structured and credible means of study. Figure 1.2 illustrates the overall research scope.

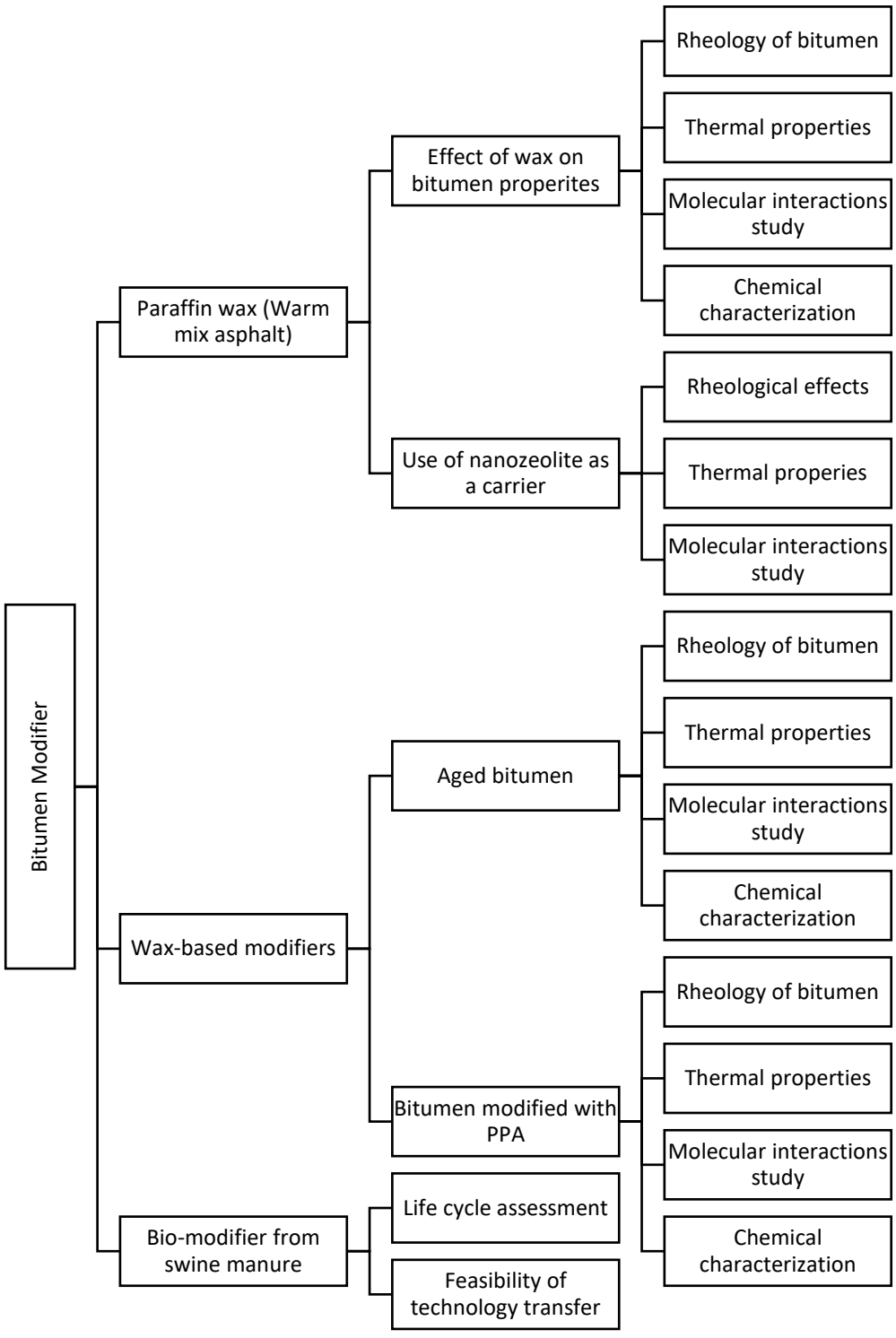

Figure 1.2 Schematic research scope

2 PARAFFIN WAX AS A WARM MIX ASPHALT ADDITIVE

2.1 Introduction and Literature Review

Warm-mix asphalts (WMA) are asphalt mixtures that can be manufactured and used at temperatures of 20°C - 40°C lower than those for hot-mix asphalt (EAPA 2016). The use of warm-mix asphalt has reduced the pollution emission and energy consumption caused by manufacturing and utilizing hot-mix asphalt (Rubio et al. 2012). WMA's lower viscosity and consequent improved workability at lower temperatures are the result of using organic or chemical additives or water-based asphalt mixtures (Vaitkus et al. 2009; You and Goh 2008).

Wax additives are different from bitumen's inherent wax. Currently, wax additives with the chemical structure of n-alkanes are used in WMA technology and are available in the market (Król et al. 2013; Lu et al. 2008; Morea et al. 2012; Sanchez-Alonso et al. 2011). Due to this difference between two substances, the n-alkane wax additive should be selected in a way so that the changes in the original bitumen will not be degrading (Król et al. 2013). Alkane is a saturated hydrocarbon (C_nH_{2n+2}), also called wax that can be in the form of a gas for n less than 5, a liquid for n between 5 and 17, and a solid for n greater than 17 (Gawel and Czechowski 1998). The melting temperature of new n-alkane additives is higher (ranges from 70°C to 145°C) than that of the inherent wax of bitumen (ranges from 20°C to 40°C) (Krol et al. 2015).

Bitumen consists of four main chemicals that are specified by their polarity. Bitumen's fractions are classified by their solubility in n-heptane. The insoluble part is

called asphaltene, and the soluble fraction is maltene (Merino-Garcia et al. 2009). The soluble part can be categorized as saturates, aromatics (polar aromatics), and resins (Corbett 1969; Lesueur 2009). The highly polar asphaltene micelles are dispersed in the maltene phase. Research has found that different concentrations of asphaltenes in the bitumen cause a variety of different mechanical behaviors in the asphalt matrix (Hofko et al. 2016). In recent research, the asphaltene molecule and its micelle formation have been characterized as primarily responsible for the mechanical behavior of bitumen (Eberhardsteiner et al. 2015).

Previous experiments on the effect of carbon chain length of n-alkanes on the precipitation of asphaltene molecules show a reduction of aggregation as the number of n-alkane carbons increases in a mix of asphaltene and n-alkane solvent (Rassamdana et al. 1996). Sahimi et al. (1997) showed the same conclusion using thermodynamic models and comparing the results with experimental results. They studied the precipitation of asphaltene molecules in *n*-C_5, *n*-C_6, *n*-C_7, *n*-C_8, *n*-C_9, and *n*-C_{10} (Sahimi et al. 1997).

Edwards et al., 2006 studied the effect of commercial waxes on asphalt mixtures performance using tensile stress restrained specimen test (TSRST), dynamic creep test, and complex modulus. Authors found that by adding 6% FT paraffin wax to a non-waxy bitumen, the fracture temperature increases from -34 to -32, but it doesn't change for the addition of the same amount of polyethylene wax. On the other hand, researchers showed that the physical hardening resulted by adding wax is observed in the BBR test but not in the TSRST test, which makes this test not suitable for identifying this effect. The results of

dynamic shear modulus showed a higher modulus for the specimens containing wax at lower frequencies (Edwards et al. 2006).

Edwards et al., 2007 studied the effect of commercial waxes in bitumen 160/220. The results of this study show a small change in complex modulus at higher temperatures while the authors stress on the probable rutting effect of wax with an n-alkane structure. Furthermore, a lowering effect on viscosity is reported by adding wax (Edwards et al. 2007).

Su et al., 2009 studied war mix asphalt mixtures made at two production temperatures (30 and 50 °C lower than control sample production temperature). Results show that for the samples that were produced at 50 °C lower than the control, the rutting depth is much higher (approximately 9mm more) than those produced at 30°C lower (Su et al. 2009).

Besides the macro-scale studying of the warm mix additives, many researchers studied the micro-scale properties of the bitumen. The so-called bee structures showed by using atomic force microscopy (AFM) of bitumens were attributed to the effect of the inherent wax of bitumen. De moraes et al., 2010 (De Moraes et al. 2010) studied the surface morphology of bitumen using AFM. Researchers showed that the bee structures changed considerably at temperatures between 50 and 56 °C, and they were completely disappeared at temperatures above 57 °C. Furthermore, the study shows by decreasing temperature from 170 °C, the formation of bee structures starts at 57 °C. Schmets et al., 2010, Pauli et al., 2011 and Fischer et al., 2014 have drawn a similar conclusion on wax-induced phase

separation in bitumen (Fischer et al. 2014; Pauli et al. 2011; Schmets et al. 2010). Qin et al., 2014 theorized that these surface morphologies are attributed to paraffin and polymer crystallization (Qin et al. 2014).

There are other researches on the effect of using wax and polymer in bitumen at the same time (Rossi et al. 2013), which focuses on the micro-scale study of interactions, but research has not been done on the effect of wax at nano-scale and molecular level (Rossi et al. 2013). Two obstacles to a full wax-bitumen study are the inherent complexity of the molecular structure of bitumen and the difficulty in understanding the simultaneous interaction of different molecules. Previous studies have shown that the structure and interactions of asphaltene molecules effectively affect the rheological and mechanical properties of bitumen (Li and Greenfield 2014; Mullins 2010). In order to understand the aforementioned interaction and its relationship to the mechanical properties of bitumen, a molecular-level study is needed to characterize the effect of wax on asphaltene molecules' behavior: the interaction of wax and asphaltene molecules, the mechanism of this interaction, its effects on the colloidal system of bitumen, and its relationship to the mechanical properties of warm-mix asphalt.

For the purposes of this study, an equilibrium molecular dynamics simulation has been performed using Large-scale Atomic and Molecular Massively Parallel (LAMMPS) software in the MedeA® environment version of 2.2. The MedeA® software consists of three levels, a graphical user interface, databases, and simulation programs.

2.2 Experimental Plan

2.2.1 Material Preparation

The bitumen used in this study was graded as PG 64-22, which is commonly used in the United States; it was acquired through Associated Asphalt Inc. in Greensboro, NC. The wax that was used for bitumen modification was a paraffin wax (P31, with melting point of 53–57°C, acquired from Fisher Scientific). The wax was introduced at 1%, 3%, 5%, and 10% dosage by weight of the initial bitumen, and was blended into asphalt at 135°C for 30 minutes.

2.2.2 Testing Methods

2.2.2.1 Differential scanning calorimetry

Bitumen samples with 1, 3, 5 and 10% added wax along with the base bitumen and wax were tested to determine the heat capacity and glass transition temperature (Tg) and to illustrate the effect of wax on the bitumen properties. The heat capacity was determined by the three-run method (ASTM E1269-11 2018), and the glass transition temperature (Tg) was determined by MDSC® in a heating cycle (Slough and Hesse 2006). The three-run heat capacity approach uses an isothermal – ramp – isothermal DSC method. This method consists of empty pans, sample, and a reference material such as sapphire. A high heating rate of 20°C/min is used to provide good signal to noise that can't be achieved with slower heating rates. For this method, provisions need to be made to correct or compensate the data for differences in the mass of the sample pan and the reference pan. In order to minimize the effect of instrument drift, the isothermal segments are used. The empty pan

baseline was subtracted from the reference results to determine a conversion factor of heat flow (mW) to heat capacity (J/°C). Then the heat flow difference between the sample and the empty pan baseline is determined, divided by the sample mass, and converted to heat capacity (J/g°) using the conversion factor. Replicate heat capacity determinations using the three-run method typically agree within about 3% or less. The three-run method can be done on almost any DSC with a minimal amount of instrument preparation. The test started at -80°C to 160°C. The samples (5-7 mg) were place in Tzero aluminum pans with hermetic lids. The traditional measurement of C_p, as outlined in ASTM E1269, requires three separate experiments for baseline, calibration, and sample analysis (ASTM E1269-11 2018). Calculating the C_p normally is obtained using computer software. In an MDSC experiment, modulation of the sample temperature permits the heat flow to be split into two components, one of which is dependent upon sample C_p and changes in C_p. The measurement of C_p by MDSC is more accurate than the three-run method, easily obtaining values with 2-3% error because it is a properly calibrated system (Slough and Hesse 2006).

2.2.2.2 Rotational Viscometer

Measurements of viscosity were conducted following ASTM D4402, using a Brookfield Viscometer RV-DVIII Ultra by applying a rotational shear on the selected material. Test specimens were prepared by pouring 10.5 grams into a specific aluminum chamber, then allowing it to cool to room temperature (ASTM D4402 2015). Samples were preheated in an oven for 30 minutes before being placed into the temperature-controlled thermoset. After thermal equilibrium within the sample was reached, three viscosity

readings were collected at three-minute intervals until the readings had a range of less than 100 cP (0.1 Pa*s). The average of these three numbers was record as apparent viscosity. The rotational speed chosen for this study was 20 rpm, with measurements conducted at 105°C, 120°C, 135°C, and 150°C.

2.2.2.3 Dynamic Shear Rheometer Test

A dynamic shear rheometer was used to investigate the elastic and viscous behavior of wax-modified bitumen by measuring the shear stress and shear strain, which was then used to calculate the complex modulus (G*) of the material. G* is typically defined as a measure of a bitumen's resistance to deformation when repeatedly sheared. In order to determine G*, a relatively wide range of oscillations were applied to the sample, ranging from 0.1 rad/s to 100 rad/s, at temperatures ranging from 70°C to 46. From the resulting data, G* master curves were generated using the principle of time-temperature superposition at a reference temperature of 61°C. Shift factors were generated using Williams, Landel and Ferry (WLF) method (Williams et al. 1955). For temperatures from 70°C to 52°C, the 25 mm spindle was used; for temperatures from 52°C to 46°C, the 8 mm spindle was used. Furthermore, the point at which the elastic and viscous modulus intersected was determined as the crossover temperature of the specimen. Crossover temperature is defined as the temperature at which the loss moduli and elastic moduli become equal.

2.2.2.4 Bending Beam Rheometer Test

The bending beam rheometer (BBR) was used to evaluate the modified unaged and aged bitumen's stiffness and ability to relax (m-value) at low temperature and compare it to that of unmodified bitumen. For the low-temperature testing, -12°C was selected, following the SuperPave bitumen PG specification, which requires the bitumen to be tested at the low-temperature grade of the bitumen (PG 64-22) plus 10°C, as mentioned in ASTM D6648 (ASTM D6648 2016). Bitumen sample beams were prepared by pouring the bitumen into six aluminum molds (four replicates). The samples were allowed one hour to cool to room temperature, then placed in a freezer for five minutes before being demolded. A constant load of 100 grams was applied on the middle point of specimens as the deflection was measured continuously.

2.2.2.5 Direct Tension Test

The direct tension test (DTT) was used to study low-temperature stress and strain and fracture properties of the modified unaged and aged bitumen. Six dog-bone-shaped bitumen specimens were prepared (dimensions of 40mm long, 6mm width, and 6mm thick) according to ASTM D6723 . The bitumen was poured into six aluminum molds, allowed to cool to room temperature for one hour, and then trimmed and placed in a freezer for seven minutes before demolding, to prevent deflection. The samples were then placed in the DTT's cooling bath at -12°C, following SuperPave bitumen PG specification (ASTM D6723-12 2012). Samples remained at -12°C for one hour for thermal equilibrium. The test started when the load reached 2 N with a strain rate of 3

percent/minute. During the test, load and displacement of the sample up to failure point were recorded and then used to calculate fracture energy (the amount of energy required to create two new

2.3 Results and Discussion

2.3.1 Differential Scanning Calorimetry

The DSC test results show a reduction of glass transition temperature (Tg), as shown in the graphs of cooling cycles generated from software associated with the instrument. Figure 2.1 shows the plot from the DSC test instrument, and Table 2.1 shows the Tg values by the bitumen paraffinic wax content. In this case, the Tg was considered as the midpoint of the glass transition phase. As the test results illustrate, the glass transition temperature of doped bitumen decreases as the wax content of the bitumen increases. This phenomenon can lead to better low-temperature behavior of the bitumen, since the formation of wax crystals can contribute to a weakening of the bitumen matrix because of lower strength of bitumen along crystal formation lines, as shown in previous studies (Pahlavan et al. 2016).

On the other hand, the heat capacity of the bitumen calculated from the heat flow of a heating cycle shows an increase of heat capacity up to the 5% wax bitumen compared to the neat bitumen, but a reduction is observed with the 10% wax bitumen. Because of the presence of wax crystals in the bitumen matrix up to the melting point (T_{mp}), a higher heat capacity is expected and seen in 1%, 3%, and 5% wax bitumen, but as the wax content increases beyond 5%, the heat capacity shows a reduction. The melting of wax is an

endothermic process, which cause the DSC results to peak. The DSC endotherm peaks of paraffinic wax exhibit two characteristic peaks as shown in Figure 2.2; these are attributed to the presence of n-paraffin structures without apparent presence of branching chains or iso-paraffin (Qin et al. 2014). By increasing the wax content in bitumen, these two peaks become more distinct, as shown in Figure 2.3.

Based on the Gibbs–Thomson effect (Qin et al. 2014), the depressed melting points indicate a smaller crystal size, which is favorable for wax-modified bitumens.

Table 2.1 Glass transition and melting point temperature of neat and doped bitumen

Property	Bitumen	1% wax	3% wax	5% wax	10% wax	Pure wax
Glass transition temperature T_g (°C)	-16.77	-16.95	-18.22	-21.07	-24.99	N/A
Melting point temperature T_{mp} (°C)	30	34	37	43	43	59.5

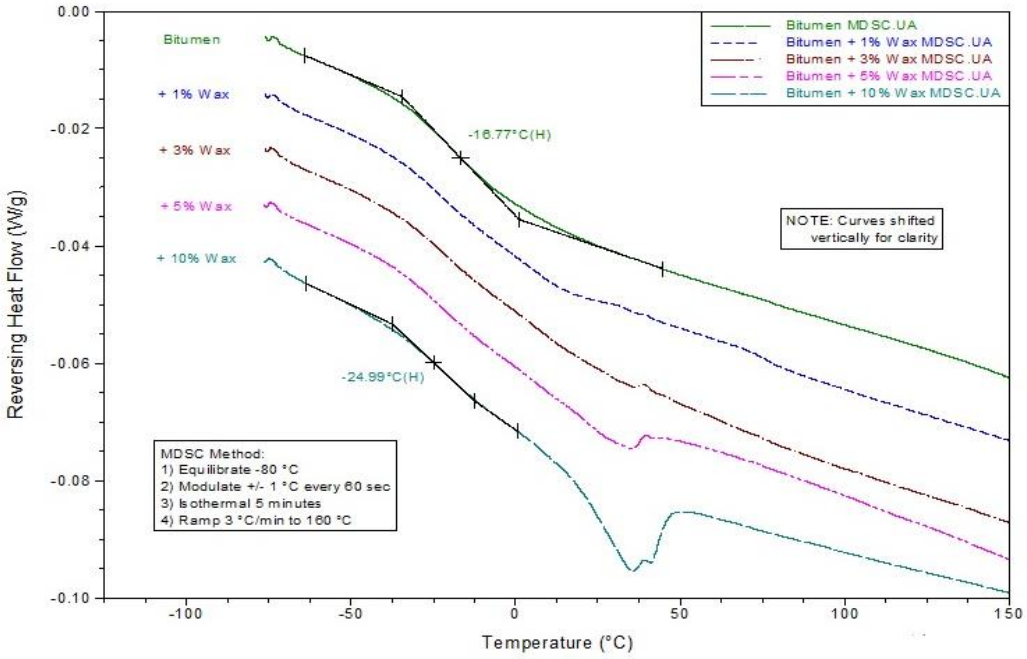

Figure 2.1. Glass transition temperature calculated by software

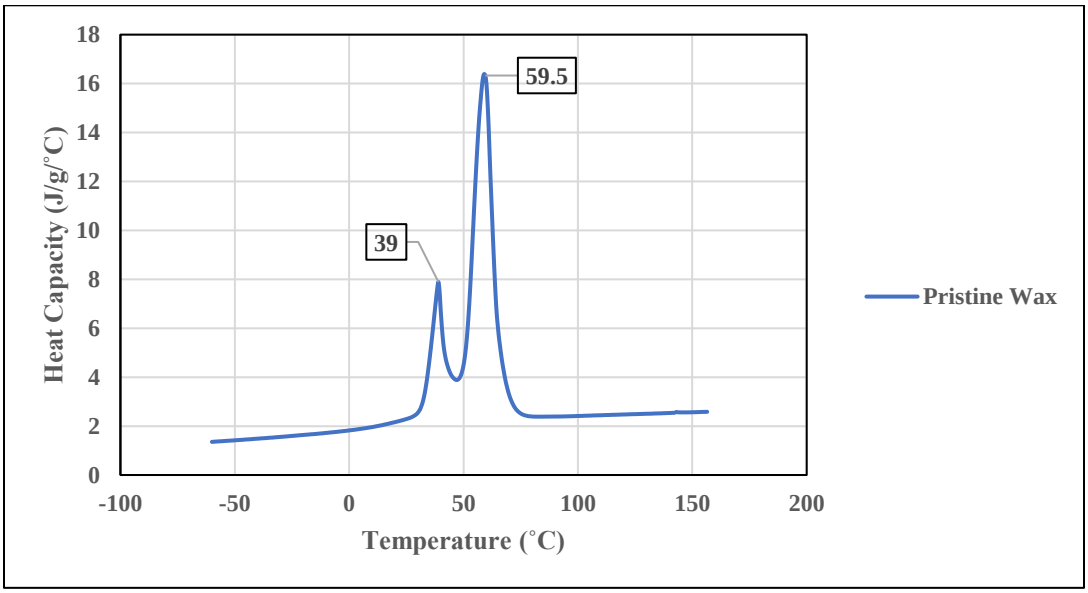

Figure 2.2. Heat capacity results for pure wax

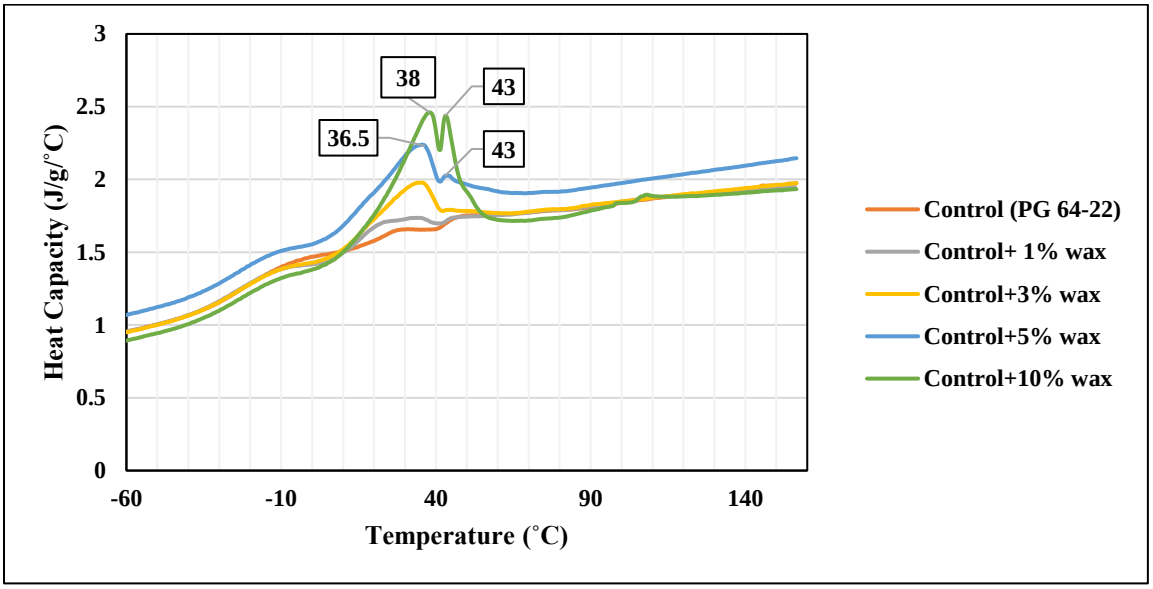

Figure 2.3. Heat capacity results for 0%, 1%, 3%, 5%, and 10% wax-modified bitumen

2.3.2 Viscosity

The effect of wax concentration on the doped asphalt's viscosity was investigated at different temperatures. Figure 2.4 shows the viscosity measurements at 0%, 1%, 3%, 5%, and 10% wax for different temperatures at 20 rotations per minute (rpm). The graph shows a significant decrease in viscosity values as wax dosage increases from 0% to 10% wax at 105°C. Also, an increase in temperature reveals a rapid decrease in viscosity, with the lowest viscosity observed at 150°C. This indicates that the addition of wax to bitumen improves bitumen workability by lowering the viscosity.

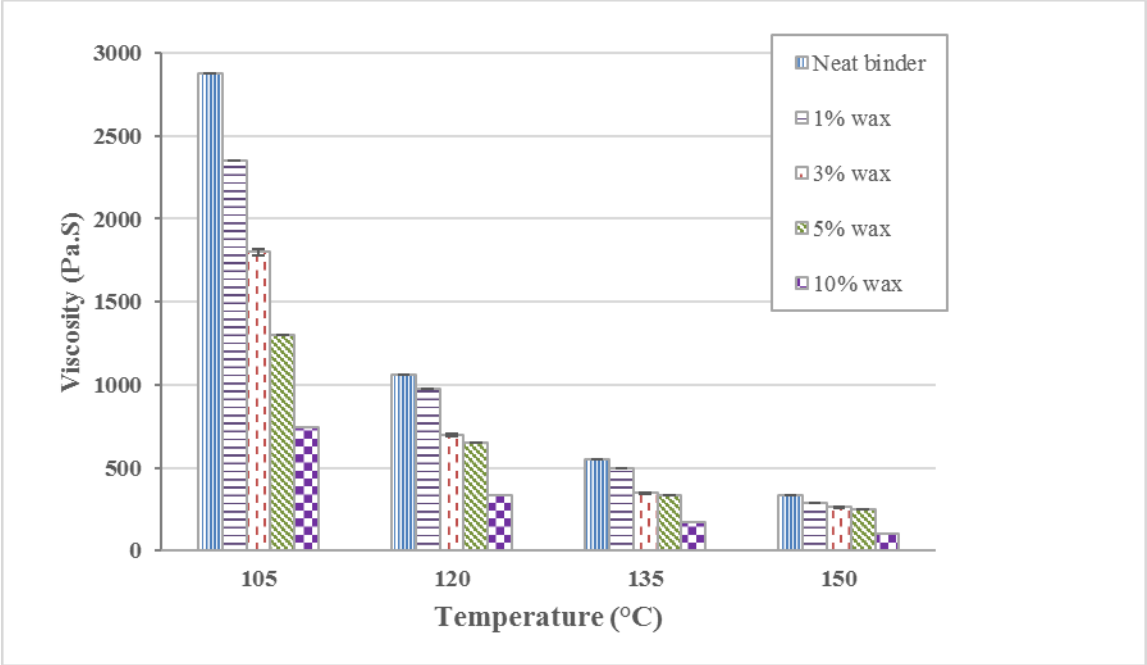

Figure 2.4 Viscosity versus temperature at 0%, 1%, 3%, 5%, and 10% wax at 20 rpm

2.3.3 Complex Modulus and Crossover Temperature

In Figure 2.5, the generated G* master curves for 0%, 1%, 3%, 5% and 10% wax are shown. The corresponding graph of shift factors is shown at the upper left. Figure 2.5 shows an overall decreasing effect of doping wax on the complex modulus, resulting in a softer bitumen. This effect is more profound at higher frequency, indicating that the presence of wax can lead to an overall softening of the matrix based on the definition of complex modulus which is the ratio of maximum shear stress to maximum strain (Yusoff et al. 2011). The softening effect of wax at higher wax contents aligns with DSC test results that show a reduction of crystal size of wax at intermediate temperatures. This phenomenon

can cause the wax-doped bitumen to be more susceptible to rutting at intermediate temperatures.

At lower frequencies, the difference in complex modulus between virgin and doped bitumen is not significant. It shows that at lower frequencies (higher temperatures), bitumen doped with paraffinic wax behaves similarly to virgin bitumen.

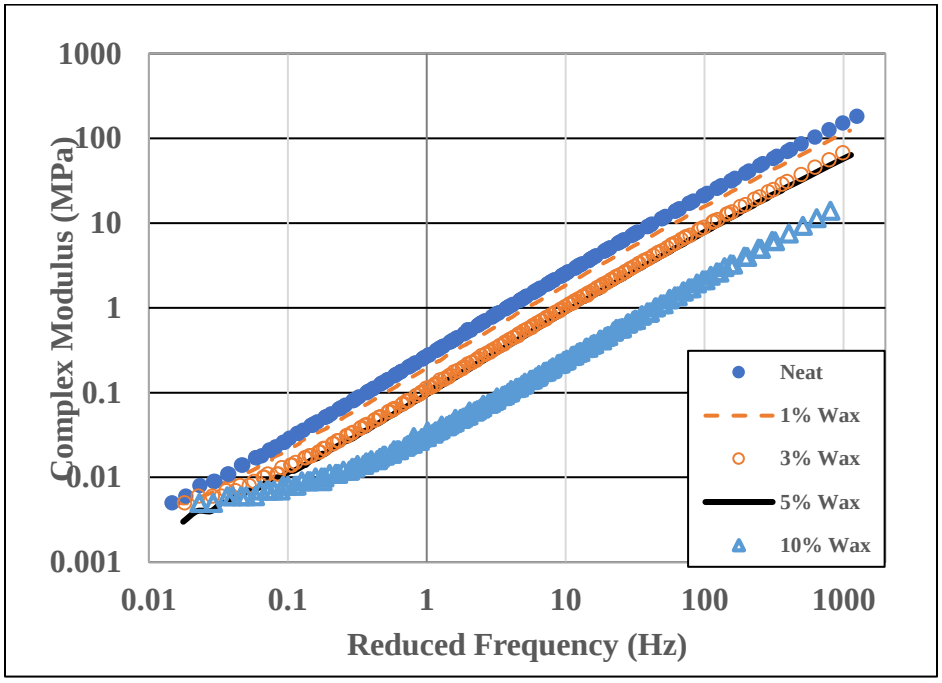

Figure 2.5 Complex modulus master curves for 0%, 1%, 3%, 5%, and 10% wax-modified bitumen at 61°C

To investigate aforementioned phenomenon more closely, the Dynamic Shear Rheometer (DSR) was used to determine the crossover temperature, which is the temperature at which the elastic and viscous modulus intersect (Figure 2.6). The

unmodified bitumen was shown to have a crossover temperature of 9°C. The difference of crossover temperature after adding 1% wax is not noticeable, as the complex modulus shows the same results. However, at 3%, 5%, and 10% wax-doped bitumen, the crossover temperature increased significantly. These results show that by increasing the wax content, wax-doped bitumen reaches its elastic behavior faster as the temperature drops, which also shows that wax-doped bitumen is stiffer at lower temperatures. To investigate the effect of the wax further, low-temperature characterization is needed to determine if this trend can be consistently observed.

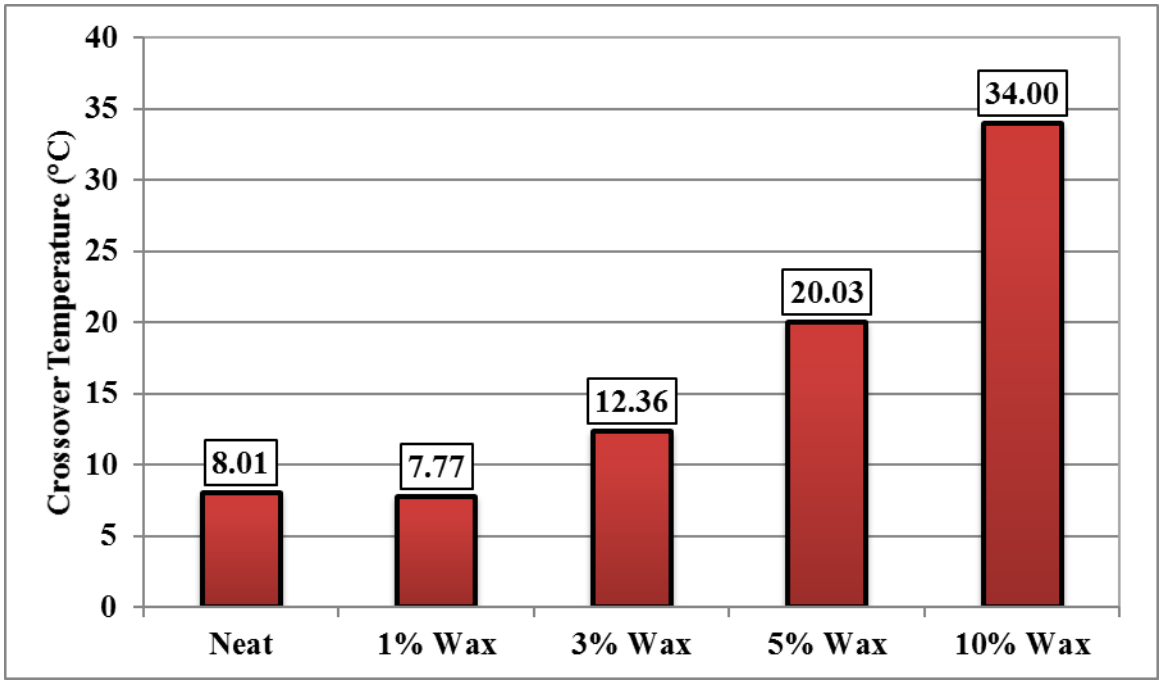

Figure 2.6 Crossover temperature of 0%, 1%, 3%, 5%, and 10% wax-modified bitumen

2.3.4 Stiffness and M-Value

Figure 2.7 shows the stiffness and m-value results that were determined using the bending beam rheometer. The stiffness results (left axis) show that increasing the wax percentage leads to an increase in stiffness value. This is consistent with the increased crystallization effect of the paraffin wax. This is also reflected in the wax-doped bitumen's decreased ability to relax stress, as shown by a decrease in the m-value as wax dosage was increased (right axis).

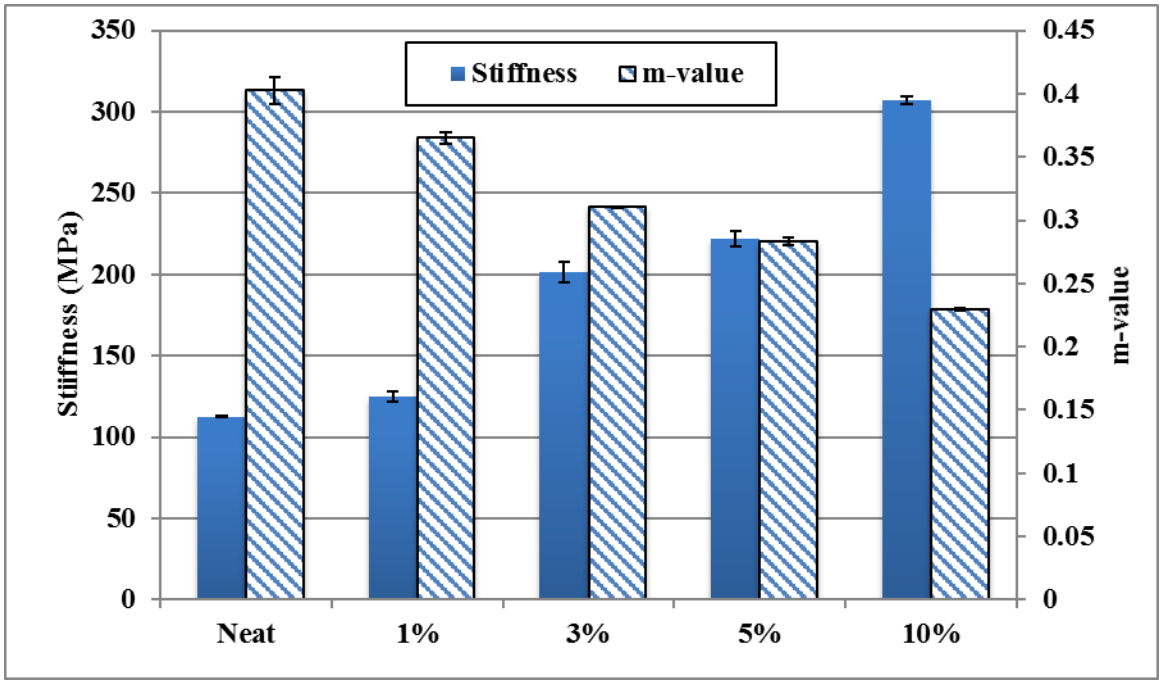

Figure 2.7 Stiffness and m-value results for 0%, 1%, 3%, 5%, and 10% wax-modified bitumen at -12°C

2.3.5 Fracture energy and ductility

Figure 2.8 shows the fracture energy calculated from the area under the load-displacement curve recorded using the direct tension test (DTT). This relates to the bitumen's cohesive properties, as the amount of energy required to bring the sample to failure is determined. The results show that fracture energy was consistently reduced with increasing the wax percentage with an increase for 10% wax sample. Since fracture energy is a function of both peak load and ductility results, it is important to analyze both measured properties to better understand the fracture energy results in Figure 2.8.

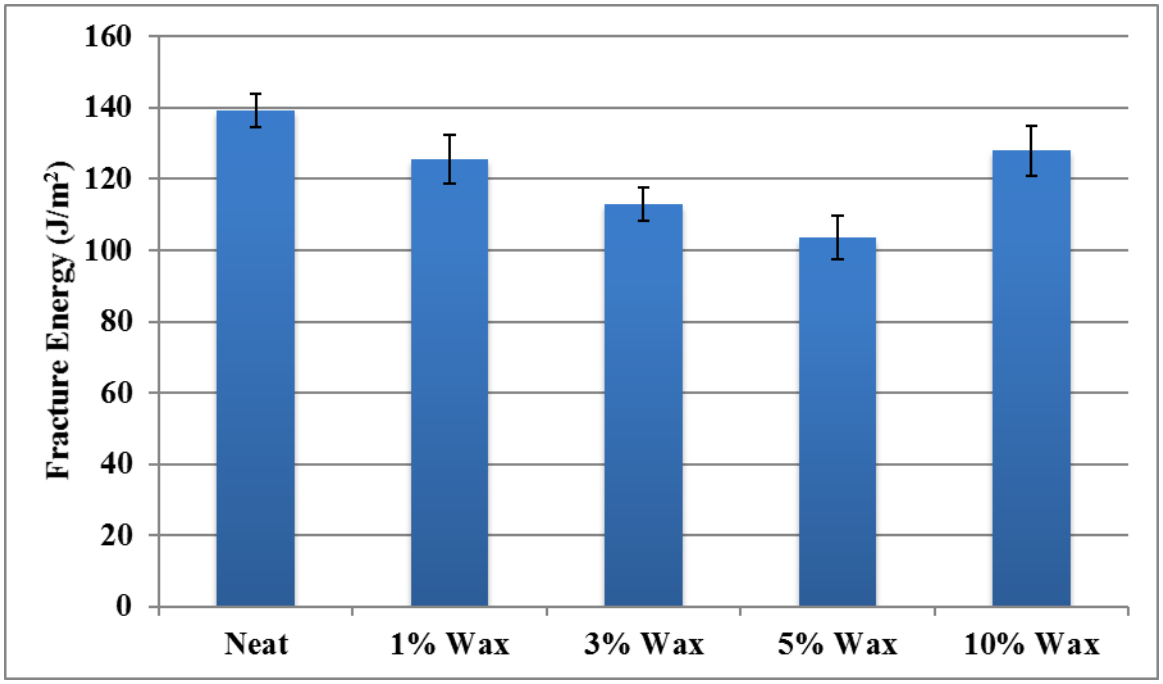

Figure 2.8 Fracture energy results for 0%, 1%, 3%, 5%, and 10% wax-modified bitumen obtained from direct tension test at -12°C

Figure 2.9 shows that peak load increases and ductility decreases with increasing of wax content. Having a higher peak load, and a lower ductility with increasing wax content shows that by increasing the wax content, the samples show stiffer and less ductile behavior. The loss in ductility can be attributed to the bitumen's decreased compliance, which is also reflected in the significant increase in peak loads for the corresponding samples. Therefore, the increase in fracture energy of 10% wax sample shown in Figure 10 is a result of the increased peak load of the sample. Increasing peak loads, in combination with decreasing ductility, indicate a more brittle failure with increased wax percentages, compared to the neat sample. While the peak load continues to increase with increasing wax percentage, the ductility appears to be less susceptible to wax percentage above 5%.

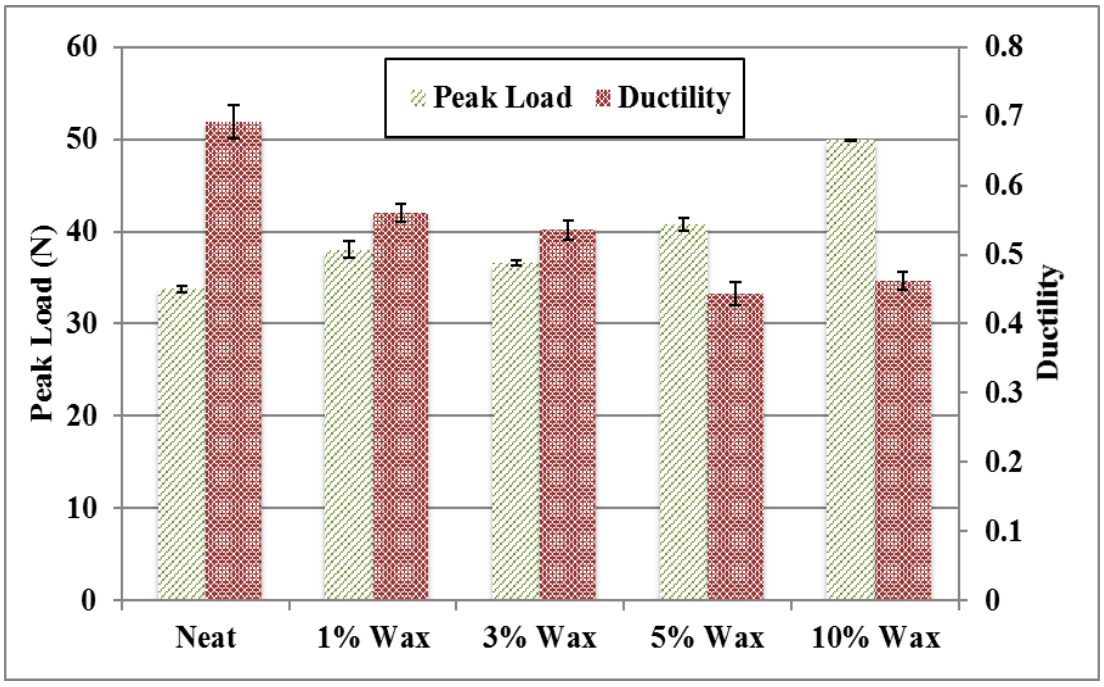

Figure 2.9 Ductility and peak load of 0%, 1%, 3%, 5%, and 10% wax-modified bitumen obtained from direct tension test at -12°C

2.4 Investigation of Interactions of Paraffinic Wax and Unoxidized Asphaltene

An equilibrium molecular dynamics simulation was performed using Large-scale Atomic and Molecular Massively Parallel (LAMMPS) software in the MedeA® environment version 2.2 to study interaction between asphaltene molecules in the presence of wax molecules.

The model was built in the MedeA® environment using the molecular builder, which allows step-by-step interactive building of polyaromatic units with attached alkyl chains and thiophenic rings. This study used the PCFF+ force field, which is an extension of the PCFF force field; PCFF+ is an all-atom force field designed to provide excellent accuracy on liquid properties and hydrocarbon modeling from ab initio simulations (Waldman and Hagler 1993). In the context of molecular modeling, a force field (a special case of energy functions or interatomic potentials) refers to the functional form and parameter sets used to calculate the potential energy of a system of atoms or coarse-grained particles in molecular mechanics and molecular dynamics simulations (Sun et al. 1994).

The asphaltene molecule proposed by Martin-Martinez et al. (Martín-Martínez et al. 2015)has been used to perform the analysis, because of its lower energy state compared to other model asphaltene molecules. This model is originally known as the modified Yen-Mullins model (Dickie and Yen 1967) which was later modified by Greenfield and Li (Li and Greenfield 2014)to alleviate the pentane effect by changing some aliphatic side chains. Martin-Martinez et al. then further enhanced the stability of the structure using Clar sextet

theory leading to rearranging of aromatic rings to find a model asphaltene that is a more stable monomer of an asphaltene molecule, due to its optimized distribution of π electrons and minimized geometrical strain. The second point at issue with the aim of exploring the effect of wax on the rheological and colloidal systems of bitumen is specification of the wax model. The wax model used in this study as an elementary unit of doped wax is the n-paraffin wax that is typically selected as n-$C_{11}H_{24}$ and has been used by other researchers (Pahlavan et al. 2016). The n-paraffin is a polymethylene sequence–(CH2)- that regularly stacks in layers (Pahlavan et al. 2016). The proposed models for asphaltene and n-paraffin wax are shown in Figure 2.10.

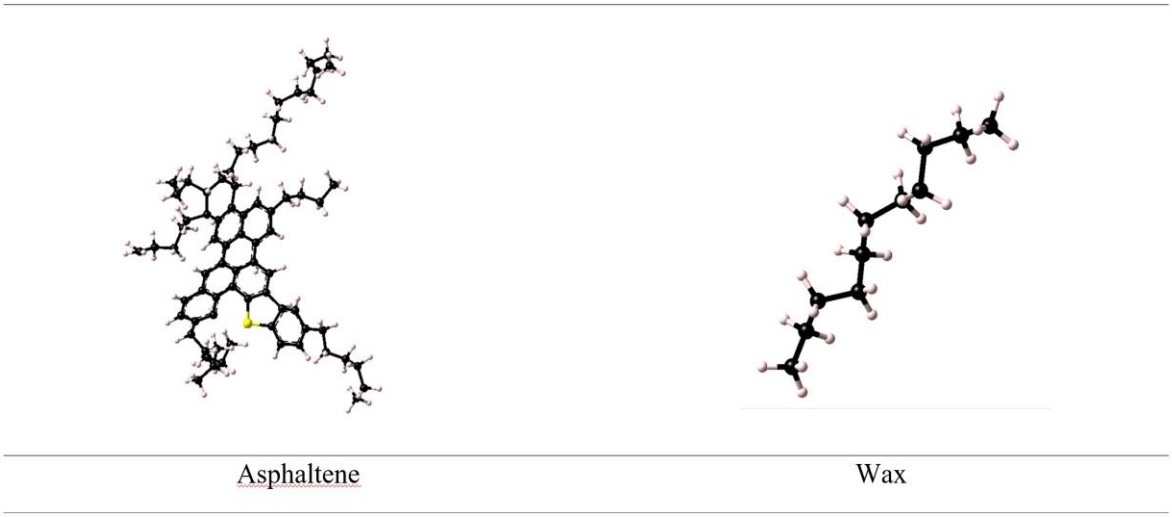

Figure 2.10 Asphaltene and wax molecular structures

In this paper to investigate the effect of wax on the formation of nano-aggregates of asphaltene molecules, a complex of different mass percentages of wax-asphaltene matrix

has been studied. The selected percentages are 1%, 3%, 5%, and 10%, which specify the mass fraction of wax in the system. The average aggregate size of asphaltene molecules was calculated using Equation 1 (Headen et al. 2017; Ungerer et al. 2014).

$$< \boldsymbol{m} >= \frac{\sum \boldsymbol{mN_m}}{\sum \boldsymbol{N_m}} \qquad \textbf{Equation 2.1}$$

where N_m is the number of aggregates containing m asphaltene molecules.

To examine the movement of wax molecules in the asphaltene matrix and the effect of wax concentration, the diffusion coefficient of the wax molecules was calculated using the Einstein Relation, which for diffusion in three dimensions can be written as Equation 2 (Einstein 1905).

$$< \boldsymbol{r^2} >= \boldsymbol{q_i Dt} \qquad \textbf{Equation 2.2}$$

where $< r^2 >$ is the mean square displacement (MSD), D is the diffusion coefficient,

q_i is a numerical constant that depends on dimensionality, and t is the elapsed time.

The above equation can be represented conceptually by Equation 3 to measure the diffusion coefficient:

$$D = [Slope\ of\ MSD\ curve\ over\ the\ elapsed\ time\ (t)]/[2d] \qquad \text{Equation 2.3}$$

where D is the diffusion coefficient, d is dimensionality, and t is the time over which we are calculating the diffusion coefficient. The unit for diffusion coefficient is $Å^2/ps$ (or 10^{-4} cm^2/s)

In the current study, all the wax molecules were considered as one subset of the entire system, and the mean square displacement was calculated for this subset.

To better study the effect of different concentrations of wax in bitumen and to better interpret the relationship of that effect with simulation, different wax concentrations in an asphaltene matrix were investigated.

2.4.1 Details of Simulations

In this study, to examine the effect of wax molecules on the stacking distance and self-association of asphaltene molecules, an NPT ensemble (constant number of atoms, constant pressure and constant temperature) was used comprising 120 molecules of C_{11} paraffinic wax and a dimer of asphaltene molecules at different temperatures from 105°C to 150°C with an interval of 15°C. From the results, the stacking distance of asphaltene dimer was measured to see the effect of temperature on stacking distance and self-association of asphaltene molecules in a waxy (non-polar) environment. The results were compared to the stacking distance of asphaltene dimer in a vacuum to better understand the effect of wax molecules on asphaltene stacking behavior.

To study the effect of wax on the formation of asphaltene nano-aggregates and asphaltene self-association at a larger scale, five different configurations were used: pure asphaltene, and asphaltene doped with 1%, 3%, 5%, or 10% wax. The samples were analyzed to capture an effect of different percentages of wax on asphaltene under vacuum, in an NVT ensemble (constant number of atoms, constant volume of the cell and constant temperature) that is similar to what was used in previous research (Pacheco-Sánchez et al. 2003). Each ensemble has 31 asphaltene molecules and a different number of wax molecules (from 2 to 20) to represent different dosages. The purpose of this part of the simulation is to look at the interaction of asphaltene molecules in the presence of wax without pressurizing the system. Simulations underwent two LAMMPS steps. The first step raised the temperature to 800 K (526.85°C) to speed up the movement of molecules, then gradually lowered the temperature to target temperature. Using Equation 1, the average aggregation size of asphaltene molecules was calculated.

To measure the diffusion coefficient of wax molecules within the asphaltene matrix, the next step of the simulation was performed in a two-stage process in which each step was composed of an NVT ensemble followed by an NPT ensemble in a vacuum environment with periodic boundary condition. To obtain a fast convergence of energy, the initial simulation started at a pressure of 200 atm and a temperature of 800 K (526.85°C) for 200 ps for each ensemble. Then decreased to a pressure of 1 atm and a temperature of 423 K (150°C). For the second stage of LAMMPS analysis, the simulation was done using

an NVT following by an NPT for the stabilized ensemble at first-stage temperature 423 K (150°C) in which duration was 15 ns using a time step of 1 fs at target temperature. The diffusion analysis was performed for 5 ns.

In all simulations, the short-range interactions were computed directly; long-range contributions were measured with the particle-particle particle-mesh method. The second-stage molecular calculation was performed initializing with an energy minimization at constant volume. A Nose-Hoover thermostat and barostat was used to maintain constant temperature and pressure during all the simulations. Non-bonded terms were calculated with a simple cutoff of 9.5 Å. The matrix of asphaltene and wax was started with a low average density to avoid molecular overlaps. The geometry of the system of molecules goes through a simple force field minimization and force field dynamics to ensure that none of the atoms are too close to each other.

2.4.2 Molecular Simulation Results and analysis

2.4.2.1 Effect of Wax on Self-Association of Asphaltene

The geometric conformation of two asphaltene monomers with the presence of wax at four different temperatures was studied to investigate the effect of temperature on possible conformations and to calculate the π-π stacking distance. Because of the presence of hetero atoms (in this case, sulfur) and saturated cycles, the occurrence of totally parallel polyaromatic sheets is unlikely. The simulation was performed at four temperatures between 105°C and 150°C. The stacking distance was calculated as the closest distance between carbon atoms in the two fused aromatic sheets in the parallel portion of a dimer.

The initial configuration was chosen according to the literature by exposing an asphaltene dimer to 120 n-$C_{11}H_{24}$ paraffin wax molecules as the solvent. The NPT ensemble was used, and the duration of the analysis was 20 ns for the system to equilibrate. The calculated stacking distances are presented in Figure 2.11.

As shown in Figure 2.11, the presence of wax solvent causes a decrease in the stacking distance of an asphaltene-asphaltene dimer. Increasing the temperature increases the stacking distance of an asphaltene dimer in both cases (in a vacuum and in wax solvent), which has a direct correlation with a reduction of viscosity by increasing temperature. Although an asphaltene dimer in waxy solvent shows a smaller stacking distance compared to stacking in a vacuum, there may be an intermediate component that affects the stacking of asphaltene molecules.

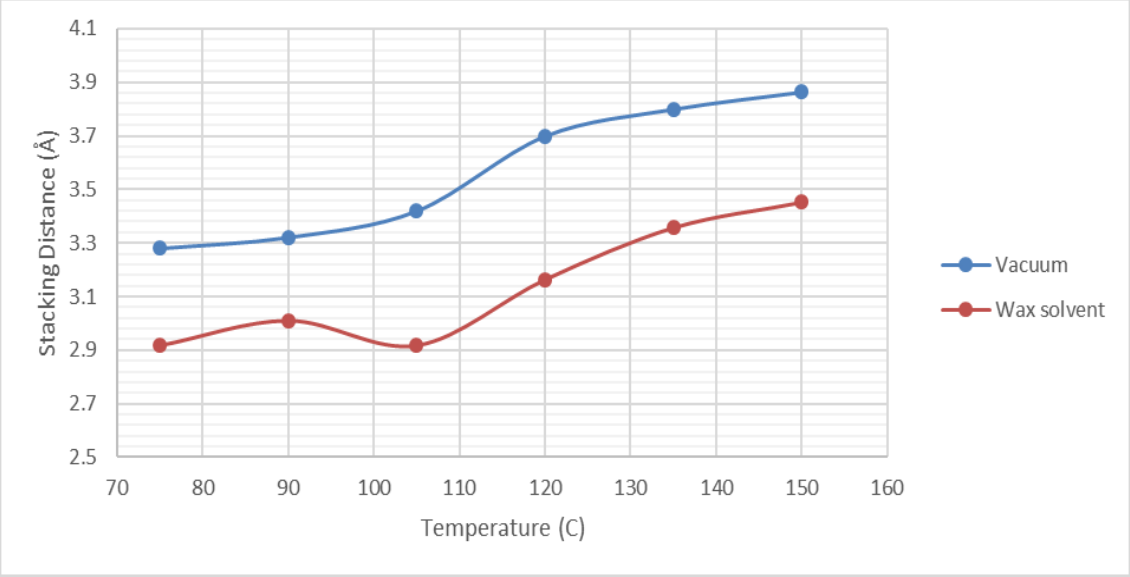

Figure 2.11 Stacking distance of an asphaltene dimer in vacuum and wax solvent at different temperatures

To evaluate the effect of n-paraffin wax on clustering of asphaltene molecules, a complex of asphaltene-wax was investigated using an NVT ensemble equilibration at a temperature of 423 K (150 ºC), using a cubic cell with dimension of 50 Å and a simulation time of 10 ns, under vacuum conditions. The continental model asphaltene used in this work stacks in clusters of 2 to 5 molecules with a large overlap of polyaromatic sheets. As a reference, for two molecules to be considered as a cluster, the overlap should be more than 50% of the area of a polyaromatic unit, which is observable by rotating the configuration around the axis normal to the tangent plane (Ungerer et al. 2014).

Figure 2.12 shows the final ensemble for 0%, 1%, and 10% wax cell. The numbers on Figure 2.12 show the number of molecules involved in the formation of a nanoaggregate. It also shows one nanoaggregate formed with five asphaltene molecules at the end of simulation and equilibration of the system.

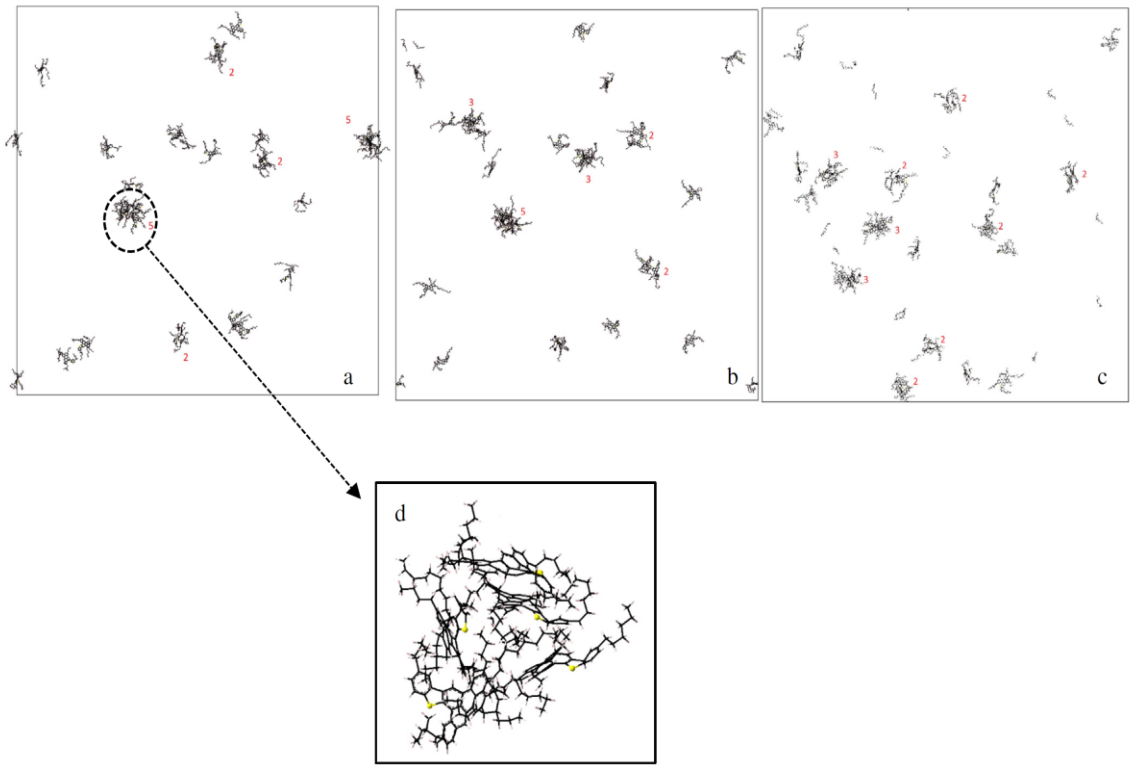

Figure 2.12 Studied ensembles to capture self-association of asphaltene molecules in the presence of wax molecules: a) Final configuration for asphaltene, b) 1% wax-asphaltene, and c) 10% wax-asphaltene ensemble, and d) magnified picture of a nano-aggregate of fiv

The average aggregation size for different conformations of wax-asphaltene was determined based on Equation 2.1. The studied ensembles were composed of 0%, 1%, 3%, 5%, and 10% wax based on overall asphaltene fraction. On the other hand, it was observed that the number of formed nanoaggregates reduces after an increase of wax content. It shows by inducing the wax molecules into the asphaltene matrix, the size of

nanoaggregates (the number of molecules involved in a nano-aggregate) shows a decrease, but the number of nanoaggregates increases. The average aggregation size and the number of nanoaggregates in each ensemble is shown in Figure 2.13.

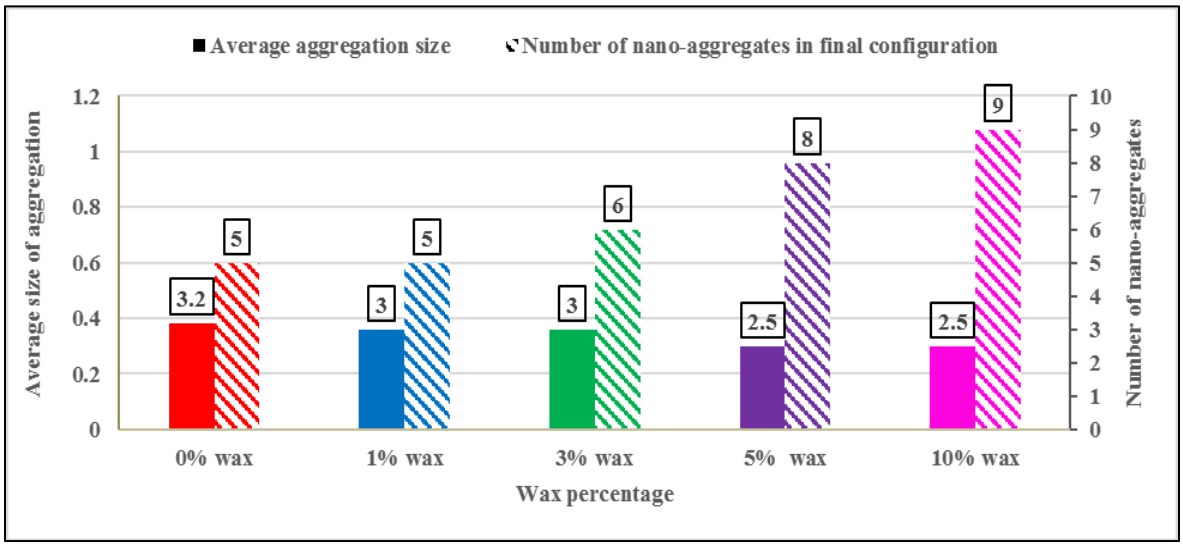

Figure 2.13 Average cluster size (number of molecules) and number of nano-aggregates in final configuration versus wax weight fraction of asphaltene

The cluster size shows a reduction with an increase of the wax weight fraction. This can be attributed to the steric repulsion of paraffin wax with the side chains of the asphaltene molecule, which would counteract the effect of π-π interactions between fused aromatic cores of asphaltene molecules, reducing their aggregation.

2.4.2.2 Diffusion Analysis

For each of four concentrations of wax, the MSD of the wax subset of the asphaltene-wax matrix was calculated over 5 ns of simulation at 423 K (150°C) using an

NPT ensemble. The studied ensembles were composed of 1%, 3%, 5% and 10% wax weight fraction of asphaltene, to represent commonly used wax dosage in the asphalt industry. The best-fit lines were then calculated, and their slopes were reported as diffusion coefficients. The MSD trend curves are illustrated in Figure 16, and the calculated diffusion coefficients are shown in Table 2.2.

Table 2.2 Diffusion coefficient and calculation uncertainty of wax molecules within the wax-asphaltene matrix

(10^{-7} cm^2/s)

Wax concentration	**1%**	**3%**	**5%**	**10%**
Diffusion coefficient	5.48	10. 59	23.34	38.89
Uncertainty	0.17	0.14	0.19	0.15

The diffusion analysis of wax shows that as the concentration of wax increases, the diffusion of the wax molecules increases within the entire matrix to the point that at 10% wax, the diffusion was 7 times higher than when 1% wax was present.

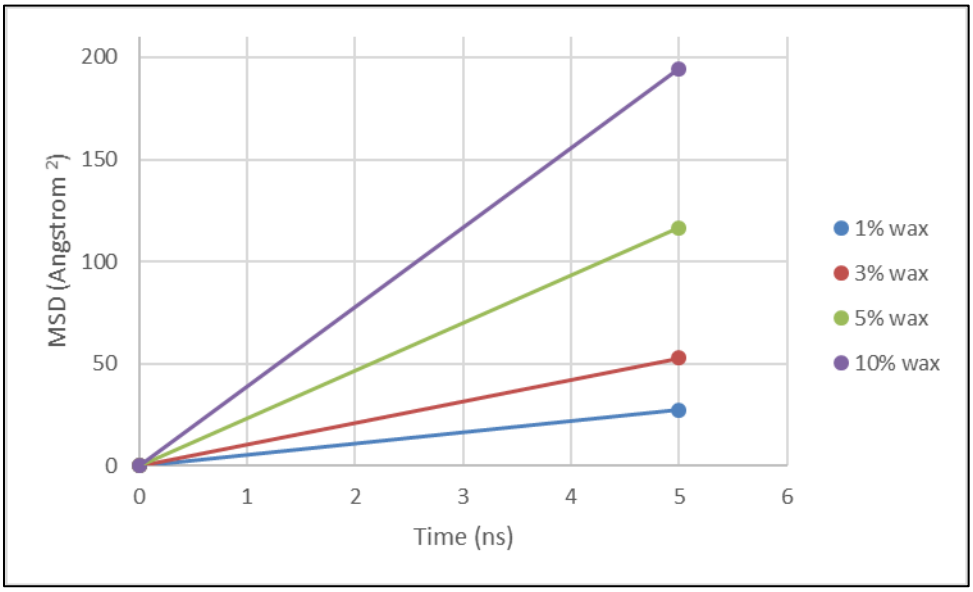

Figure 2.14 MSD curves for different conformations of asphaltene-wax simulations

2.5 Summary

This chapter investigates the effect of introducing n-alkane paraffin wax into bitumen as a warm-mix additive. To do so, the underlying interaction mechanisms between wax and asphalt molecules were examined both experimentally and via computational modeling. It was observed that presence of wax leads to improved workability of the asphalt mixture; this in turn allows lowering the mixing and compaction temperatures of the asphalt, which can promote pavement sustainability metrics. The research presents a comprehensive rheological characterization followed by computational modeling geared toward the use of molecular dynamics simulation to understand the mechanisms of

interaction between bitumen and paraffin wax molecules. Based on the results of experiments and modeling, the following conclusions were drawn:

- The glass transition temperature decreased by adding paraffinic wax to bitumen. Furthermore, there was a depression in melting point (endothermic peak in the DSC test) compared to pure wax, which can be attributed to reduction of wax crystal size when wax is mixed into the bitumen.
- The viscosity results showed a decreasing trend as the wax concentration in bitumen increased.
- The complex modulus decreased at high frequencies (at reference temperature of 61^{o}C) as the wax content increased. At low frequencies, there wasn't much difference between the complex modulus of neat bitumen and that of wax-doped bitumen. The low frequencies in the complex modulus represent temperatures close to wax melting point. Latter temperature was determined based on DSC analysis to the temperature at which the crystal structure of wax molecules starts to collapse. Accordingly, it may indicate that the presence of wax (above its melting point) may cause a disruption in asphaltenes molecular packing leading to a softer bitumen.
- Crossover temperature showed an increasing trend as the wax concentration increased from 1% to 10% in the bitumen. This phenomenon demonstrates that by increasing the wax content, the overall matrix of bitumen become more elastic.
- The stiffness of bitumen measured using a bending beam rheometer showed an increasing trend as the wax concentration increased, with the stiffness of bitumen

containing 10% wax being almost three times higher than that of neat bitumen. In addition, the observed reduction in m-value indicates bitumen's stress relaxation capability is reduced as the wax content increased.

- The fracture energy of bitumen decreased consistently as the wax content increased. Further analysis shows that, increasing wax content resulted in less ductility and a higher peak load at the failure point, which shows a more brittle fracture. This can be due to the formation of paraffinic wax crystals that changes the behavior of bitumen from ductile to more brittle behavior.
- The stacking distance of asphaltene dimer in a wax matrix increases with the increase of temperature, which aligns with the observed reduction in viscosity. Furthermore, the asphaltene dimer's stacking distance was found to be lower inside a wax matrix compared to the scenario without presence of wax.
- The average size of asphaltene aggregates reduces with an increase of wax concentration in the asphaltene-wax complex. However, the number of clusters of asphaltene increases as wax content increases from 1% to 10% in the system.
- The diffusion coefficient of wax molecules within an asphaltene-wax complex increased about seven times when the wax concentration was increased from 1% to 10%.

3 ROLE OF WAX TO RESTORE MOLECULAR PACKING OF ASPHALT

3.1 Introduction and Literature Review

The bitumen used in hot mix asphalt is always susceptible to reaction with oxygen in the air, a process called oxidative aging (Petersen 2009; Xu and Wang 2017).

Oxidative aging is a major factor responsible for hardening and rheological changes in asphalt, resulting in degradation of desirable asphalt properties (Bowers et al. 2014; Durrieu et al. 2007; Traxler 1961; Vargas et al. 2008). The oxidative aging process happens in two stages; for each stage, there is a laboratory test method to simulate it. The rolling thin-film oven (RTFO) test is used to simulate short-term aging that happens during the construction phase; the pressured aging vessel (PAV) test is used to simulate long-term aging of bitumen (De Filippis et al. 1995; Houston et al. 2007; Ruan et al. 2003; Siddiqui and Ali 1999; Wang et al. 2015). The use of reclaimed asphalt pavement (RAP) has been highly promoted by both road authorities and asphalt contractors; mainly due to increase and fluctuation of bitumen price from $235 per ton in 2006 to $635 in 2015 and to $409 in 2018 based on asphalt price index (Oklahoma department of transportation). Another motivation for promoting use of RAP is its abundance in the US., as well as the potential environmental benefit from reduction of use of natural resources and virgin bitumen which can off-set some of the consumption of depleting resources of virgin bitumen and mineral aggregate (Oldham 2015). To allow usage of high RAP asphalt mixture, a rejuvenator is needed to retrieve the original mechanical properties of virgin bitumen. Currently, different

types of rejuvenator for aged asphalt have been introduced to the market; these rejuvenators have different origins such as bio-based (wood pellets, animal waste, soybean and corn stover), waste engine oil, and some refinery-based oils that have portions of paraffinic oil bases (Chen et al. 2014; Oldham et al. 2014; Zaumanis et al. 2013).

Many newly used rejuvenators contain paraffinic wax or paraffinic oil (Mogawer et al. 2015); these still have the viscosity-lowering effect, but there is still the question of their effectiveness in chemically rejuvenating aged asphalt. Previous researches studied rejuvenators which contained paraffinic oil base. Mogawer et al. (2015) used paraffinic oil as rejuvenator and showed that it improved cracking properties of asphalt mixtures containing 50% RAP bitumen. For instance, fatigue test shows a much higher number of cycles (two times of control bitumen) to failure point (Mogawer et al. 2015). Zaumanis et al. (2013) introduced waste engine oil with paraffin wax to mixtures made from 100% RAP bitumen; the latter showed improvement in creep compliance which was increased by 25% compared to reference bitumen (Zaumanis et al. 2013). Wang et al., 2017 used a warm mix additive with structure of a polyethylene wax as rejuvenator for high RAP mixtures and showed improvement of high and low temperature properties (Wang et al. 2017). Among the four different chemical groups known as SARA (saturates, aromatics, resins and asphaltenes) (Eberhardsteiner et al. 2015), asphaltenes are the highly polar constituents of bitumen that are dispersed in the maltene phase (Allen et al. 2014). A change in the concentration of asphaltenes in bitumen causes a variety of changes in the asphalt's rheology as well as the asphalt's mechanical properties. The asphaltene

molecules and their self-interaction are recognized to strongly affect the rheological and mechanical behavior of bitumen (Li and Greenfield 2014; Mullins 2010). During the aging process of bitumen, one of the major factors that contributes to the stiffening of bitumen is the oxidation of polar aromatics, and asphatenes, leading to an increased aggregation due in polar fraction of asphalt components (Speight 1999). It has been documented that oxidation increases the asphaltene fraction of bitumen as the aromatics convert to asphaltenes (Qin et al. 2014). The results of gel permeation chromatography (GPC) indicated an increase in high molecular size species after asphalt was exposed to oxidation; the latter was attributed to asphaltene molecules becoming more prone to aggregation due to oxidation (Sharma et al. 2017). Other studies focused on examining interactions of wax with other constituents of bitumen in micro scale (Pauli et al. 2011; Schmets et al. 2010). The effects of paraffin wax on unaged bitumen at both macro scale and nano scale was also studied by Samieadel et al., 2017 (Samieadel et al. 2017). However, the effect of paraffin wax materials on aged bitumen and understanding the connection between molecular interactions and rheological properties of aged asphalt is yet to be investigated.

Furthermore, there are limited study of the effect of wax on asphaltene behavior (as one of the key players of asphalt properties), especially after oxidation of asphaltene during aging process, and its effect on asphaltene nano-aggregates formation.

In this chapter, molecular conformation and packing of oxidized asphaltene molecules in presence of paraffin wax is studied via both computational modeling and

experiments. Accordingly, the chapter presents a comprehensive thermos-mechanical characterization of aged bitumen doped with different dosages of paraffin wax utilizing a rotational viscometer, a dynamic shear rheometer, a bending beam rheometer, and a direct tension test. The Size exclusion chromatography was done to study the effect of paraffin wax on the formation of nano-particles. To further study the intermolecular interactions between paraffin wax and aged asphaltene molecules, an equilibrium molecular dynamics simulation has been performed using Large-scale Atomic and Molecular Parallel software in the MedeA® 2.2 environment. The simulations took place on a simplified model of the wax and oxidized asphaltene complex in two stage: first, the effect of doped n-Paraffin wax on the self-association of oxidized asphaltene molecules was studies; second the behavior of wax molecules in a complex of asphaltene-wax in methanol as a solvent medium was studied. The result of this study provides in-depth understanding on how paraffin wax affects molecular packing of oxidized bitumen, and consequently its thermo-mechanical properties.

3.2 Experiment Details

3.2.1 Material preparation

The bitumen used in this study was graded as PG 64-22 and donated by Associated Asphalt Inc. of Greensboro NC; it was aged based on RTFO (short term aging simulator) and PAV (long term aging simulator based on the standards (ASTM D2872-12e1 2012; ASTM D6521-13 2013) and doped with different paraffin wax dosages. For the aging process, the bitumen was initially aged using a rolling thin-film oven followed by two

durations of the regular aging procedure of a pressure aging vessel. The test using two durations is known as 2XPAV, total of 40 hours. 2XPAV has been shown to give better results with regard to the long-term aging that happens in the field (Bowers et al. 2014). The wax that was used for aged bitumen modification was a petroleum-based paraffin wax (P31, with melting point of 53 to 57°C, purchased from Fischer Scientific). The wax was blended at 1%, 3%, 5%, and 10 %wt of the initial aged bitumen, and samples were hand-blended at 135°C for 30 minutes.

3.3 Testing Methods

3.3.1 Rotational viscometer

The viscosity results were determined using a rotational viscometer (RV). Measurements were conducted following ASTM D4402 using a Brookfield Viscometer RV-DVIII Ultra, by applying a rotational shear on the selected material. Samples were prepared by pouring 10.5 grams of each sample (aged bitumen with different concentrations) into an aluminum chamber following by cooling to room temperature (ASTM D4402 2015). Samples were preheated in an oven for 30 minutes before testing in the temperature-controlled thermoset apparatus. After reaching thermal equilibrium, three viscosity results were taken at three-minute intervals until the results had a range of less than 100 cP (0.1 Pa.s). The average value of three readings was taken as the viscosity value. The speed chosen for this study was 20 rpm performed at 120, 135, and 150°C.

3.3.2 Dynamic shear rheometer test

The complex moduli results were determined using the Malvern Kinexus Pro dynamic shear rheometer (DSR) following ASTM D7552 – 09 (ASTM D7552-09 2014). The samples (three replicates for each sample) for each were tested at 31 different frequencies ranging from 0.1 to 100 rad/s at a temperature range of 76 to 10°C with 6-degree increments. The 25mm spindle was used for the high intermediate temperature range of 64 to 76°C, while the 8 mm spindle was used for 58 to 10°C due to increased stiffness of the bitumen at lower temperatures (Laukkanen 2017). From the resulting data, master curves were generated using the principle of time-temperature superposition (TTS) using the Williams-Landel-Ferry method (WLF) (Williams et al. 1955) at a reference temperature of 43°C. Furthermore, the temperature at which the loss moduli and storage moduli meet (known as the crossover temperature) was measured as a property of the material. In general, viscoelastic materials with higher crossover temperature reach their elastic behavior faster as temperature drops and behave more as a stiffer material (Huang et al. 2014; Samieadel et al. 2017).

3.3.3 Bending beam rheometer test

The bending beam rheometer (BBR) was used to evaluate the modified aged bitumen's stiffness and ability to relax (m-value) at low temperature and compare it to that of unmodified aged bitumen. For the low-temperature testing, -12°C was selected, following the SuperPave bitumen PG specification, which requires the bitumen to be tested at the low-temperature grade of the bitumen (PG 64-22) plus 10°C, as mentioned in ASTM

D6648 (ASTM D6648 2016). Bitumen sample beams were prepared by pouring the bitumen into six aluminum molds (six replicates). The samples were allowed one hour to cool to room temperature, then placed in a freezer for five minutes before being demolded. A constant load of 100 grams was applied on the middle point of specimens as the deflection was measured continuously.

3.3.4 Direct tension test

The direct tension test (DTT) was used to study low-temperature stress and strain and fracture properties of the modified aged bitumen. Six dog-bone-shaped bitumen specimens were prepared (dimensions of 40mm long, 6mm width, and 6mm thick) according to ASTM D6723 (ASTM D6723-12 2012). The bitumen was poured into six aluminum molds, allowed to cool to room temperature for one hour, and then trimmed and placed in a freezer for seven minutes before demolding, to prevent deflection. The samples were then placed in the DTT's cooling bath at -12°C, following SuperPave bitumen PG specification (ASTM D6723-12 2012). Samples remained at -12°C for one hour for thermal equilibrium. The test started when the load reached 2 N with a strain rate of 3 percent/minute. During the test, load and displacement of the sample up to failure point were recorded and then used to calculate fracture energy (the amount of energy required to create two new surfaces) and ductility (the change in length divided by the original length).

3.3.5 Size exclusion chromatography

The Size Exclusion Chromatography (SEC) analysis was conducted using a Thermofisher RefractoMax 521 RI detector and Malvern H100-3078 column (7.8mm ×

300mm). A WPS-3000TSL analytical auto-sampler was fully controlled by the Chromeleon chromatography management system. Samples (3% w/w in Tetrahydrofuran, THF) were filtered using 0.45-µm Millipore PTFE to remove suspended particulates; a pump flow rate of 1.0 mL/min with THF as the carrier solvent and injection volumes of 25 µL were used. The separation of the multi-component mixture took place in the column. A constant flow of fresh eluent was supplied to the column via a pump to detect analytes. The analysis was conducted based on size separation of analytes. The resulting chromatographic data was processed using Chromeleon software.

3.4 Results and Discussion

3.4.1 Viscosity Test

The effect of wax content on the viscosity aged bitumen was investigated at different temperatures (Figure 3.1). The viscosity results show that by increasing the wax concentration from 1% to 10%, the viscosity of the blend decreases. Furthermore, the increase in temperature shows a swift reduction in bitumen viscosity. The viscosity difference for different dosages also decreases as the temperature increases. This change in viscosity at high temperatures occurs when wax crystals can't be formed and the wax molecules can move freely in the bitumen medium.

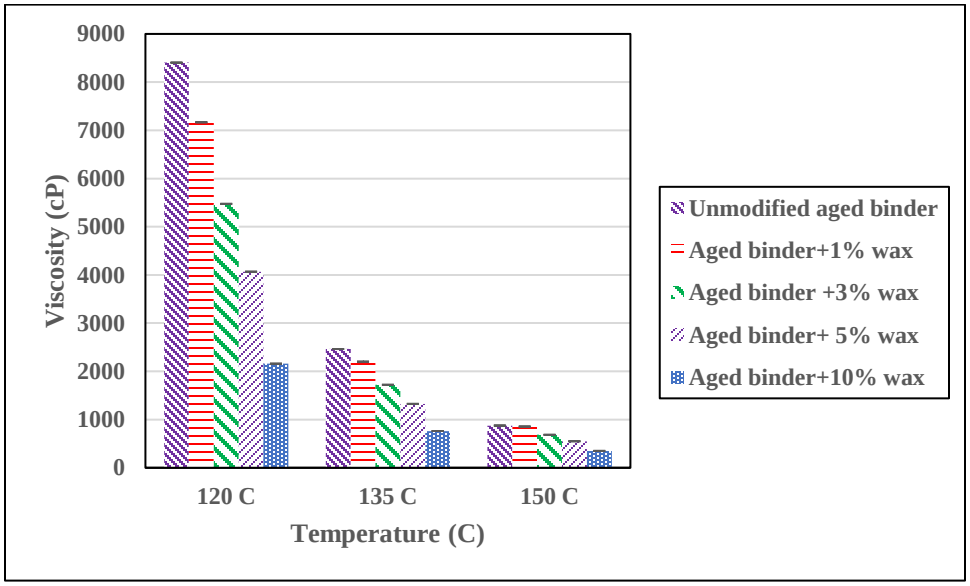

Figure 3.1 Viscosity vs temperature at 0%, 1%, 3%, 5% and 10% wax under 20 rpm.

3.4.2 Complex Modulus and Crossover Temperature

Using the dynamic shear rheometer (DSR), the complex modulus (G*) master curves for 0%, 1%, 3%, 5%, and 10% wax-modified aged bitumen were calculated and plotted in Figure 3.2. The results indicate that at a higher percentage of wax content, the aged bitumen becomes softer, especially for 5% and 10% wax. This softening effect is more noticeable at lower temperatures. At lower temperatures (higher frequencies), the bitumen becomes softer with an increase of wax content, while at higher temperatures, there is not much change after 5% wax. The results show that, for a temperature range of 10 °C to 76°C,

adding more than 3% wax is needed before a noticeable softening effect in aged bitumen starts.

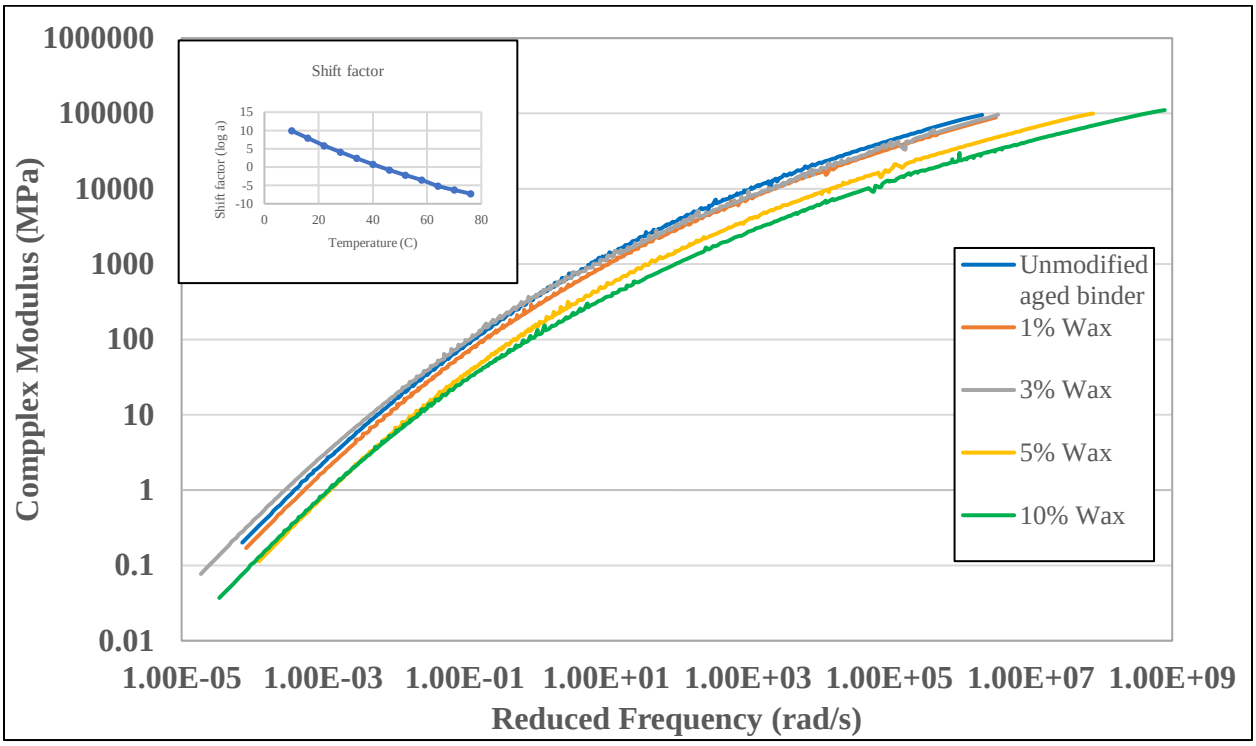

Figure 3.2 Complex modulus master curves for 0%, 1% 3%, 5% and 10 % wax-modified aged bitumen

To investigate the aforementioned phenomenon more closely using the DSR, the point at which the storage and loss moduli intersect (at a phase angle of 45^{o}) was also determined as an indicator of the hardness of a material. This point is also known as the crossover temperature and is a physical property of a material. The crossover temperatures of unmodified aged bitumen, and aged with different wax concentrations are presented in Figure 3.3. The crossover temperatures show that by aging the bitumen, the crossover

temperature of the material increases significantly. By adding wax to aged material, a small reduction is observed at lower concentrations followed by an increase at higher dosages. This can be related to the formation of wax crystals at lower temperatures than its melting point.

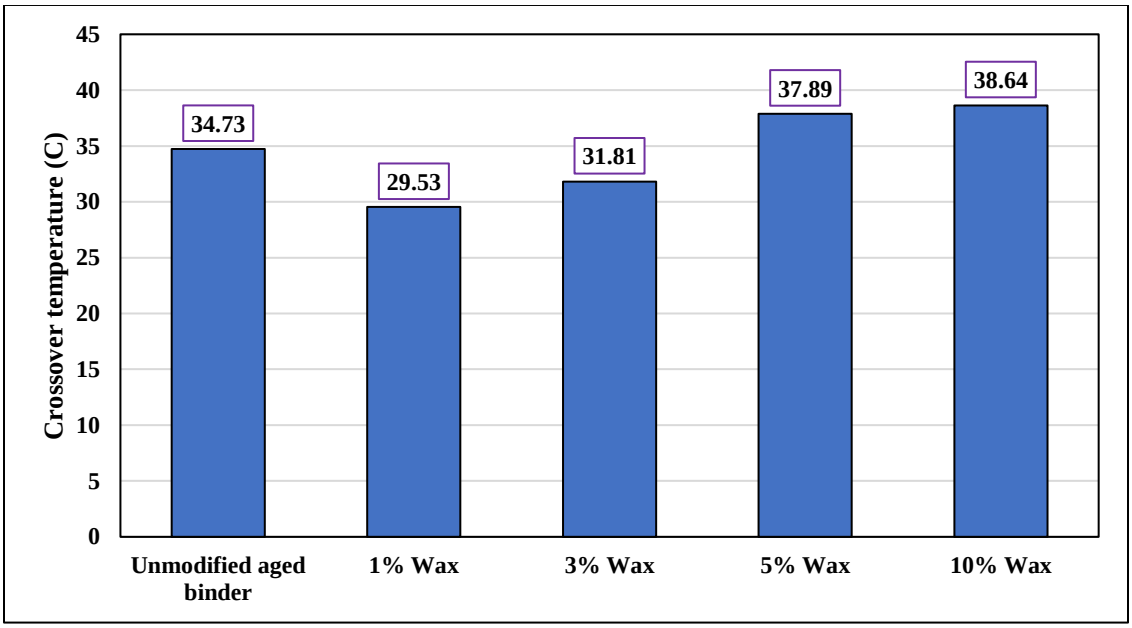

Figure 3.3 Crossover temperatures for 0%, 1% 3%, 5% and 10 % wax-modified aged bitumen

3.4.3 Stiffness and M-Value

Figure 3.4 shows the stiffness and m-value results that were determined using the BBR. The stiffness results (left axis) show that an increase in wax content leads to a higher stiffness value in which by adding 10% wax the stiffness increases by almost 30%. This phenomenon can be due to an increase in the formed crystallized networks of the paraffin

wax in the bulk of aged bitumen. This is also shown with the modified aged bitumen's decreased ability to relax stress, as shown by the constant decreasing of the m-value up to 20% less than unmodified aged bitumen after adding 10% paraffin wax (right axis).

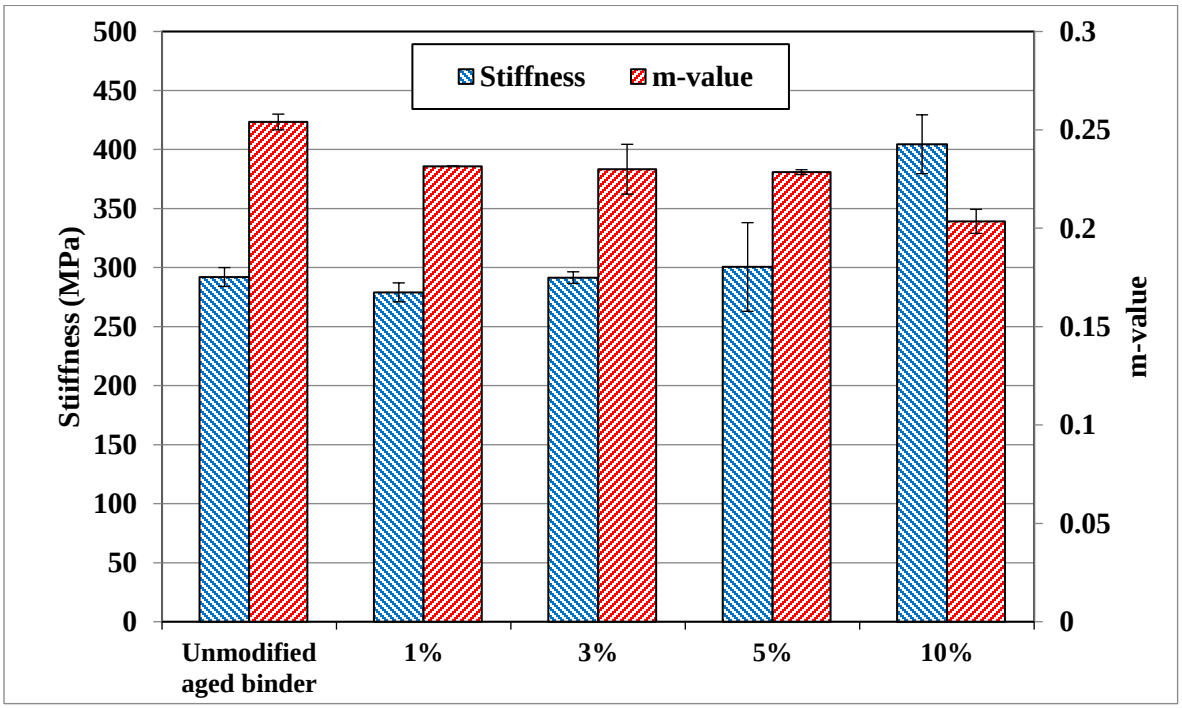

Figure 3.4 Stiffness and m-value results for unmodified aged bitumen, 0%, 1%, 3%, 5%,

3.4.4 Fracture Energy and Ductility

Figure 3.5 shows the fracture energy obtained from a DTT test by calculating the area under the curve of load-displacement. The fracture energy represents the cohesive strength of the material and the energy that is needed to bring the material to cohesive failure. The results indicate that by adding wax to aged bitumen, the material becomes extremely brittle. The results from ductility also show that by adding wax, the ductility of

aged material decreases by 30 percent (Figure 3.6). A lower peak load along with lower fracture energy and ductility does not show any improvement from added wax in aged bitumen's low-temperature rheological properties.

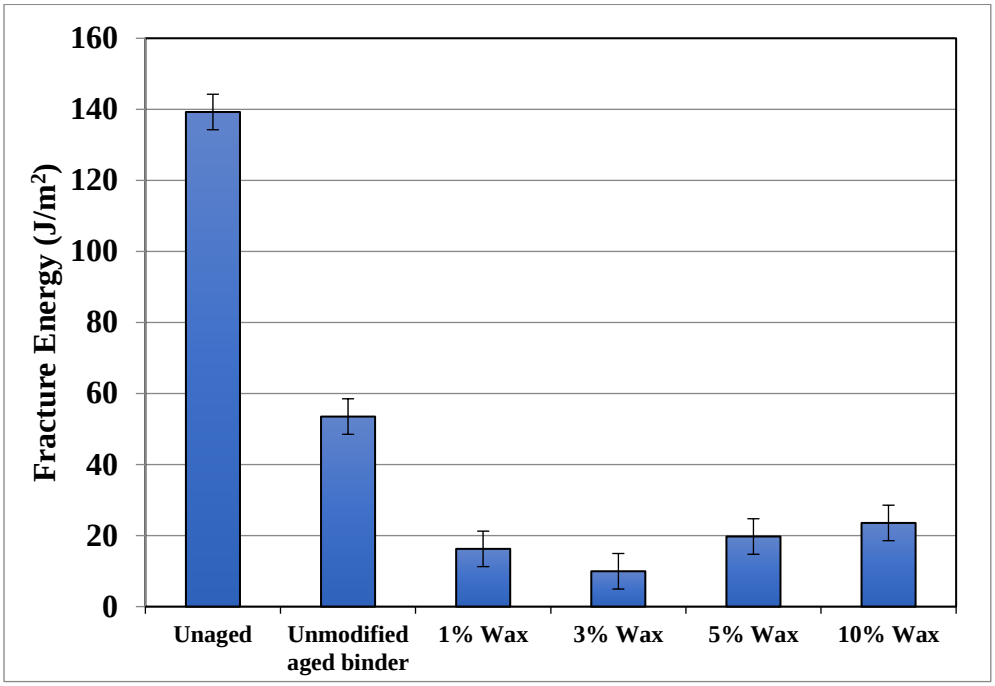

Figure 3.5 Fracture energy results for 0%, 1%, 3%, 5% and 10% wax-modified aged bitumen

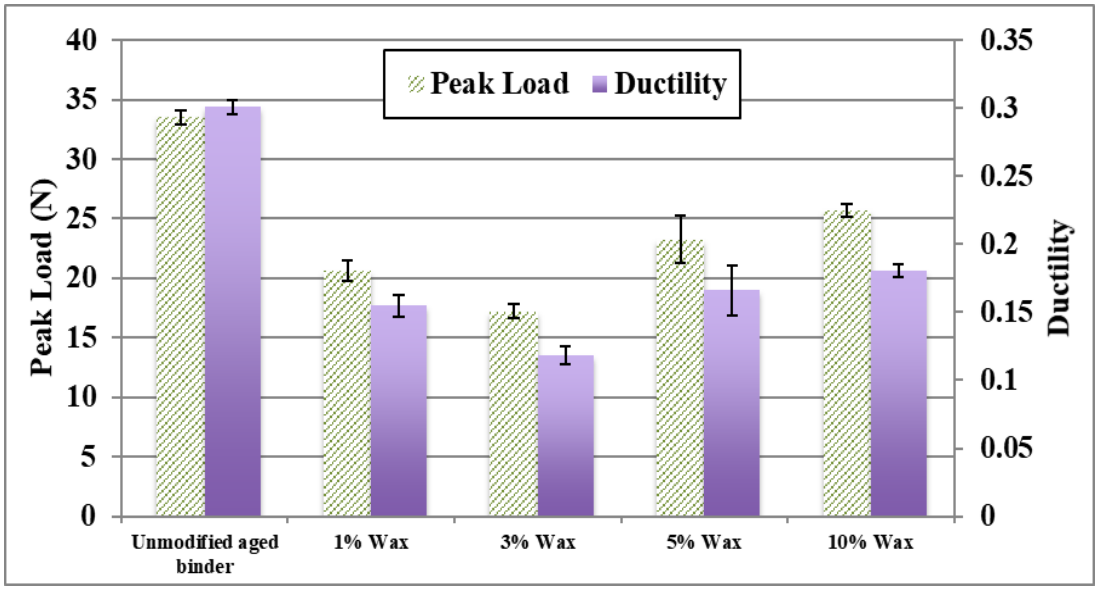

Figure 3.6 Ductility and peak load for 0%, 1%, 3%, 5% and 10% wax-modified aged bitumen

This change in properties of aged bitumen can be explained as being caused by the formation of more weak crystal networks inside the bulk of aged bitumen which decrease the resistance of bitumen from tensile stress. The reason for ununiform trend for fracture test is the fact that mechanism for destructive tests are different from the non-destructive tests as DSR showing a more consistent trend with increase of wax content. This further confirms that at specific wax content fracture mechanism transitions from bulk fracture to a crack growth at the interface between wax and asphalt

3.4.5 Size Exclusion Chromatography (SEC)

Figure 3.7 shows the chromatogram of unaged bitumen, aged bitumen, and aged bitumen + 10% wax. The Figure shows that the peak intensity at early elution time (around 4.91 minutes) is increasing, and the shoulder around 5.6 minutes converted to a noticeable peak from unaged to aged bitumen. But after introducing 10% wax, there is a reduction in the intensity of the areas of both peaks. In size exclusion chromatography, material with a higher molecular weight appears at an earlier elution time. The enhancement in the peak area shows an increase in molecular weight after aging. Table 3.1 shows the cumulative percentage of area from the start time of elution up to 5.8 minutes for all three chromatograms. Based on size exclusion analysis, the large molecular size increase after aging, and it was reduced after 10% wax inclusion.

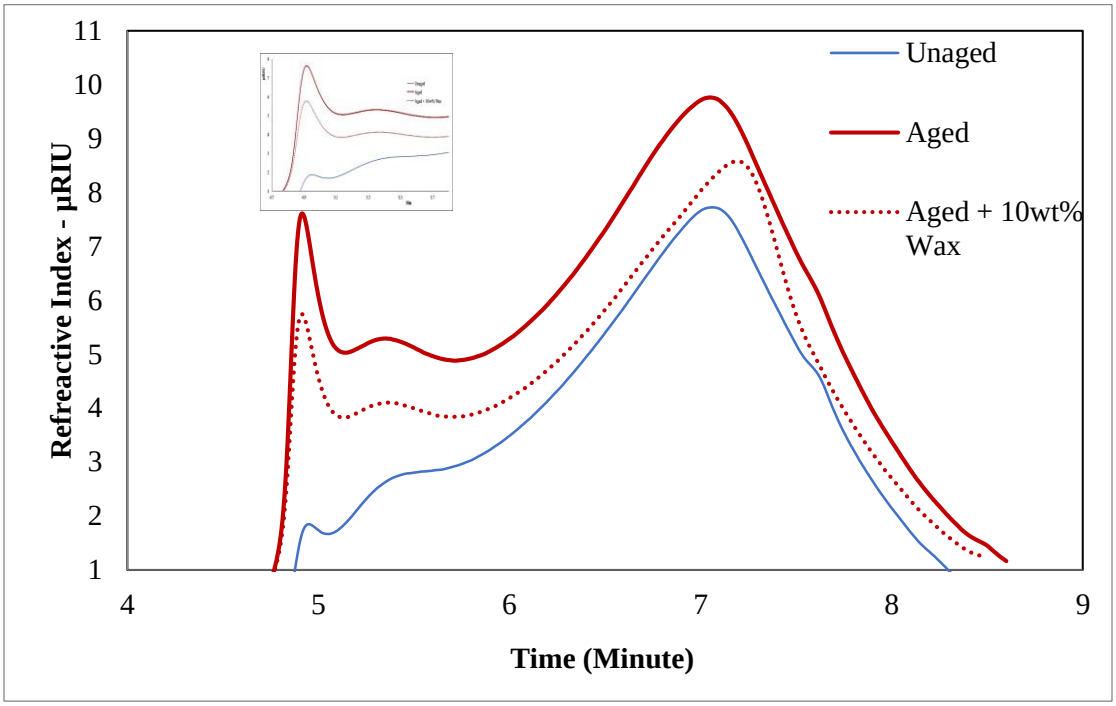

Figure 3.7 Cumulative Percentage Area of Refractive Index

Table 3.1 SEC test results for unaged bitumen, aged bitumen, and aged bitumen+10%wax.

Name of sample	Cumulative% (start of slice to 5.8 minutes)
Unaged	155.47
Aged	256.66
Aged + 10wt% Wax	226.02

3.5 Paraffin Wax and Oxidized Asphaltene Molecular Interaction

Molecular dynamics simulation (MDS) was performed on a system at equilibrium state composed of oxidized asphaltene, paraffinic wax, and methanol as a solvent, using Large-scale Atomic and Molecular Massively Parallel (LAMMPS) software in MedeA® environment version 2.2 to investigate the interaction of paraffinic wax molecules on oxidized asphaltene molecules. The model was built in the MedeA® environment using the molecular builder. This study used the PCFF+ force field, which is an extension of the PCFF force field. It includes a Lenard-Jones 9-6 potential for intermolecular and intramolecular interactions and specific stretching, bending, and torsion terms to involve 1-2, 1-3, and 1-4 interactions .

3.5.1 Methods of Analysis

In this study, to study the effect of the presence of wax molecules on the self-association or stacking of oxidized asphaltene molecules, the change in interaction energy and stacking distance of a dimer was measured. The interaction energy of an oxidized asphaltene dimer is a measurement of the thermodynamic stability. The interaction energy (E_{int}) can be calculated by subtraction of the total energy of the complex from the sum of the fragments' energy (Equation 4). This method is widely used in other research (Liu et al. 2015; Pahlavan et al. 2016; Silva et al. 2016).

$$\boldsymbol{E_{int} = E_{complex} - \left(\sum E_{fragment}\right)} \qquad \textbf{Equation 3.1}$$

To further investigate the effect of paraffin wax on the self-interaction of oxidized asphaltene molecules, the average aggregation size of oxidized asphaltene molecules induced with different dosages of wax was calculated. The average aggregation size (<*m*>) was determined according to Equation 2 (Ungerer et al. 2014).

The pairwise radial distribution function or RDF (g(r)) was used in the determination of stacking distance between atoms or molecules. In this study, g(r) was calculated between oxidized asphaltene molecules. The most centered carbon atom on polyaromatic sheet of oxidized asphaltene molecules was used to calculate the RDF.

To examine the mobility of wax molecules in an oxidized asphaltene matrix, first a subset of wax molecules was defined and the mean square displacement (MSD) graph was plotted. Referring to the Einstein relation of Brownian motion and the definition of the diffusion coefficient, the value of the diffusion coefficient was measured according to Equation 2.3.

3.5.2 Structure of Oxidized Asphaltene, Paraffin Wax and solvent

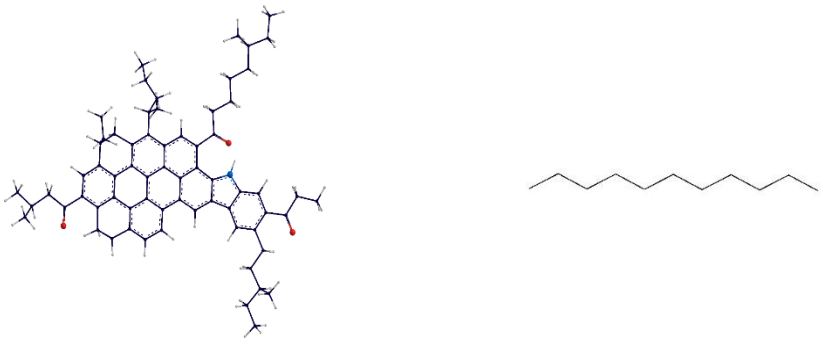

Figure 3.8 Oxidized asphaltene (red atoms are oxygens and blue atom is nitrogen) (Left) and wax ($C_{11}H_{24}$) (Right) molecular structures.

The oxidized asphaltene molecule used in this study was proposed by our research group; the molecule's properties and structure were developed recently. It is an oxidized asphaltene-pyrrole including 3 carbonyl groups placed at the most probable locations of the structure (Pahlavan et al. 2017). The wax model used in this study as an elementary unit of doped wax is the n-C_{11} paraffin wax that is a polymethylene sequence of –(CH2)- that regularly stacks in layers.

The chain length selected for this research was n-$C_{11}H_{24}$, which has been used before for understanding the interactions between wax and unoxidized asphaltene (Pahlavan et al. 2016). The selected wax structure may have a shorter length than the ones actually used for doping bitumens, but it helps with regard to the limitations on simulation size and computational cost on simulations that can be conducted. The proposed structures for oxidized asphaltene and n-paraffin wax are shown in Figure 3.8.

In this study methanol solvent was used to provide an aggregation effect on oxidized asphaltene molecules. In most asphaltene related researches, n-heptane is the selected solvent. However, in this study, since the effect of n-C_{11} is of interest, the solvent needed to have a different chemical structure than an aliphatic chain hydrocarbon. Otherwise, the effect of wax molecules will be overlooked.

The geometry of the system of molecules goes through a simple force field minimization and force field dynamics to ensure that none of the atoms are too close to each other.

3.5.3 Simulation Method

The interaction energy of a dimer of oxidized asphaltene was studied using a two-stage LAMMPS. The first stage started with an NVT at a high temperature (800K) for 100ps and an NPT with a high pressure (200 atm) for 500 ps, both annealed to 298.15 K(25°C) and 1 atm to shake the system and prevent trapping at local minimum energy states. The second stage of the two-stage LAMMPS was started with an NVT (constant number of atoms, volume, and temperature) ensemble with a temperature of 298.15 K(25°C) followed by an NPT (constant number of atoms, pressure, and temperature) ensemble with a temperature of 298.15 K(25°C) and a pressure of 1atm. The ensemble was composed of two oxidized asphaltene molecules and 600 molecules of methanol as solvent. Methanol was chosen because of its tendency to aggregate oxidized asphaltenes. The NVT duration was 2 nanoseconds(ns) to reach an equilibrated state for atomic and molecular configuration, followed by an NPT simulation for 30 ns at 298.15 K(25 °C) and a pressure of 1atm. To measure the effect of wax on the interaction energy of oxidized molecules, another simulation was performed with the same procedure except for one change: the replacement of 6.5 wt% of methanol solvent with wax molecules. For outcomes, the interaction energy and stacking distance of oxidized asphaltene dimers were measured with and without the presence of wax. An oxidized asphaltene dimer was considered stacked when 50 percent or more of the polyaromatic area was overlapped, which is observable by rotating the configuration around the axis normal to the tangent plane. The stacking distance was measured between the closest points of molecules.

To better understand the effect of wax on the self-association formation of nanoaggregates of oxidized asphaltene molecules, an ensemble of 17 oxidized asphaltenes, 2000 methanol molecules and a different number of wax molecules equal to 1%,3%, 5% and 10% by weight fraction of oxidized asphaltene was built. The simulation was performed in two stages with two LAMMPS. The first LAMMPS stage was exactly like the previous method, while the second stage started using an NVT simulation of 2ns follow up by an NPT simulation of 10 ns, both at 298.15 K(25°C) and 1 atm. The diffusion analysis was conducted over 1ns for the wax subset. To have a better understanding of the computational cost, second stage of LAMMPS in simulation was done in 947481seconds (approximately 74s for each step)

The short-range interactions were calculated directly, and long-range interactions were computed with the particle-particle-particle mesh (PPPM) method. The first-stage molecular calculations were performed initializing with an energy minimization at constant volume using the conjugate gradient method. For the purpose of this study, a Nose-Hoover thermostat and barostat was used to maintain constant temperature and pressure during the simulation. Non-bonded interaction terms were calculated with a simple cutoff of 9.5 Å. The matrix of methanol, oxidized asphaltene, and wax was started with a low average density for both simulation methods to avoid molecular overlaps. In the current study, all the wax molecules were considered as one subset of the whole system, and the mean square displacement was calculated for this subset.

3.5.4 Results and analysis

3.5.4.1 Effect of Wax on Self-Association of Oxidized Asphaltene

The geometric conformation and stability of an oxidized asphaltene dimer in methanol solvent was studied. For comparison purposes, two ensembles were studied: one with methanol only, and one contained wax equal to 6.5 wt% of solvent. The solvent was replaced with wax (instead of just adding wax to the system) to keep the mass ratio equal in both configurations. Figure 3.9 illustrates the final configuration of the simulation (solvent molecules are hidden for clarity). The procedure was explained earlier in the methods section. The stacking distance (closest point of polyaromatic sheets) and the interaction energy were calculated and are presented in Table 3.2. The results for the interaction energy and stacking distance show that the presence of wax molecules (or n-alkanes in general) promotes dimerization of oxidized asphaltene molecules. The interaction energy of an oxidized asphaltene dimer is showing that the dimer that is formed in the presence of wax molecules is more stable than the one formed in undoped solvent. The stacking distance also shows the same trend; its value is lower when wax molecules are around asphaltene molecules. These results show that wax by itself doesn't have a peptizing effect on oxidized asphaltene molecules, because wax brings an oxidized asphaltene dimer to a lower energy state and stabilizes it.

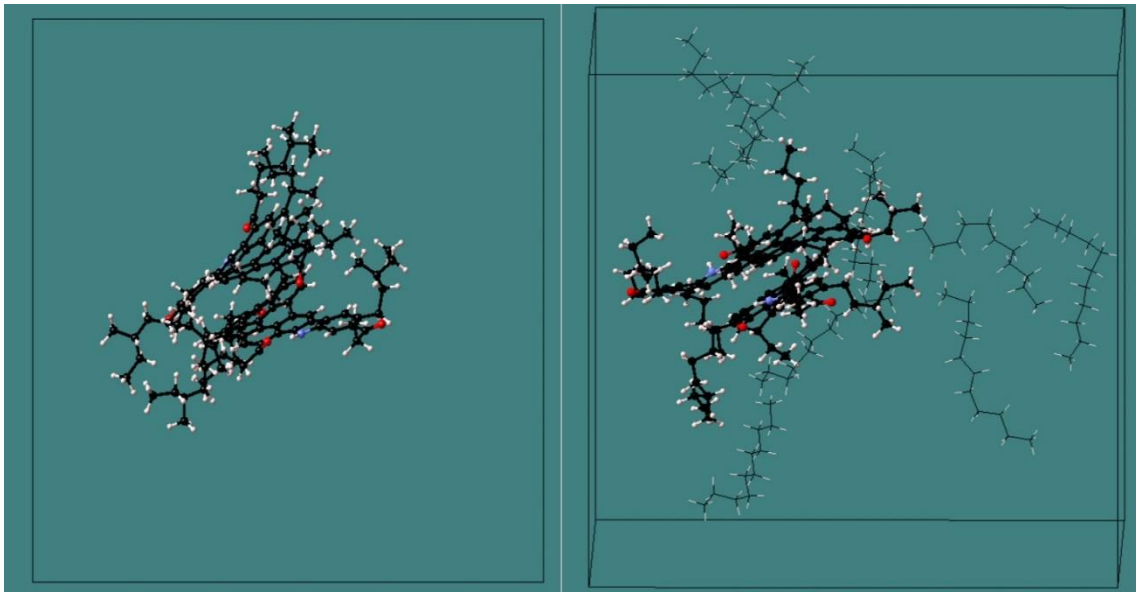

Figure 3.9 The final configuration of a dimer of oxidized asphaltene in methanol solvent: (a - left) without wax, (b - right) with the presence of wax.

Table 3.2 Interaction Energy for Oxidized Asphaltene Dimer and Stacking Distance Without and With the Presence of Wax

Measurement	Oxidized asphaltene dimer without wax in solvent	Oxidized asphaltene dimer with 6.5 wt% of solvent replaced with wax
Interaction energy (kJ/mol)	-15	-58
Stacking distance (Å)	3.267	3.166

To evaluate the effect of n-paraffin wax on the formation of nanoaggregates of oxidized asphaltene, a system of oxidized asphaltene molecules, wax molecules, and methanol as solvent was studied. Each ensemble was composed of 2000 molecules of methanol, 17 molecules of oxidized asphaltene, and 1 to 10 molecules of paraffin wax as a weight fraction of the oxidized asphaltene molecules (1%, 3%, 5%, and 10% of oxidized asphaltene molecules weight fractions). The simulation procedure was elaborated in the simulation methods section. The results of the number of formed nanoaggregate and the average aggregation size are shown in Figure 3.10. The results show a reduced size of aggregation (number of molecules forming a nanoaggregate) after adding wax to the system of oxidized asphaltene in solvent. Although the results show a general reduction in size, a specific trend was not observed. The results also show that by adding wax to the system, oxidized asphaltene molecules pack in a smaller size of nanoaggregates but nanoaggregates become more frequent.

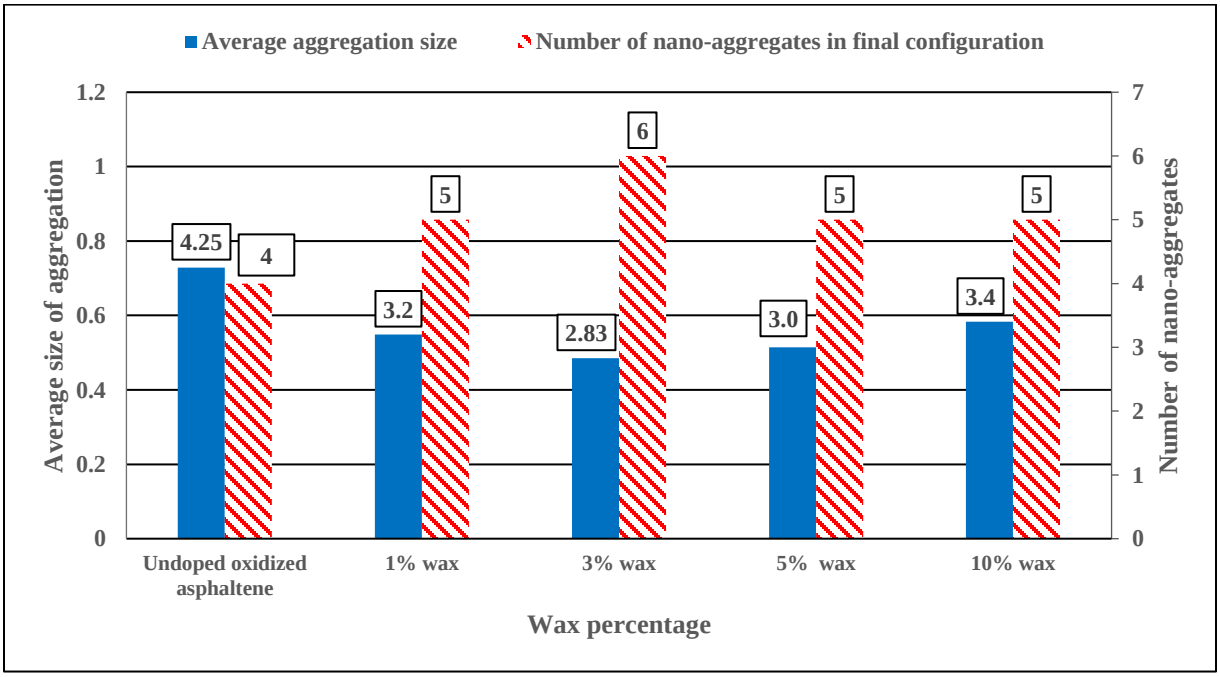

Figure 3.10 Average aggregation size (number of molecules forming a nano-aggregate) and number of nano-aggregates in final configuration versus wax weight fraction of oxidized asphaltene in methanol solvent at 298.15K (25°C).

3.5.4.2 Radial Distribution Function (Pair Correlation Function)

To obtain better insight into the aggregation of oxidized asphaltene molecules with and without presence of wax molecules, the radial distribution function (RDF), g(r), was calculated for the system with just oxidized asphaltene and another with 10 wt% wax relative to asphaltene portion. Figure 3.11 illustrates the results of the RDF analysis. The most centered carbon atom of polyaromatic sheet of oxidized asphaltene molecules was selected as a subset to calculate RDF. The results show that addition of wax content

results in higher probability of stacking of oxidized asphaltene molecules at lower distance. The intensity of occurrence of π-π stack of oxidized asphaltene molecules (first peak) at distance of 4.6 Å is higher in presence of wax molecules compared to the ensemble without wax which is aligned with results of interaction energy. The second peak may represent the T-shaped stacking of asphaltene molecules which occurs at 7.3 Å.

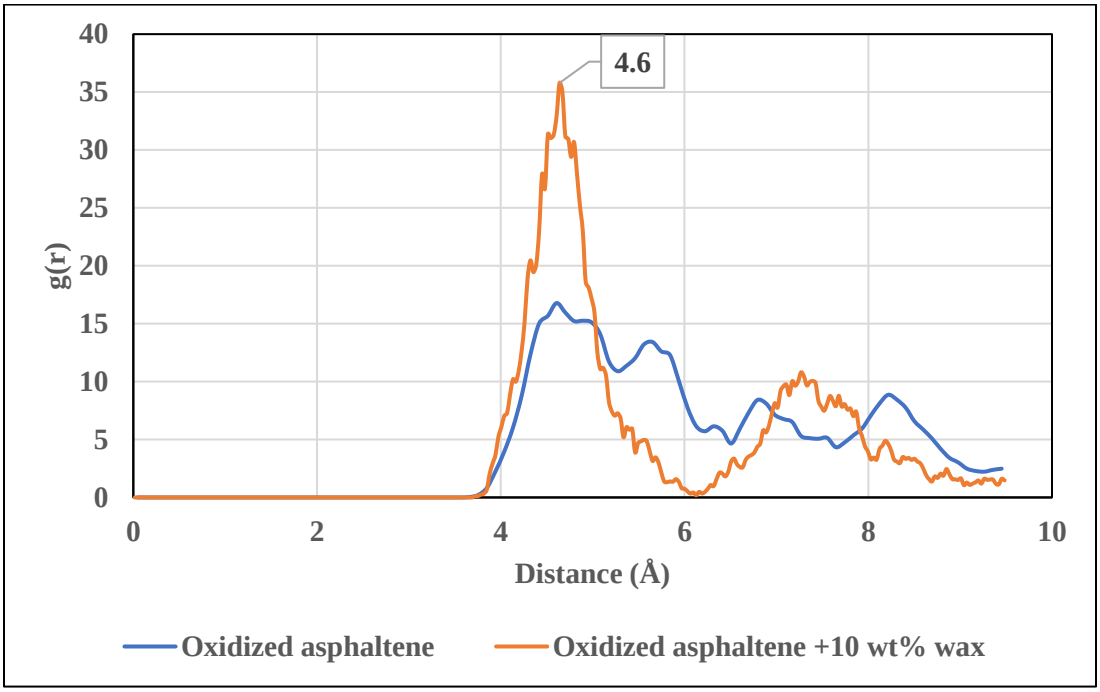

Figure 3.11 Oxidized asphaltene molecules g(r) after 10 ns simulation time in methanol solvent at 298.15 K (25°C).

3.5.4.3 Diffusion Analysis

Using Equation 2.3, the mean squared displacement (MSD) of the wax subset was calculated for 1ns to evaluate the diffusion coefficient of the wax molecules in an ensemble

of oxidized asphaltene and solvent. The purpose of this analysis was to study the effect of an increase of wax concentration on the diffusion of wax molecules into the oxidized asphaltene matrix in solvent. The results of the diffusion coefficient are shown in Table 3.3. The results indicate that the diffusion of wax molecules increases as the wax concentration increases. This can be attributed to the alteration of aggregates size due to presence of wax. Accordingly, the diffusion coefficient results are in-line with the trend observed for the change of nanoaggregate size as the wax content increases. It was shown that nanoaggregates size decreases 20% when wax content increases from 0% to 10%. In the same token, it was observed that by increasing the wax concentration from 1% to 10%, the diffusion of wax increases by over 100%.

Table 3.3 Diffusion Coefficient and Calculated Uncertainty of Wax Molecules Within the Wax and Oxidized Asphaltene Matrix in Solvent at 298.15 K (25°C) (10^{-5} cm^2/s)

Wax concentration	**1%**	**3%**	**5%**	**10%**
Diffusion coefficient	0.632	0.640	1.115	1.473
Uncertainty	0.022	0.0078	0.0051	0.0078

3.6 Summary

Using two perspectives (rheology and molecular interaction), this chapter evaluated the effects of n-alkane paraffin wax doped into aged bitumen. Paraffin wax has previously shown good results as an additive to aged bitumen that can improve the workability of the

asphalt mixture along with lowering the mixing and compaction temperatures of unaged and high RAP contained asphalt. This study also provided further insights on the mechanisms of interaction between n-paraffin wax and oxidized asphaltene molecules that has been shown to play an important role in bitumen rheology. These are the results from both the rheology experiments and the molecular simulations:

- Viscosity results from the RV test show that at high temperature, the viscosity decreases as more wax is added to the aged bitumen.
- The complex modulus decreased as the wax concentration increased. This increase is more distinct with a wax content of more than 3%. The complex modulus results show an overall softening effect (at temperature ranges of 10-76 ^{o}C) as wax content increased. Observed softening effect at high and intermediate temperature may be attributed to enhanced dimerization of asphaltene while reducing size of asphaltene nano-aggregates in the matrix.
- Based on molecular dynamics simulation results, the interaction energy of the oxidized asphaltene dimer reached a lower state after replacing 6.5 wt% of methanol solvent with paraffinic wax molecules. Furthermore, the $\pi-\pi$ stacking distance of oxidized asphaltene molecules decreased from 3.267Å to 3.166Å. This shows that paraffinic wax molecules promote dimerization of oxidized asphaltene molecules.
- Furthermore, the average aggregation size of oxidized asphaltene molecules decreased 20% with an increase of wax concentration from 0% to 10% in studied ensembles. This shows the ability of wax molecules to prevent the formation of

nanoaggregates of oxidized asphaltene when they have enough mobility. This phenomenon was observed in size exclusion chromatography at which addition of wax resulted in smaller particles in oxidized bitumen.

- Moreover, the diffusion coefficient of the paraffin wax molecules increased with increasing wax concentration. The results show an increase of over 100% when the wax content increases from 1% to 10%. This can be attributed to molecular conformation and relative change of nano-aggregate size in presence of wax.
- The radial distribution function of oxidized asphaltene molecules in studied ensembles containing 0 wt% and 10 wt% of wax (relative to oxidized asphaltene portion) showed the first peak appeared at 4.6 Å with a higher intensity in presence of wax. This suggests that addition of wax promotes higher interactions between oxidized asphaltene monomers (dimerization) as it was observed with interaction energy change but less formation of nano-aggregates due to intrusion of paraffinic wax molecules which is observed in average aggregation size and diffusion coefficient).

Following conclusion were derived from laboratory experiments at temperature range for which simulations could not be performed due to extensive computational time requirement:

- The stiffness results of the aged bitumen measured using a bending beam rheometer (at temperature of -12 ^{o}C) show a consistent increase by increasing the wax content of aged material. The ability to relax stress (known as the m-value) decreased with an increase of wax content in aged bitumen.

- The fracture energy of the aged bitumen, measured with a direct tension test (at temperature of -12 ^{o}C), decreased after adding paraffin wax. This also resulted in lower ductility of the aged material that continued to decrease with increasing wax percentage.

The crossover temperature of aged bitumen shows a significant increase compared to that of unaged bitumen. Adding wax does not have much of an effect on this property of bitumen. The results show a decreasing trend when 1% and 3% wax is added to aged asphalt, with a sudden increase (to a temperature higher than that of aged bitumen without wax) for 5% and 10% wax-doped asphalt samples.

4 EFFECT OF WAX-BASED ADDITIVES ON THERMOMECHANICAL CHARACTERISTICS OF OXIDATIVE AGED BITUMEN

4.1 Introduction and Literature Review

Bitumen consists of millions of different molecules including several straight-chain hydrocarbons such as wax (Gawel and Czechowski 1998; Redelius 2004). During the distillation of crude oil, the high boiling points of the wax components (up to 600 ^{o}C, depending on chain length) typically cause the wax components to remain in the residue of the refinery; this residue is referred to as bitumen (Kane et al. 2003; Musser and Kilpatrick 1998). One of the wax components commonly found in bitumen is paraffin wax, which refers to the group of n-alkanes with no or few branches and which are gas for n less than 5, liquid for n between 5 and 17, and solid for n greater than 17 (Gawel and Czechowski 1998).

It should be noted that paraffin wax is a component of several warm-mix additives, recycling agents, and rejuvenators. Use of a warm mix has been effective in reducing the environmental impact of pavement construction by lowering the mixing and compaction temperatures and extending the construction season (Chowdhury and Button 2008; Edwards et al. 2006; Hanz et al. 2010; Kim et al. 2013; Samieadel et al. 2017). The increased use of warm mix in the asphalt industry leads to increased use of wax-based additives, which are components of many commercial warm-mix additives. In addition, during oxidative aging of bitumen, the more reactive components of asphalt such as asphaltene and resin react with oxygen, but saturates such as paraffin wax remain intact

due to their low reactivity; the result is an increased relative ratio of saturates to other components (Pahlavan et al. 2018). This in turn leads to disturbing the bitumen's colloidal balance and increasing its stiffness and susceptibility to fatigue cracking (Arega et al. 2011). Several studies have been conducted to investigate the evolution of the rheological properties of warm-mix asphalts containing paraffin wax (Akisetty et al. 2009; Banerjee et al. 2012). However, the underlying molecular level interactions that control the rheological evolution have not been unveiled. Moreover, many rejuvenators that attempt to restore aged bitumen's original properties contain paraffinic wax or n-alkane structure molecules. Waste engine oil, paraffin wax, waste cooking oil, and paraffinic-based oil have been used as rejuvenators for aged bitumen (Chen et al. 2014; Mogawer et al. 2015; Moghaddam and Baaj 2016; Zaumanis et al. 2013). Therefore, there is a need for in-depth understanding of the effect of paraffin wax on bitumen's molecular conformation and packing, which in turn alters bitumen's thermo-mechanical properties and ultimately pavement performance.

Based on the polarity of molecules in bitumen, four categories of molecules are defined and referred to as the SARA fractions: saturates, aromatics, resins, and asphaltenes. Among the four SARA fractions, asphaltenes are known to have a significant role in bitumen's rheological properties (Fischer et al. 2014). Asphaltenes consist of molecules with polycyclic aromatic cores with four to ten fused rings surrounded by saturated hydrocarbon aliphatic chains; asphaltenes are insoluble in n-heptane and have an overall molecular weight of 500 to 1000 g/mol (Pahlavan et al. 2018; Pomerantz et al. 2015). One of the interactions between asphaltene molecules is known as a π-π interaction, which may

appear between delocalized π electrons (Hunter and Sanders 1990; Redelius and Soenen 2015). The π-π interactions are one of the most important interactions for polar molecules such as asphaltenes, since they directly affect the physical properties of bitumen (Mullins 2010; Redelius and Soenen 2015). The strength of such interactions increases as the number of fused aromatic rings increases. Thus, the interactions of asphaltene molecules are stronger than those of resin molecules having a lower number of aromatic rings.

During the aging process, the reaction with oxygen increases the polarity of bitumen molecules, causing stronger polar interactions as well as increasing the aromaticity, which increases π-π interactions (Pahlavan et al. 2018; Redelius and Soenen 2015). The formation of polar functional groups on asphalt fractions has been introduced as one of the dominant reasons for molecular agglomeration (Pahlavan et al. 2018). Increases in nanoaggregates and overall asphaltene content are characteristics of an oxidized bitumen (Le Guern et al. 2010; Pahlavan et al. 2018; Pahlavan et al. 2018).

The presence of wax in most virgin bitumen has shown a preventive effect on the aggregation of asphaltene molecules, with a consequent decrease in the viscosity and stiffness of the bitumen (Pahlavan et al. 2016; Samieadel et al. 2017) at high temperature. The results of the latter study provide insight into the effect of wax on virgin bitumen, as is the case when wax-based warm-mix additives are used in virgin bitumen. The promotion of using recycled asphalt pavements increases the amount of aged bitumen that is incorporated into pavement construction, exposing the aged bitumen to wax molecules

either from warm-mix additives or recycling and rejuvenating agents. Thus, there is a need to understand how aged bitumen interacts with wax molecules.

Therefore, this paper examines the effect of wax on the aggregation of molecules of aged bitumen and the consequent effect on the bitumen's thermomechanical properties. To study the effect of wax on the rheological properties of aged bitumen, a multiple stress creep recovery (MSCR) test and a bending beam rheometer test were conducted, to characterize the effect at both intermediate and low temperatures. To illustrate the tendency to crystallization of paraffin wax in most aged bitumen, X-ray diffraction was performed on bitumen samples doped with different wax dosages. Differential scanning calorimetry and thermogravimetric analysis were conducted to illustrate wax's effect on the thermal properties of aged bitumen. Molecular dynamics simulation was used to investigate the intermolecular interactions of paraffin wax with stacked and agglomerated oxidized asphaltene molecules. The result of this study helps to understand the effect of paraffin wax on aged bitumen’s rheology, thermal properties, and the connection with the interactions at nano-scale, to better comprehend any improvement or degrading effect on bitumen performance from the use of wax-based additives and modifiers.

4.2 Materials and Methods

The aged bitumen used in this study was PG 64-22. The virgin bitumen was aged in the laboratory and doped with 1, 3, 5 and 10% paraffin wax by the weight of base aged bitumen. For the aging process, the bitumen was initially aged using a rolling thin-film oven (RTFO) (ASTM D2872-12e1 2012) followed by a pressure aging vessel (PAV)

(ASTM D6521-13 2013). An asphalt sample was aged a total of 40 hours (twice the standard time) using PAV. (This process is referred to as 2XPAV.) According to the literature, 2XPAV better represents recycled pavement asphalt exposed to long-term aging in the field (Bowers et al. 2014). The wax that was used in this study was paraffin wax P31 (CAS number: 64742-51-4), with melting point of 53 to 57°C, acquired through Fischer Scientific. The wax was introduced to bitumen at 1, 3, 5, and 10 wt% dosage by the initial weight of the aged bitumen and was blended by hand for 5 minutes at 135 °C.

4.2.1 Bending beam rheometer (BBR)

BBR test results were used to calculate stiffness and stress relaxation capability, referred to as the m-value of the specimen. The lower of the two temperatures corresponding to a stiffness of 300 MPa and an m-value of 0.30 is called critical cracking temperature, based on ASTM D6648 (ASTM D6648 2016). The difference between the two temperatures (ΔT_c) has been related to the fatigue performance of bitumen by several researchers (Anderson et al. 2011; Menapace et al. 2018).

To conduct the test, bitumen samples were prepared by pouring the bitumen into aluminum molds 12.5mm wide, 127mm long, and 6.25mm thick. The samples were allowed one hour to cool at room temperature. Afterwards, the samples were placed in a freezer for five minutes before demolding. A constant load of 980 mN was applied at the middle point of each specimen as the deflection was measured continuously for 5 minutes.

4.2.2 Multiple stress creep recovery (MSCR)

The MSCR test was performed following the AASHTO T350-14 (AASHTO T 350-14 2014) specification, in which the bitumen is subjected to 10 cycles of stress and recovery of 1 and 9 seconds, respectively, at two stress levels of 0.1 and 3.2 kPa at 64°C. Before the start of the test, samples were subjected to a pre-load cycle. Afterwards, non-recoverable creep compliance (known as J_{nr}), the recovery percentage, and the recovery difference between stresses of 0.1 and 3.2 kPa was determined.

4.2.3 Differential scanning calorimetry (DSC)

DSC analysis was performed using a TA Q2000 from TA Instruments to determine the glass transition temperatures (Tg), melting temperature (Tmp), and crystallinity of aged bitumen. Samples of approximately 5-7mg were placed in hermetic Tzero aluminum pans. The modulation amplitude was set to ± 1.00 °C every 60 seconds. Ramps of 3.00 °C/min were applied to all three cycles. The first heating cycle was from – 80 to 160 °C, followed by a cooling cycle down to -80 °C, and finally followed by a second heating cycle from -80 °C to 160 °C. The second heating cycle was used to determine the desired thermal properties to standardize the results with a uniform cooling ramp. The melting temperature was determined using the peak maxima function in the known wax melting temperature range. The degree of crystallinity was determined using a commercial heat of fusion value of 220 J g^{-1} for paraffin wax.

4.2.4 Thermogravimetric analysis (TGA)

The TGA method was used to investigate the thermal resistance of each sample of aged bitumen, using a TA Q500 from TA Instruments. The measurements were performed from 50-600 ºC with a heating ramp of 10 ºC/min. Samples were placed in platinum pans under a nitrogen blanket with a flow rate of 10 ml/min.

4.2.5 X-ray diffraction (XRD)

XRD was performed on a PANalytical Empyrean diffractometer with CuKα radiation, running at 45 kV and 40 mA in the interval of 3-40°. The samples were placed on an amorphous plate sample holder to capture the crystalline structure of the samples.

4.3 Molecular Dynamics Simulation

A molecular dynamics simulation was performed on a system at equilibrium state composed of oxidized asphaltene, paraffinic wax, and methanol as a solvent medium, using Large-scale Atomic/Molecular Massively Parallel Simulator (LAMMPS) software in a MedeA® environment, version 2.2. The study focused on investigating interactions of paraffin wax molecules and oxidized asphaltene molecules. Wax was introduced to the system of oxidized asphaltene after the formation of nanoaggregates. The model was built in the MedeA® environment using the molecular builder, which allows an interactive, step-by-step construction of polyaromatic units with attached aliphatic chains and pyrrole rings. This study used the PCFF+ force field, which is an extension of the PCFF force field.

"Force field" refers to the functional form of parameters used to calculate the potential and kinetic energy of the system of atoms and molecules. PCFF+ is an all-atom force field designed to provide excellent accuracy on hydrocarbon and liquid modeling from ab initio simulations (Sun et al. 1994; Ungerer et al. 2014; Waldman and Hagler 1993). This force field includes a Lenard-Jones 9-6 potential for intermolecular and intramolecular interactions and specific terms for stretching, bending, and torsion to involve 1-2, 1-3, and 1-4 interactions (Ungerer et al. 2014).

4.3.1 Structure of oxidized asphaltene, paraffin wax, and solvent

The oxidized asphaltene molecule used in this study was a continental structure asphaltene (Pahlavan et al. 2018) containing a large core of poly-aromatic rings (Fischer et al. 2014; Morgan et al. 2010; Wiehe 2008). The selected oxidized asphaltene-pyrrole contains 3 carbonyl groups. The analysis of where the functional groups should be added was based on previous studies on hetero atoms and the molecular weight of asphaltene conducted in Strategic Highway Research Program(SHRP), taking into account the mechanism of the formation of carbonyl groups during oxidation (Figure 4.1) (Jennings et al. 1992; Lesueur 2009).

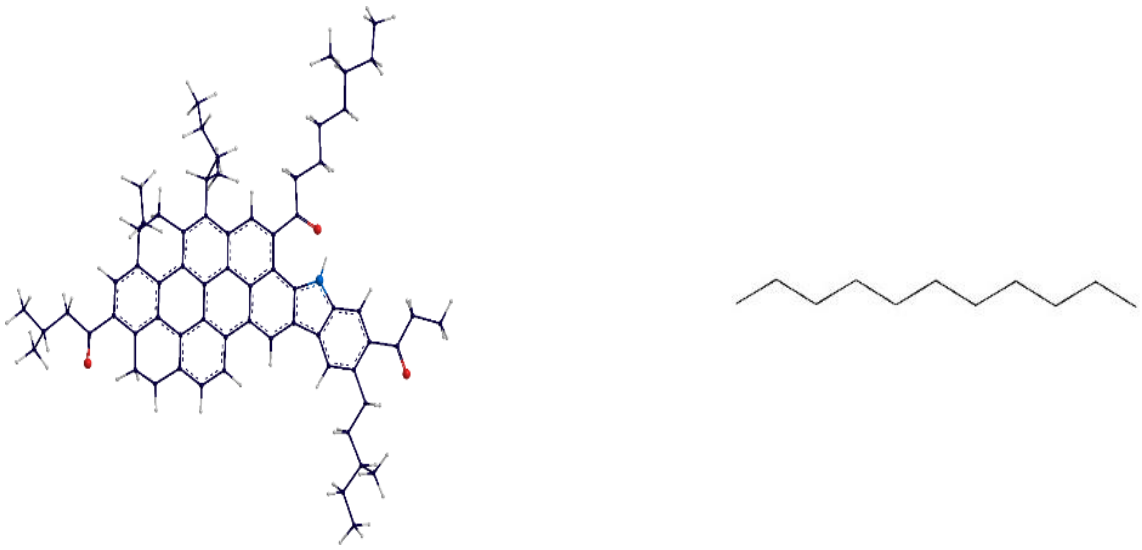

Figure 4.1 Selected structures for molecules involved in the simulation: Left-Oxidized asphaltene (red atoms are oxygen and blue atom is nitrogen); Right-Paraffin wax

The paraffin wax molecule used in this paper is the n-C_{11} paraffin wax that is a polymethylene sequence of -(CH2)- that regularly stacks in layers (Pahlavan et al. 2016). To keep the portion of wax molecules in the range of 1 to 10 wt% of oxidized asphaltene, and to prevent an increase in computational cost, the wax molecule size was chosen to be n-C_{11}. The proposed structures for oxidized asphaltene and n-paraffin wax are shown in Figure 4.1. The solvent medium in this study is methanol, which is known to be able to initiate asphaltene aggregation; this allows examining the extent of aggregation in an ensemble of wax-asphaltene. Furthermore, to study the effect of wax as a straight-chain hydrocarbon, the solvent needed to have a structure different from for the simulation to

better illustrate the effect of paraffin wax on the assembly of oxidized asphaltenes (Painter et al. 2015).

4.3.2 Simulation method

The simulation was composed of a sequence of two LAMMPS stages, starting with energy minimization using the conjugate gradients method at a constant volume with a low average density to avoid molecular overlaps. The first stage started with an NVT ensemble (constant number of atoms, volume, and temperature) at a high temperature (800K) for 100ps, followed by an NPT ensemble (constant number of atoms, pressure, and temperature) at pressure of 200 atm and temperature of 800 K for 500 ps to shake the system and prevent its trapping at a local minimum energy state. The second stage of the two-stage LAMMPS was started with an NVT ensemble with a temperature of 298.15 K (25°C) for 2ns to reach an equilibrium with no pressure on the system, followed by an NPT ensemble with a temperature of 298.15 K (25°C) and a pressure of 1atm for 20ns. During all the stages of simulation, a Nose-Hoover thermostat and barostat (Plimpton 1995) was utilized and the time step was set to 1 fs. The short-range interactions were calculated directly, while long-range interactions were measured with the particle-particle-particle-mesh (PPPM) method. Non-bonded terms were calculated with a simple cutoff of 9.5 Å. The average temperature and pressure during NPT simulations was checked to ensure the system was in equilibrium.

After equilibration of oxidized asphaltenes in methanol, two different percentages of wax with respect to the asphaltene fraction (1wt% and 10wt%) were added to the system,

and the simulation was continued for another 30ns in order to investigate the effect of paraffin wax on self-assembled stacks of oxidized asphaltenes. The average pressure and temperature were monitored during the simulation to ensure the system was in equilibrium. During the simulation, the coordinates for the center of mass of asphaltene molecules were recorded for aggregation study, and the radial distribution function results were calculated for the most-centered carbon atom of oxidized asphaltene molecules. A subset was assigned to wax molecules to track mean square displacement for calculation of the diffusion coefficient over 10ns of simulation.

4.3.3 Methods of analysis

To investigate the effect of paraffin wax on the self-assembled oxidized asphaltene molecules, the average aggregation number of oxidized asphaltene molecules in the presence of wax was calculated. The average aggregation number (g_z) was determined using Equation 4.1 (Goual et al. 2014; Nagarajan 1994; Sengers et al. 2000).

$$\boldsymbol{g_z = \frac{\sum_i n_i g_i^3}{\sum_i n_i g_i^2}} \qquad \textbf{Equation 4.1}$$

where n_i is the number of aggregates containing g_i monomers.

The radial distribution function (g(r)) was calculated for oxidized asphaltene molecules before and after wax was introduced. The results of the radial distribution function represent the most probable separation distance of oxidized asphaltene molecules. The RDF provides a way to visualize the degree of separation between a group of atoms,

which in this study is a subset composed of the most-centered carbon atom of oxidized asphaltene molecules. The RDF g(r) is calculated using Equation 4.2.

$$\boldsymbol{g(r) = \lim_{dr\to 0} \frac{V}{N(N-1)4\pi r^2 dr} \sum_i^N \sum_{j\neq i}^N \delta(r - r_{ij})} \qquad \textbf{Equation 4.2}$$

where V is the volume, N is the number of atoms included in the calculation,

δ is the Kronecker delta function, and r_{ij} is the distance between the two atoms (Levine et al. 2011; Lowry et al. 2017).

The diffusion coefficient can be calculated from the time evolution of the mean squared displacement, $u^2(t)$, using Equation 4.3 (Chitra and Yashonath 1997).

$$\boldsymbol{u^2(t) = \frac{1}{N} \sum_{i=1}^N \frac{1}{(T-t)} \int_0^{T-t} [\vec{r_i}(t+\tau) - \vec{r_i}(\tau)]^2 \, d\tau} \quad \textbf{Equation 4.3}$$

where *T* is the duration of the simulation, and $\vec{r_i}$ is the guest atomic positions.

By fitting a straight line to the points in the closed interval [t_1,t_2], a least squares straight line is obtained. The slope of this straight line is used to compute the diffusion coefficient using the Einstein relation, using Equation 4.4.

$$\boldsymbol{D = \frac{<u^2(t)>}{2dt} = \frac{u^2(t_2) - u^2(t_1)}{2d(t_2 - t_1)}} \quad \textbf{Equation 4.4}$$

where *d* is dimensionality and is equal to 3.

In other words, the diffusion coefficient can be measured using Equation 4.5.

$$\boldsymbol{D = [Slope\ of\ MSD\ curve\ over\ the\ elapsed\ time\ t]/[2d]} \quad \textbf{Equation 4.5}$$

where D is the diffusion coefficient, d is dimensionality, and t is the time over which we are calculating the diffusion coefficient. The unit for a diffusion coefficient is $Å^2$/ps (or 10^{-4} cm^2/s).

4.4 Results and Data Analysis

4.4.1 Critical low temperature

Figure 4.2 shows the critical low temperatures (Tc), which correspond to a critical stiffness and stress relaxation (m-value) of 300 Mpa and 0.300, respectively. The Tc of stiffness did not vary significantly until 10% wax, at which it showed a drastic decrease, indicating significant stiffening of the overall aged bitumen due to the addition of wax. In contrast, the Tc corresponding to m-value was found to be very sensitive to the wax dosage, showing a reduction of about 12 degrees when the wax dosage increased from 0 to 10%. ΔTc is defined as $Tc_{(stiffness)}$ - $Tc_{(m\text{-}value)}$. In Table 4.1, the calculated ΔTc shows an increase in absolute value (a larger negative value), indicating that the stiffness effect becomes more prevalent as the wax concentration increases, while bitumen loses its stress-releasing capacity. It has been reported that the increase in absolute value for ΔTc is correlated to a higher susceptibility to non-load-related cracking of asphalt pavement such as transverse cracking and block cracking (Anderson et al. 2011). This phenomenon is related to bitumen losing its ability to relax stress with an increase of paraffin wax in aged bitumen, as the ΔTc becomes more controlled by the m-value. Other studies also related the higher absolute value of ΔTc to an increase in fatigue cracking, which is a consequence of the embrittlement (loss of ductility) of the bitumen (Bennert et al. 2016). In the current paper,

the bigger gap between critical temperatures of stiffness of 300MPa and m-value of 0.3 is a result of an increase in paraffin wax, which affects the embrittlement of bitumen; this leads to a higher risk of fatigue cracking along with non-load-related cracking, due to aged bitumen's diminishing capability to relax accumulated stress.

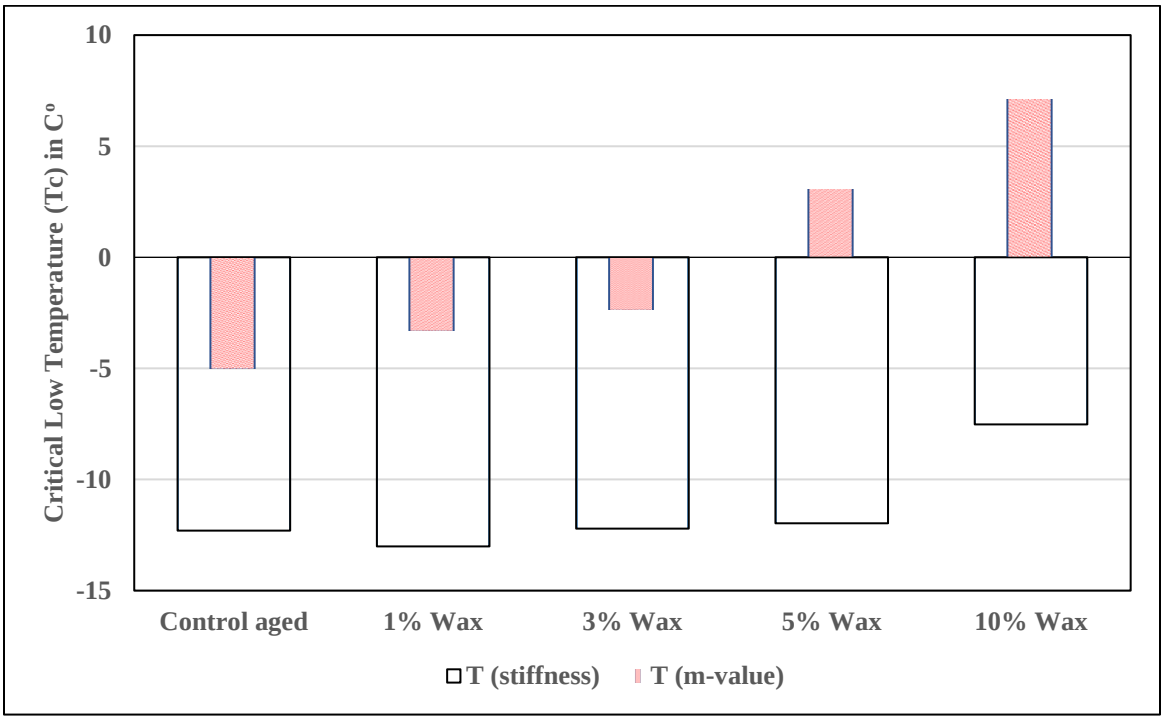

Figure 4.2 Critical low temperatures for stiffness and m-value

Table 4.1 Delta Tc results for control aged and 1, 3, 5, and 10wt% wax-doped aged bitumen

Sample	Delta Tc
Control Aged	-7.30
Aged + 1% Wax	-9.71
Aged + 3% Wax	-9.87
Aged + 5% Wax	-15.04
Aged + 10% Wax	-14.60

4.4.2 Non-recoverable creep compliance

The MSCR results at 64°C are shown in Table 4.2. After aging, the non-recoverable creep compliance, J_{nr}, decreased significantly compared to control asphalt, showing bitumen becoming stiffer due to aging. However, J_{nr} was shown to increase with increasing wax percentage, which shows more residual strain after applying creep stress. This phenomenon can be due to partial melting of paraffin wax, causing a softening effect as wax molecules increase the mobility of asphaltene molecules. In addition, percent recovery shows a continuously decreasing trend as paraffin wax content increases. This can be due to a disturbed network of asphaltene molecules in the presence of wax at high and intermediate temperatures giving rise to its viscous behavior. Previous research showed that the complex modulus and shear viscosity of aged bitumen decreases with an increase in wax content (Samieadel et al. 2018).

Table 4.2 MSCR results for control aged bitumen and 1, 3, 5, and 10wt% wax-doped aged bitumen

Sample	J_{nr} 3.2kPa^{-1}	J_{nr} diff (%)	% Recovery 3.2 kPa^{-1}
Control aged	0.0306	11.9	55.6
Aged + 1% Wax	0.0713	14.8	43.7
Aged + 3% Wax	0.1095	14.4	39.8
Aged + 5% Wax	0.1601	18.0	37.1
Aged + 10% Wax	0.3689	32.8	27.0

4.4.3 X-ray diffraction (XRD)

The results of the XRD analysis showed that the structure of the aged bitumen was primarily amorphous, independent of wax content. In order to experimentally determine the size of the particles detected, the interlayer d-spacing was calculated, using Braggs law (Equation 4.6).

$$n\lambda = 2d \sin \theta \qquad \text{Equation 4.6}$$

where λ is the incident wavelength, θ is the reflection angle,

n is the integration constant, and d is the interplanar lattice spacing (d-spacing).

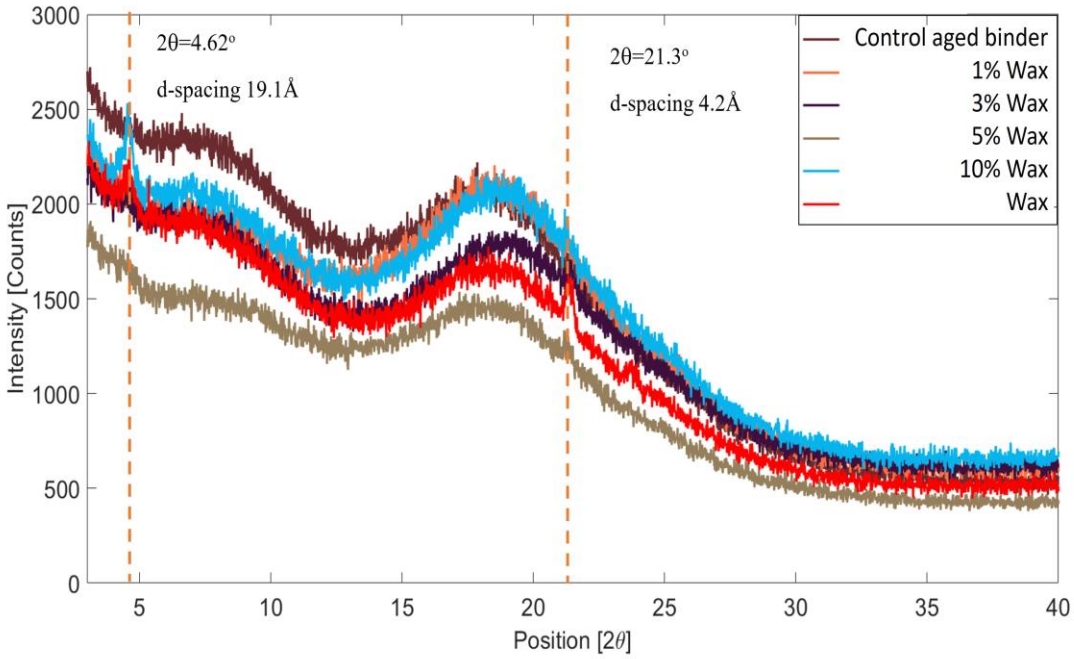

Figure 4.3 XRD results for pure wax, control aged bitumen, and 1% 3%, 5%, and 10wt% wax-doped aged bitumen

Figure 4.3 shows the XRD results for pure wax, control aged bitumen, and aged bitumen doped with different percentages of paraffin wax. A sharp peak appeared at 4.6° for both pure paraffin wax and the aged asphalt doped with 10% wax, with a corresponding d-spacing of 19.1 Å. This peak can be attributed to the formation of lamellar paraffin wax inclusions, which was also shown in previous studies using atomic force microscopy (Pahlavan et al. 2016). The d-spacing between the lamellae is about 20nm when wax is added to the aged bitumen (Pahlavan et al. 2016). Most commercial paraffin wax has a highly ordered structure and therefore would not be amorphous (Żbik et al. 2006). Reported peaks for paraffin wax are around 2θ =21.6° and 2θ = 24.0°, which are attributed

to the diffractions of (110) and (200) crystal planes of monoclinic paraffin (Li et al. 2013; Li et al. 2014; Rao and Zhang 2011). The peak at 2θ =21.33° is clearly observed in aged bitumen doped with 10% wax, corresponding to the wax component. The formation of paraffin wax lamellae is evidenced by the d-spacing of 20nm; this can cause weak points in the bulk of bitumen that can contribute to crack initiation at sub-zero temperatures, where crystal formation is more stringent (Pahlavan et al. 2016).

4.4.4 Glass transition temperature and degree of crystallinity

The heat flow results for paraffin wax show two endothermic peaks that are well-known for petroleum paraffin wax (Figure 4.4). The first peak shows a solid-solid transition in wax crystals; it is closely followed by a melting peak (Luyt and Krupa 2008). A study of glass transition temperature showed that aged bitumen has a higher glass transition temperature (-17.56 ^{o}C) compared to unaged bitumen (-18.07 ^{o}C); this could be due to the loss of volatile, light components of bitumen during aging (Kriz et al. 2008). The addition of wax to aged bitumen led to a reduction in glass transition temperature, with 10% wax-doped specimens having a glass transition temperature nearly 9 degrees lower than the control sample; this can be attributed to the contribution of wax to the maltene phase (a fraction with lower molecular weight and higher mobility) of bitumen. It has been reported that the glass transition temperature is mainly affected by the maltene portion (Lesueur 2009), but the role of asphaltene nanoaggregates cannot be ignored (Samieadel et al. 2018). Glass transition is a phenomenon that occurs in amorphous polymers whose chains are not

arranged in ordered crystals; since pure paraffin wax has a highly ordered crystalline structure, glass transition does not occur in pure paraffin wax.

However, the wax appears to have a dominant effect on melting behavior; 10% wax-doped samples have a melting temperature closer to that of pure wax, as seen in Figure 4.5. With increasing wax content, the heat of fusion for melting also increases, but it is lower than that of pure wax; this suggests the formation of smaller wax crystals when wax is blended into aged bitumen, as shown in Table 4.3 (Qin et al. 2014).

A reduction in glass transition temperature can improve bitumen's rheological properties; the embrittlement of aged bitumen would take place at a lower temperature. However, the formation of wax crystals and a lamellar structure at low temperatures could make the cracking behavior of bitumen be dominated by the bitumen's stiffness more than its relaxation capability, as evidenced by the high ΔT_c in wax-doped bitumen. The formation of a lamellar structure can also promote crack initiation, due to the presence of weak points at the interfaces of a lamellar structure. The latter phenomenon has been studied using a direct tension test and atomic force microscopy (Pahlavan et al. 2016; Samieadel et al. 2018).

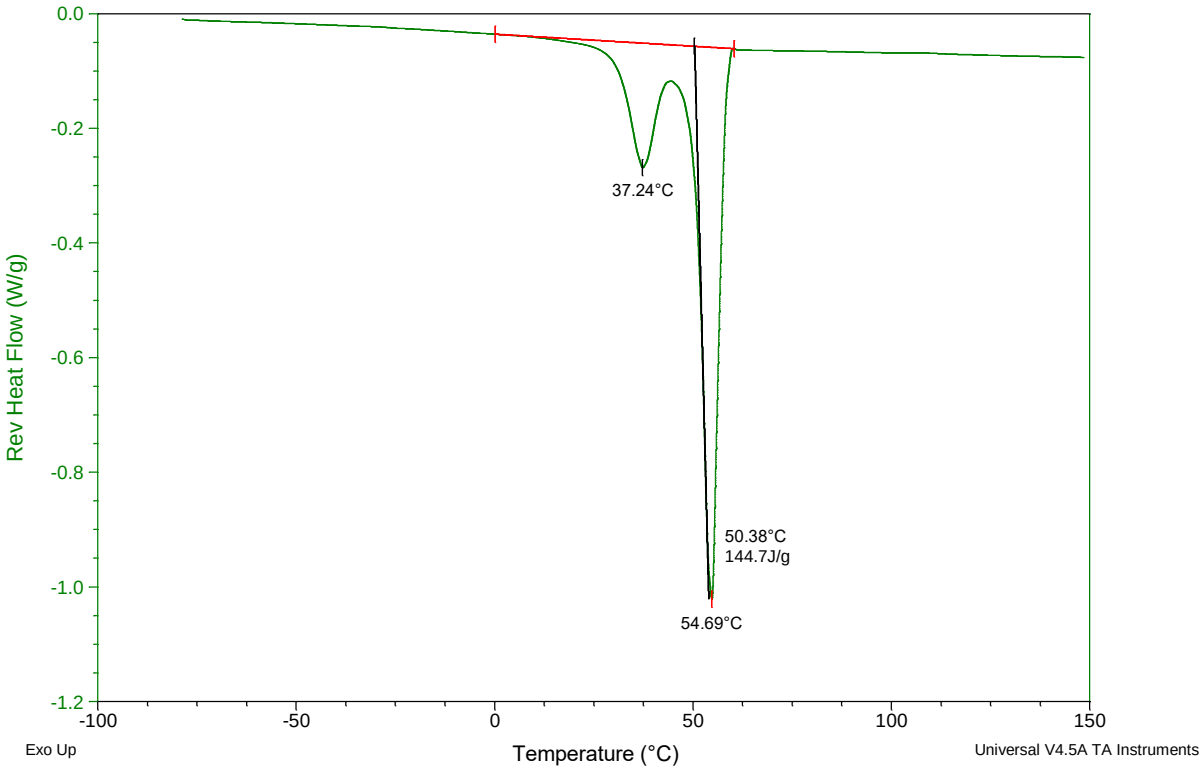

Figure 4.4 Reverse heat flow results for paraffin wax

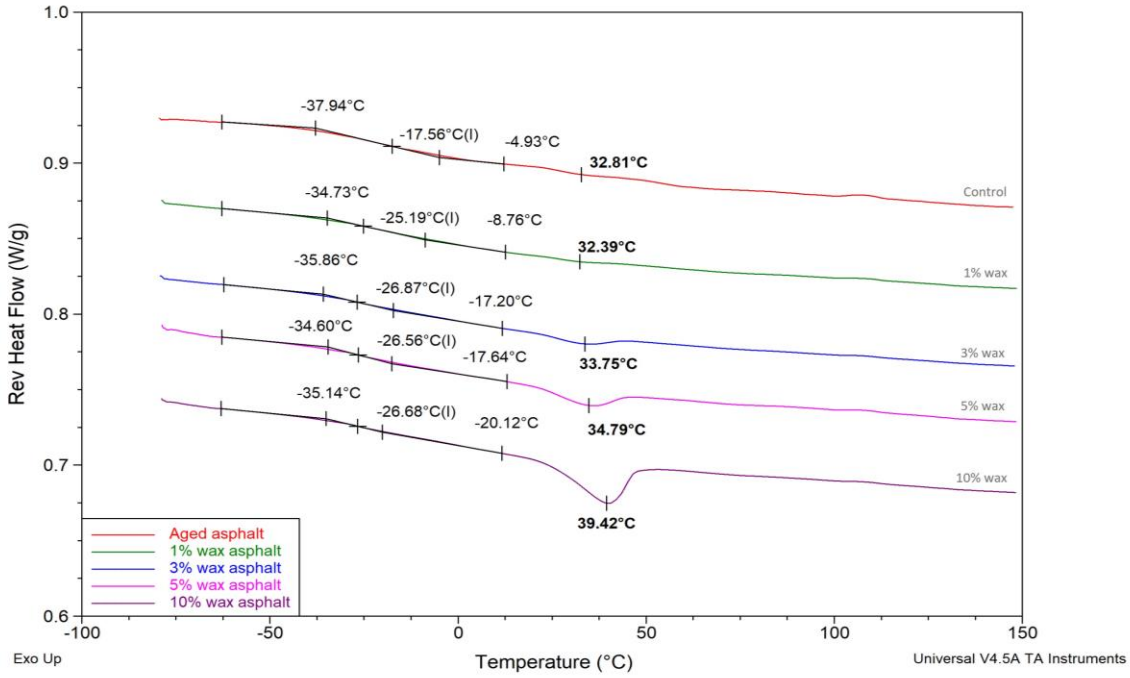

Figure 4.5 Second heat cycle results for control aged bitumen and aged bitumen doped with 1, 3, 5, and 10 wt% paraffin wax.

Table 4.3 Thermal properties based on the second heating cycles measured using a differential scanning calorimeter for control aged bitumen and aged bitumen doped with 1, 3, 5, and 10wt% wax

Property	Control Aged Bitumen	1% Wax	3% Wax	5% Wax	10% Wax	Pure Wax
Glass transition temperature Tg (°C)	-17.56	-25.19	-26.87	-26.56	-26.68	NA
Melting point temperature Tmp (°C)	32.81	32.39	33.75	34.79	39.42	54.69
Measured enthalpy of fusion [J/g]	0.092	0.5643	1.614	3.111	7.982	144.7

4.4.5 Thermal resistance

TGA was used to study the flash point and weight loss curve of each aged bitumen doped with wax. A nitrogen environment was used to ensure that the observed thermal decomposition of specimens was not convoluted by other mechanisms such as oxidation in air. The degradation onset temperatures for unaged and aged bitumen were determined to be 326.9 ^{o}C and 307.9 ^{o}C, with residual masses of 17.24% and 29.7% at 600 ^{o}C, respectively. The lower degradation onset temperature observed in aged specimens compared to unaged specimens can be attributed to the presence of a greater asphaltene content in aged specimens; it has been documented that oxidative aging promotes the conversion of resins and aromatics to asphaltenes, increasing the asphaltene fraction (Sharma et al. 2017; Yu et al. 2014). In addition, the presence of graphene oxide (GO)-like structures in aged asphalt has been reported (Pahlavan et al. 2018). It has also been documented that increase in asphaltenes have a decreasing effect on the thermal stability of bitumen (Firoozifar et al. 2011). Therefore, the relatively higher asphaltene content in aged asphalt can contribute to its having a lower degradation onset temperature compared to unaged asphalt.

Furthermore, all doped specimens had higher degradation onset temperatures than the control sample (Table 4.4). Paraffin wax increased the degradation onset temperature and restricted the decomposition of material, as also documented elsewhere (Ge et al. 2017). This phenomenon is believed to be in agreement with previous studies evaluating

the reactivity of bitumen's components, which showed that the saturates components (such as paraffin wax) have lower reactivity compared to asphaltenes (Mousavi et al. 2016). Thus, wax-doped specimens have a relatively higher amount of components with low reactivity, and their degradation onset temperature is shifted to a higher temperature.

Figure 4.6 shows that even though the degradation onset temperature is shifted to a higher temperature, the residual mass for each doped sample is lower than the control, with residual mass continuously decreasing with an increase in wax percentage from 1% to 5%. This indicates that the presence of wax increases the decomposition of the materials. This can be attributed to the role of wax in breaking asphaltene nanoaggregates into smaller nanoaggregates, exposing a higher surface area to degradation mechanisms. However, the 10% wax-doped specimens showed relatively less degradation than the 5% wax-doped specimens, which could be due to significant crystalline regions formed due to a relatively high wax concentration.

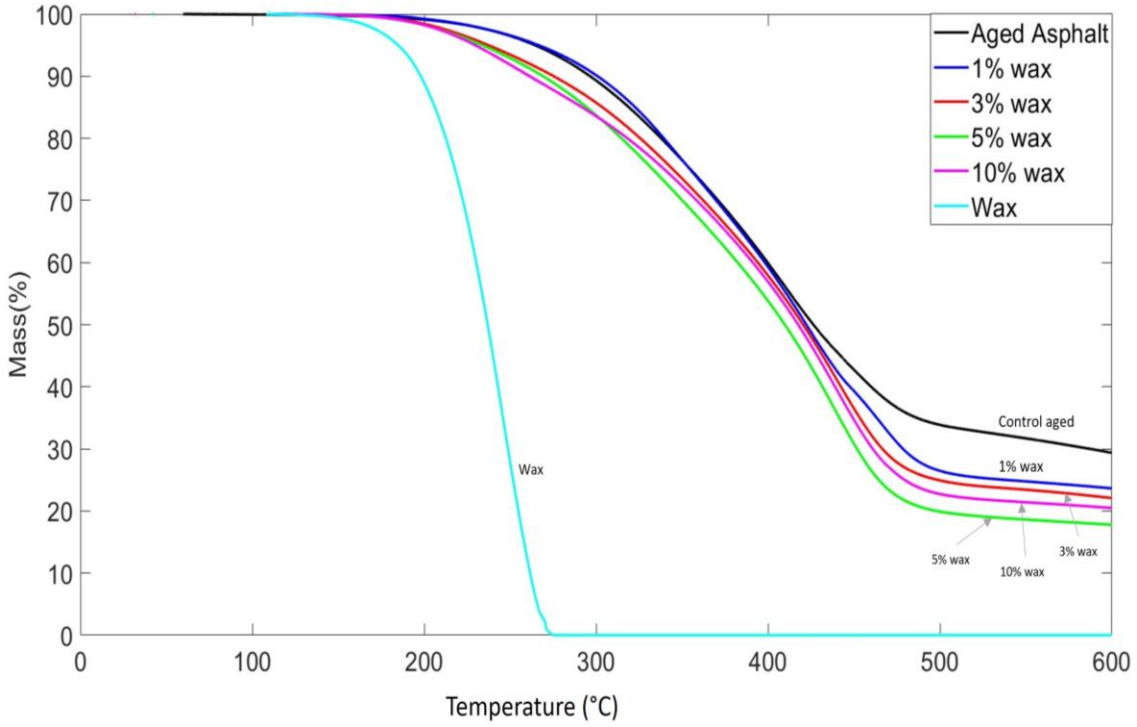

Figure 4.6 Measurements of thermal resistance for wax, control aged bitumen, and aged bitumen doped with 1, 3, 5, and 10wt% wax, using thermogravimetric analysis

Table 4.4 Onset temperature of degradation and residual mass of control aged bitumen and aged bitumen doped with 1, 3, 5, and 10wt% wax, using thermogravimetric analysis

Property	**Control Aged Bitumen**	**1% Wax**	**3% Wax**	**5% Wax**	**10% Wax**	**Pure Wax**
Onset temperature (°C)	307.9	321.6	314.5	309.8	332.9	211.0
Residual mass at 600 °C [w%]	29.7	23.7	22.0	17.9	20.8	0

4.5 Molecular Dynamics Simulation Results

4.5.1 The effect of wax on self-aggregation of oxidized asphaltene

To evaluate the effect of n-paraffin wax on the formation of nanoaggregates of oxidized asphaltene, a system of oxidized asphaltene molecules was equilibrated in methanol solvent for 20ns, and then two different percentages of wax were introduced into the system. The purpose of this simulation is to investigate the effect of straight-chain paraffin wax on post-aging molecular conformations. Figure 4.7 shows the equilibrated asphaltene system before adding paraffin wax molecules. (Solvent molecules have been removed for clarity.)

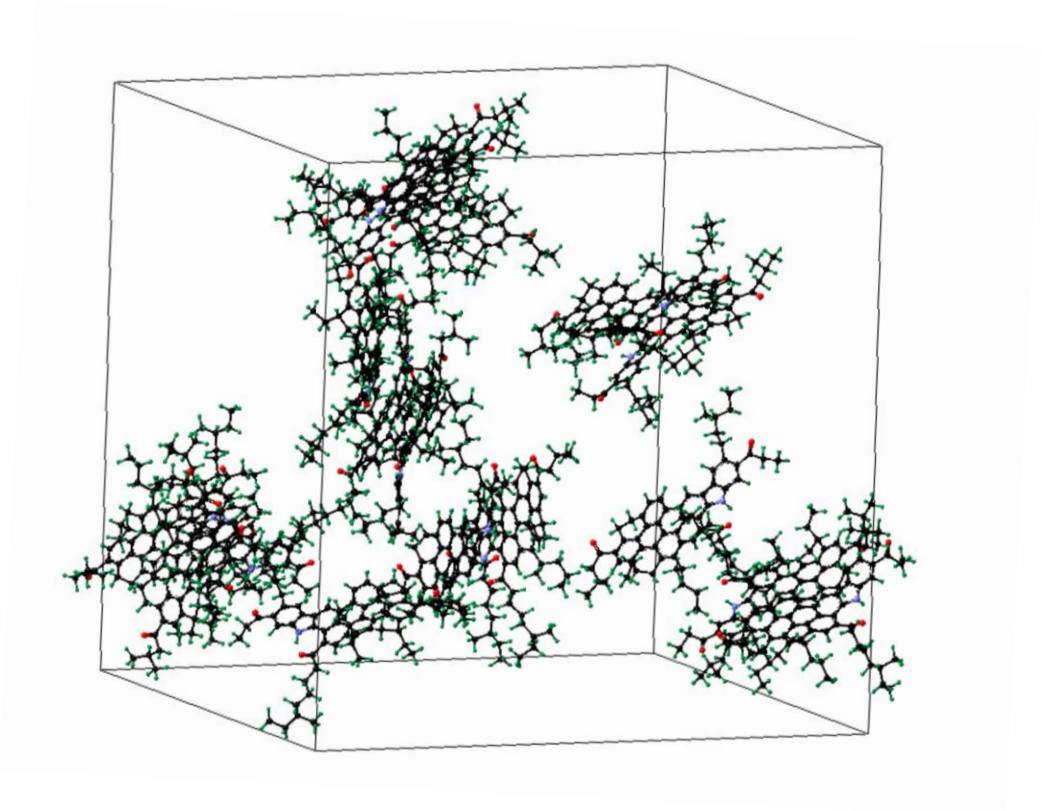

Figure 4.7 Equilibrated system of 17 oxidized asphaltene molecules in methanol solvent after 20ns simulation in an NPT ensemble

To study the aggregation pattern for two extreme cases of asphaltene doped with 1% and 10% wax, after equilibration of oxidized asphaltene molecules in methanol, 1 and 10 paraffin wax molecules with respect to asphaltene mass were added to the system. The distance between each pair of oxidized asphaltene molecules was measured every 50ps during the simulation, using the coordinates of each asphaltene's center of mass. Any two molecules were considered as stacked if the distance between their respective centers of mass was less than 0.85; the aggregation number was defined as the number of molecules

involved in a cluster of stacked molecules (Goual et al. 2014). The Molecular Dynamics (MD) simulations results show that the average aggregation number is reduced by 25% after adding 10% paraffin wax (Figure 8). This phenomenon can be due to the intrusion of paraffin wax molecules into self-assembled stacks of oxidized asphaltene, weakening their π-π interaction. Such a weakening effect can lead to the formation of nanoaggregates with fewer molecules involved in them. This dispersive effect of paraffin wax on oxidized asphaltene can help restore the conformation of asphaltene molecules before aging. This effect of paraffin wax is due to its mobility in the system, which is noticeable at temperatures

around and higher than the melting point of paraffin wax (Samieadel et al. 2018).

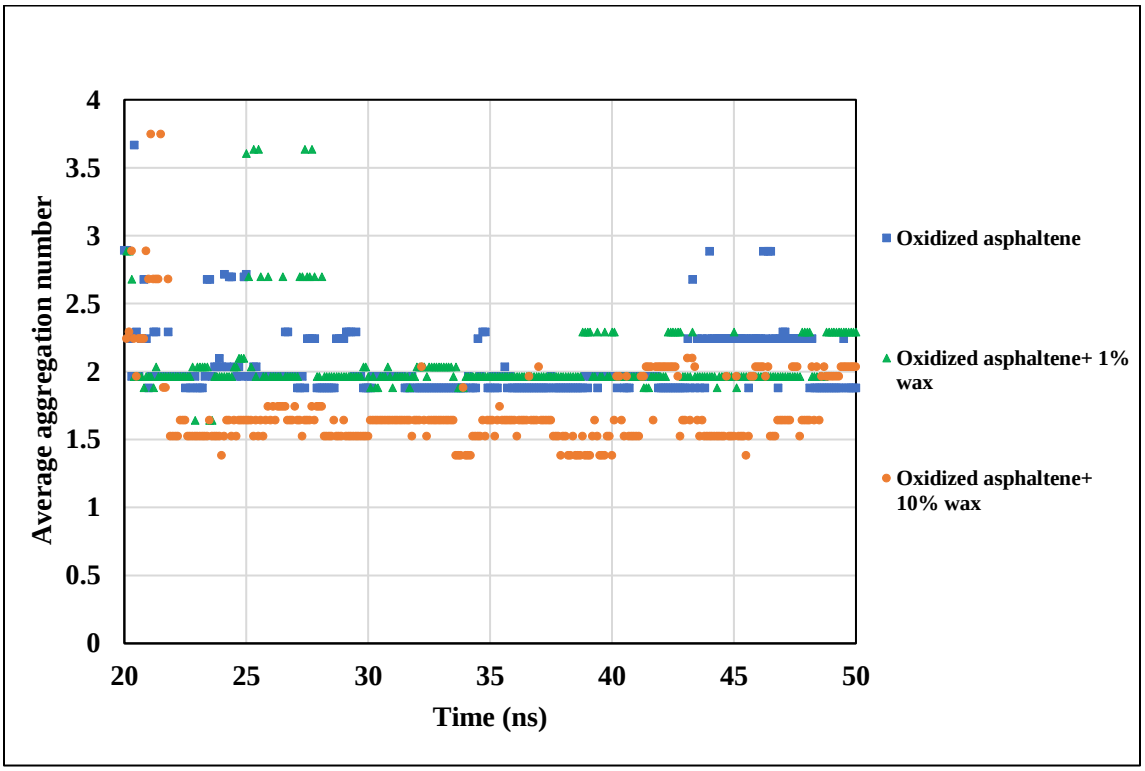

Figure 4.8 Average aggregation number for oxidized asphaltene in methanol solvent with and without the presence of paraffin wax molecules, at 298.15K (25°C)

The study results shows that upon the introduction of wax to the system, wax molecules reach to polyaromatic sheets of oxidized asphaltene, changing the positions of the asphaltene molecules relative to each other from parallel to displaced parallel This structural deformation can increase the interlayer spacing and facilitate the intercalation of wax molecules into the stacks of oxidized asphaltenes. This intercalation occurs mostly through the CH-π interaction and is followed by a disturbance in the π-π interaction between polyaromatics in stacks. This in turn facilitates the de-agglomeration of oxidized asphaltene molecules (Pahlavan et al. 2018). Furthermore, CH-π interactions between the CH sites of the aliphatic chains of paraffin wax and the acceptor π-clouds of aromatic sheets of asphaltenes have a destructive effect on the π-π interactions of asphaltene-asphaltene (Maresca et al. 2008). Therefore, the CH groups of the aliphatic chains of paraffin wax molecules provide polar surfaces of interaction for the aromatic cores of oxidized asphaltene molecules, dispersing the aggregates of asphaltenes while blocking the reformation of nanoaggregates (Pahlavan et al. 2018).

The reduction in size of oxidized asphaltene nanoaggregates can contribute to restoring the rheology that aged bitumen had prior to aging, as shown in previous studies (Samieadel et al. 2018). During oxidative aging, as determined by thin-layer chromatography with flame ionization detection, polar molecules such as resin react with oxygen, becoming more polar and less soluble in n-heptane, and consequently increasing

the asphaltene fraction (Zhang et al. 2011). Increased polarity promotes stronger intermolecular interactions and plausibly the aggregation of asphaltenes (Yu et al. 2014). This phenomenon will affect the rheology of bitumen, causing a stiffening effect in bitumen (Epps Martin et al. 2016). However, paraffinic wax has been shown to have a decreasing effect on the complex modulus of aged bitumen (Samieadel et al. 2018) and an increasing effect on the creep compliance modulus, which can be due to deagglomeration of structured oxidized asphaltene molecules and disruption of the stacking mechanism of polar molecules.

Adding wax to bitumen leads to the formation of crystals with smaller size compared to pure wax; the reason for this can be the trapping of paraffin wax molecules between polar components, which will lead to a lower melting point and a lower heat of fusion compared to pure wax. Figure 4.9 shows the mechanism of penetration, deformation, and deagglomeration of oxidized asphaltene nanoaggregates by paraffin wax molecules

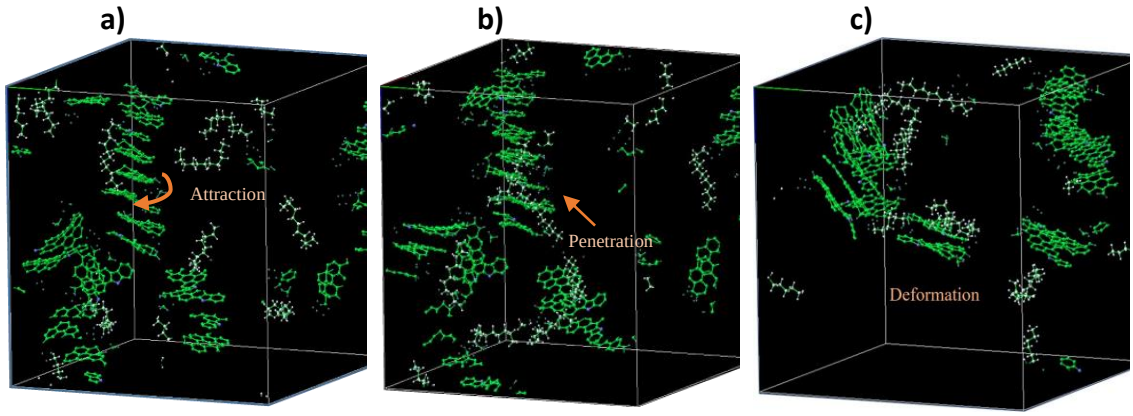

Figure 4.9 Deagglomeration mechanism of paraffin wax molecules: a) Attraction of paraffin wax to the center of nanoaggregate, b) Penetration of paraffin wax molecule into the nanoaggregate by opening the interlayer space, c) Deformation and deagglomeration of nanoaggregate of asphaltene molecules (Solvent molecules and side chains of asphaltenes have been removed for clarity.)

The aforementioned CH-π interaction of paraffin wax molecules and polyaromatic sheets of oxidized asphaltenes also contributes to blocking other asphaltenes from being attracted to newly separated nanoaggregates. Figure 4.10 illustrates the blocking mechanism of paraffin wax molecules to prevent the reformation of nanoaggregates of asphaltene after deagglomeration.

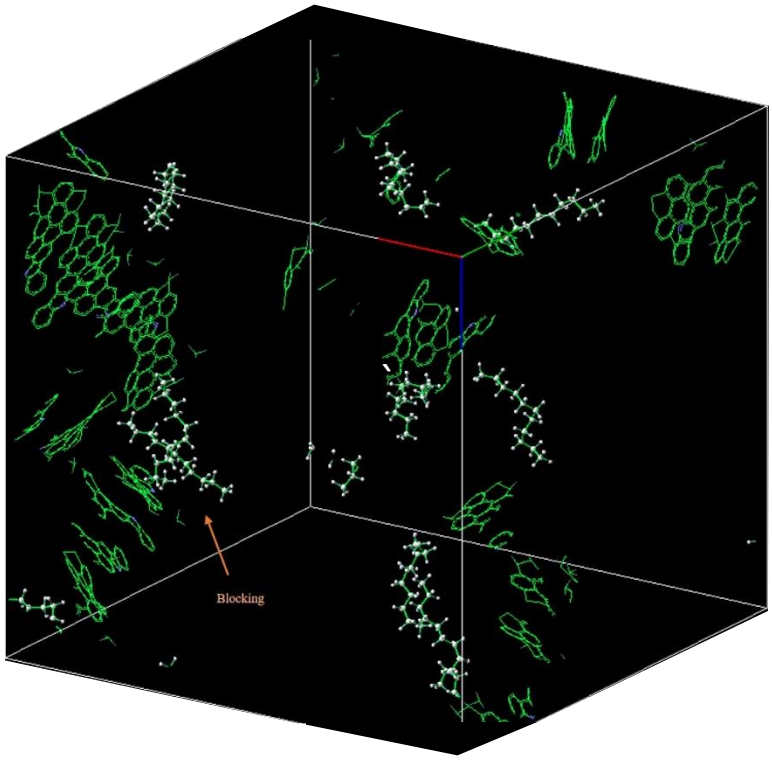

Figure 4.10 Illustration of blocking mechanism of paraffin wax molecules to prevent reforming nanoaggregates of oxidized asphaltene

It should be noted that a reduction in the size of nanoaggregates is not directly correlated to better mechanical properties. The simulation was done in solvent, which gives the paraffin wax molecules a higher mobility, so they can more easily attract to polar sites of asphaltene molecules. However, it should not be assumed that higher wax content is beneficial to mechanical the properties of aged bitumen in general. With a lowering of temperature, the samples with higher wax content will form more crystalline structures that can result in more weak points, leading to more sites for initiating the formation of cracks

(Pahlavan et al. 2016). Previous studies (Lu and Redelius 2007) proposed a limit on wax content to prevent low-temperature mechanical deterioration.

4.5.2 Radial distribution function (RDF)

The radial distribution function (g(r)) was calculated for the most-centered carbon atom of oxidized asphaltene in each selected subset. The results of the radial distribution function (Figure 4.11) illustrate the degree of separation for asphaltene molecules based on the coordinates of centered carbon atoms. The results of the RDF indicate that oxidized asphaltene molecules form parallel stacks at 4.7Å. Such a distance between asphaltene molecules is within the range that has been reported elsewhere as parallel stacking distance (Mousavi et al. 2016; Yaseen and Mansoori 2018). Such orientation and relative distance between asphaltene molecules is attributed to the strong π-π interactions of polyaromatic sheets of oxidized asphaltene molecules. After introducing paraffin wax to the system of oxidized asphaltene molecules, the intensity of the peak corresponding to 4.7Å spacing decreases by 50 and 23 percent for 1 and 10% wax concentration, respectively, indicating fewer parallel stacks formed between asphaltene molecules. This can be due to paraffin wax disturbing stacks of oxidized asphaltene while weakening self-assembled nanoaggregates.

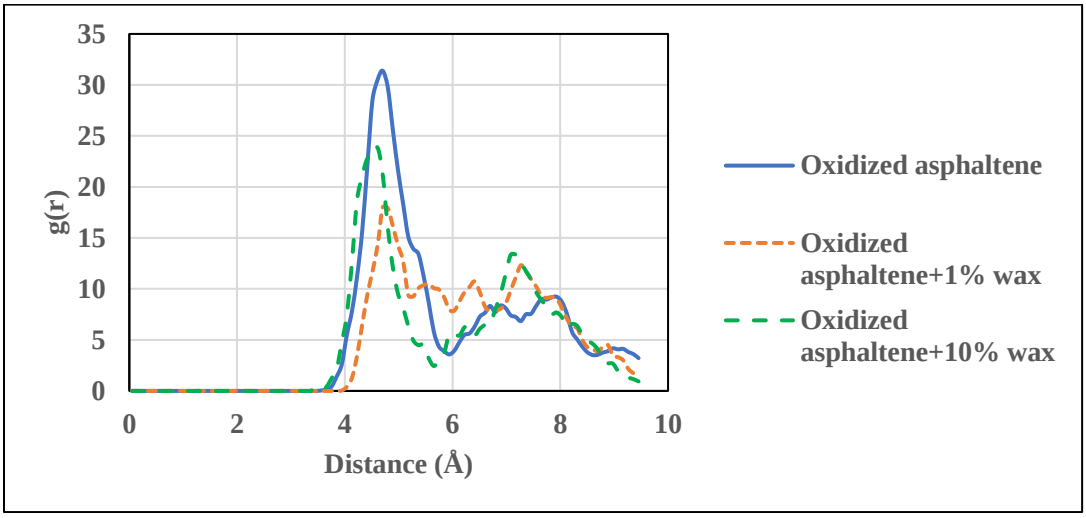

Figure 4.11 Radial distribution function for the most-centered carbon atom of polyaromatic sheets of oxidized asphaltene after 50 ns simulation in methanol solvent at 298.15K (25°C)

4.5.3 Diffusion analysis

Using Equation 4.5, the mean squared displacement (MSD) of the wax subset was calculated for 10ns to evaluate the diffusion coefficient of the wax molecules in an ensemble of oxidized asphaltene and solvent. The purpose of this analysis was to study the effect of an increase in wax concentration on the diffusion of wax molecules into the oxidized asphaltene matrix. The results of the diffusion coefficient indicate that the diffusion of wax molecules increases as the wax concentration increases (Table 4.5). This can be the result of variation of aggregates' size due to the presence of wax. Accordingly, the diffusion coefficient results are aligned with the results of average aggregation number which shows a higher mobility of wax molecules can result in breakage of formed nanoaggregates of oxidized asphaltene in aged bitumen. Such breakage further promote

diffusion within a matrix of reduced nanoaggregates. This phenomenon can result in softening of aged bitumen at temperatures where wax molecules can have higher diffusivity into the bulk of asphalt and redistribute polar molecules; which in turn reduce viscosity.

Table 4.5 Diffusion coefficient and calculated uncertainty of wax molecules within the oxidized asphaltene matrix in methanol solvent at 298.15 k (25°c) (10^{-5} cm^2/s)

Wax concentration	**1%**	**10%**
Diffusion coefficient	0.534	0.854
Uncertainty	0.0085	0.0044

4.6 Summary

With increased emphasis on the use of recycled asphalt pavements, as well as usage of wax-based additives such as many warm-mix additives, recycling, and rejuvenation agents, there is a need for in-depth understanding of the effect of wax on the performance characteristics of bitumen. In addition, due to the low reactivity of wax molecules, they typically remain intact as asphalt ages during pavement service life, consequently increasing the relative ratio of wax molecules to asphaltene molecules and making the role of wax more prominent. This paper provides a comprehensive understanding of the underlying molecular-level interactions controlling the thermo-mechanical properties of aged bitumen doped with wax. This is a summary of the results:

1- The difference between the absolute values of critical low temperatures (S=300 MPa and m-value=0.3) increased from -7.3 ^{o}C to -14.6 ^{o}C when the wax content of

aged bitumen increased from 1% to 10%; this may be attributed to the formation of lamellar structures in bitumen. Such an increase in ΔTc can increase a bitumen's susceptibility to thermal cracking and fatigue cracking.

2- The percent strain recovery decreased up to 50% with an increase of wax from 1% to 10%; this can be attributed to the role of wax in disturbing the asphaltene network by reducing the formation of nanoaggregates.

3- XRD results show the formation of wax crystals in the bulk of bitumen with a corresponding d-spacing of 19.4Å at 10% wax dosage. Another peak with lower intensity was observed at d-spacing of 4.2Å for the 5% and 10% sample. No peak could be captured in specimens containing 1% and 3% wax dosages.

4- The glass transition temperature decreased 9 ^{o}C after the addition of 10% wax to aged bitumen. This decrease can be attributed to wax contributing to the maltene component of bitumen, promoting the mobility of the overall matrix.

5- The melting point of a 10% wax-doped specimen was found to be 15 ^{o}C lower than that of pure wax. This can be attributed to the formation of smaller wax crystals when wax is blended into the bitumen; smaller wax crystals can be a result of trapping wax molecules between polar components. A similar reduction trend was observed in samples with lower wax concentrations.

6- The onset temperature for decomposition of bitumen decreases with aging, due to an increase in reactive components. However, after the addition of paraffin wax,

the onset temperature increases, mainly because wax is less reactive than other asphalt components.

7- In simulation, paraffin wax molecules in a medium that gives them sufficient mobility were found to be able to break the nanoaggregates of oxidized asphaltene, leading to smaller nanoaggregates. This in turn increases the exposed surface area in samples with high wax content, making them more prone to degradation. High exposed surface area may be the cause of the low residual mass observed in samples with high wax content.

8- In simulation, the mechanism of breakage of nanoaggregates is initiated by CH-π interaction between paraffin wax and aromatic sheets of oxidized asphaltene, weakening the stacked structure of asphaltene molecules. This is followed by wax penetration into the self-assembled stacks of oxidized asphaltenes, promoting breakage of nanoaggregates. This was also evidenced by a 25% reduction in the average aggregation number of oxidized asphaltenes when 10 wt% paraffin wax molecules were added to the system.

9- In simulation, the radial distribution function shows a reduction of peak intensity at around 4.7Å, which is the stacking distance of oxidized asphaltene. This indicates that after adding wax to the ensemble, asphaltene molecules are less likely to form parallel stacks, and are mostly prevented from the formation of large stacked molecules.

10- In simulation, the diffusion coefficient of the paraffin wax subset increases with an increase of wax content. An increase of wax content from 1% to 10% increases the diffusion coefficient by 35%.

5 INTERPLAY BETWEEN WAX AND POLYPHOSPHORIC ACID AND ITS EFFECT ON BITUMEN THERMOMECHANICAL PROPERTIES

5.1 Introduction and Literature Review

Wax-based additives have been commonly used in warm-mix asphalts (WMA) and many industrial rejuvenators. Warm-mix asphalts are paving mixtures that can be manufactured and placed at temperatures of 20-40 ^{o}C lower than those for hot-mix asphalts (Samieadel et al. 2017). One of the warm-mix additives is paraffin wax, a white crystalline powder with a chemical structure of n-alkanes and a melting point of 50-60 ^{o}C (Krol et al. 2015; Morea et al. 2012; Samieadel et al. 2017; Sanchez-Alonso et al. 2011). Paraffin wax can improve the workability of asphalt mixture and extend the construction season (Edwards and Redelius 2003; Lu and Redelius 2007; Pahlavan et al. 2016). N-alkanes are saturated hydrocarbons that are solid with carbon number higher than 17 (Gawel and Czechowski 1998). However, wax additives can be different from a bitumen's inherent wax (Samieadel et al. 2017). The two waxes commonly recognized in crude oils and distillates are paraffin waxes and microcrystalline waxes(Edwards and Redelius 2003). Paraffin waxes are mainly composed of n-paraffins (n-alkanes) with minor amounts of isoparaffins and cycloparaffins; they crystallize as plates or needles(Edwards et al. 2006). The melting point of paraffin wax is in the range of 50 to 70 ^{o}C; it is reduced to 20-30 ^{o}C when blended with bitumen (Butz et al. 2000; Samieadel et al. 2017). Microcrystalline waxes are aliphatic hydrocarbon compounds containing a considerable amount of iso-paraffins and

cycloparaffins; they have a less distinct melting point and a high average molecular weight (Musser and Kilpatrick 1998).

Depending on the source, bitumen can be rich in wax or almost wax free (Schmets et al. 2010). The presence of wax can highly affect the temperature sensitivity of bitumen, since wax has a melting point and changes its phase with temperature change (Samieadel et al. 2018). At higher service temperatures, it has been shown that wax can soften the bitumen and lower the viscosity; at lower temperatures, wax stiffens bitumen, causing bitumen to be more susceptible to low-temperature cracking (Baldino et al. 2012; Samieadel et al. 2017). The low-temperature cracking can be attributed to wax crystallization and the formation of lamellar structures, which can play as weak points for crack nucleation at low temperatures (Pahlavan et al. 2016).

Bitumen's chemical components have been categorized into saturates, aromatics, resins, and asphaltenes (Bissada et al. 2016). Bitumen is known to have a colloid structure, where asphaltenes are dispersed in the maltene phase composed of saturates, resins, and aromatics (Redelius and Soenen 2015). Depending on the amount of each portion, the properties of bitumen can vary significantly (Redelius and Soenen 2015). It has been shown that there is a close relationship between the asphaltene fraction and the mechanical properties of bitumen (Yu et al. 2014). The interplay between different components in bitumen as well as bitumen components and modifiers can highly affect a bitumen's rheology and compromise its mechanical performance.

Among commonly used bitumen modifiers are elastomers, plastomers, thermosets, sulfur, and acids such an polyphosphoric acid (PPA)(Al-Adham and Wahhab 2015; Brasileiro et al. 2019; Gama et al. 2018; Naveed et al. 2019). PPA has gained attention as a modifier to increase the high-temperature grade of bitumen without compromising its low-temperature grade (Baumgardner et al. 2005; Masson 2008; Masson and Collins 2008). High-purity PPA, an oligomer of H_3PO_4, is produced either from the dehydration of H_3PO_4 at high temperatures or by heating P_2O_5 dispersed in H_3PO_4 (Corbridge 1980; r se Averbuch-Pouchot and Durif 1996; Xiao et al. 2014). The dehydration method tends to produce short chains, whereas the dispersion method usually produces chains with more than 10 repeat units (Baumgardner et al. 2005). PPA can be used as a modifier to improve the high-service temperature of bitumen and bump the grade without air-blowing the bitumen; air-blowing is known to cause oxidation of highly polar molecules of bitumen and increase bitumen's aging susceptibility (Giavarini et al. 2000).

Baumgardner et al. observed that after the addition of PPA to waxy bitumen, the asphaltene fraction increased; they concluded that the addition of PPA led to coprecipitation of asphaltenes with insoluble PPA-adducts (Al-Adham and Wahhab 2015). Mason and his co-workers performed a similar study and showed that the interaction of PPA and resin molecules leads to an increase in the heptane-insoluble fraction, which is reflected as an increase in the asphaltene portion (Masson 2008). Orange et al. proposed a model for the interaction of PPA with bitumen components based on the reactivity of asphaltenes with PPA; the model shows that acid-base reactions and esterification can

cause a deagglomeration of the asphaltene aggregates, leading to an improvement in the bitumen's rheology (Giavarini et al. 2000).

Xiao et al. showed that adding 0.5% PPA to bitumen can account for using 1% less rubber while maintaining the same high-temperature grade (Xiao et al. 2014); however, it was noted that the effect of PPA on bitumen is dependent on the bitumen's composition (Schmets et al. 2010). Baldino et al. showed that the rheological glass transition temperature of bitumen is reduced with an increase in PPA (Baldino et al. 2012). Liu et al. studied the effect of PPA on warm-mix asphalt and showed that PPA causes an increase in the complex modulus and a decrease in the phase angle when measured at intermediate service temperature (Liu et al. 2016). It was also observed that PPA decreases the creep stiffness at subzero temperatures but it does not affect the m-value at the studied concentration (Liu et al. 2016). Yan et al. showed that adding PPA to bitumen causes a decrease in the resin fraction of bitumen and an increase in the asphaltene fraction, while the saturates and aromatic portions remain unchanged (Yan et al. 2013).

While there are several studies of the effect of PPA on bitumen solubility and rheology, there is limited research on a molecular-level understanding of the effect of PPA and its interplay with bitumen’s inherent wax and/or wax-based additives. Therefore, this paper incorporates laboratory experiments and molecular dynamics simulations to relate

the molecular interactions between PPA and the components (including wax) of bitumen on its phase changes and rheological properties.

5.2 Materials Preparation

The bitumen used in this study was graded as PG 64-22, which is commonly used in the United States and has been found to have a very low content (<0.5%) of inherent wax. Here, we refer to it as a low-wax bitumen. The wax that was used for bitumen modification was a petroleum paraffin wax (CAS number: 64742-51-4, with melting point of 53‑57 ºC, acquired from Fisher Scientific). The wax was introduced at 5% and 10% dosages by weight of the initial bitumen and was hand-blended at 135 ºC for 10 minutes. In this study, the bitumen with 5% wax is called medium-wax bitumen, and the bitumen with 10% wax is called high-wax bitumen. After mixing the wax into the bitumen, the PPA was hand-blended for 10 minutes at a concentration of 1% (of total mass of sample).

5.3 Test Methods

5.3.1 Differential scanning calorimetry (DSC)

Differential scanning calorimeter (DSC 2500) by TA instrument was used to determine glass transition temperature and melting peak of each specimen. The glass transition of bitumen was measured using modulated DSC with a modulation of ±1 ºC every 60 seconds and a ramp of 3 ºC/min. The calculation was done using data collected in the second heating cycle. To provide a more precise measurement of glass transition and remove the noise of regular DSC the modulated DSC was used for samples with wax

and PPA. In an MDSC experiment, modulation of the sample temperature permits the heat flow to be split into two components, one of which is dependent upon sample Cp and changes in Cp. The measurement of Cp by MDSC is more accurate than the other methods (such as three-run method), easily obtaining values with 2–3% error because it is a properly calibrated system (Pilař et al. 2014)

For this experiment, the samples (5‑7 mg) were placed in Tzero aluminum pans with hermetic lids. It should be noted that for this method, provisions need to be made to correct or compensate the data for differences in the mass of the sample pan and the reference pan. To minimize the effect of instrument drift, the isothermal segments are used for 15 minutes.

5.3.2 Dynamic shear rheometer (DSR)

A dynamic shear rheometer by Anton Paar Modular Compact Rheometer MCR 302 was used to perform several rheological characterization tests as described below.

5.3.2.1 Frequency sweep test

An oscillatory test was performed at 0.01strain rate and frequencies of 0.1 rad/s to 100 rad/s at temperatures ranging from 76 ºC to 4 ºC. To perform the test, parallel plate spindles of diameter 8mm and 25mm were used for temperatures below and above 40 ºC respectively to measure shear stress and shear strain. From the measured shear stress and shear strain, the complex modulus (G*) and phase angle were calculated, to investigate

the elastic and viscous behavior of each specimen. The complex modulus is defined as a measure of bitumen's resistance to deformation when repeatedly sheared. Complex modulus is calculated based on equation 5.1.

$$G^* = \frac{\tau_{max}}{\gamma_{max}} \qquad \textbf{Equation 5.1}$$

Where τ_{max} = maximum applied stress and γ_{max} = maximum resultant strain.

Phase angle is the time lag between occurrence of τ_{max} and γ_{max}. The time lag can be measured in seconds and then converted to an angular measurement by dividing it by the oscillation frequency and then multiplying by 360° (or 2π radians).

5.3.2.2 Shear rate sweep test

To further investigate the change in particle size and the intermolecular interactions of wax and PPA-modified bitumen, a shear rate sweep test from 0.1 to 30 (1/s) was performed at 52 ^{o}C using an 8mm parallel plate. This test reveals the thixotropy characteristic of bitumen, which is indicative of the intermolecular interaction in bitumen.

As the shear rate increases (>10 1/s), shear thinning occurs, and the data can be fitted to a power law model (Chhabra 2010) using Equation 5.2.

$$\sigma = K\dot{\gamma}^n \quad \textbf{and} \quad \eta = K\dot{\gamma}^{n-1} \qquad \textbf{Equation 5.2}$$

where η is viscosity, $\dot{\gamma}$ is shear rate, σ is shear stress, and n is the power law index. K is the flow consistency index, a measure of viscosity under non-Newtonian flow (Ajienka and Ikoku 1990).

5.3.2.3 Multiple stress creep recovery (MSCR) test

The MSCR test was performed following the AASHTO T350-1433 (AASHTO T 350-14 2014) specification, in which the bitumen is subjected to 10 cycles of stress and recovery of 1 and 9 s, respectively, at two stress levels of 0.1 and 3.2 kPa at 58 °C. Before the start of the test, samples were subjected to a preload cycle. Afterward, the nonrecoverable creep compliance (known as J_{nr}) and the difference between creep compliance of 0.1 and 3.2 kPa were determined.

5.3.3 X-Ray powder diffraction method

X-ray diffraction (XRD) analyses were carried out by employing a Siemens D5000 Diffractometer equipped with an FK 60-04 air insulated X-ray diffraction tube with Cobalt anode, the XRD spectrums were taken with Co Kα radiation (1.7889 nm) at 45 kV and 40 mA in the range of $2\theta = 5^{o}–50^{o}$ with a rate of 1^{o}/min.

5.3.4 Thin-layer chromatography with flame ionization detection (TLC-FID)

The fractional composition of the bitumen modified with PPA and wax was investigated using an Iatroscan MK-6s model TLC-FID analyzer. The hydrogen flow rate

and air flow rate were set to 160 mL/min and 2 L/min, respectively. The part insoluble in n-heptane, the asphaltene content, was separated and determined following the (ASTM D3279-07 2007) standard. Later, 20 μg of n-heptane soluble (maltene) was spotted on the chromrods; pentane, toluene, and chloroform solutions were used for solvent development. The chromrods were developed in a pentane tank for 35-40 minutes, then dried in the air for 2-5 minutes. The dried chromrods were then transferred into a second developing chamber filled with a 9:1 ratio of toluene:chloroform solution for 9 minutes. Finally, the rods were dried in the oven at 85 °C, and each prepared specimen was scanned for 30s using the Iatroscan with FID detector.

5.3.5 Moisture susceptibility index using contact angle measurement

A ramé-hart Model 260 standard contact angle goniometer was used to image a droplet of each specimen at room temperature. The contact angle between the droplet and the substrate was measured using the DROPimage Advanced software package. The percent of change in contact angle after conditioning the specimen in water was calculated as an indicator of moisture susceptibility (Equation 5.3).

The equipment is composed of a light source, a sample stage, a lens, and image capturing tools. The contact angle is defined as the angle between the tangent to the bitumen interface and the tangent to the bitumen-solid interface. A lower value of the contact angle indicates good wettability between the droplet and the substrate (Lamarre et al. 2016). In this study, contact angles were measured in dry conditions and wet conditions to study the effect of water exposure on the adhesion of bitumen samples. The substrate

used was silica platelets as representative of siliceous stone aggregates. Figure 5.1 illustrates a droplet of bitumen before and after water conditioning.

To prepare specimens, the glass slides were sterilized in acetone, isopropanol, and water, followed by sonication and drying with nitrogen gas for 10 minutes, using the procedure in the literature (Hung et al. 2017). The slides then were placed into UV ozone for 15 minutes to ensure any monolayers were removed from the surface. About 15 mg of each bitumen sample was placed on sterilized glass slides that were placed in an oven for 30 minutes at 150 ^{o}C to promote proper coating, followed by cooling at room temperature for 1 hour. To study the effect of moisture on the adhesion properties of bitumen, the samples were conditioned in a vial containing 5mL of deionized water at 80 ^{o}C for 2 hours. The percent of change in contact angle before and after water exposure was used as an indicator of moisture susceptibility, as shown in Equation 5.3 below.

$$Contact\ Angle\ Moisture\ Susceptiblty\ Index = \frac{(Contact\ Angle_{Wet} - Contact\ Angle_{Dry})}{Contact\ Angle_{Dry}} \times 100$$

Equation 5.3

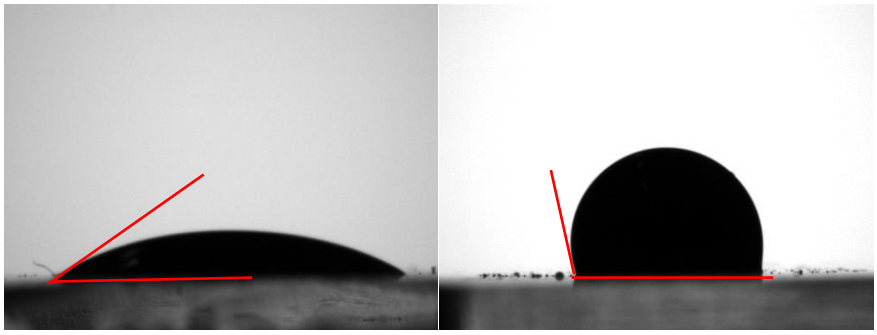

Figure 5.1 Image of a sample bitumen on glass slide: Left – a dry sample, Right: after wet conditioning

5.3.6 Bending beam rheometer (BBR)

BBR test was used to characterize the fatigue performance of bitumen at subzero temperatures and to measure stiffness and m-value of bitumen. M-value is known as the ability to relax the stress (ASTM D6648 2016) by bitumen beam sample (12.5 mm wide, 127 mm long and 6.25 mm thick) while a constant load of 980 mN is applied at the middle point of the beam. After applying the load, the deflection of beam was measured, and the stiffness and the m-value was calculated at 60 second point.

By the ASTM standard, bitumen sample should have stiffness of lower than 300 MPa and m-value of higher than 0.3 at test temperature specified for each PG grade (10 ^{o}C higher than lower PG grade) which in case of PG 64-22 is -12 ^{o}C. In this study, BBR test results are used to calculate the temperature at which the stiffness is equal to 300MPa and m-value is equal to 0.3. The lower of the two temperatures is called critical low temperature and the difference between the two temperatures (ΔT_c) has been related to non-load-related cracking of asphalt pavement and the fatigue performance of pavement by several researchers (Anderson et al. 2011; Menapace et al. 2018).

5.4 Molecular Dynamics Simulation

A molecular dynamics simulation was performed on a system at equilibrium state composed of several fused aromatic molecules to represent bitumen components, PPA, and paraffinic wax in heptane as a solvent medium; paraffinic wax was included in scenarios where the wax effect was being examined. Large-scale Atomic/Molecular Massively

Parallel Simulator (LAMMPS) software in a MedeA® environment version 2.2 was used for simulation. The study focused on investigating the interaction of PPA molecules with resin-type molecules, with and without the presence of wax. The model was built in the MedeA® environment using the molecular builder, which allows an interactive, step-by-step construction of polyaromatic units with attached aliphatic chains and pyrrole rings. This study used the PCFF+ force field, which is an extension of the PCFF force field. The force field refers to the functional form of parameters used to calculate the potential and kinetic energy of the system of atoms and molecules. PCFF+ is an all-atom force field designed to provide excellent accuracy on hydrocarbon and liquid modeling for *ab initio* simulations (Sun et al. 1994; Waldman and Hagler 1993). This force field includes a Lenard-Jones 9-6 potential for intermolecular and intramolecular interactions and specific stretching, bending, and torsion terms to involve 1-2, 1-3, and 1-4 interactions (Ungerer et al. 2014).

5.4.1 Simulation method

In this study, a simulation box of resin molecules with a concentration of 20 wt% in heptane was created containing 20 resin molecules. The molecular structures of resin were selected from the literature (Fischer et al. 2014; Mousavi et al. 2016). The chemical structures of PPA and paraffin wax are presented in Table 5.1. To investigate the effect of PPA and wax on the interaction of resin-like molecules, a simulation box containing heptane was made with the supercell feature of Medea software. The simulation contained two LAMMPS stages: an NVT ensemble (constant number of atoms, volume,

and temperature), followed by an NPT ensemble (constant number of atoms, pressure, and temperature). Both ensembles started with a high temperature and pressure of 800 K and 200 atm, with an annealing pressure and temperature to target values of 350 K and 1 atm. The second LAMMPS stage was set to simulate the resin in heptane for 20 ns to reach equilibrium. After that, the PPA and wax molecules were added to the system and the simulation continued for another 10 ns to reach a total simulation time of 30 ns.

Table 5.1. Molecular structures used in molecular simulation

Sample ID	**Chemical formula**	**Chemical Structure**	**Reference**
Resin	$C_{40}NH_{59}$	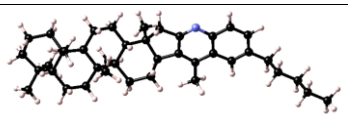	(Fischer et al. 2014)
Polyphosphoric Acid	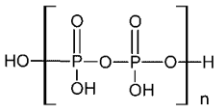	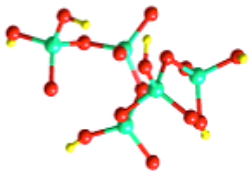	(Masson 2008)
Paraffin wax	$C_{11}H_{24}$	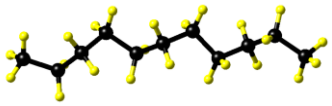	(Samieadel et al. 2018)

The radial distribution function (RDF) (g_r) was calculated for the subset comprising the most-centered carbon atom of each resin molecule. The RDF results help to understand the extent of the interaction between molecules based on the increase or decrease of distance between them. The RDF is calculated in histogram from binning of pairwise

distance to the maximum force cutoff of 9.5 Å using the "compute rdf" command of LAMMPS source code. The results of the radial distribution function represent the most probable separation distance of resin molecules. The RDF helps to visualize the degree of separation between a group of molecules, which in this study is a subset comprised of resin molecules. The RDF g(r) is calculated using Equation 5.4.

$$g(r) = \lim_{dr \to 0} \frac{V}{N(N-1)4\pi r^2 dr} \sum_i^N \sum_{j \neq i}^N \delta(r - r_{ij}) \qquad \text{Equation 5.4}$$

Where V is the volume, N is the number of atoms included in the calculation, δ is the Kronecker delta function and r_{ij} is the distance between the two atoms (Levine et al. 2011; Lowry et al. 2017).

5.5 Results and Discussion

5.5.1 Glass transition and melting peak test results

The modulated method that was used in this study starts with an isothermal equilibration at -80 ºC for 5 minutes. Then the heating ramp of 3 ºC/min starts with modulation of +/-1 ºC every 60 seconds up to 160 ºC. The data in the second heating cycles was used for analysis (Figure 5.2).

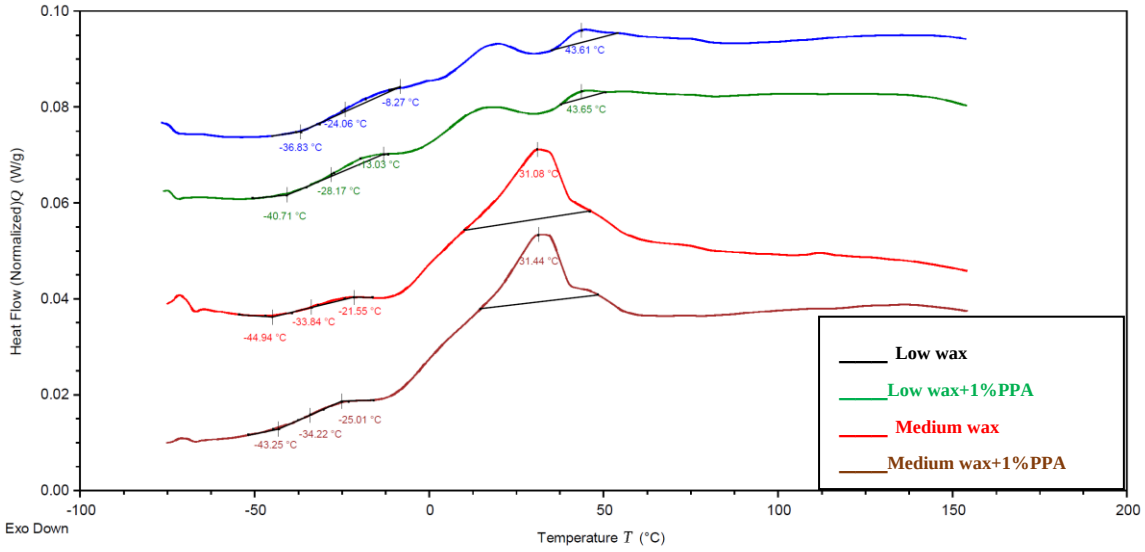

Figure 5.2. Heat flow plot for control and modified bitumen

Table 5.2 shows the results of the modulated DSC for samples of bitumen with low wax, medium wax, and high wax, with and without PPA modification. The results in this table show a glass transition temperature decrease as the wax content increases, which aligns with previous studies. In other words, the presence of wax shifts the glass transition temperature toward a more negative value (a larger absolute value) (Samieadel et al. 2017). The observed reduction in glass transition temperature is attributed to wax molecules having low weight and high mobility compared to other components of bitumen. The presence of PPA has shown a further reduction in glass transition temperature toward even lower (more negative) values. This lowering effect is more pronounced at a higher dosage of wax.

Table 5.2 Results of MDSC for control sample and samples containing different percentages of wax and PPA

Sample	Onset of glass transition (ºC)	Glass transition temperature (ºC)	End temperature of glass transition (ºC)	Melting Peak (ºC)
Low wax	-36.83	-24.06	- 8.27	43.61
Low wax +1%PPA	-40.71	-28.17	-13.03	43.65
Medium wax	-44.94	-33.84	-21.55	31.08
Medium wax +1%PPA	-43.25	-34.22	-25.01	31.44
High wax	-42.33	-24.99	-15.41	34.78
High wax +1%PPA	-40.22	-29.94	-19.57	35.31

5.5.2 Frequency sweep test results

Figure 5.3 shows the complex modulus results for two service temperatures: one at high range (58 °C), and one at low range (22 °C). These particular temperatures were selected since one is above melting temperature of wax and one is below based on MDSC results of melting peak. The results show that wax at high temperature has a softening effect on bitumen, since the complex modulus is lower in wax-doped specimens. However, the results at low temperature show that wax has a hardening effect when the test temperature is below the melting point of wax as obtained from the DSC. This phenomenon can be due to the formation of wax crystals at low temperature. However,

the addition of PPA to waxy bitumen has a softening effect at temperatures lower than the melting point of wax. This shows that presence of PPA can mildly soften the overall bitumen containing wax crystals. It has been documented that presence of wax crystals stiffen bitumen at temperatures lower than melting point of wax in bitumen (Pahlavan et al. 2016; Samieadel et al. 2018; Samieadel et al. 2017).

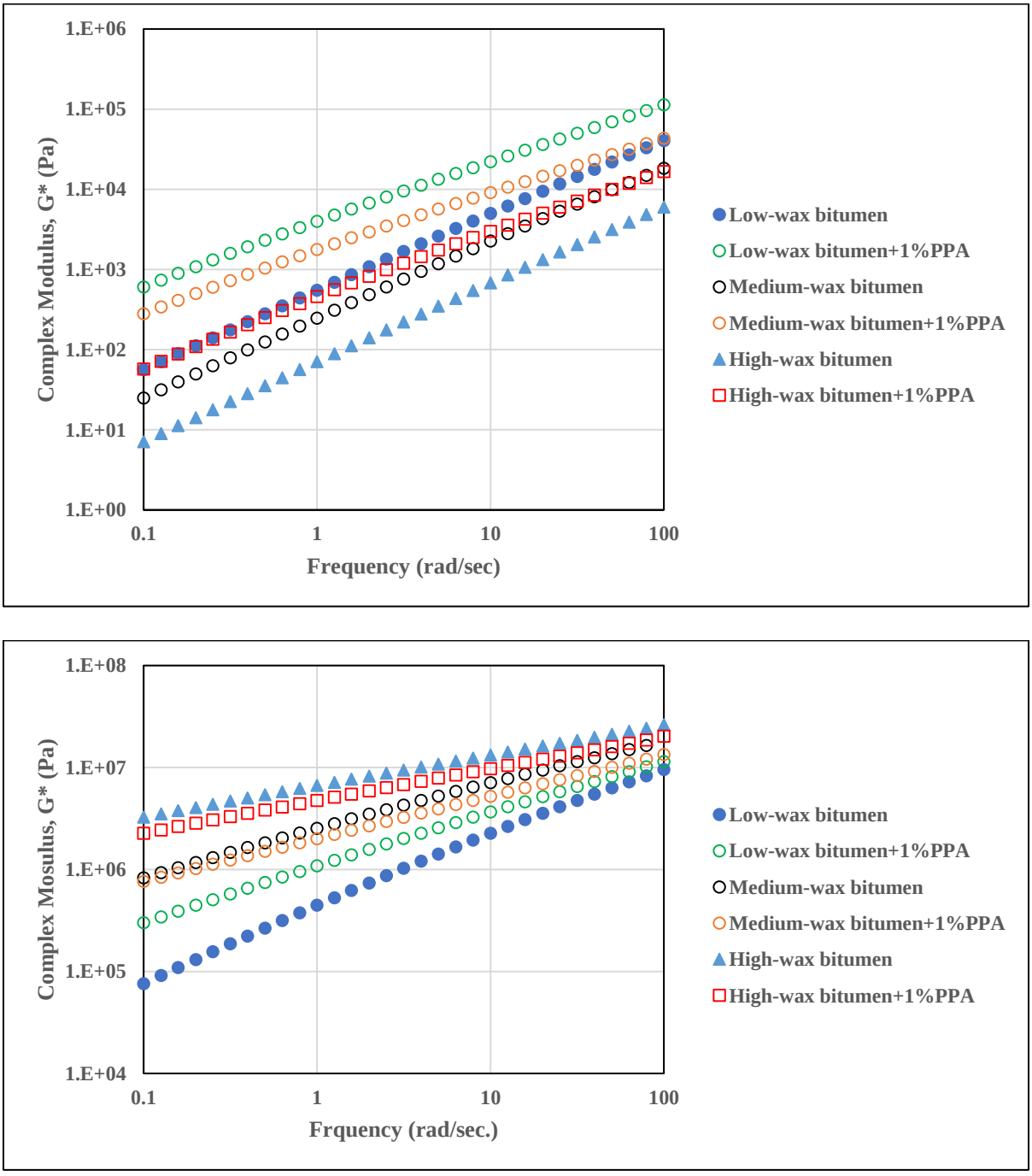

Figure 5.3. Complex modulus vs. Frequency: Top) High service temperature (58 ºC);

Bottom) Low service temperature (22 ºC)

Figure 5.4 illustrates the phase angle values for two service temperatures of 58 ^{o}C and 22 ^{o}C. At low temperature, adding PPA reduces bitumen's phase angle, indicating that bitumen is behaving as a more elastic solid. This trend doesn't change dramatically with the presence of wax crystals. However, at high temperature, adding wax leads to a bitumen with a more viscous behavior, due to the softening effect that paraffin wax imparted on bitumen above the melting point of wax. The presence of PPA improves the elastic behavior of wax-doped bitumen. This in turn can lead to better resistance to rutting, which is a problem typically observed in high-wax bitumen. High decrease in phase angle of bitumen after addition of PPA can be due to the enhanced intermolecular interactions as explained later via our computational analysis. In addition, it has been documented that addition of PPA increases the asphaltene fraction (insoluble part in heptane) fraction of bitumen (Baumgardner et al. 2005); this in turn can promote elastic behavior of bitumen.

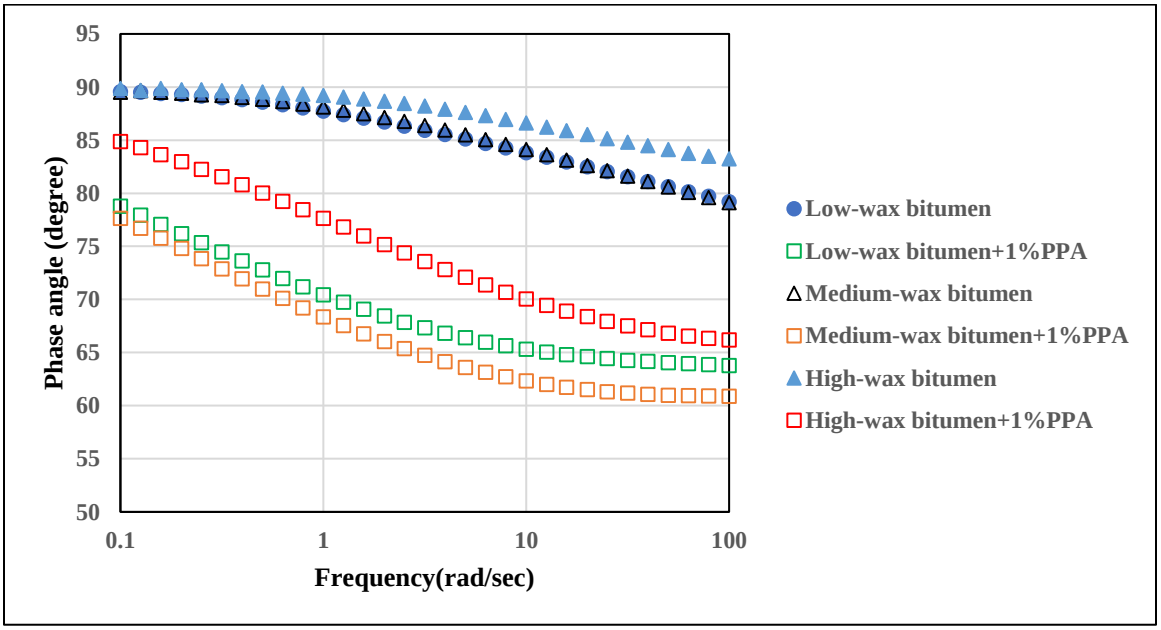

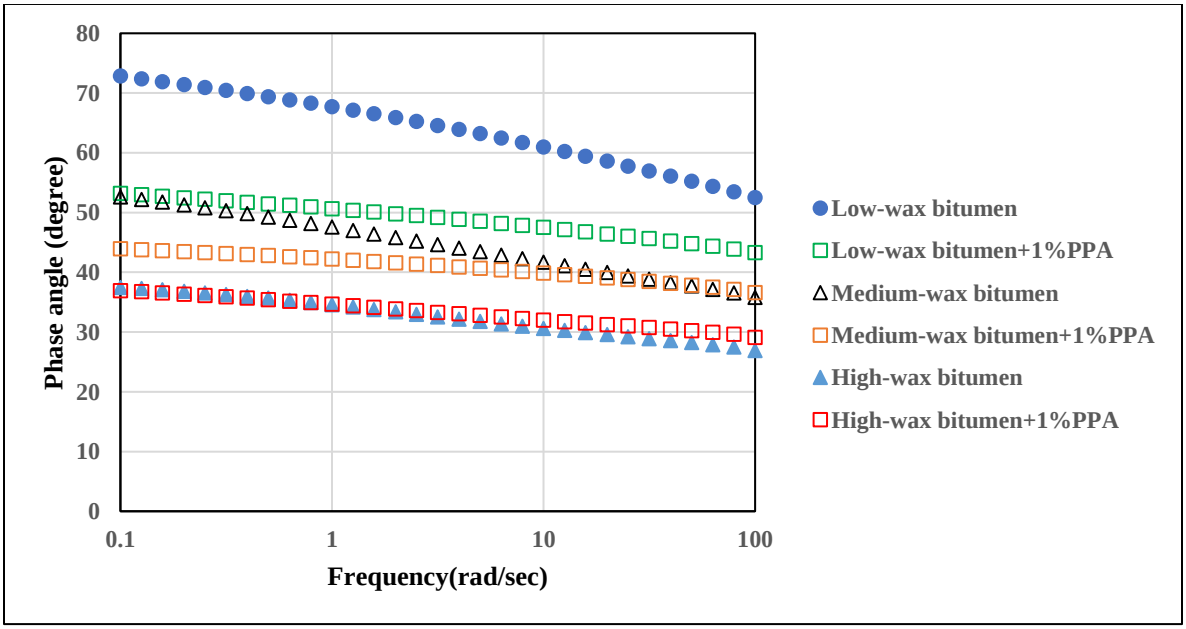

Figure 5.4. Phase angle vs. frequency: Top) High service temperature (58 ºC); Bottom) Low service temperature (22 ºC)

The crossover frequency and modulus results at 40 ºC are shown in Table 5.3. The crossover point in rheological terms is the point at which the loss modulus and storage modulus are equal. The results indicate that at 40 ºC, the crossover frequency is highly affected by the addition of PPA, since it shifts to lower values.

The reducing effect of PPA on the crossover frequency shows that bitumen preserves its elasticity for a longer time as temperature increases. The lower the crossover frequency, the higher the polydispersity index. This indicates that the average molecular weight is higher than number averaged molecular mass, leading to wider distribution of molecular mass (Setz et al. 2013). Increase in solid fraction of bitumen results in an increase in relaxation time of the structures.

This phenomenon takes place when there is high interaction between molecules of a colloid, which in bitumen's case shows that PPA increases the average molecular weight of nano-particles. However, this happens while the complex modulus (the overall stiffness) of bitumen reduces, showing the material becomes softer at crossover. Wax appears to have a reduction effect on crossover frequency, which can be due to formation of wax clusters. But it is significantly less pronounced than PPA’s effect on crossover frequency. This could be attributed to role of PPA on promoting self-assembly in resins and formation of secondary bonds as explained later in our computational analysis.

Table 5.3 . Crossover modulus and frequency of control sample w/o modifier at 40 ºC

Sample	Crossover frequency (rad/sec)	Crossover modulus (MPa)	Crossover frequency % change	Crossover modulus % change
Low-wax bitumen (PG 64-22)	11257.46	1.35E+07	NA	NA
Low-wax bitumen +1%PPA	816.84	3.11E+06	-92.74	-76.98
Medium-wax bitumen	7327.66	8.79E+06	-34.91	-34.96
Medium-wax bitumen +1%PPA	410.53	9.97E+05	-96.35	-92.62
High-wax bitumen	13030.52	7.75E+06	15.75	-42.63
High-wax bitumens +1%PPA	1695.57	1.59E+06	-84.94	-88.24

The complex viscosity of modified bitumen at 22ºC and 58 ºC is shown in Figure 5.5. The obtained shear rate and viscosity values can be used to characterize how a material is likely to flow under an imposed shear stress (Xiao et al. 2014). Based on the Krieger-Dougherty equation, by increasing the volume fraction of solid particles in a colloid, the viscosity increases (Ogawa et al. 1997). In the case of PPA-modified bitumen, the increase of solid fractions (as demonstrated later in the TLC-FID results) can cause the bitumen to show stiffer behavior in terms of viscosity. However, an increase of wax reduces the absolute value of the viscosity while the reduction trend versus frequency does not change at 58 ºC. This trend is reversed at 22 ºC, when the presence of wax imparts a stiffening effect on bitumen when measured at low temperature, and the addition of PPA alleviates the stiffening effect.

The results presented in Figure 5.5 further illustrate that at temperatures lower than the melting point of wax, bitumen shows higher responsiveness to change of frequency.

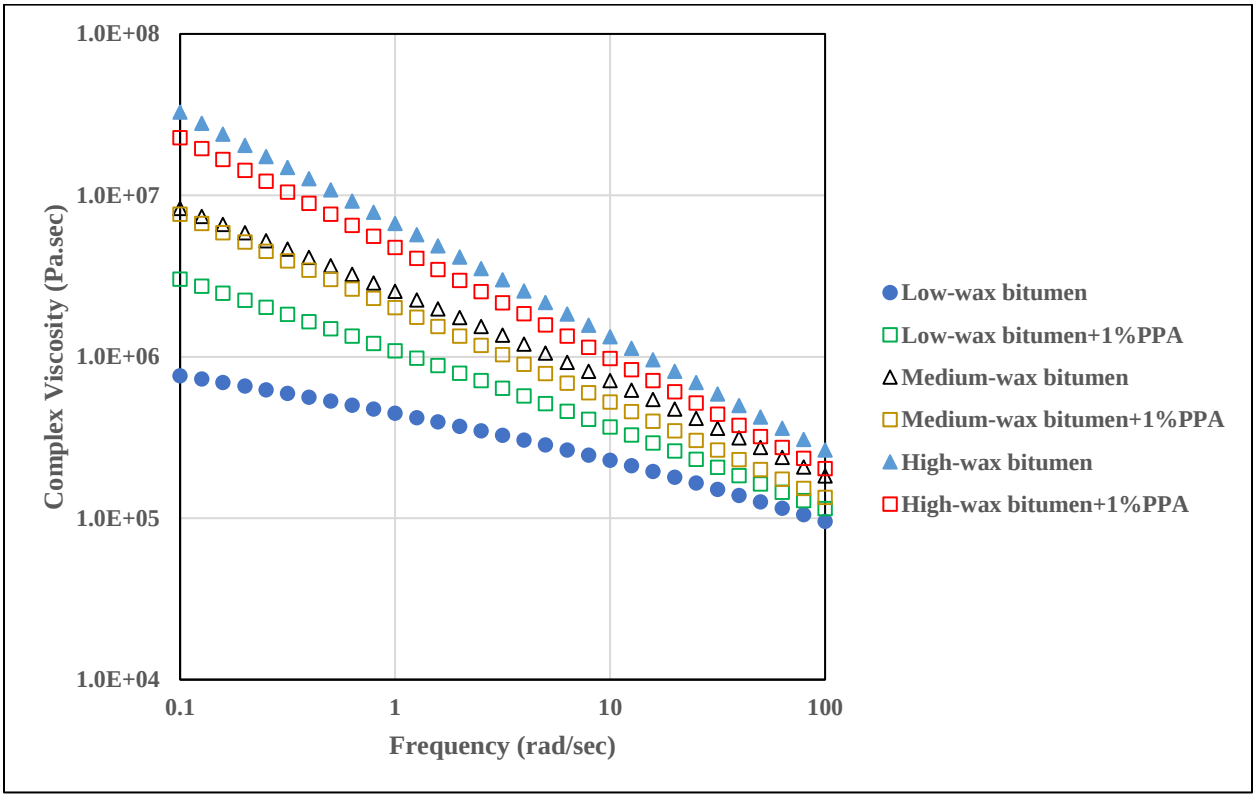
1.0E+08
1.0E+07
1.0E+06
1.0E+05
1.0E+04
Complex Viscosity (Pa.sec)
0.1
1
10
100
Frequency (rad/sec)
Low-wax bitumen
Low-wax bitumen+1%PPA
Medium-wax bitumen
Medium-wax bitumen+1%PPA
High-wax bitumen
High-wax bitumen+1%PPA

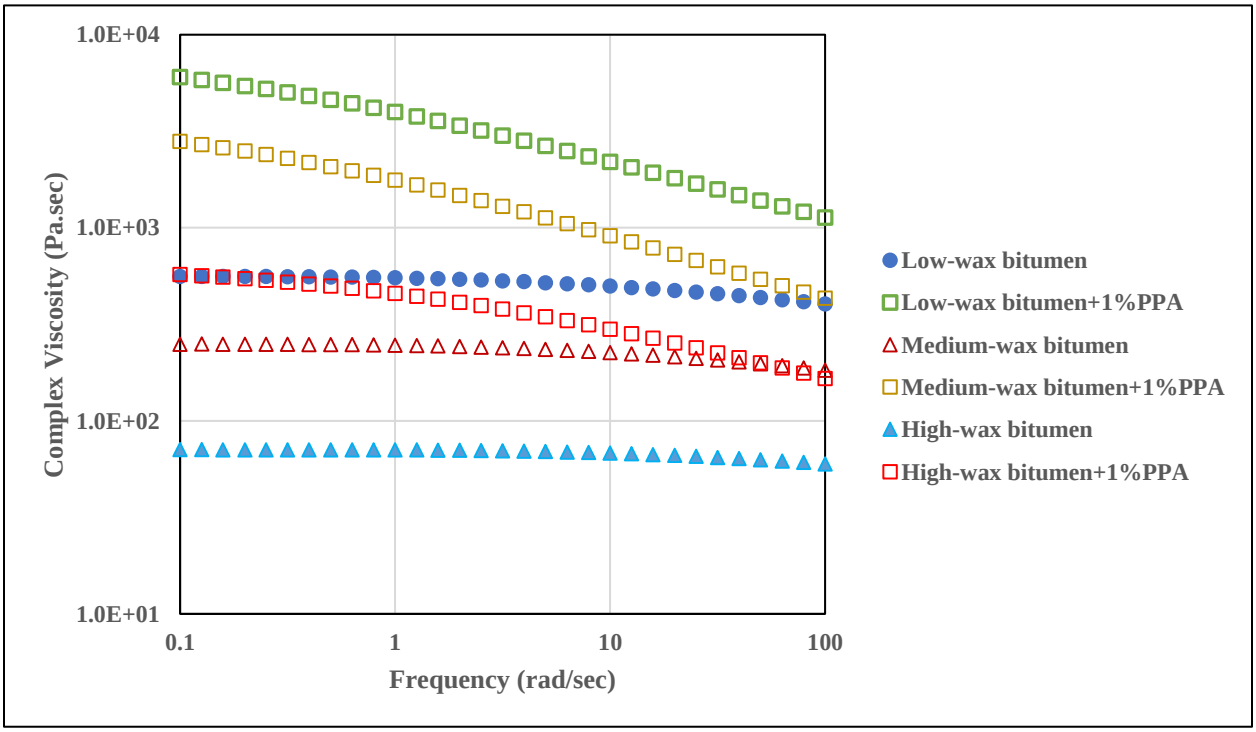
1.0E+04
1.0E+03
1.0E+02
1.0E+01
Complex Viscosity (Pa.sec)
0.1
1
10
100
Frequency (rad/sec)
Low-wax bitumen
Low-wax bitumen+1%PPA
Medium-wax bitumen
Medium-wax bitumen+1%PPA
High-wax bitumen
High-wax bitumen+1%PPA

Figure 5.5. Complex viscosity vs. frequency: Top) Lower service temperature (22 ^{o}C);Bottom) Higher service temperature (58 ^{o}C) above wax melting point

5.5.3 Shear rate sweep test results

To further investigate the intermolecular interactions of bitumen modified with wax and PPA, a shear rate sweep test was done for bitumen containing wax and PPA at a temperature of 52 ^{o}C (Figure 5.6). Equation 1 was used to calculate the power law index and consistency parameter of each sample (Table 5.4). The power law index value increased (in absolute value) after the addition of PPA to control bitumen, indicating the nano-particle size of the solid fraction increased (Chhabra 2010). When PPA is added to wax-doped samples, the power law index increases, which is a result of an increase in the solid fraction because of the formation of PPA-resins assemblies. However, the presence of wax moderates this increase in overall particle size by increasing the volume of low-molecular weight fraction.

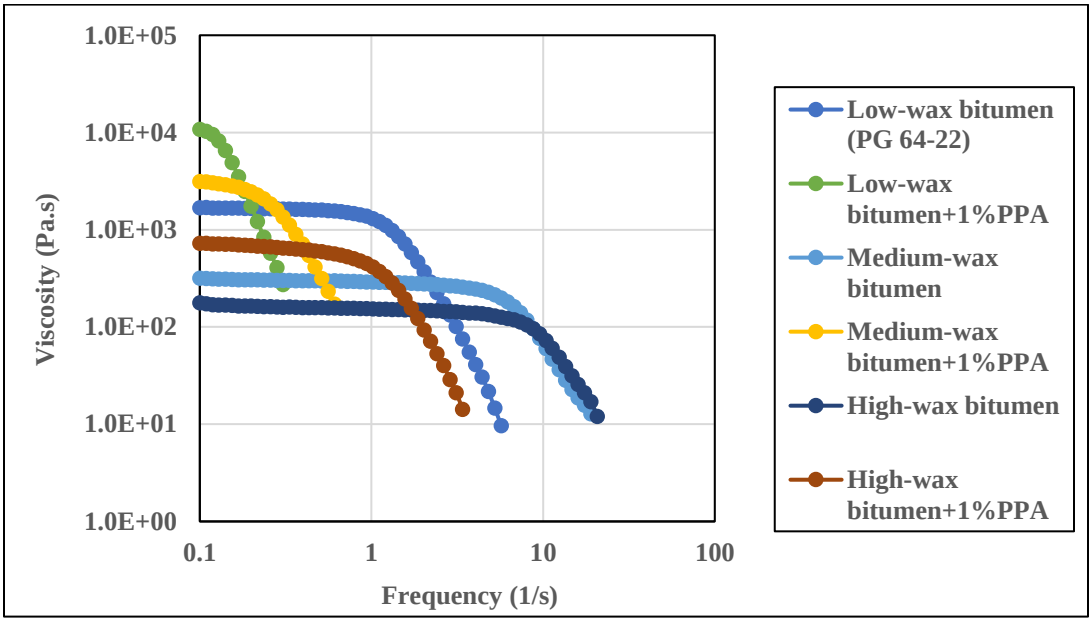

Figure 5.6. Viscosity results as a function of shear rate for low-, medium-, and high-wax samples modified with PPA, at 52 ºC

Table 5.4 . Power law parameters of shear-thinning for low-, medium-, and high-wax samples with and without PPA

Sample	Temperature °C	Power law index (n)	Consistency parameter (K)
Low-wax bitumen (PG64-22)	52	-2.35	4.0E+06
Low-wax bitumen+1%PPA	52	-3.21	1.9E+03
Medium-wax bitumen	52	-1.65	3.0E+07
Medium-wax bitumen+1%PPA	52	-2.12	3.8E+04
High-wax bitumen	52	-1.58	3.0E+07
High-wax bitumen+1%PPA	52	-2.36	9.7E+05

5.5.4 Multiple stress creep recovery test results

Multiple stress creep recovery results for bitumen, wax-doped bitumen, and PPA-modified wax-doped bitumen at 58 °C are presented in Figure 5.7 and Table 5.5. The results show that the addition of PPA to bitumen reduces the deformation, indicating that bitumen behaves as a more elastic solid. However, the addition of wax leads to higher deformation, indicating a more viscous behavior. The results show that the stiffening effect of introducing PPA is more dominant than the softening effect of wax.

The non-recoverable compliance (J_{nr}) shows an overall reduction compared to control and waxy samples. This can improve the rutting resistance associated with wax-modified bitumen and reduce permanent deformation. The high-wax samples showed the same trend as the medium-wax samples.

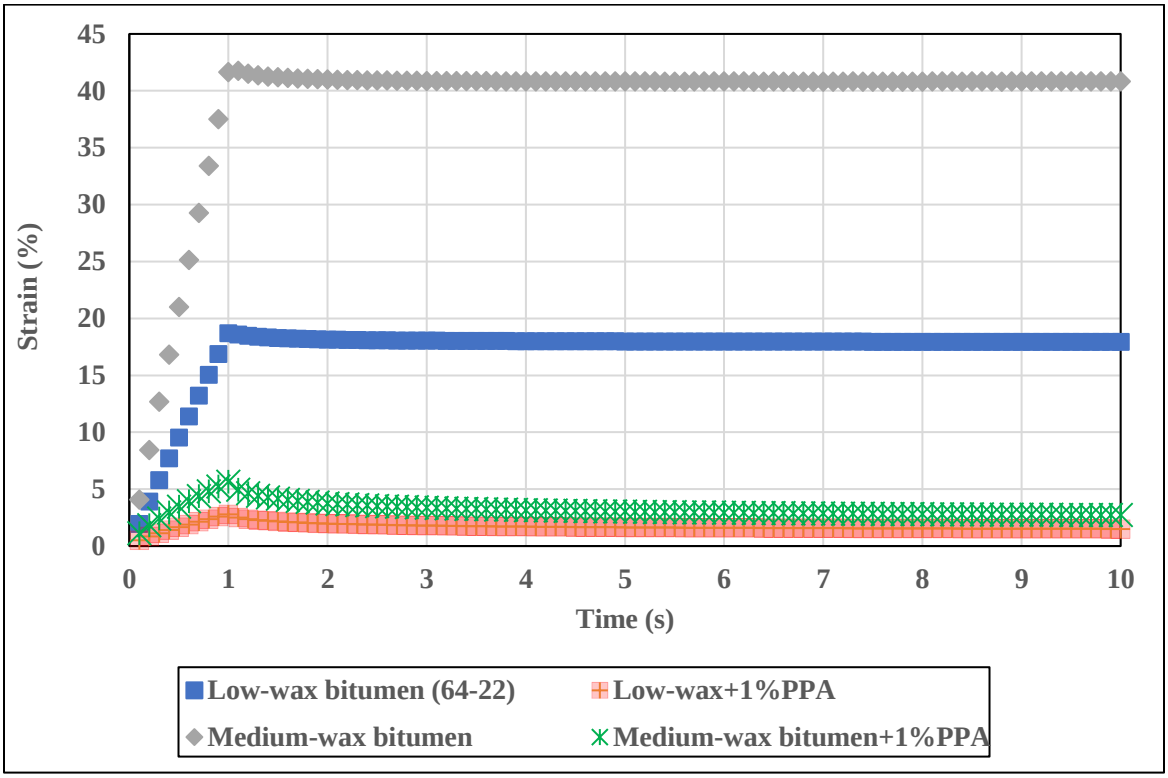

Figure 5.7 Creep recovery of first cycle of MSCR test at 0.1 kPa

Table 5.5 . Multiple stress creep recovery test results

MSCR Test Parameter	Low-wax bitumen	Low-wax bitumen+ 1% PPA	Medium-wax bitumen	Medium-wax bitumen+1%PPA	High-wax bitumen	High-wax bitumen+1%PPA
Jnr 0.1(1/kPa)	1.80	0.12	4.08	0.21	17.79	1.21
Jnr 3.2(1/kPa)	1.99	0.17	4.70	0.48	21.06	2.95
Jnr diff (%)	10.69	35.49	15.03	118.90	18.34	142.39

5.5.5 X-ray diffraction test results

The XRD results presented in Figure 5.8 illustrate the effect of PPA on wax crystallization in the bulk of bitumen. The results show that the presence of PPA did not change the extent or structure of wax crystals. The location of peaks associated with the wax in modified specimens is the same as that of the pure wax, which shows PPA doesn't affect wax crystallization.

It has been documented that low m-value and high stiffness of wax-doped bitumen is due to wax crystallization at low temperatures (Samieadel et al. 2018; Samieadel et al. 2017). On the other hand, Liu et al. showed that PPA is able to improve the rheological properties of wax-doped bitumen at low temperture (Liu et al. 2016). However, our XRD results show that PPA was not able to eliminate wax crystallization; therefore, the documented improvement is not due to change in crystallization of wax.

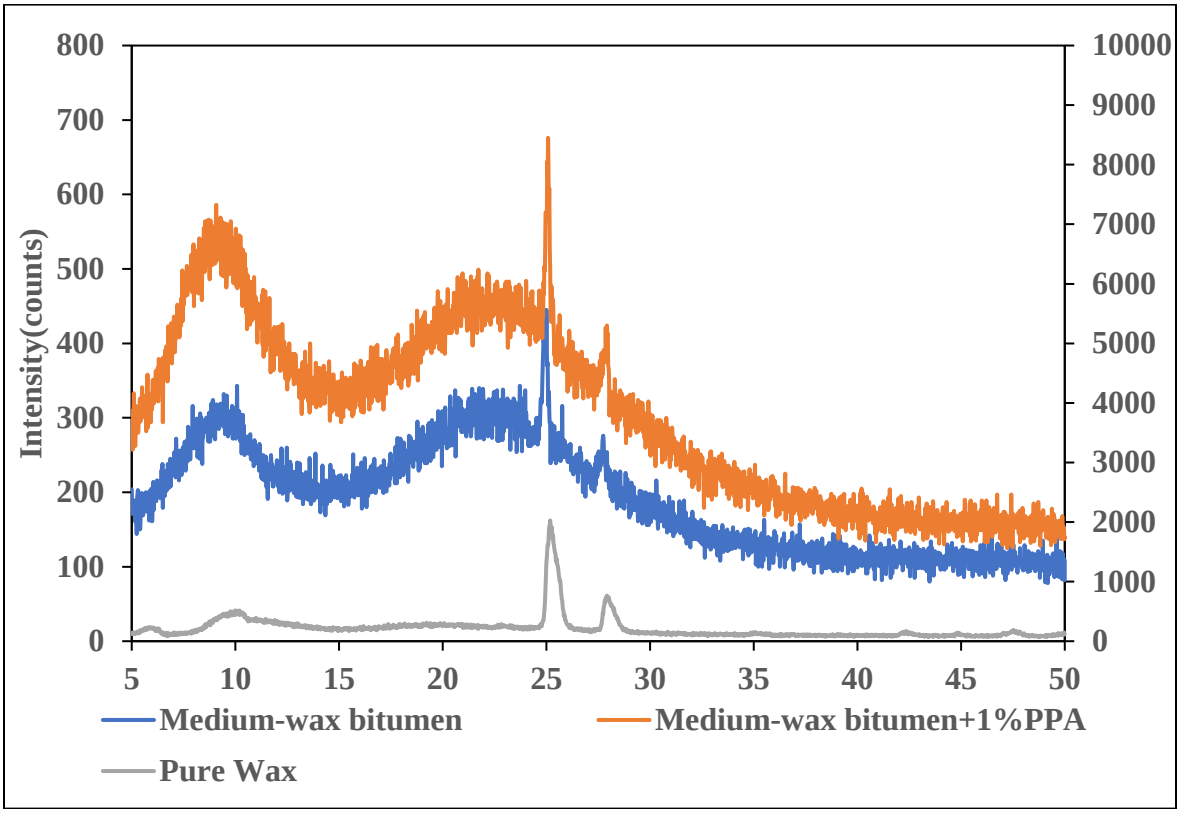

Figure 5.8. XRD results for medium-wax bitumen with and without PPA

5.5.6 TLC-FID analysis results

The fractions of saturates, aromatics, resins, and asphaltenes (SARA) were determined using TLC-FID and are presented in Figure 5.9. The results show that the addition of PPA to wax-doped bitumen reduces the resin fraction and increases the asphaltene fraction. Based on the mechanism explained by Baumgardner et al. (Baumgardner et al. 2005), this increase can be explained by interaction between resins and PPA, adding to the fractions which are insoluble in heptane or categorized as asphaltene.

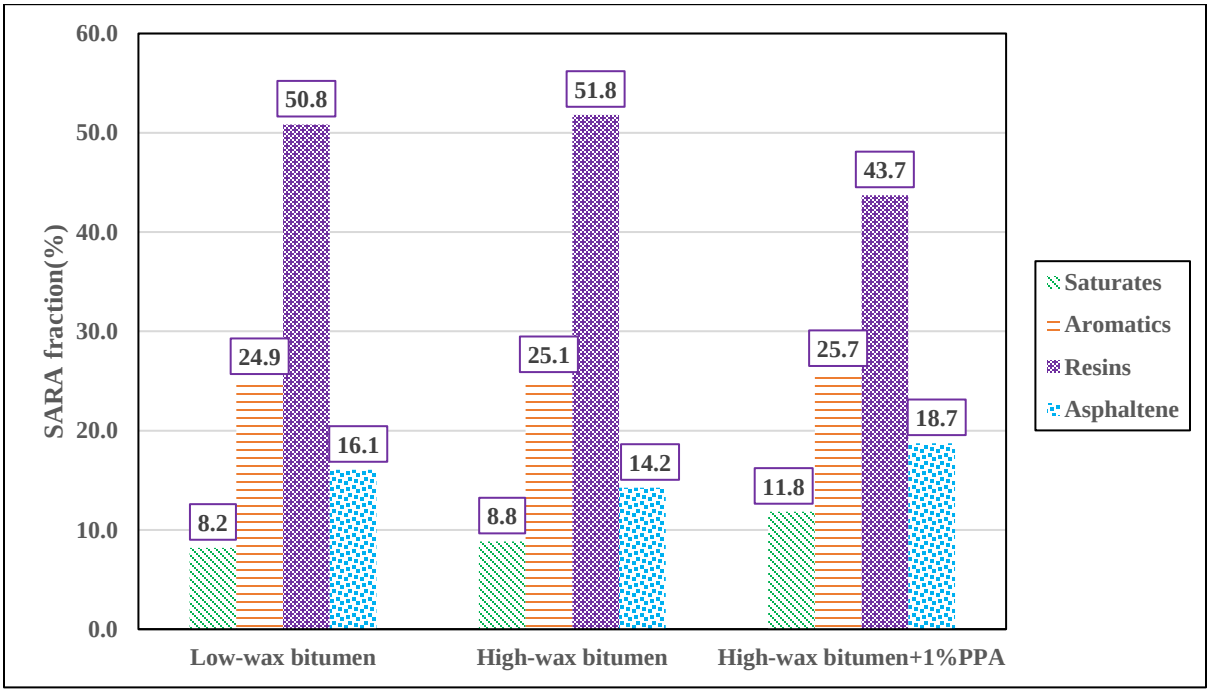

Figure 5.9. SARA fractions of low-wax and high-wax bitumen with and without PPA

5.5.7 Moisture susceptibility index test results

The moisture susceptibility index calculated by Eq 5.3 for low-, medium-, and high-wax bitumen with and without the presence of PPA are shown in Figure 5.10. The results show that the presence of wax increases the moisture susceptibility of bitumen, which can lead to less adhesion of bitumen to stone aggregate. However, the addition of PPA significantly reduces the moisture susceptibility of each wax-doped bitumen.

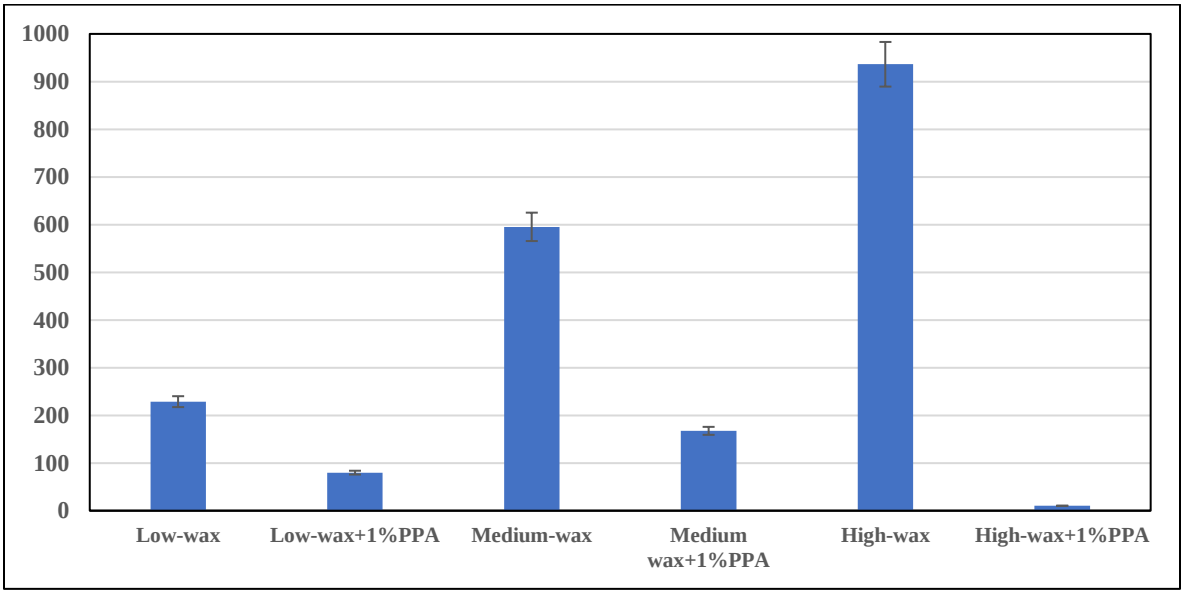

Figure 5.10. Moisture susceptibility index (percent change in contact angle before and after water exposure)

5.5.8 Critical low temperature results from BBR test

The results of stiffness and m-value at -12 ^{o}C are shown in Figure 5.11-top. The results indicate that addition of wax stiffens the bitumen while presence of PPA can moderate this effect of wax and reduce the stiffness. To further investigate the effect of each modifier, the critical low temperatures were studied using two temperatures of -12 ^{o}C and -18 ^{o}C.

Low temperature limits are referred to temperatures at which stiffness is 300 MPa or m-value is 0.3 (Figure 5.11) (Samieadel et al. 2018); the lower value between these two are referred to as critical low temperature (T_c). The difference between these two are referred to as Delta Tc (ΔTc) and is shown in Table 5.6. It can be observed that presence of wax leads to reduction of Tc from -17 ^{o}C in low wax to -12C in medium wax; this is a

clear evidence of wax increasing susceptibility of bitumen to cracking at low temperature. It can be also observed that PPA has opposite effect on the low-wax and medium-wax bitumen. PPA addition found to have positive effect on Tc in low-wax bitumen, however its effect on medium wax bitumen was negative. Addition of wax increases the stiffness of material and lowers the m-value which has been evidenced in previous research (Samieadel et al. 2018).

Delta Tc ($Tc_{\text{(corresponding to stiffness of 300MPa)}} - Tc_{\text{(corresponding to m-value of 0.3)}}$) is controlled by stiffness in low-wax scenario as shown by positive values, but it becomes m-controlled in medium-wax scenarios (negative values). This in turn shows strong effect of wax on dismantling stress relaxation capability of bitumen irrespective of its stiffness. The change in delta Tc due to addition of PPA to low-wax scenario is not significant, however in medium-wax scenario addition of PPA caused delta Tc to increase by nearly 5 times; this is a strong evidence of PPA's amplifying negative effect of wax on bitumen's low temperature performance.

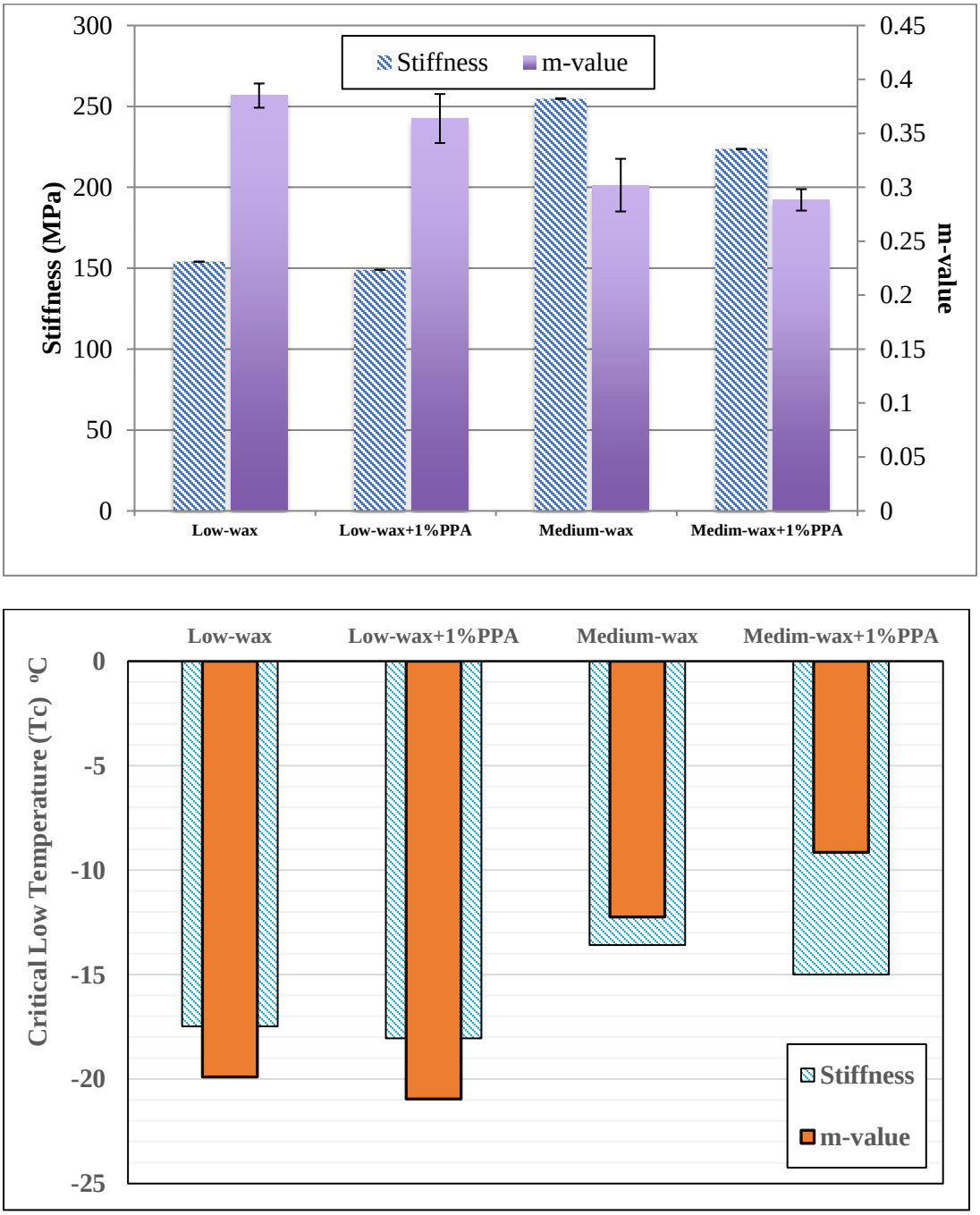

Figure 5.11. Bending Beam rheometer results: Top- Stiffness and m-vlaue at -12 °C.

Bottom- Critical low temperatures values for different samples

Table 5.6 ΔTc results for low wax and medium wax bitumen samples with and without presence of PPA

Sample	**ΔT_c**
Low-wax bitumen	2.43
Low-wax bitumen+1%PPA	2.9
Medium-wax bitumen	-1.34
Medium-wax bitumen+1%PPA	-5.85

5.6 Molecular dynamics simulation results

5.6.1 Radial distribution function

Figure 5.12 shows the results for the radial distribution function for 20 resin molecules in a box of heptane medium (blue line) calculated based on Eq 5.2. The radial distribution function shows an increase in the presence of PPA, with a peak appearing at 7.5 Å; this can indicate higher accumulation of resins in the presence of PPA. Furthermore, in snapshots presented in Figure 5.13 an accumulation of resin molecules close to PPA molecules can be observed. This can be attributed to the formation of hydrogen bonds between the hydrogen in a PPA molecule and the nitrogen in resin molecules (Figure 5.14). The criteria for hydrogen bond are defined in forcefield

equations which in PCFF+ forcefield the maximum hydrogen donor and acceptor distance should be 3Å.

However, after the addition of wax to the box, the resin molecules become more dispersed, resulting in a reduction of RDF (Figure 5.11). A lower RDF means that resin molecules are less probable to locate at a specific distance with respect to each other, indicating smaller size of fluctuates of resin-PPA. This may be attributed to wax hindering the effect of PPA in bringing resins together.

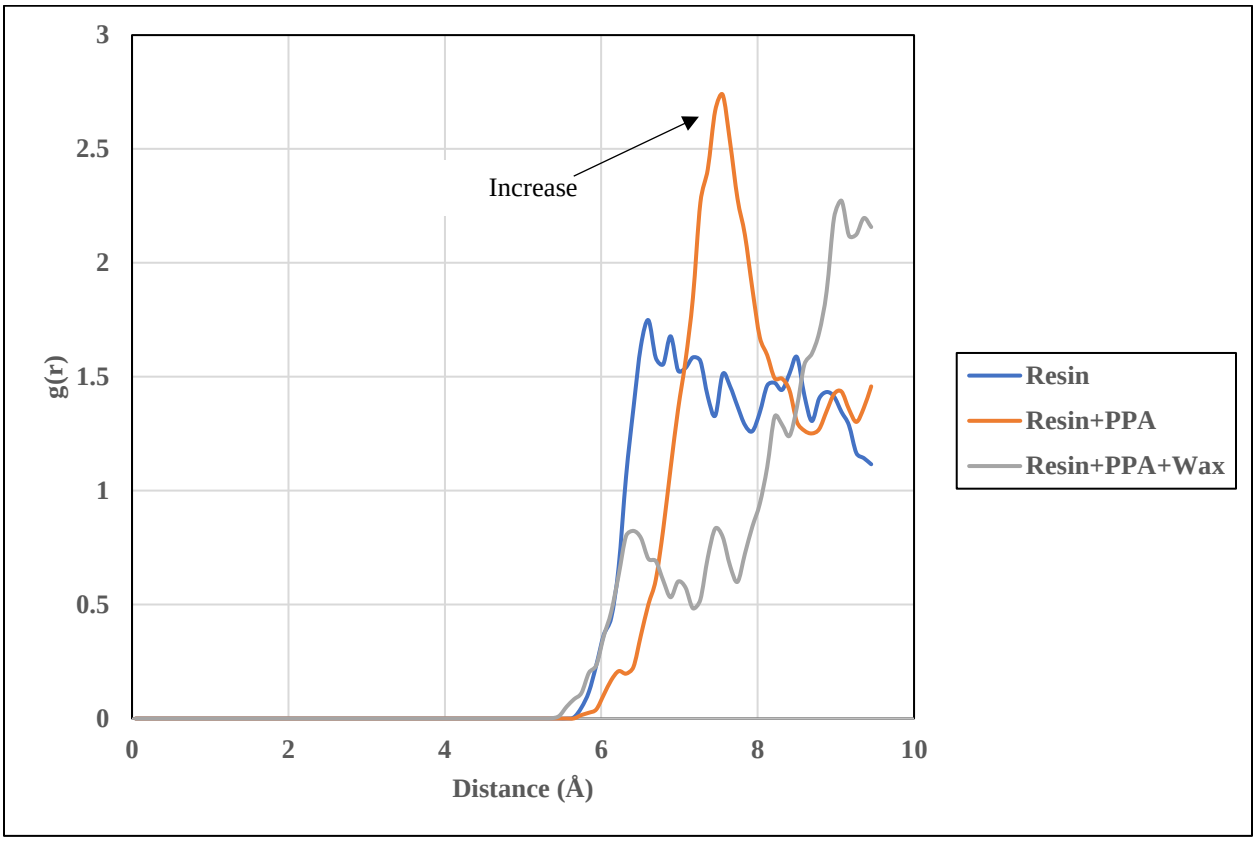

Figure 5.12. Radial distribution function results for 20 resin molecules with and without the presence of PPA and wax

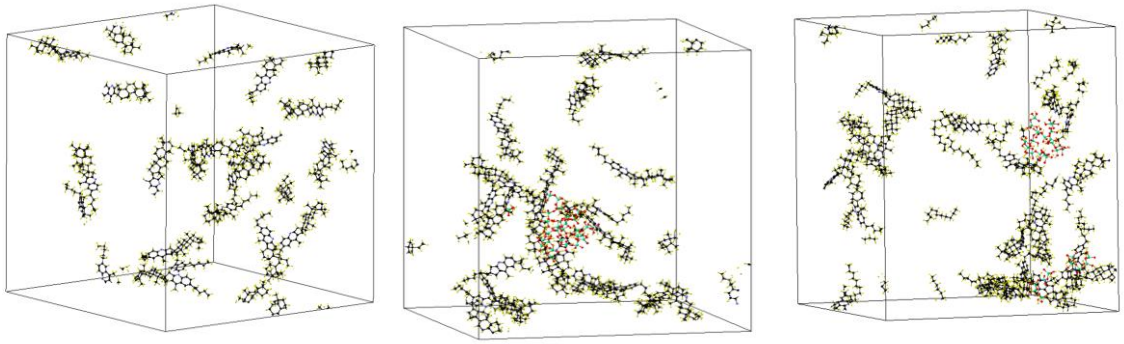

Figure 5.13. Snapshot of resin molecules: Left- Isolated resin molecules; Middle- Resin and PPA combination; Right- Resin with both PPA and wax (heptane molecules are hidden for clarity). Red circle in middle snapshot shows accumulation of resin molecules around PPA molecules.

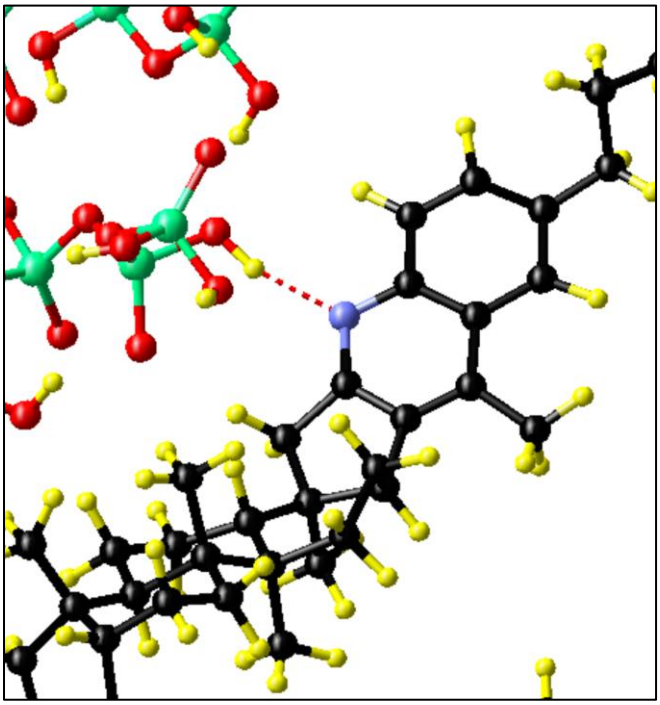

Figure 5.14. Formation of hydrogen bond (red dashed line) between PPA hydrogen (yellow) and resin nitrogen (blue) indicated by software outputs

5.7 Summary

Using comprehensive laboratory experiments and computational modeling, this paper examined the interplay between wax and PPA in a bitumen matrix. The results of computational modeling showed that PPA has a strong interaction with fused aromatics such as those classified as resins in bitumen. This strong interaction was attributed to hydrogen bonding between PPA oxygen as donor and resin's nitrogen as acceptor atoms. Computational analysis further showed that the interaction between resin molecules was amplified in the presence of PPA, leading to a 70% increase in the radial distribution

fucntion. However, resin molecules intercation was reduced when wax was present, causing resins to become more scattered, as evidenced by a 60% decrease in the radial distribution function.

Such interactions were evidenced in laboratory experiments by the reduced solubility of resins in heptane, causing the resins to precipitate out in heptane. This in turn led to 8.1% decrease in resin content upon introduction of 1% PPA. The abovementioned interactions further promoted elastic behavior within the bitumen matrix through the formation of resin-PPA assemblies and improvemed bitumen's glass transition temperature (Tg). The results showed that crossover frequency was reduced by 93% and Tg was reduced from -36 ^{o}C to -40 ^{o}C when 1% PPA was introduced to bitumen. A study of moisture susceptibility showed all bitumen specimens containing PPA (regardless of wax content) had better resistance to de-wetting when exposed to water than their counterparts without PPA.

The interplay of PPA and wax showed to be temeprture dependent since paraffin wax changes its phase with temperature. The presence of wax showed to hinder the effects of PPA on bitumen at high temperture, and applify it as low temperture. The effect of the above interplay was more evident when the wax content increased from low to medium to high concentrations.

Previous studies showed that wax crystallization can lead to higher stiffness and lower m-value (Pahlavan et al. 2016; Samieadel et al. 2018; Samieadel et al. 2017). Addition of PPA to wax modified bitumen has shown to increase m-value and decrease

stiffness (Liu et al. 2016); our study confimed the reduction of stiffness but did not show any increase in m-value of waxy bitumen upon addition of PPA. Also, our XRD results didn't show any change in crystallization of wax with presence of PPA suggesting that reduction of stiffness of waxy bitumen is not due to prevention of wax crystallization. The observed reduction in stiffness can be due to wax preventing self-assmebly of resins molecules. The critical low temperatures cracking of bitumen showed that interplay of wax and PPA amplifies negative effect of wax on bitumen's low temperture performance causing the bitumen to be more prone to cracking as evidenced by a five times increase in delta Tc of waxy bitumen upon introduction of PPA. The study results help inform formulators and manufacturers about unseen interplay between bitumen additives such as wax and PPA causing unwanted consequences on pavement performance.

6 USING NANOPARTICLES AS CARRIER FOR WAX DISPERSION

6.1 Introduction

Paraffin wax has been used as a softener and to improve the workability of asphalt (Samieadel et al. 2017). The term “wax” usually refers to a material that is a white solid at ambient temperature and melts at higher temperature to form a low-viscosity liquid (Soenen et al. 2014). All bitumen contains a fraction of wax that can affect the rheological properties of the bitumen (Canestrari et al. 2013). Besides the natural wax in bitumen, adding wax to bitumen lowers the mixing and compaction temperature of asphalt by 20 to 40°C, which helps to reduce energy consumption and extend the construction season (Croteau and Tessier 2008; Edwards and Redelius 2003; Lu and Redelius 2007; Pahlavan et al. 2016). This type of asphalt, which maintains lower viscosity at lower temperatures, is known as warm-mix asphalt (WMA).

The two waxes commonly recognized in crude oils and distillates are paraffin waxes and microcrystalline waxes (Edwards and Redelius 2003). Paraffin waxes are mainly composed of n-paraffins (n-alkanes), with minor amounts of isoparaffins and cycloparaffins. Paraffin waxes crystallize as plates or needles (Edwards et al. 2006), and their melting points are in the range of 50 to 70°C; their melting points are reduced to 20-30°C when blended with bitumen (Butz et al. 2000; Samieadel et al. 2017). Microcrystalline waxes are aliphatic hydrocarbon compounds containing a considerable amount of isoparaffins and cycloparaffins. Microcrystalline waxes have a less distinct melting point and a high average molecular weight (Musser and Kilpatrick 1998).

Paraffin wax also has some adverse effects. Paraffin wax is able to decrease the viscosity of bitumen and make bitumen softer, but its melting point at 60°C (Rathod and Banerjee 2014) will increase bitumen's sensitivity to rutting distress. Furthermore, wax easily crystallizes at low temperature, which results in an increase in stiffness and cracking at low temperature (Richter 2002; Samieadel et al. 2018; Samieadel et al. 2018). The low adhesive property may also cause issues with stripping of aggregates in pavements (Lu and Redelius 2007).

In order to solve the problem of wax crystallization in the bulk of bitumen and to better blend paraffin wax with bitumen, this study introduces nano-zeolites as carriers for paraffin wax. Nano-zeolites are the nanocrystalline form of zeolites, which are a type of nanoporous (pore size < 2 nm) crystalline aluminoslicate material. Compared to conventional micron-sized zeolites, nano-zeolites not only have improved external surface area due to the reduction of size to nanoscale, they also have additional inter-particle meso-pores (2 – 50 nm) and small macro-pores (50 – 200 nm). Because of these unique features, nano-zeolites have demonstrated an improved efficiency in their conventional catalysis (Choi et al. 2009), separation (Xu et al. 2019), and other emerging applications in areas such as medicine, antimicrobials, and the food industry (Chen et al. 2017; Mintova et al. 2015). In this study, nano-zeolites are believed to be a promising carrier for large paraffin molecules due to nano-zeolites' large external surface areas and large pore volumes. The scalable synthesis recently developed (Chen et al. 2019) makes nano-zeolites more promising for further practical uses.

The hypothesis is to use nano-zeolite impregnated with paraffin wax molecules as a warm-mix additive to make paraffin wax more dispersed in the bulk of asphalt. Theoretically, nano-zeolite has a stiffening effect, so once it is mixed with paraffin wax to modify bitumen, it is capable of counteracting the softening effect of paraffin wax at higher intermediate temperature and reducing the susceptibility of wax-modified bitumen to rutting. Second, paraffin wax will be melted and mixed with nano-zeolite prior to mixing with bitumen. Nano-zeolite pores will be impregnated with melted paraffin wax to promote an isomerization process to better disperse paraffin wax and prevent the crystallization process. Furthermore, the chance of agglomeration of nano-zeolite particles will decrease, and nano-zeolite will be able to play the role of a carrier for paraffin wax. As a result, wax molecules are released after addition of Winz (nano-zeolite impregnated with wax) to asphalt. The acidic compounds of bitumen then replace the wax on nano-zeolite. As a result, the released wax will be less prone to crystallization while diversion of acidic compounds help improving resistance of interface of bitumen and stone aggregate to moisture damage.

6.2 Material Preparation

Nano-zeolites for this study were synthesized by first preparing an aluminosilicate precursor mixture with the composition of $2.5Na_2O$: $1.0Al_2O_3$: $4.0SiO_2$: $33H_2O$. The mixture was prepared by dissolving 17.028 g of NaOH pellets (acquired from Sigma-Aldrich) and 55.046 g of water glass (also from Sigma-Aldrich) in deionized water (35.498 g), followed by the addition of 27.473 g of metakaolin (MetaMax® from BASF, SiO_2:

53.0%, Al_2O_3: 43.8%, Na_2O: 0.23%, K_2O: 0.19%, TiO_2: 1.7%, and Fe_2O_3: 0.43%). After stirring with a mechanical mixer (IKA RW 60 digital mixer) at 800 rpm for 40 min, a visually homogeneous and free-flowing solution was obtained. The solution was then poured into 500-ml autoclavable polypropylene bottles, and the bottles were tightly closed and placed in a laboratory oven at 90 °C for 48 hours. After the heating, the products were taken out and washed with deionized water multiple times until the pH of the supernatant was about 8. The final product was collected after centrifugation; then it was dried in a laboratory oven at 90°C overnight and stored in sealed glass vials at room temperature for further use.

The bitumen used in this study is graded as PG 64-22, which is commonly used in the United States; it was acquired through Western Asphalt Inc. in Arizona. The wax that was used for bitumen modification is a paraffin wax (P31, with melting point of 53–57°C, acquired from Fisher Scientific). The wax was introduced at 1%, 3%, and 5% dosage by weight of the initial bitumen and was blended into the bitumen at 135°C for 30 minutes.

To impregnate the nano-zeolite with paraffin wax, the nano-zeolite was first heated in the oven at 100°C for two hours to reduce the moisture content. Then the weighted nano-zeolite was placed in a glass container on a hot plate at 100°C. The wax granules were then poured around it and hand-blended until there was no remaining liquid paraffin wax. The samples were sieved by a 425 μm sieve. Figure 6.1 shows the process of preparation of nano-zeolite impregnated with wax (Winz). To prepare the Winz-modified bitumen, the amount of Winz was calculated based on the amount of wax to reach the same percentages

of 1%, 3%, and 5% of bitumen. For instance, 2g of Winz was added to 20g of bitumen to produce a 5% Wax (Winz) bitumen sample, since each gram of Winz has equal portions of wax and nano-zeolites. For the sake of comparison, in a second scenarios nano-zeolite and wax were added to bitumen separately; the latter scenario was titled as "Control+5%Wax+5%NZ".

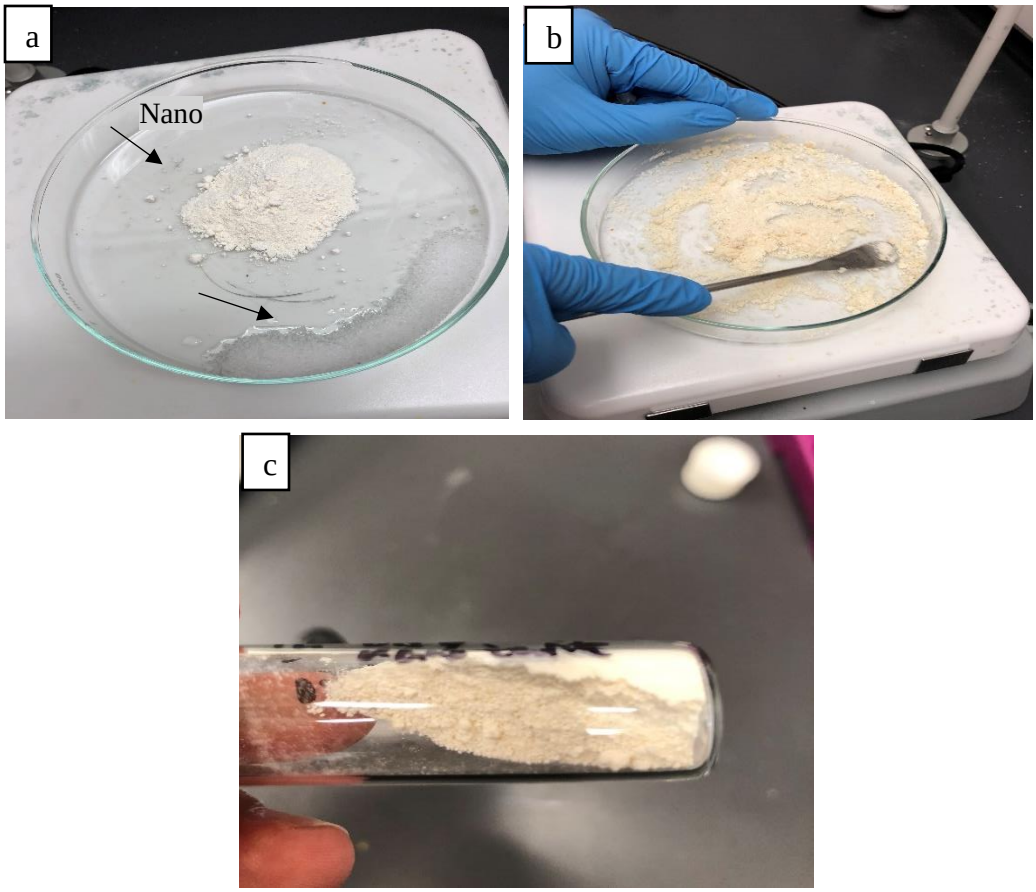

Figure 6.1 Different stages of producing Winz particles: a) nano-zeolite powder and wax were placed on a hot plate. b) nano-zeolite and melted wax are mixed with a spatula. c) The Winz powder was saved for bitumen modification.

6.3 Testing Methods

6.3.1 Scanning electron microscopy

Scanning electron microscopy (SEM) images of Winz samples and nano-zeolite samples were collected using an XL30 environmental FEG (FEI) microscope operating at 10 kV acceleration voltage. For SEM, the sample powders were sprinkled onto the SEM stub affixed with carbon conducting tape, and the samples were then coated with Au/Pt for ~ 6 nm before imaging. The coupled energy dispersive X-ray spectroscopy (EDS) analysis was performed at 20 kV and ~ 11 mm working distance.

6.3.2 Rotational Viscosity

Measurements of viscosity were conducted following ASTM D4402 (ASTM D4402 2015), using a Brookfield Viscometer RV-DVIII Ultra by applying a rotational shear on the selected material. Test specimens were prepared by pouring 10.5 grams into a specific aluminum chamber, then allowing it to cool to room temperature. Samples were preheated in an oven for 30 minutes before being placed into the temperature-controlled thermoset. After thermal equilibrium within the sample was reached, three viscosity readings were collected at three-minute intervals until the readings had a range of less than 100 cP (0.1 Pa.s). The average of these three numbers was recorded as apparent viscosity. The rotational speed chosen for this study was 20 rpm, with measurements conducted at 105°C, 120°C, 135°C, and 150°C.

6.3.3 Dynamic shear rheometer: frequency sweep test

A dynamic shear rheometer was used to investigate the elastic and viscous behavior of wax-modified bitumen by measuring the shear stress and shear strain, which was then used to calculate the complex modulus (G*) of the material. Complex modulus is typically defined as a measure of a bitumen's resistance to deformation when repeatedly sheared. In order to determine G*, a relatively wide range of oscillations were applied to the sample, ranging from 0.1 rad/s to 100 rad/s, at temperatures ranging from 76°C to 4°C at 6-degree intervals using 31 frequencies. From the resulting data, G* master curves were generated using the principle of time-temperature superposition at a reference temperature of 40°C. Shift factors were generated using the Williams, Landel, and Ferry (WLF) method (Williams et al. 1955). For temperatures from 70°C to 40°C, the 25 mm spindle was used; for temperatures from 40°C to 4°C, the 8 mm spindle was used. The frequency at which the graphs for elastic modulus and viscous modulus intersect is the crossover frequency of the specimen. The crossover temperature is the temperature at which the loss modulus and elastic modulus are equal.

6.3.4 Dynamic shear rheometer: shear rate sweep test (SRST)

To further investigate the change in particle size and the intermolecular interactions of wax and WINZ-modified bitumen, a shear rate sweep test from 0.1 to 30 (1/s) was performed at 52°C using an 8mm parallel plate. This test reveals the thixotropic

characteristics of bitumen, which is indicative of the intermolecular interaction in bitumen.

As the shear rate increases (>10 1/s), shear thinning occurs, and the data can be fitted to a power law model (Chhabra 2010) using Equation 1.

$$\boldsymbol{\sigma = K\dot{\gamma}^{n}} \quad \textbf{and} \quad \boldsymbol{\eta = K\dot{\gamma}^{n-1}} \qquad \textbf{Equation 6.1}$$

where η is viscosity, $\dot{\gamma}$ is shear rate, σ is shear stress, and n is the power law index. K is the flow consistency index, a measure of viscosity under non-Newtonian flow (Ajienka and Ikoku 1990).

6.3.5 Multiple stress creep recovery (MSCR)

The MSCR test was performed following the AASHTO T350-1433 (AASHTO T 350-14 2014) specification, in which the bitumen is subjected to 10 cycles of stress and recovery of 1 and 9 s, respectively, at two stress levels of 0.1 and 3.2 kPa, at 58 °C. Before the start of the test, samples were subjected to a preload cycle. Afterward, nonrecoverable creep compliance (known as Jnr) and the recovery difference between stresses of 0.1 and 3.2 kPa were determined.

6.3.6 Differential scanning calorimetry (DSC)

Bitumen samples with 1%, 3%, and 5% of added wax along with the base bitumen and wax were tested to determine the heat capacity and glass transition temperature (Tg) and to illustrate the effect of wax and the method of impregnation of nano-zeolite with wax on the bitumen properties. The heat flow measurements were determined by the three-run method (ASTM E1269-11 2018), and the glass transition temperature (Tg) was determined

in a second heating cycle (Slough and Hesse 2006). The three-run heat capacity approach uses an isothermal – ramp – isothermal DSC method. This method consists of empty pans, sample, and a reference material such as sapphire. A high heating rate of 20°C/min is used to provide good signal to noise that can't be achieved with slower heating rates. For this method, provisions need to be made to correct or compensate the data for differences in the mass of the sample pan and the reference pan. To minimize the effect of instrument drift, the isothermal segments are used. The empty pan baseline was subtracted from the reference results to determine a conversion factor of heat flow (mW) to heat capacity (J/°C). Replicate heat capacity determinations using the three-run method typically agree within about 3% or less. The three-run method can be done on almost any differential scanning calorimeter with a minimal amount of instrument preparation. The test started at -80 and ended at 160°C The samples (5-7 mg) were placed in Tzero aluminum pans with hermetic lids. The calculations of glass transition point and enthalpy associated with endothermic peaks were done using TRIOS software developed by TA Instruments.

6.3.7 Bending beam rheometer (BBR)

The BBR test was used to characterize the mechanical performance of bitumen at subzero temperatures and to measure the stiffness and m-value of bitumen (ASTM D6648 2016). The M-value measures the ability of a bitumen beam sample (12.5 mm wide, 127 mm long, and 6.25 mm thick) to relax stress while a constant load of 980 mN is applied at the middle point of the beam. After applying the load, the deflection of the beam was measured, and the stiffness and the m-value were calculated at the 60-second point.

To meet the ASTM standard, a bitumen sample should have a stiffness lower than 300 MPa and an m-value higher than 0.3 at the test temperature specified for each PG grade (10^{o}C higher than the lower PG grade). In the case of PG 64-22, the test temperature is -12^{o}C. In this study, BBR test results are used to calculate the temperature at which the stiffness is equal to 300MPa and the m-value is equal to 0.3. The lower of the two temperatures is called the critical low temperature; the difference between the two temperatures (ΔT_c) has been related to non-load-related cracking of asphalt pavement and the fatigue performance of pavement (Anderson et al. 2011; Menapace et al. 2018).

6.4 Molecular Dynamics Simulations

A molecular dynamics simulation was performed on a system at equilibrium state composed of three parts: a slab of silica (SiO_2) in crystal form with a separation of 80 Å, to represent nano-zeolite particles; wax molecules of $C_{11}H_{24}$; and decanoic acid, which is commonly found in the acidic part of bitumen. The study of acid-silica interaction in bitumen is due to the increase in moisture susceptibility of bitumen because of the presence of the acidic part. This increase is because of the hydrophilic nature of acids and the consequent interaction with water, which results in a reduction in the cohesion and adhesion properties of bitumen.

To investigate the interaction of silica-based structures with wax and acid, Large-scale Atomic/Molecular Massively Parallel Simulator (LAMMPS) software in a MedeA® environment version 2.2 was used for simulation. The study focused on investigating the interaction of wax and acid molecules with silica. The model was built in the MedeA®

environment using the molecular builder. In this study, the PCFF+ force field, which is an extension of the PCFF force field, is used. The force field refers to the functional form of parameters used to calculate the potential and kinetic energy of the system of atoms and molecules. PCFF+ is an all-atom force field designed to provide excellent accuracy on hydrocarbon and liquid modeling for *ab initio* simulations (Sun et al. 1994; Waldman and Hagler 1993). This force field includes a Lennard-Jones 9-6 potential for intermolecular and intramolecular interactions and specific stretching, bending, and torsion terms to involve 1-2, 1-3, and 1-4 interactions (Ungerer et al. 2014).

6.4.1 Simulation method

A slab of silica (SiO_2) was made using the MedeA interface with periodic boundary condition applied. The ensemble of wax molecules was simulated separately and then merged to the cell that includes the silica structure. The silica walls were separated by a distance of 80 Å, to simulate the nano-pores of nano-zeolite. Initially, the wax and silica were equilibrated in an NVT ensemble for 500 ps; then the decanoic acid molecules (at equilibrium state) were added to the system to study the interaction preferences of the three materials (wax, acid, and silica). The simulations started at a high temperature of 800K, annealing to 370K, which was selected as the target temperature.

6.5 Results and Discussion

6.5.1 Scanning electron microscopy images

The morphology of the 5% Winz sample and its wax distribution were investigated by scanning electron microscopy (SEM) (Figure 6.2). As shown in the low-magnification SEM image (Figure 6.2 a), the particle sizes macroscopically are quite large and heterogeneous, ranging in size from a few µm up to 500 µm. Higher-magnification imaging reveals that each of those large particles consists of sub-micron-sized particles that agglomerate together (Figures 6.2 b – c). Those sub-micron-sized particles exhibit smooth surfaces and relatively uniform sizes in the range of 200 – 500 nm (Figure 6.2c). The sizes of primary Winz particles are consistent with those of pure nano-zeolites before wax impregnation. However, the pure nano-zeolites show surfaces that are much more textured (Figure 6.2d); this confirms that in the Winz samples, the nano-zeolites are impregnated by waxes, leading to the smooth surfaces. Notably, areas examined in the Winz sample revealed a homogeneous distribution of smooth-surface wax-impregnated particles, without segregation of a region of pure wax. Nonetheless, small regions of pure wax were still observed, as shown in the SEM image and EDS result in Figure AA1 (Appendix A); this could be due to a limitation of the hand-blending method.

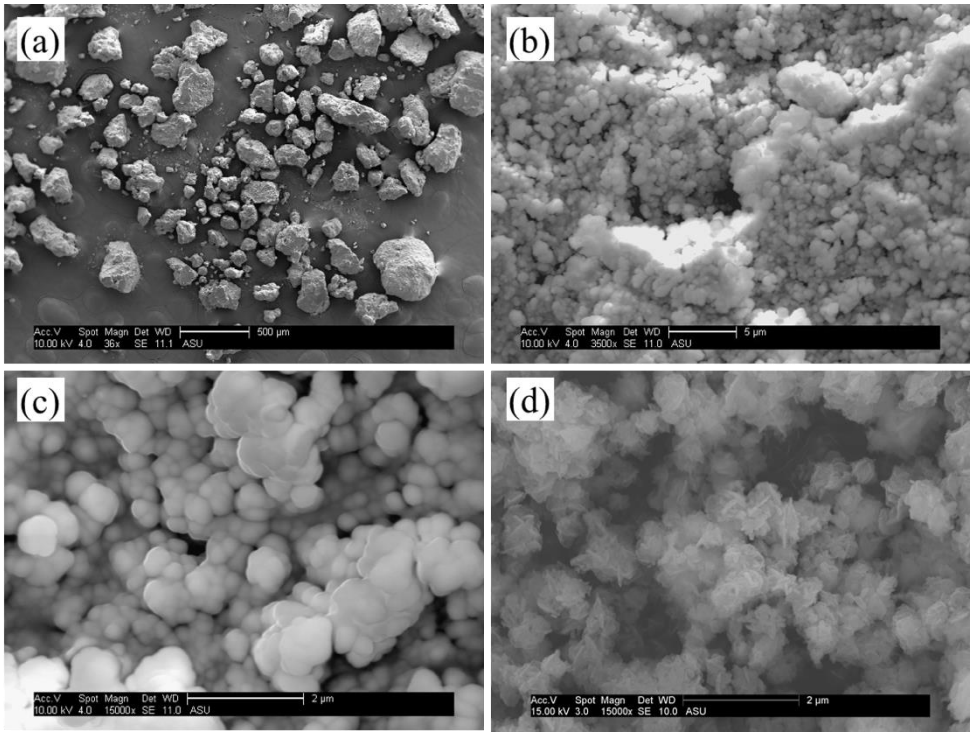

Figure 6.2 Scanning electron microscopy (SEM) images of nano-zeolite impregnated with wax (Winz). Samples (a – c) are different magnifications. Sample (d) is pure nano-zeolite.

6.5.2 Rotational viscosity

Figure 6.3 shows the viscosity results for control samples and samples modified with either wax-impregnated nano-zeolite (Winz), or separately added nano-zeolite and wax. The results show that the addition of wax decreases the viscosity at all temperatures. The addition of nano-zeolite and wax separately had the same effect as wax-impregnated nano-zeolite; this suggests that wax molecules are released from nano zeolite and blended into the bitumen.

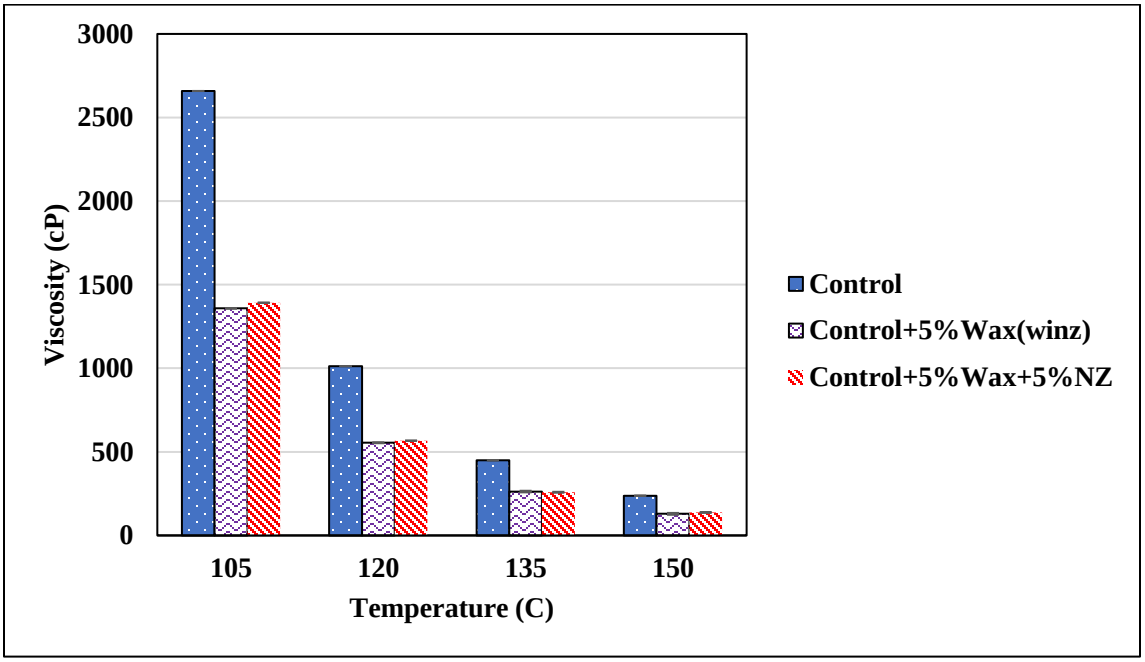

Figure 6.3 Rotational viscosity results for bitumen modified with either nano-zeolite impregnated with WINZ, or separately added nano-zeolite and wax

6.5.3 Complex modulus and crossover frequency

Figure 6.4 shows the results for the complex modulus of bitumen modified with either wax, nano-zeolite impregnated with wax (Winz), or separately added nano-zeolite and wax. All the graphs were made using time-temperature superposition laws at a reference temperature of 40°C. The complex modulus at higher frequency shows lower values for the samples containing wax, which is an indication of softer bitumen at higher frequency or lower temperatures. The 5% Winz sample is slightly stiffer than the 5% Wax modified sample, which can be due to the presence of nano-zeolite particles. The results also show there is no difference in high temperature properties between adding nano-

zeolite and wax separately and adding wax-impregnated nano-zeolite. The latter is an indication of wax being released when added via wax-impregnated nano-zeolite.

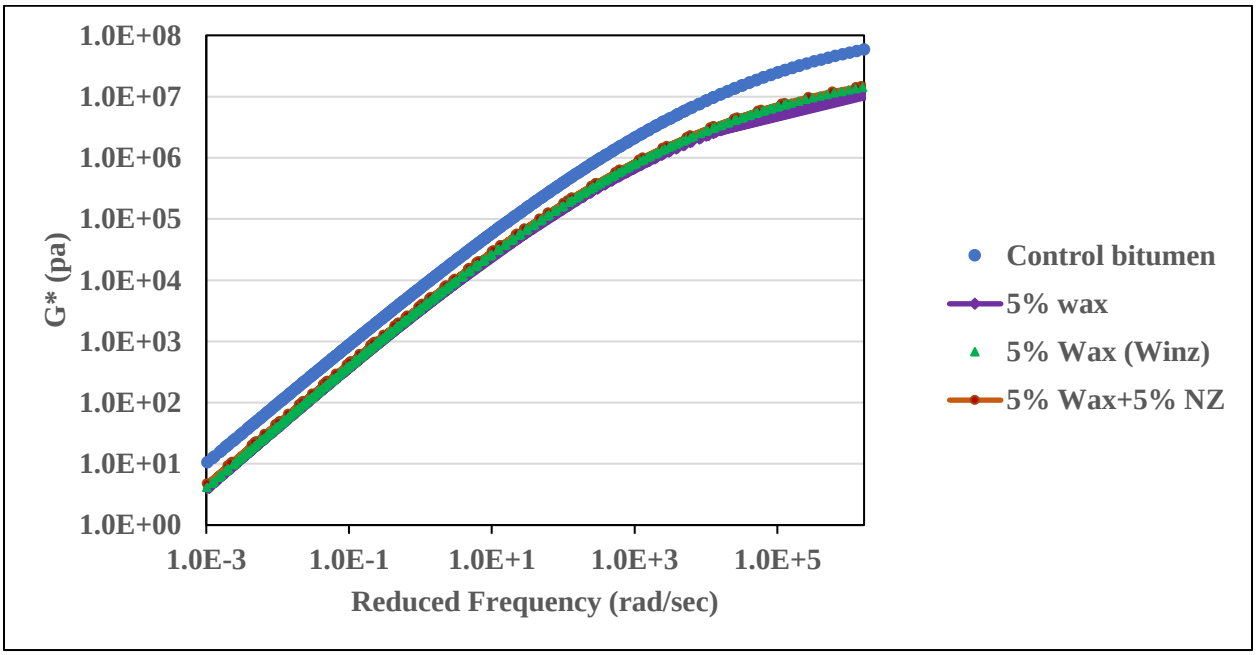

Figure 6.4 Complex modulus results for samples containing wax, wax-impregnated nano-zeolite (Winz), and wax and nano-zeolite added separately

Figure 6.5 shows the graphs for storage and loss modulus, and Table 6.1 presents the values for crossover frequency and modulus at 13°C. Crossover frequency is a measure of stiffness: material with a higher value of crossover frequency has less molecular interaction, and material with smaller value of crossover frequency has higher molecular interaction (Oldham et al. 2019). This result shows that as the wax amount increases in bitumen, the crossover frequency shifts to a lower value. A lower crossover frequency is an indication of stiffer material, which can be attributed to crystallization of wax in

bitumen. Furthermore, the results show that when wax was introduced through nano-zeolite instead of being directly added to bitumen, the resulting sample showed a higher crossover frequency that can be due to enhanced dispersion of wax due to presence of nano-zeolite. It further shows that wax is released from nano-zeolite into the bitumen.

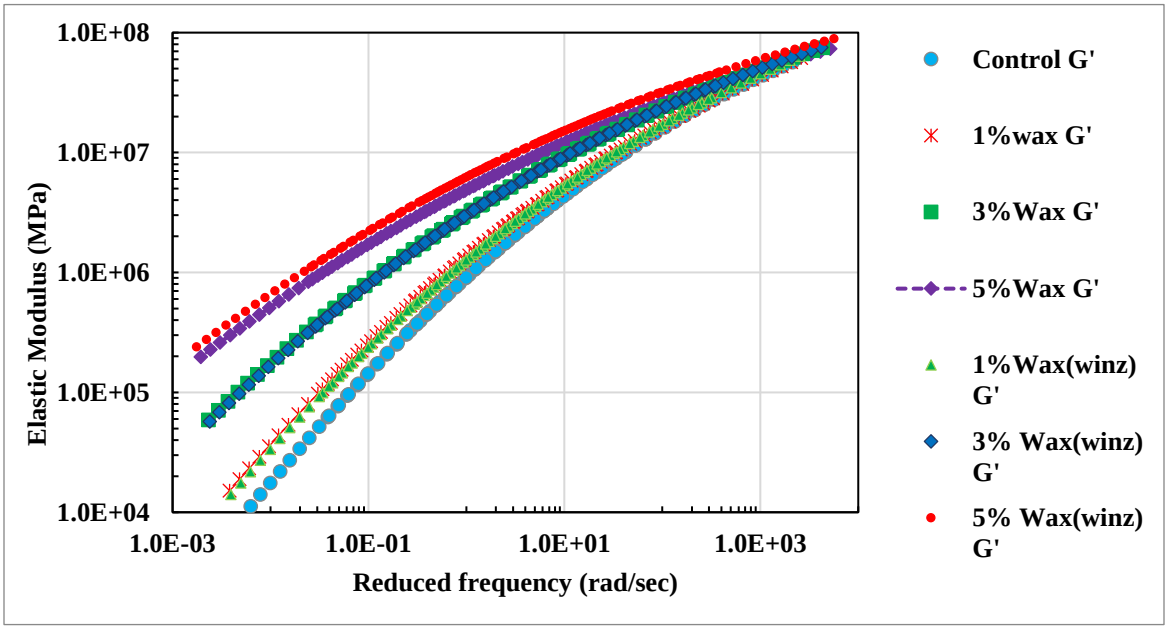

Figure 6.5-a. Elastic modulus results of control and modified samples at reference temperature of 13 ºC

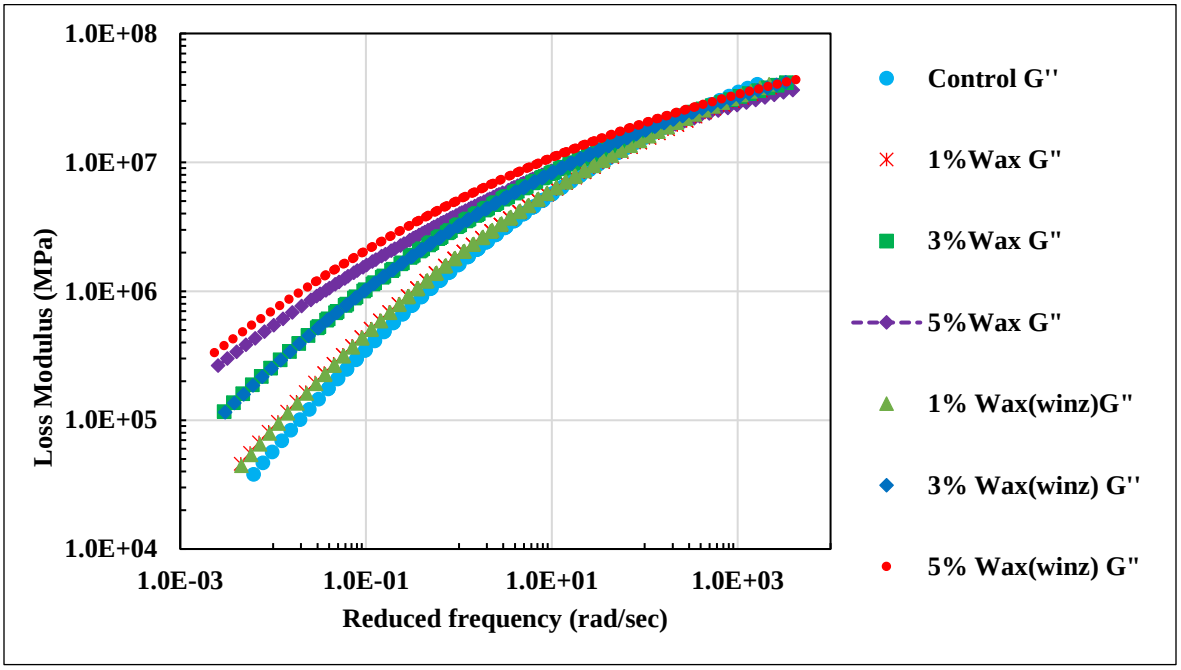

Figure 6.5-b. Loss modulus results of control and modified samples at reference temperature of 13 ºC

Table 6.1.Crossover frequency and crossover modulus at reference temperature of 13 ºC

Sample	Crossover Frequency (rad/sec)	Crossover Modulus
Control	26.8	7.95
Control+1%Wax	23.55	8.40
Control+3%Wax	1.02	3.27
Control+5%Wax	0.05	1.12
Control+1%Wax (Winz)	27.97	9.46
Control+3%Wax (Winz)	3.93	5.79
Control+5%Wax (Winz)	0.30	3.22

6.5.4 Rutting performance criteria

From the complex modulus results, the values at 10 rad/s were determined and used to calculate the Superpave specification parameter as an indicator of the material's susceptibility to rutting, based on ASTM D6373-16 (ASTM D6373 - 16). The results (presented in Figure 6.6 and Table 6.2) show that adding wax changes the grade of bitumen based on the limit of 1 kPa for G*/sin (δ). However, when wax was added via nano-zeolite, stiffness and rutting resistance parameters increased. The latter effect is an improvement for rutting performance of bitumen modified with wax. Adding wax and nano-zeolite separately (Control+5%Wax+5%NZ) or as wax-impregnated nano-zeolite (Winz) appeared to be nearly the same in terms of rutting performance (Figure 6.6-b).

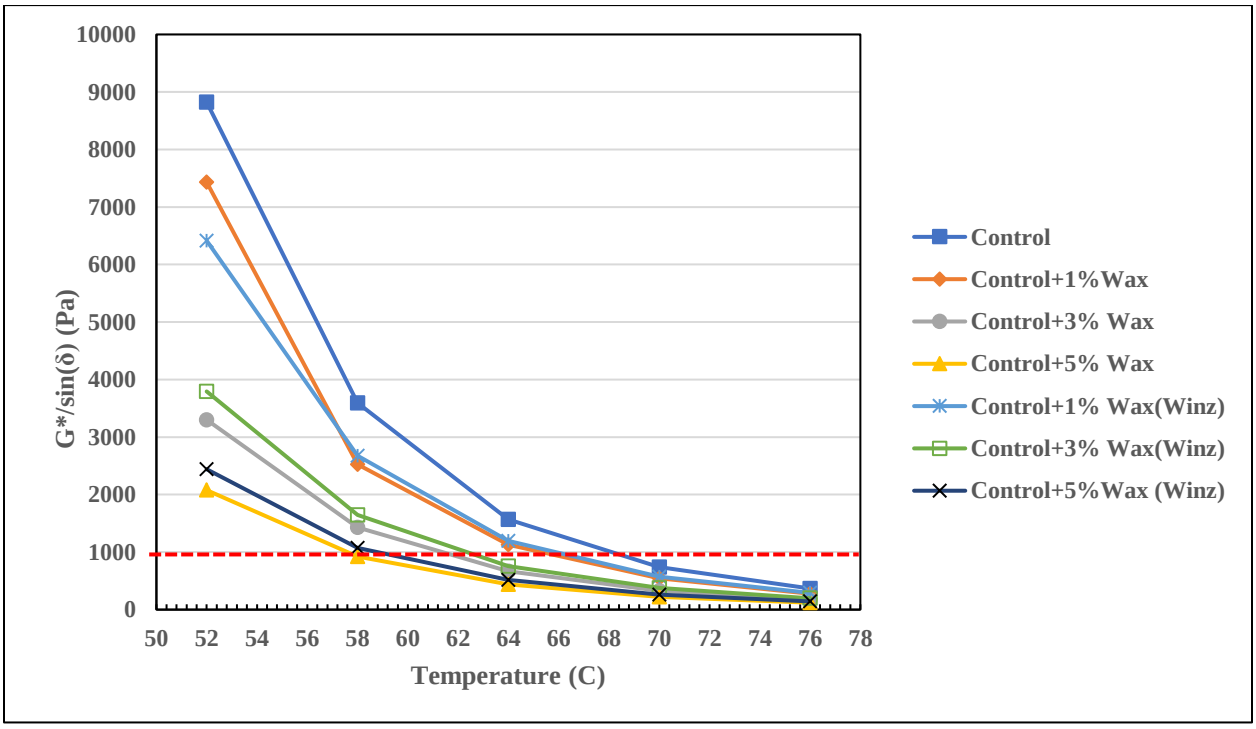

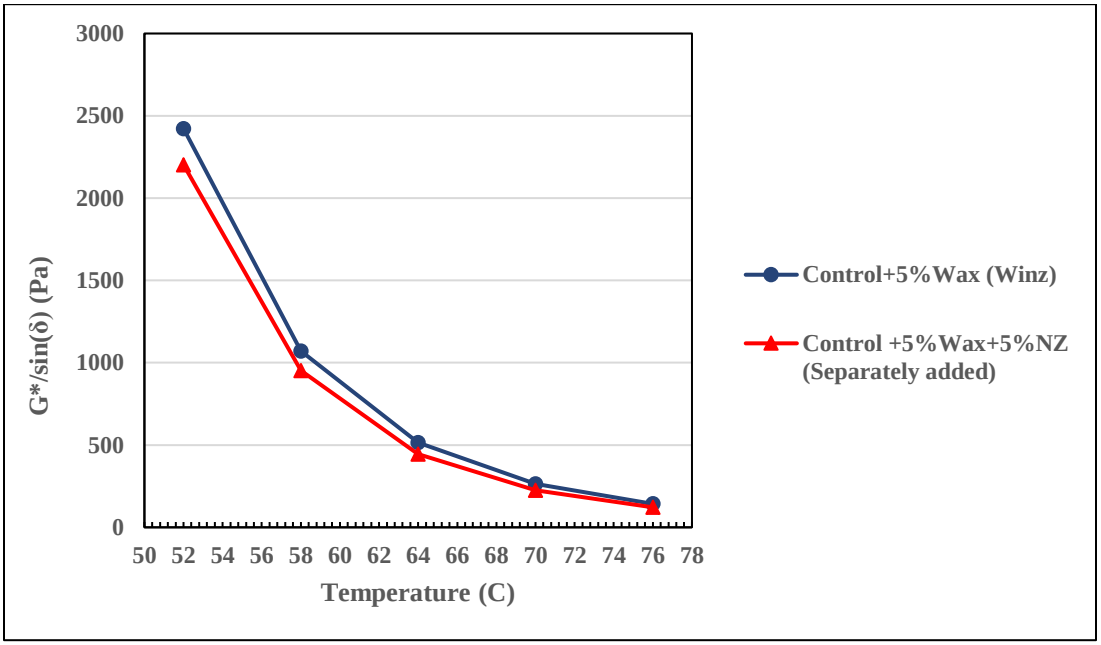

Figure 6.6 Rutting performance measurements results: a) Rutting parameter for control bitumen and modified samples. b) Comparing the results of adding Winz powder and adding nano-zeolite and wax separately.

Table 6.2 High service temperature test results of G*/sin(δ)

Sample	G*/sin(δ) (Pa)					Criterion	High-temperature grade
	52	58	64	70	76		
Control	8821	3592.7	1570.6	736.9	367.45	>1000	64
Control+1%Wax	7430.6	2523.6	1129.4	541.66	276.72		64
Control+3% Wax	3300.6	1431.3	664.5	328.8	173		58
Control+5% Wax	2077.2	920.6	439.84	222.71	120.45		52
Control+1%Wax (Winz)	6413.9	2675.9	1194	571.93	291.31		64
Control+3%Wax (Winz)	3793.5	1644.4	757.86	374.81	196.71		58
Control+5%Wax (Winz)	2440.7	1073.8	514.94	263.29	142.69		58

6.5.5 Shear rate sweep test (SRST)

The shear thinning behavior of dry and water-conditioned samples were compared to examine the effect of moisture on intermolecular interactions in asphalt (Figure 6.7). To investigate the effect of moisture on internal structure of bitumen containing Winz, a sample of bitumen doped with 5% Win was conditioned in water for 24 hours at a temperature of 60 ^{o}C. The power law parameters calculated from Equation 1 for the shear thinning part of the graph are presented in Table 6.3. The results show that after water conditioning, the internal forces in asphalt specimens doped with Winz are significantly reduced as evidenced by a lower onset frequency for shear thinning and a lower power law index. These observations are attributed to hydrolysis of acidic compounds at the interface of Winz and bitumen when exposed to water. Such phenomenon has been associated to

dissolution of acidic compounds of bitumen which are migrated to siliceous surfaces as documented by Fini's groups (Hosseinnezhad et al. 2019; Hung et al. 2017; Hung et al. 2019; Zadshir et al. 2019). This observation was further confirmed by our molecular dynamics results presented in following sections of this paper.

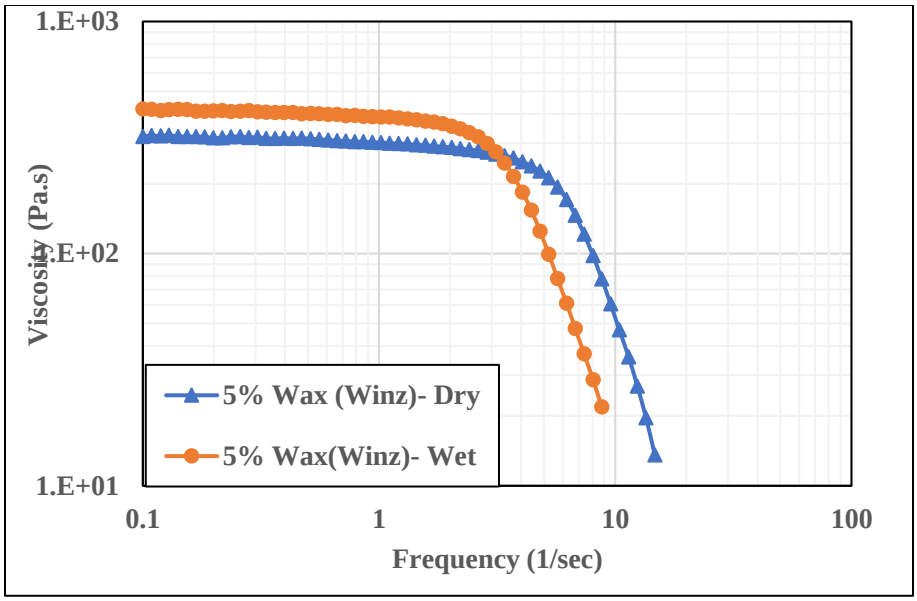

Figure 6.7 Shear rate sweep test results on bitumen containing Winz

Table 6.3. Shear Rate Sweep Test Results in wet and dry conditions

Sample	Temperature ºC	Zero shear viscosity (Pa.s)	Power law index (n)	Consistency parameter (K)
Control+5%Wax (Winz)-Dry	60	320	-3.25	9.0E+08
Control+5%Wax (Winz)-Wet	60	420	-1.89	1.0E+07

6.5.6 Multiple stress creep recovery (MSCR) test

The results for the MSCR test at 58 ºC are shown in Table 6.4. The non-recoverable creep compliance (Jnr) is higher for samples with higher percentages of wax, indicating that bitumen samples show higher flow as percentages of wax increases. However, samples modified with Winz have a lower Jnr for all scenarios at both 0.1 and 3.2 kPa. This in turn indicates more elastic behavior of bitumen containing Winz due to presence of nano zeolite which indicates better resistance to permanent deformation and rutting in pavment. The values of Jnr_{diff} increases as the content of Winz in bitumen increases with Jnr_{diff} increasing from 11% in control asphalt (0% Winz) to 15% in samples having 5%Winz.

Table 6.4. Multiple stress creep recovery test results at 58 ºC

Samples	Jnr 0.1	Jnr 3.2	Jnr diff (%)
Control	2.69	2.99	11.13
1% wax	3.60	4.05	12.65
3% wax	7.01	7.78	10.91

5% wax	10.91	12.24	12.25
1% Wax(Winz)	3.48	3.93	12.64
3% Wax(Winz)	6.21	7.03	13.1
5% Wax(Winz)	9.38	10.84	15.57

6.5.7 Glass transition and melting enthalpy

Figure 6.8 and Table 6.5 show the results from differential scanning calorimetry. After the addition of wax, the glass transition temperature didn't change dramatically. On the other hand, the melting temperature shows a reduction for Winz samples compared to that of wax samples. Presence of nano-zeolite in 5% wax sample led to higher enthalpy of melting meaning a higher amount of energy needed to melt wax. This can be due to adsorbing of energy by nanozeolite particles or higher number of wax crystals in the bulk of bitumen.

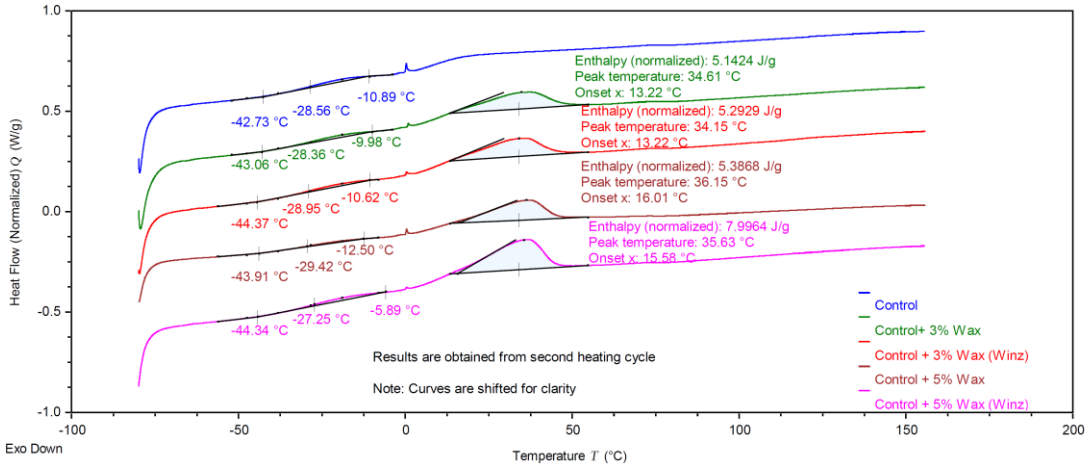

Figure 6.8 Second heat cycle results for control and modified bitumen samples

Table 6.5. Thermal properties of control and modified bitumen samples

Sample	Onset glass transition (ºC)	Glass transition midpoint(ºC)	End point of glass transition (ºC)	Onset melting temperature (ºC)	Peak melting temperature (ºC)	Enthalpy of melting (J/g)
Control	-42.73	-28.56	-10.89	N/A	N/A	N/A
Control+3% wax	-43.06	-28.36	-9.98	13.22	34.61	5.14
Control +3% Wax (Winz)	-44.37	-28.95	-10.62	13.22	34.15	5.29
Control+5% Wax	-43.91	-29.42	-12.5	16.01	36.15	5.38
Control+5% Wax (Winz)	-44.34	-27.25	-5.89	15.58	35.63	7.99

6.5.8 Critical low temperature

Figure 6.9 shows the stiffness and m-value for different samples at -12ºC. To be able to decouple the results, a control sample was also prepared by adding separately the same amounts of wax and nano-zeolite as in the Winz samples, to investigate whether impregnation makes a difference. As the results illustrate, the addition of wax increases the stiffness and reduces the m-value at subzero temperatures. However, the addition of wax in the form of impregnated nano-zeolite particles reduced the stiffness and increased the

m-value at the same time. Furthermore, modifying the bitumen by adding the wax and nano-zeolite separately also resulted in approximately the same values for stiffness and m-value. The results suggest that the presence of nano-zeolite is the most effective factor on stiffness and m-value. In the presence of nano-zeolite, there was little difference between impregnating the wax and just adding the wax separately.

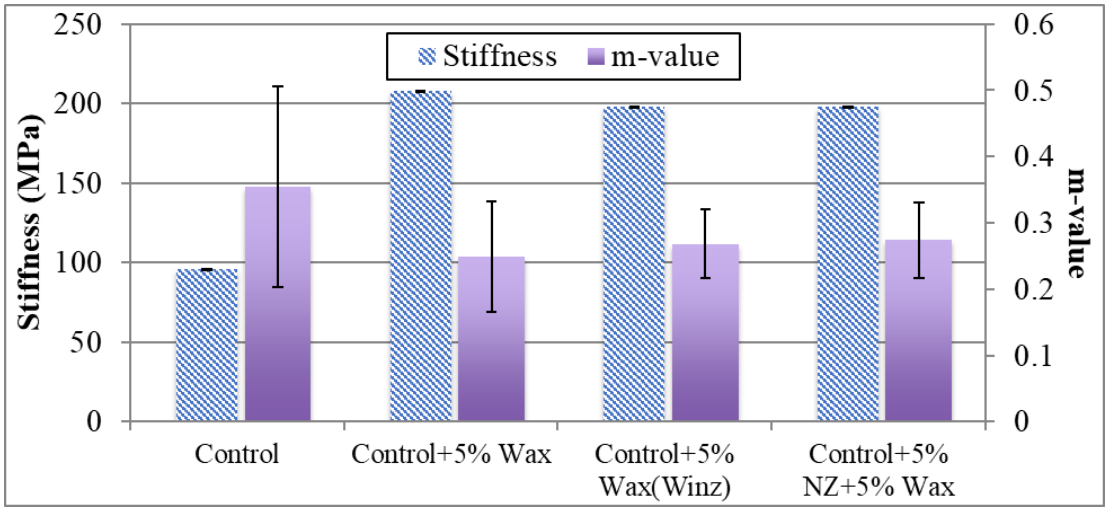

Figure 6.9 Stiffness and m-value for different samples at -12ºC

To study the effect of modification on critical low temperatures (the temperature where the material meets the standard criteria), data from at least two points need to be acquired. The second temperature was selected as -18ºC. The results of critical low temperatures for all samples are presented in Figure 6.10. The measures of the difference between the critical low temperatures ($T_{stiffness}$-$T_{m\text{-}value}$) for control, control+5% wax, control+5%winz, and control +5%wax+5% NZ are -1.25, -8.64, -8.5, and -8.94ºC, respectively. The results show that the addition of nano-zeolite particles lowers the stiffness

and increases the m-value at both -18ºC and -12ºC. This in turn indicates improved stress relaxation capacity in the case of winz where wax is carried within nano-zaolite. This can be attributed to reduced stacking and crystallization of wax in bitumen due to enhance dispersion enabled by nanozeolite. This was also evidenced in higher value of delta Tc for samples where wax was directly added to bitumen.

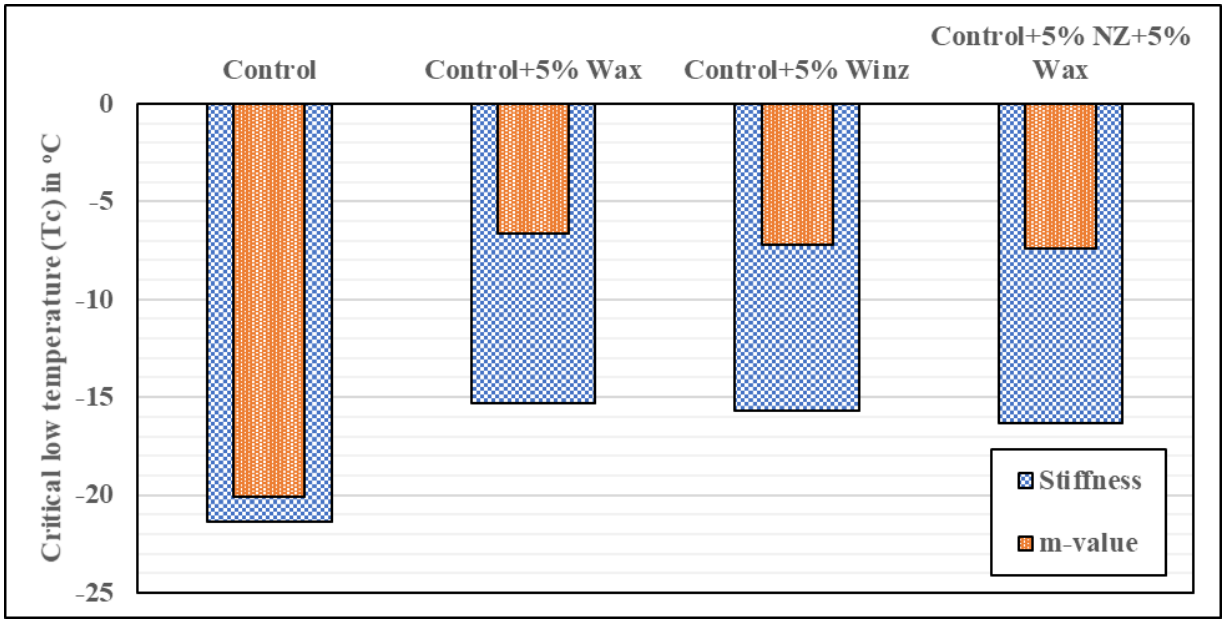

Figure 6.10. Critical low temperatures of tested samples

6.6 Molecular Simulation Results

The MD results show that at NVT ensemble, the wax molecules are attracted by active sites of the silica structure, as it can be seen in Figure 6.11.

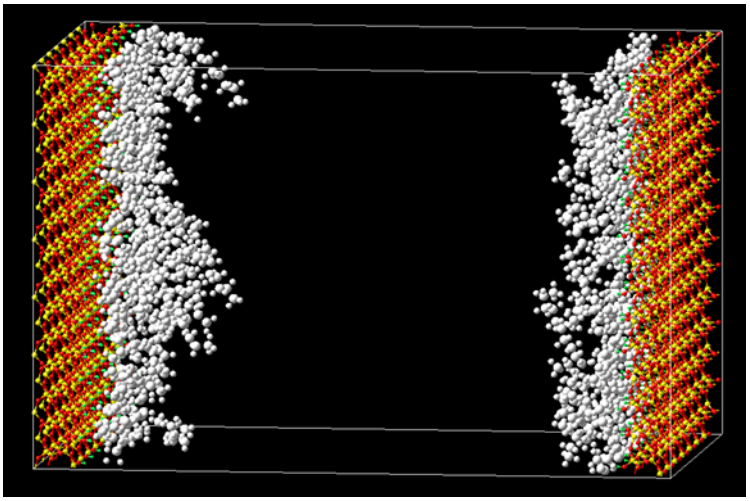

Figure 6.11. Interaction between wax molecules (white) and silica (orange and red)

Figure 6.12 shows the initial ensemble for the second stage of the simulation, which starts with the addition of a droplet of acid to the wax-silica system. After 500ps of simulation, the final ensemble (Figure 6.13) suggests that acid molecules will replace wax on the surface of silica and also occupy the vacant active sites of a silica crystal. This phenomenon results in the release of wax, which was shown in the results of experiments. Absorbing the acid from bitumen can

improve the moisture susceptibility of pavement (Mousavi et al. 2019).

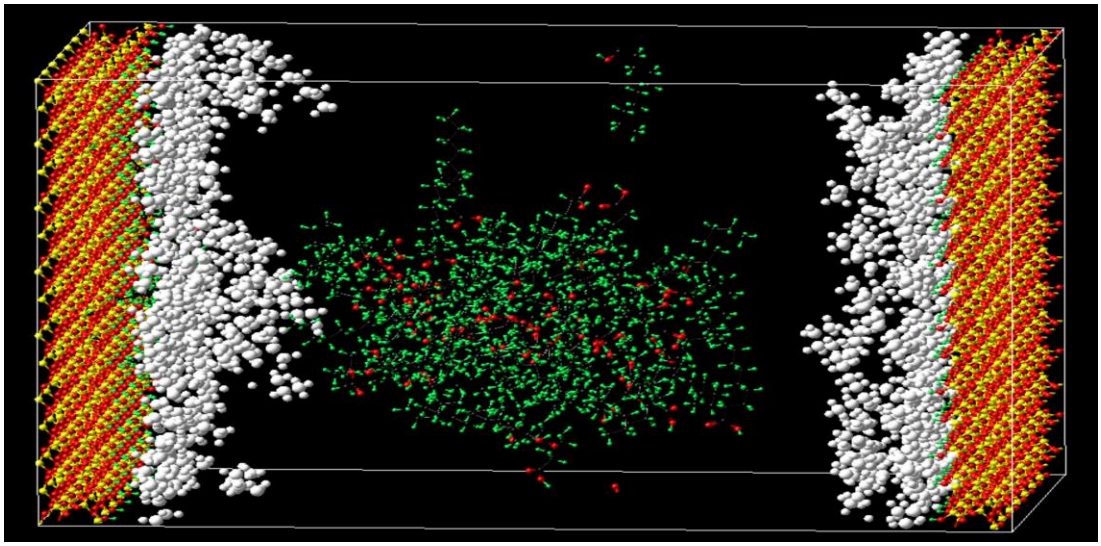

Figure 6.12. Addition of droplet of acid (middle) to system of silica-wax

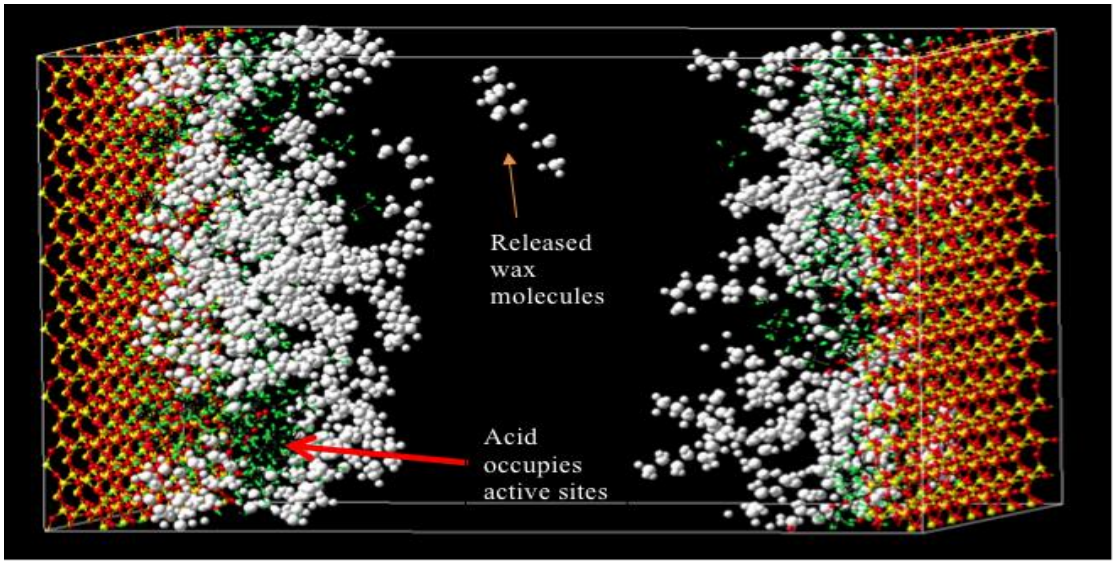

Figure 6.13. Acid molecules replaced the wax on the surface of silica, releasing the wax.

6.7 Summary

In this study, a new method for blending paraffin wax with bitumen was introduced. The purpose of this method is to reduce the adverse effects of wax on the low-temperature properties of bitumen due to wax crystallization, which is the underlying reason for the stiffening and embrittlement of bitumen containing wax. The study results can be summarized as follows:

- SEM images confirmed that the nano-zeolites were impregnated by paraffin waxes producing wax-impregnated nanozeolite referred to as Winz.
- Rheometry study showed the crossover frequency of bitumen containing Winz are nearly twice that of bitumen containing isolated paraffin wax; this can be a result of enhanced wax dispersion preventing formation of wax crystals.
- Study of the thermal properties showed that the Winz samples had a higher enthalpy of melting compared to bitumen containing isolated paraffin wax. This could indicate smaller but more frequent wax crystals. This was in-line with the above rheometry results indicating enhanced dispersion.
- At high service temperatures, bitumen modified with wax-impregnated nano-zeolite showed the same softening effect as wax-modified samples as evidenced by complex modulus and viscosity results. This was expected due to wax being in liquid form.
- Asphalt containing Winz showed to have higher $G^*/\sin\delta$ indicating enhanced elasticity and higher resistance to rutting than asphalt modified with isolated wax.

- The significant change in shear thinning behavior of bitumen containing Winz when exposed to water showed that nano-zeolite adsorbs acidic compounds of bitumen.
- At sub-zero temperatures, bitumen containing wax and nano zeolite had a lower stiffness and higher stress release capacity compared to bitumen containing isolated wax.
- The molecular dynamics simulation results show that the siliceous surfaces absorb wax molecules. However, the adsorbed wax can be easily replaced by carboxylic acids present in bitumen. In addition, adsorption of acids by nano zeolite detract them from the interface of bitumen and stone aggregate, which can enhance resistance to moisture damage in asphalt mixture.

7 LIFE CYCLE ASSESSMENT OF A SUSTAINABLE BITUMEN MODIFIER

7.1 Introduction and Literature Review

In the United States, there is increasing demand for new roads as well as the widening, maintenance, and rehabilitation of existing roads. Additionally, more attention is being paid to sustainable development in civil engineering. Sustainable development can be defined as development that meets the needs of the present without compromising the ability of future generations to meet their own needs. Construction that fits this description is known as sustainable construction (WCED 1987).

Bio-binder produced from bio-mass is a promising partial replacement for bitumen that has been shown to improve the mechanical properties of the bitumen (Fini et al. 2011). The production of bio-binder is performed using a hydrothermal liquefaction (HTL) process on swine manure. HTL turns swine manure into bio-oil and also prevents carbon dioxide (CO_2) and other greenhouse gases from being emitted into the air (Cantrell et al. 2008). Because bio-binder and bitumen have some similarities in their rheological and chemical properties, bio-oil can be considered a good resource to produce the bio-binder to be used as an additive to asphalt pavement to improve the asphalt's properties (Fini et al. 2012; Fini et al. 2010; Mills-Beale et al. 2014). Furthermore, the chemical characterization and similarity in chemical compounds made bio-binder a prominent candidate for the production of bio-modified bitumen (Fini et al. 2011; Fini et al. 2010). It has been documented that in the presence of bio-binder, the stiffness of

bitumen at subzero temperature reduces, and the ability to relax the stress increases (Fini et al. 2012). It also showed that bio-binder has a reducing effect on the viscosity at high temperatures, which in turn, can improve the workability and consuming less energy to bring the bitumen to the desired state to mix with aggregates (Fini et al. 2012). Researchers also concluded that adding bio-binder to bitumen can decrease the critical cracking temperature of virgin bitumen when bio-binder is added at 10 wt% of the base bitumen (Fini et al. 2011). Overall, the bio-binder has shown to be a promising candidate as a modifier for conventional bitumen to enhance its mechanical and chemical properties. In terms of cost, there has not been an exact procedure of cost estimation yet, but as an approximation (Goudriaan et al. 2000) estimated a cost of $0.54/gal for bio-oil obtained from different sources using an HTL process.

Because bio-oil and bituminous bitumen have some similarities in their rheological and chemical properties, bio-oil can be considered a good resource to produce the bio-binder to be used as an additive to asphalt pavement to improve the asphalt's properties (Fini et al. 2010). Using a closed system to convert biomass to oil, pollution problems caused by runoff of the manure to ground and surface waters can be prevented (Ocfemia et al. 2006). In general, manure decomposition can cause the production of greenhouse gases and cause a significant burden on the environment. Storing swine manure in lagoons or using it as fertilizer leads to emission of CO_2, methane (CH_4), and N_2O. Only about 5% of U.S cropland is fertilized with livestock manure, which is a very small portion (Fini et al. 2011). On the other hand, using bio-binder from swine manure

as a partial replacement for bituminous bitumen was shown to be promising in both mechanical and sustainability aspects (Fini et al. 2011). Also, the production of bio-oil from swine manure and then converting it to bio-binder as an additive to asphalt can increase the value of manure and assimilate the carbon into bio-binder instead of emitting it to the air (Fini et al. 2011).

HTL usually takes place between 200 ^{o}C and 374 ^{o}C and from 4 to 20 MPa (Akiya and Savage 2002). To produce bio-binder, the operating temperature of HTL at a laboratory scale is in the range of 200 ^{o}C to 400 ^{o}C, and the time required for the process (residence time) is less than 2 hours. HTL is followed by filtration under vacuum and vacuum distillation to obtain bio-binder. During vacuum distillation, the pressure above the liquid mixture is reduced to less than its vapor pressure, which causes the most volatile liquids to evaporate (Harwood et al. 1989).

The question of whether a product meets the sustainability criteria, or even whether the product is beneficial from an environmental perspective, can be investigated using an LCA of that product. ISO14014 and ISO14040 define the LCA as the compiling and evaluation of the inputs and outputs and also the environmental impacts associated with a product over its life cycle (Finkbeiner et al. 2006; ISO14040 2006). An LCA can identify the environmental hotspots of a product or process and use the information to optimize the process from an environmental perspective. As a very first step in an LCA, a life cycle inventory (LCI) should be developed that involves creating an inventory of flows from and to each process in the life cycle of a product. Inventory flows include

inputs of water, energy, and raw materials and releases to air, land, and water (Rebitzer et al. 2004). For new products in which there is limited data available on the impacts and other implications, a cradle-to-gate analysis is appropriate (Franklin Associates 2011). Cradle-to-gate is an assessment of a partial product life cycle from resource extraction (cradle) to the factory gate, which in this case would be bio-binder being used in an asphalt mixture. The use phase and disposal phase of the product are omitted in this case, due to a lack of data on the long-term performance of bio-asphalt and also the end-of-life of this product.

In this study, the energy consumption and greenhouse gas emissions of 10% bio-binder have been compared with those of neat unmodified bitumen. To compare the environmental impact of the two products, the global warming potential index (GWPI) is used. Global warming potential (GWP) is a relative measure of how much heat a greenhouse gas traps in the atmosphere compared to carbon dioxide (Lashof and Ahuja 1990). This research uses different methods to build the inventory, create a cradle-to-gate LCA of bio-modified bitumen, and compare the results to conventional bitumen. A further study has been conducted beyond the boundaries of the LCA to show the effects of releasing the swine manure to nature and the environmental burdens of that compared with using it to produce bio-binder. GaBi software and databases were used to build the life cycle inventory.

7.2 Research Scope and Functional Unit

In the bio-binder production process, the HTL process uses a high pressure and temperature reactor to heat the slurry feedstock and convert it to bio-oil. After purging the residual air, the reactor is then heated to the designated experiment temperature, and the temperature is kept constant for the proper reaction time. After the reaction is done, the reactor is rapidly cooled by running tap water through the cooling coil inside the reactor. Afterward, the gas is released, and the pressure is reduced. After obtaining bio-oil through this process, acetone is added to the product, and by filtration under vacuum, the bio-char is separated. The light components of the product are separated using a vacuum distillation process.

Figure 6.1 shows the bio-binder production process chain studied in this research.

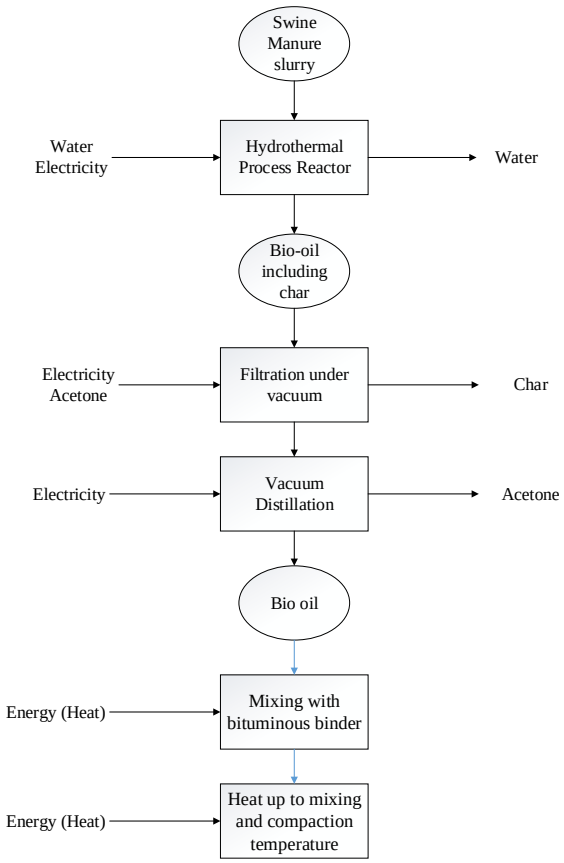

Figure7.1 Bio-binder Production Process Chain Overview

To build the life cycle inventory of the bio-binder production process, experiment procedures are utilized. The system boundary of the comparative LCA selected for this research is shown in Figure 7.2 for the production process chain is from the first phase, which is material preparation for production of bio-binder and conventional bitumen to the mixing of the bio-binder and bitumen to have 10% bio-modified bitumen.

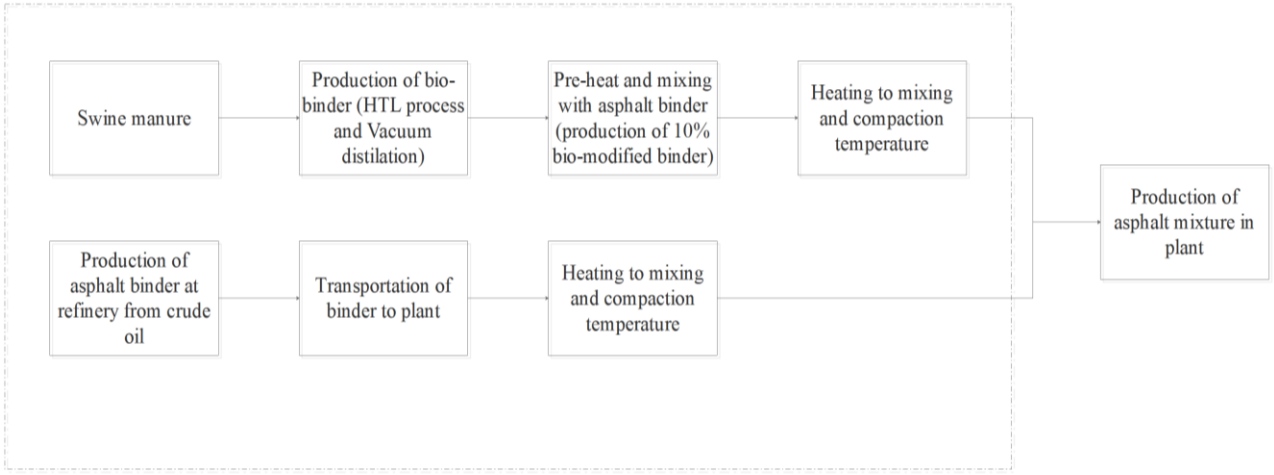

Figure7.2 System Boundary For LCA

To perform an LCA on a product, the functional unit should be defined. A functional unit quantifies a standard amount to be compared between alternatives that serve this function. Equivalent functionality shall be maintained for all candidates of an LCA model (Yu and Lu 2012). In this study, the LCA of the production of 50 kg of bio-modified bitumen (required for the production of 1000 kg (1 ton) of bio-modified asphalt mixture) is compared with the production of 50 kg of conventional petroleum-based bitumen. The results are shown for bio-modified bitumen containing 10 wt% bio-binder.

7.3 Materials and Methods

The yield of bio-oil based on a residual time of 120 minutes at 340 ^{o}C shows 51% of the conversion of swine manure slurry (Hosseinnezhad et al. 2016). After vacuum distillation, 10% of the bio-oil is converted to bio-binder.

7.3.1 Energy consumption

7.3.1.1 Bio-binder production

Energy consumption in the production of bio-binder occurs in two stages. First, the reactor provides enough heat through three heat sleeves with a total power of 2,300 W. The second stage is vacuum distillation, in which the light components of bio-oil are separated under vacuum and blowing nitrogen gas. The heat needed to increase the slurry temperature to the setpoint of 340 ºC can be calculated as equation 7.1 (Ocfemia et al. 2006):

$$E_i = \frac{MC\int_{20}^{T} C_{pw}dT + (1-MC)\int_{20}^{T} C_{ps}dT}{\varepsilon} \cong m \times C_{pw} \times \Delta T \qquad \text{Equation 7.1}$$

where: E_i = energy input (kJ/kg),

MC = moisture content of slurry feed,

m= mass of manure slurry (kg),

ΔT = temperature difference (ºC),

C_{pw} = specific heat capacity of pure water,

C_{ps} = average specific heat of the solids, and

ε = efficiency of heating

As a simplifying assumption, the specific heat capacity of the manure slurry was approximated to be equal to that of pure water (4.18 kJ/kg ºC), based on the assumptions that almost 80% of the feedstock is water including the inherent water in manure-based

on literature (Xiu and Shahbazi 2012; Xiu et al. 2010) and the presence of solids would lower the specific heat insignificantly. Furthermore, the heat losses from the processes were neglected (ε=1.0, assuming 100% heating efficiency).

The vacuum filtration and distillation process consume energy to separate the biochar and the light component (acetone) that was added to increase the separation of biochar from bio-oil. The amount of these energies was calculated using GaBi software and the specifications of the instruments used.

7.3.2 Mixing and compaction

Mixing and compaction temperatures can be obtained through different methods; the most popular method uses AASHTO T 245 and T 312 (AASHTO 2004). This method uses a viscosity of 0.17±0.02 Pa-s for mixing and 0.28±0.03 Pa-s for compaction for unmodified bitumens (AASHTO 1998; AASHTO 2004)(AASHTO, 1998 and 2004). There are other studies on mixing and compaction temperatures of asphalt, which documents the HMA plant mixing temperature to be in a range of 265 to 320 ^{o}F with a midpoint of 292 ^{o}F (Asphalt Pavement Environmental Council and Association 2000). The rheological analysis of bio-binder showed that the addition of bio-binder to the base bitumen could allow for the reduction of mixing and compaction temperatures because it reduces the viscosity of the base bitumen (Fini et al. 2011).

Because bio-binder lowers the viscosity of the base bitumen, it is reasonable to use the same criteria as the AASHTO method to calculate the mixing and compaction temperature of bio-modified bitumen.

Another method for calculating mixing and compaction temperatures is the Casola method, which considers the phase angle for that purpose (West et al. 2010). According to recent research on bio-binder's effects on asphalt mixtures, bio-binder can allow reduction of the mixing and compaction temperature by 15 ^{o}C (Mogawer et al. 2012).

To calculate the energy needed to increase the bitumen temperature to get suitable viscosity and workability, the heat capacity of the bitumen is required. For this study, the heat capacity of the neat bitumen as well as the bitumen modified with 10% bio-binder was calculated using a differential scanning calorimetry (DSC) test. The heat capacity was determined using the three-run method (ASTM E1269-11 2018). This method uses empty pans, the sample, and reference materials such as sapphire. A high heating rate of 20 °C/min is used to provide a good signal-to-noise ratio that cannot be achieved with slower heating rates. For this method, provisions need to be made to correct or compensate the data for differences in the mass of the sample pan and the reference pan. To minimize the effect of instrument drift, isothermal segments are used. The empty-pan baseline was subtracted from the reference results to determine a conversion factor of heat flow (mW) to heat capacity (J/°C). Then the heat flow difference between the sample and the empty pan baseline was determined, divided by the sample mass, and converted to heat capacity (J/g^{o}) using the conversion factor. Replicate heat capacity determinations using the three-run method typically agree within about 3% or less. The three-run method can be done on almost any DSC with a minimal amount of instrument

preparation. The test was performed from -60 ºC to 160 ºC. The samples (5-7 mg) were placed in Tzero aluminum pans with hermetic lids. Using the DSC test results, the amount of energy needed to raise the temperature of the bitumen from ambient temperature to achieve the desired workability was then calculated.

7.3.3 Feedstock energy and energy intensity factors

There are some controversies regarding the inclusion or exclusion of the feedstock energy of an asphalt mixture in LCA methodology. As a hydrocarbon, bitumen has a specific amount of inherent energy that is trapped in the asphalt mixture. By ISO standards, this chemical energy needs to be included in any energy assessment (ISO14040 2006; Santero et al. 2011). Four pavement LCA studies considered this energy in their inventory (Athena Research Institute 2006; Häkkinen and Mäkelä 1996; Nisbet et al. 2001; Stripple 2001). Different feedstock energy estimates that result in the exclusion or inclusion of this energy change lead to different conclusions within pavement LCA studies. The feedstock energy in bitumen is reported to be 40.2 MJ/kg (Intergovernmental Panel on Climate Change 1995), which is over six times the maximum energy factor of bitumen production. On the other hand, the energy intensity factors for bitumen covers a range of 0.7 to 6.0 MJ/kg, due to different scopes and system boundaries used in different methodologies (Santero et al. 2011). A 2010 pavement LCA-related workshop defined the feedstock energy as the heat of combustion of a material input that is not used as an energy source to a product system, measured in higher heating value or lower heating value (Santero et al. 2011).

7.4 Emissions to Air

Different test methods are used to measure pollutant emissions to air through the whole process chain.

Three different test methods were used to determine the amount of each pollutant in HTL gases. (ASTM D1946-90, 2015) and EPA method 18 were utilized, which describes the process to measure volatile organic compounds by gas chromatography. (ASTM D1946-90 2015)(EPA measurement of gaseous organic compound emissions by gas chromatography, 2017) was used to measure sulfur compounds in the exiting gas of the HTL process reactor. As positive sample pressure is required by the analytical process, samples with insufficient pressure are pressurized with helium to the minimum required pressure for the analysis (usually 5 psi). Dilution factors for pressurized samples are calculated and used to correct the corresponding analytical results. Data resulting from ASTM D1946 and D1945 fuel gas and natural gas analyses are reported in mole percentage and are normalized (components sum to 100%) in the analytical section of this report.

7.5 Results and Discussion

7.5.1 Life cycle inventory (LCI) analysis

Different sources have been used to obtain data for a better understanding of the uncertainty of the system. For clarity, five different references are mentioned for energy consumption of bitumen production with different system boundaries and scopes in Table 7.1 to emphasize the importance of attention to system boundary. However, to produce

the life cycle inventory of bitumen, the results from Gabi software was used. The feedstock of crude oil is excluded to be able to compare the results with that of bio-binder. The emission amounts are showing the direct emissions of the production of bio-binder. The life cycle inventory data for the production of bitumen and bio-binder is presented in Table 7.2 and Table 7.3, respectively.

Table 7.1 Bitumen production energy consumption in different studies

Amount	Unit	Reference
0.63×10^9	J/Ton of Material	(Stammer Jr and Stodolsky 1995)
0.42×10^9	J/Ton of Material	(National Crushed Stone Association 1977)
6×10^9	J/Ton of Material	(Häkkinen and Mäkelä 1996)
2.93×10^9	J/Ton of Material	(Stripple 2001)
5.81×10^9	J/Ton of Material	(Athena Research Institute 2006)

Table 7.2 Life cycle inventory of conventional bitumen

Parameter	Amount	Unit	Reference
Production energy consumption	6.58×10^9	J/Ton of Material	Gabi software database
Mixing and compaction temperature energy consumption for 10% bio-modified bitumen	0.47×10^9	J/Ton of Material	DSC test results
Feedstock Energy	41.28×10^9	J/Ton of Material	Bomb calorimeter measurement

Emissions from production of bitumen			
Carbon dioxide	401.18	Kg/Ton of Material	GaBi software database
Nitrous oxide	0.0027	Kg/Ton of Material	GaBi software database
Methane	4.71	Kg/Ton of Material	GaBi software database

Table 7.3 Life cycle inventory of bio-binder and 10% bio-modified bitumen

Parameter	Amount	Unit	Reference
Production of bio-binder energy consumption	1.19×10^9	J/Ton of Material	(Ocfemia et al. 2006)
Vacuum distillation	0.19×10^9	J/Ton of Material	Readings from device
Emissions of production of bio-binder			
Carbon dioxide	76.87	Kg/Ton of Material	Gas chromatography
Nitrous oxide	0.0017	Kg/Ton of Material	FTIR test
Methane	1.6	Kg/Ton of Material	Gas chromatography
Mixing and compaction of 10% bio-modified bitumen	0.21×10^9	J/Ton of Material	DSC test results
Feedstock energy of 10% bio-modified bitumen	41.23×10^9	J/Ton of Material	Bomb calorimeter measurement

7.5.2 Life cycle impact assessment (LCIA)

This study takes into consideration the emissions related to the process stages of the production and preparation of bitumen and bio-modified bitumen.

The results of a batch HTL process developed at North Carolina A&T State University yields almost 18% bio-binder. This is in good agreement with Ocfemia et al.,

2006 study. The results of the following batch are as shown in Figure 7.3. The process of hydrothermal liquefaction of swine manure generates 2.5 kg slurry of biomass for each batch, with a yield of 450 g bio-binder. The comparative results of emissions from the production of Bio-binder and conventional bitumen are shown in Figure 7.4. A significant reduction in all three studied GHG gases is observable. Furthermore, the results of emission for the products of bio-modified bitumen and conventional bitumen show that using bio-binder reduces the emission factors of the bitumen. To have a better reference of comparison, the emission factors and the global warming potential index of 50 Kg of each product have been calculated and presented in Figure 7.5. The conversion factors of 1 for carbon dioxide, 21 for methane, and 310 for nitrous oxide are used based on (Chan et al., 2015) research. The results show an improvement of this index after using bio-binder as a sustainable modifier.

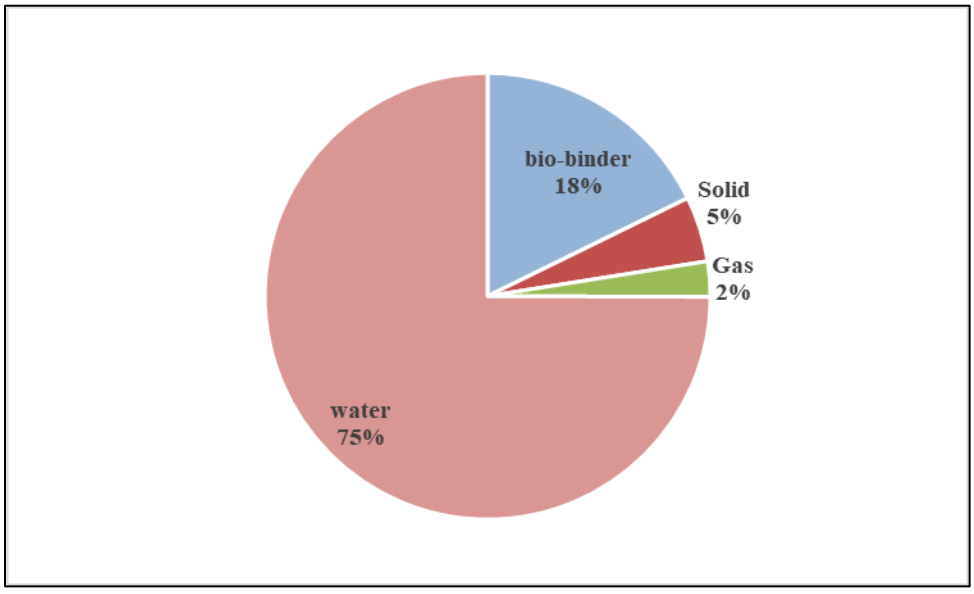

Figure 7.3 Product Mass Distribution

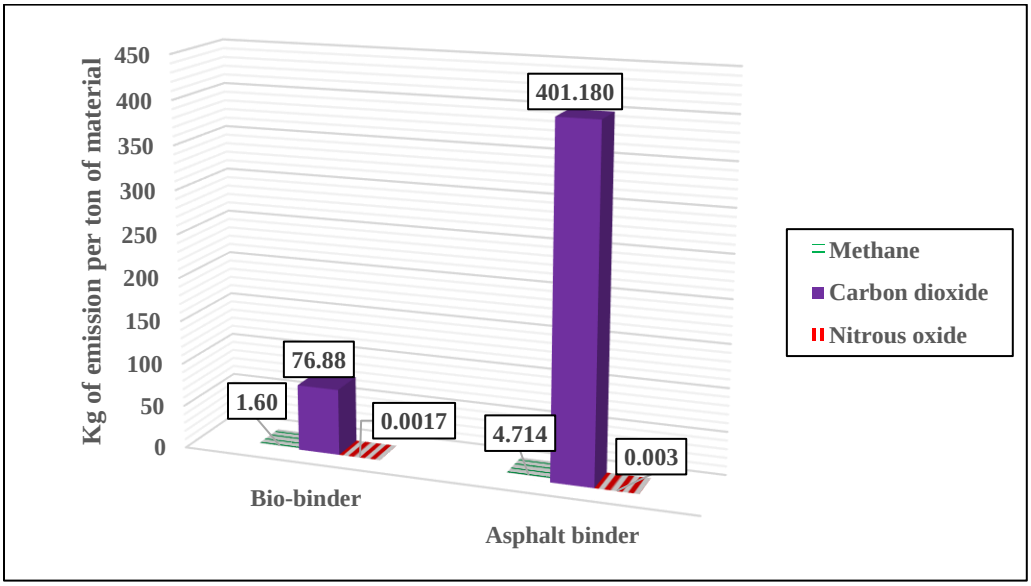

Figure7.4 Greenhouse Gas Emissions for Bio-binder And Bitumen

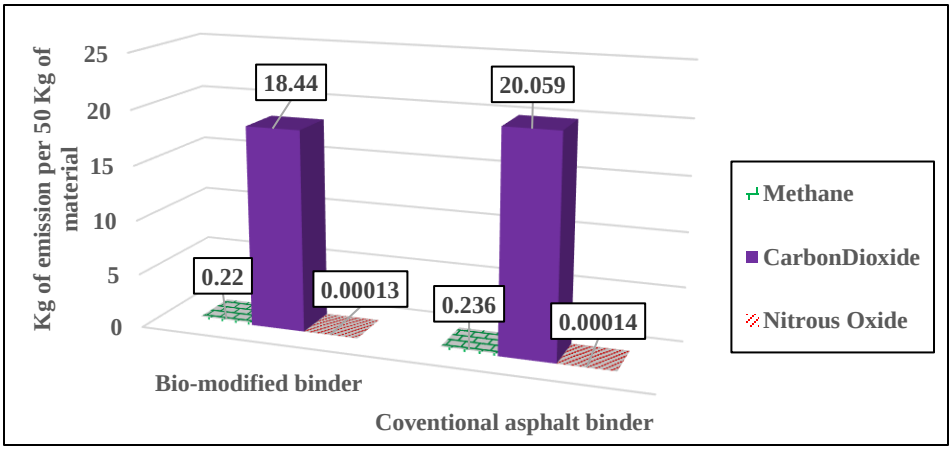

Figure 7.5-a Greenhouse Gas Emissions For 50 kg of Bio-Modified Bitumen (containing 10% of bio-binder and 90% virgin bitumen) And Conventional Bitumen.

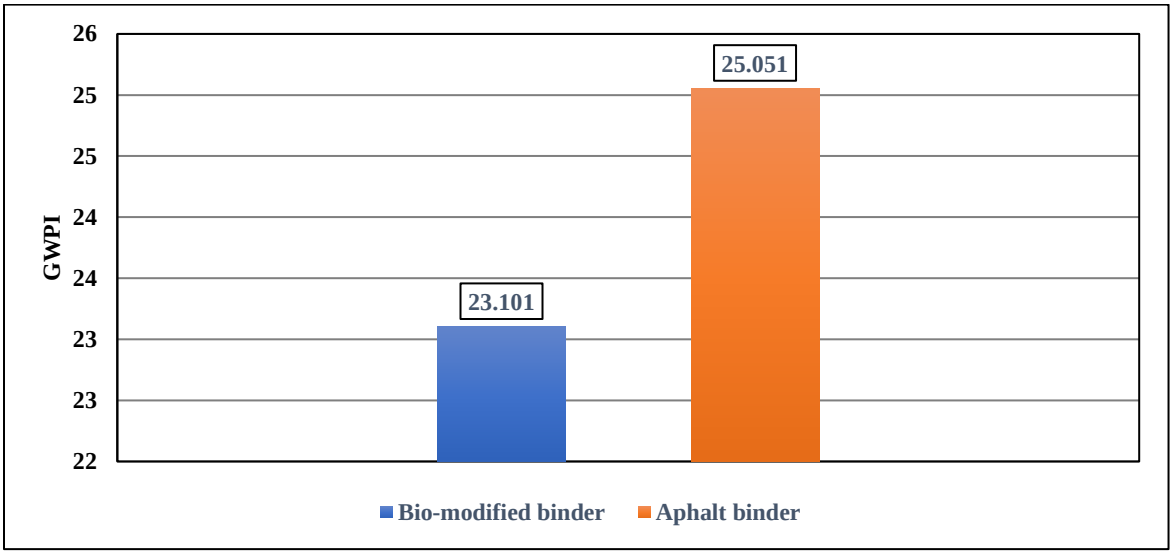

FIGURE 7.5-b Global Warming Potential Index For 50 kg of Bio-Modified Bitumen and Conventional Bitumen.

7.6 Beyond the Boundaries

To better understand the effect of the production of bio-binder on the environment, this study compared the environmental impact of not converting swine manure to bio-binder and instead letting it be landfilled. A literature review has been conducted to estimate the emission of each gas from the manure produced by one swine in each day. Then it is compared with the equivalent amount that is needed for HTL and the production of bio-binder.

7.6.1 Swine manure in a lagoon

7.6.1.1 CO_2 emission from pig manure

There are three approaches to the estimation of CO_2 emissions. The level of CO_2 due to pig manure was omitted in some studies because the main CO_2 release was from pigs' exhalation(Anderson et al. 1987; Van't Klooster and Heitlager 1994).

There are other studies that estimate the CO2 released from pig manure is about 4-5% of the CO_2 from exhalation (Dong et al. 2007; Pedersen and Sällvik 2002; Sousa and Pedersen 2004). Other studies have reported the CO_2 release at 10-30% of the respiratory production (Jeppsson 2000; Pedersen et al. 2008; Philippe et al. 2007; Philippe et al. 2007; Philippe et al. 2012). Ni et al. (1999) stated that emissions from manure are about 40% of the tranquil CO_2 exhalation rate. For the purpose of this research, the average amount of 30% of exhalation CO_2 is used (Ni et al. 1999).

Table 7.4 shows four different equations for estimating the exhaled CO_2 emissions of pigs. In these equations, "*BW*" is the bodyweight of a pig.

Table 7.4 Equations proposed to estimate CO_2 exhalation by pigs ($E\text{-}CO_{2\ pig}$, in kg/day)

REFERENCES	EQUATIONS
(Ni et al. 1999)	$E\text{-}CO_2$, PIG = 0.224 $BW^{0.46}$
(Brown-Brandl et al. 2004)	$E\text{-}CO_2$, PIG = 0.123 $BW^{0.62}$
(Pedersen et al. 2008)	$E\text{-}CO_2$, PIG = 0.0998 $BW^{0.646}$
(Philippe and Nicks 2015)	$E\text{-}CO_2$, PIG = 0.136 $BW^{0.573}$

7.6.1.2 CH_4 emission from pig manure

The emission of methane from swine manure initiates from the temporal succession of microbial processes (Hellmann et al. 1997; Monteny et al. 2006). There are several parameters that increase the CH_4 emission: lack of oxygen, high temperature, high moisture content, high level of degradable organic matter, low redox potential, neutral pH, and C/N ratio between 15 and 30 (Amon et al. 2006; Kebreab et al. 2006; Møller et al. 2004).

7.6.1.3 N_2O emission from pig manure

In pig houses, N_2O originates only from manure. Its formation mainly occurs during incomplete nitrification/denitrification processes performed by micro-organisms that normally convert NH_3 into non-polluting N_2 (Philippe and Nicks 2015).

7.6.2 Results and Discussion

7.6.2.1 GHG emissions (manure in lagoons)

This study used GHG emissions from manure in lagoons for 5,000 head of pigs. A regular pig's body weight starts at 65 lb and finishes at 265 lb after full fattening that takes 20 weeks. The average amount of manure over 20 weeks is 3.5 lb per day. The manure management system is pit storage.

The CO_2 emissions were calculated using four different methods (Table 7.5), and the average value was used in the analysis.

Table 7.5 CO_2 emission from pig manure in lagoons for one pig

References	Equations	CO_2 (kg/pig/day)
(Ni et al. 1999)	E _ CO_2, PIG = 0.224 $BW^{0.46}$	2.345798
(Brown-Brandl et al. 2004)	E _ CO_2, PIG = 0.123 $BW^{0.62}$	2.915716
(Pedersen et al. 2008)	E _ CO_2, PIG = 0.0998 $BW^{0.646}$	2.701626
(Philippe and Nicks 2015)	E _ CO_2, PIG = 0.136 $BW^{0.573}$	2.536046
	Average	2.624796

CH_4 emission from manure can be estimated using the following equation, based on three assessments: the excreted volatile solids (*VS*) or organic matter (*OM*) in kg; the maximum methane-producing capacity (B_0) in m^3 CH_4 per kg *VS* or *OM*; and the methane conversion factor (*MCF*), in percentage (IPCC Intergovernmental Panel On Climate Change 2006).

$$E\_CH_4 = VS \times B_0 \times MCF$$ **Equation 7.2**

The recommended value for VS for North America in the IPCC publication is 0.27 kg/pig/day. In the literature, B_0 has a value from 0.29 to 0.53 m^3 per kg *VS* (Chae et al. 2008; Jarret et al. 2011; Møller et al. 2004; Vedrenne et al. 2008). For the purpose of this study, the B_0 value selected is 0.48 m^3 CH_4/kg *VS* specified for Northern America. In the literature, *MCF* values range from 2% to 80%, according to manure type (Dämmgen et al. 2012; Jarret et al. 2011; Møller et al. 2004; Rodhe et al. 2012).

According to the (IPCC Intergovernmental Panel On Climate Change 2006), the amount of MCF for a liquid/slurry manure management system for the average temperature of Greensboro, North Carolina, is 27%. Table 7.6 shows the assumptions and the calculated amount.

Table 7.6 CH_4 emission from manure in lagoons for one pig

B_0 (m^3 CH_4 per kg VS)	VS(kg/pig/day)	MCF (%)	CH_4 (m^3/day)	CH_4 (kg/pig/day)
0.48	0.27	0.27	0.034992	0.027889

The guidelines for the National Greenhouse Gas Inventories (IPCC Intergovernmental Panel On Climate Change 2006) recommend estimating direct N_2O emissions by multiplying the N excreted by animals (Nex) by a specific conversion factor for each type of manure management system. For North America, the estimate for excreted nitrogen is 20 kg/animal/year, and the emission factor for pit storage under animals is 0.2% (Gibbs et al. 1999). So, it is reasonable to assume that the average amount of 0.11 g N_2O is produced by each pig during a day.

To make 50 kg of a 10% bio-modified bitumen, the production of 5 kg Bio-binder is required. Using 1.25 kg for the solid portion of manure in a batch of slurry used to produce 450g of Bio-binder, the production of 5 kg Bio-binder requires enough manure to have 13.9 kg of solids. Data gathered from farmers of North Carolina states that the average amount of manure per pig over 20 weeks is 1.58 kg/day; of this amount, 10 wt%

is solid waste, and the rest is liquid. Therefore, one pig produces 0.158 kg/day of manure solids, and 88 pigs produce 13.9 kg/day of manure solids from 139 kg/day of manure. Figure 6-a shows the comparative results of emissions from storing 139 kg of manure in lagoons versus using it to produce 5 kg of Bio-binder. Using the previously used conversion factors of 21 for methane and 310 for nitrous oxide, the GWPI for bio-binder and for swine manure in nature are presented in Figure 7.6.

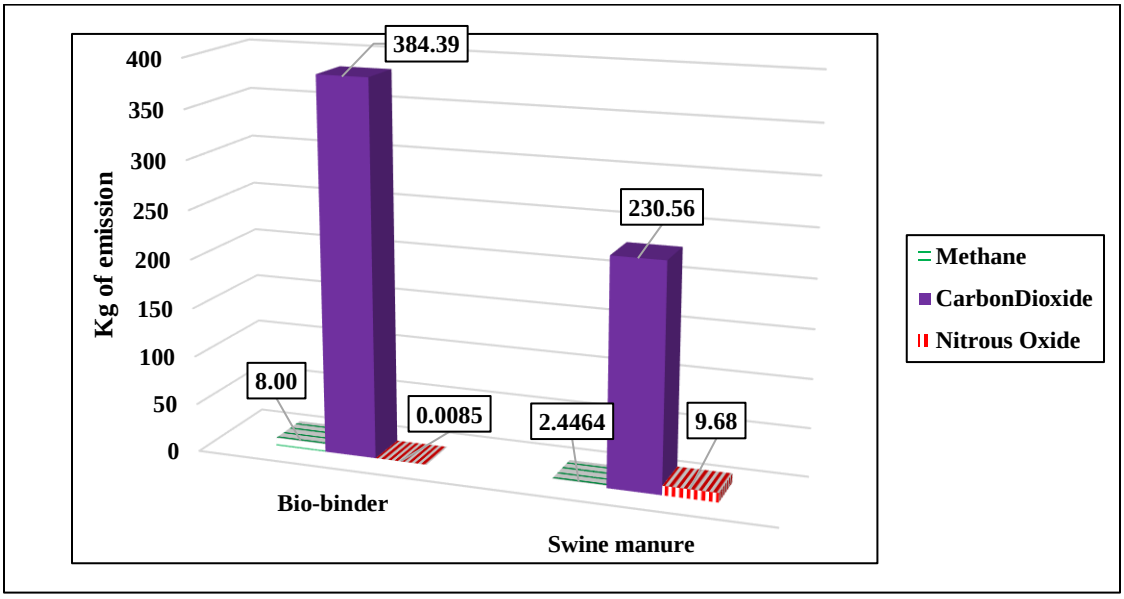

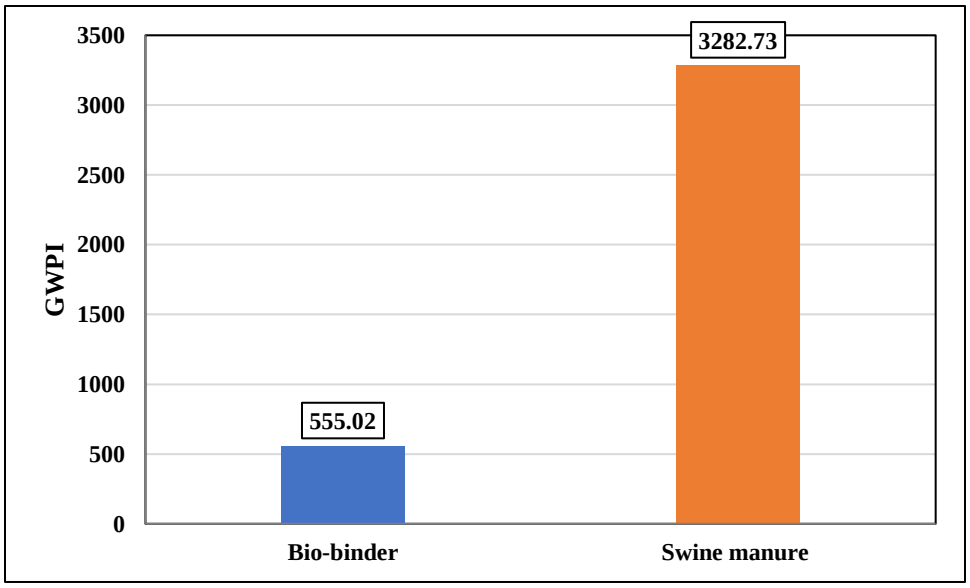

Figure 7.6- Top: Gas emissions for Storing 139 kg of Manure in A Lagoon Versus Using It to Produce 5 Kg of bio-binder; Bottom: Global Warming Potential Index for Storing 139 kg of Manure in A Lagoon Versus Using It to Produce 5 Kg of bio-binder.

7.7 Summary

In this study, a comparative life cycle assessment was conducted on conventional bitumen and a bio-modified bitumen that is 90 wt% bitumen and 10 wt% bio-binder obtained from HTL of swine manure. The results of the analysis show an improvement in the environmental impact of the bitumen after replacing 10 wt% of it with bio-binder from swine manure. Both the GWP and the energy consumption of the cradle-to-gate LCA show a lower impact of the bio-modified bitumen. Mixing and compaction energy needed to maintain the proper workability of asphalt showed a reduction of over 50%.

The emission results showed that the production of conventional bitumen emitted over 5 times more carbon dioxide and approximately 3 times more methane to the environment compared to that of bio-binder. Global warming potential index of bio-modified bitumen improved by 7.8% compared to that of conventional bitumen. Furthermore, a comparative analysis of gas emissions from storing 139 kg of manure in a lagoon versus using it to produce 5 kg of bio-binder showed a decrease of over 80% in the global warming potential index.

8 FEASIBILITY OF TECHNOLOGY TRANSFER

In this chapter, we are going to discuss the economic viability of bio-binder (bio-rejuvenator) from swine manure as a partial replacement for bitumen and/or using as a rejuvenator to revitalize aged bitumen from reclaimed asphalt pavement (RAP) and recycled asphalt shingles (RAS).

8.1 Industry Pain

Bio-rejuvenator provides a sustainable solution to treat swine manure, which is a major challenge, both environmentally and economically. One pig produces more than 5000 gallons of manure per year. With more than 120,000,000 hogs being produced a year, we have more than 6 billion gallons of swine manure for treatment each year, and this is just the US. Swine manure is either stored in open lagoons – resulting in serious health and environmental issues - or being sold to the farmers as fertilizers –with added costs to the hog farmers to store and deliver it. This disruptive technology completely resolves these issues by converting swine manure to the bio-rejuvenator, which is then used as liquid asphalt for paving and construction applications or as a rejuvenator to reuse the recycled asphalt pavements.

From the demand side, the price of liquid asphalt has increased dramatically from $250 per ton in 2003 to $605 per ton in 2015 and $560 per ton in late 2018. The fluctuation of price makes decision making in the asphalt industry harder each year. The

pavement/construction industry is looking to use recycled asphalt pavements (RAP) and recycled asphalt shingles (RAS). Currently, in the US, more than 90 million tons of asphalt pavement were reclaimed every year, making asphalt the most frequently recycled material. In the process of construction of asphalt pavement (including materials, plant production, trucking, and lay down), materials are the most expensive production cost category, comprising about 70 percent of the cost to produce hot mix asphalt. There are pains on both sides of the supply chain.

According to the survey conducted by National Asphalt Pavement Association (NAPA), about 66.7 million tons of reclaimed asphalt pavement (RAP) and 1.2 million tons of reclaimed asphalt shingles (RAS) were collected in the U.S. during 2011 for use in new pavements. In 2017, RAP usage in new asphalt pavement mixtures reached 76.2 million tons, a greater than 36 percent increase from 2009. An additional 3.4 million tons of RAP were used as aggregate. At year-end 2017, some 102.1 million tons of RAP was estimated to be stockpiled for future use across the country. More than 99 percent of asphalt pavement reclaimed from roads, and parking lots were reclaimed for use in new pavements instead of going into landfills. In the survey, 98 percent of producers reported using RAP in their mixes for new construction, pavement preservation, rehabilitation, and other projects. RAS usage also continued to be widespread, with nearly 950,000 tons being used in 2017. RAS includes both manufacturers' scrap shingles and post-consumer

roofing shingles, and about 9 percent of the total supply of waste shingles nationwide are reclaimed for use in asphalt pavements.

The use of RAP and RAS during the 2011 paving season translates to a saving of 21.2 million barrels of liquid asphalt binder, saving taxpayers some $2.2 billion. When reclaimed asphalt pavement and shingles are processed into new pavement mixtures, the liquid asphalt binder in the recycled material is reactivated, reducing the need for virgin bitumen. Using reclaimed materials also reduces demands on aggregate resources. With RAP, old roads can be effectively mined for the raw materials needed to create their replacements. As per the findings of Asphaltrecycling.com, recycled asphalt is a huge cost saver for the local government. The savings amount to $30-$80 a ton. Contractors and municipalities recycle asphalt at $18/ton using a PT-PRO series Recycler. A hot mix costs $78/ton. Therefore, the saving is phenomenal at $60/ton. Hence, if a person uses 50 tons of asphalt for 30 days, he could save up to $90,000. The same logic applies to recycled asphalt shingles (RAS). Currently, over 11 million tons (22 billion lbs) of asphalt roofing materials are dumped in U.S. landfills each year. At an average of $125 per ton to dispose of this material, contractors are taking a gigantic hit on their job cost, which ultimately gets passed down to the homeowners looking to re-roof. Asphalt shingles can be turned into RAS, or recycled asphalt shingles, which can be reused for products such as roads, asphalt-based sealants, and more. At the same time, dump fees can be reduced to as little as $75 or less depending on the location.

Presently, state DOTs permit a limited use of RAP and RAS in asphalt pavements due to the degrading effect on the performance of the final product. A survey of U.S. States conducted by the Materials Engineering and Research Office of the Ministry of Transportation of Ontario, Canada, (MTO) found that for base and binder courses, 20–50 percent RAP was typically permitted. Permitted levels of RAP were higher in base courses and for light traffic roadways, as compared to medium or heavy traffic roadways. Some States commented that although high amounts of RAP were permitted, contractors typically did not submit mix designs for amounts greater than 25 percent. The goal of asphalt rejuvenators is to return aged asphalt materials to a pre-aged conditions and restore the pavement's desired performance in areas such as ductility, strain and resistance to various forms of cracking.

On the environmental side, it is documented that storing swine manure in lagoons increases the global warming potential 6 folds compared to the production of bio-binder.

In both cases, hog farmers pay to get rid of their manure. The innovative and revolutionary (patented) process converts swine manure to a bio-rejuvenator that can be used to restore desirable properties of asphalt binder in recycled asphalt pavement and shingles. Bio-binder is a sustainable (low cost, durable and eco-friendly) alternative resource developed from a thermochemical conversion of swine manure; it sequesters manure's carbon and greenhouse gases otherwise released into the atmosphere.

The following results were observed during our research on the feasibility of usage of bio-rejuvenator from swine manure:

- Bio-rejuvenator reduced stiffness of RAP by 40%
- Bio-rejuvenator improved workability of RAP
- Bio-rejuvenator improved cracking characteristics and had no negative effect on moisture susceptibility
- Bio-rejuvenator had a good degree of compatibility with both RAP and bitumen

And in case of using bio-rejuvenator for RAS:

- Bio-binder led to the improvement of recycled asphalt shingle (RAS) properties (You et al. 2011).
- Addition of bio-binder improved low-temperature properties of RAS asphalt (You et al. 2011).
- Application of 10% bio-binder alleviated the negative impacts of RAS on asphalt.
- Bio-modified RAS showed four degrees improvements in cracking temperature.

- Rheological properties of RAS asphalt were improved after bio-modification.

8.2 Customer/Market Analysis

Worldwide annual consumption of asphalt is 150 million tons, which makes it a $90 billion industry in 2013. According to a Specialists in Business Information (SBI) report, the U.S. market for liquid asphalt totaled $16 billion in 2013, up 45% from $8.7 billion in 2007. Global demand for asphalt is expected to increase 8.2 percent annually to reach to more than 198 million barrels in 2015. As the refineries are using coking technologies to convert crude oil into other value-added products, there has been a shortage of liquid asphalt in the market. According to the industry reports, the need for liquid asphalt is growing across the globe while the supply is shrinking.

9 CONCLUSION AND FUTURE RESEARCH

Asphalt pavement behavior at a macro-scale and its mechanical properties have been well studied. However, the underlying reasons for the occurrence of that behavior have not been well explained. Given the continuing pavement failures despite many experiments on asphalt pavement and macro-scale studies, it is necessary to understand the relationship between asphalt binder's mechanical behavior, chemical components, and molecular interactions. Using a multi-scale approach to characterize the effect of a modifier on bitumen can be one of the first steps towards a better understanding of the shortcomings and failure mechanisms of asphalt pavements. The following sections explain the conclusions of this research and the contributions to the body of knowledge, followed by recommendations for future work.

9.1 Contributions to the Body of Knowledge

In this research, a multi-scale approach was used to understand bitumen behavior and make a connection between macro-scale, micro-scale, and nano-scale behavior of the material before and after modification. The experiment part of the study was used to characterize bitumen based on thermo-mechanical and chemical characteristics. The molecular dynamics simulations were used to study the nano-scale interactions between bitumen molecules and modifier molecules to explain the underlying mechanisms controlling the macro-scale behavior of modified asphalt.

The modification of virgin bitumen containing straight-chain wax was studied as an analogue for wax-based modifiers in warm-mix asphalt. Wax-based modifiers are commonly used to reduce the mixing and compaction temperature of asphalt by increasing the workability of asphalt. It was shown that the softening effect of wax at higher service temperature could be due to disruption in the agglomeration of asphaltene molecules. However, at lower temperatures than the melting point of the wax, the crystallization of wax made the bitumen stiffer and more brittle.

Wax is also a constituent of many rejuvenators such as waste engine oil and waste vegetable oil that are used as softening agents and rejuvenators for aged bitumen. Therefore, to understand the working mechanism of wax-based rejuvenators, interactions between wax and aged bitumen were studied. It was shown that wax molecules could deagglomerate oxidized asphaltene molecules due to the CH-pi interaction between the wax's aliphatic chain and the asphaltene's polyaromatic structure. The results of experiments showed that the overall molecular size of bitumen was reduced after modification with wax. at lower temperatures, wax caused bitumen stiffening; the increased stiffness reduced the capability of bitumen to relax stress. Such a finding is critical to help synthesize and design highly effective rejuvenators and avoid unexpected side-effects from the application of wax-based rejuvenators.

The use of multiple modifiers in asphalt binder is common; for instance, introducing wax-based additives to a bitumen containing polyphosphoric acid (PPA) is commonly practiced. However, the interplay of modifiers and its plausible negative

effects on asphalt properties are not well understood. Therefore, we studied the interplay of wax-based modifiers with polyphosphoric acid, and we showed how polyphosphoric acid affects bitumen's mechanical properties as an elastomer. In this study, it was shown that wax molecules could hinder the effectiveness of PPA by counteracting the PPA mechanism of forming hydrogen bonds with the resin fraction of bitumen.

One of the concerns with the use of wax-based modifiers is their crystallization and lack of proper dispersion in asphalt. The crystallization of wax could lead to asphalt's brittle behavior, making it more prone to cracks at low temperatures. To enhance dispersion and avoid crystallization, we examined the role of nanoparticles as carriers for wax. It was found that nano zeolite particles can absorb paraffin wax molecules in their pores and release them when added to bitumen. After releasing the wax molecules, the nano zeolite particles continue by adsorbing the acidic molecules of bitumen, thereby reducing the moisture susceptibility of bitumen.

In addition, this study assessed the economic and environmental impact of a bio-based modifier as a partial replacement for bitumen, using a life-cycle assessment to emphasize the fact that rejuvenators should provide beneficial changes over neat bitumen. To facilitate the transition of research outcomes to the market, a market analysis was performed to highlight the opportunities and challenges associated with the adaptation and deployment of research outcomes. It was shown that a bio-modifier derived from swine manure has the merits of meeting market needs and competing with similar products currently available by enhancing bitumen's properties at a lower cost.

9.1.1 Critique of Current Literature

In the case of warm-mix asphalt technology using chemical additives such as wax, the literature explains that the presence of wax can soften the bitumen and make it workable at temperatures 20 - 40^{o}C lower than conventional asphalt (Kristjánsdóttir et al. 2007). The same effect was observed for the use of wax or additives that contain paraffinic materials in aged bitumen obtained from reclaimed asphalt pavement (RAP) or recycled asphalt shingles (RAS). At intermediate service temperatures of asphalt (25-70^{o}C), the presence of wax (with melting temperature of 30 to 70 ^{o}C) increases the chance of rutting due to the softness of asphalt. On the other hand, a number of research studies showed that the use of Fischer–Tropsch wax could improve the rutting behavior of asphalt due to its branched structure (Richter 2002; Richter 2002).

On the other hand, the use of wax in asphalt pavement or the presence of wax in asphalt additives such as rejuvenators has been shown to increase the embrittlement of asphalt at sub-zero temperatures. This stiffening effect of wax on asphalt and the severity of the effect again depend on the wax structure as well as the chemical composition of the bitumen. Therefore, there is a need for understanding the relationship between the mechanical properties of bitumen and its chemical composition.

Furthermore, it is important to understand the interplay between different modifiers and their synergistic and antagonistic effects on asphalt performance. For instance, bitumen can contain some level of PPA that can raise the grade of bitumen and make it more elastic at higher temperatures. This usually isn’t mentioned when the

bitumen is being purchased from refineries. Modifying the PPA-modified bitumen with wax or waxy modifiers could cause adverse effects and intensify asphalt failure. The literature lacked a comprehensive study of the interplay between modifiers and their effect on bitumen properties.

Due to oxidative aging, bitumen changes chemically, and this affects the bitumen's mechanical properties and makes the pavement prone to cracking. In order to recycle asphalt pavement at the end of its service life, and to use this as material for new pavement at a rate beyond 30% of new material, the asphalt's original properties need to be chemically restored. This should be done by using rejuvenators that contain some of the lighter components of asphalt that have escaped the pavement during the service years. The literature covers experiments characterizing the effect of rejuvenators on bitumen and its mechanical properties such as viscosity and complex modulus. However, the mechanism of rejuvenation, the molecular interaction of rejuvenator and bitumen, and the connection between molecular interaction and asphalt's mechanical properties are yet to be investigated. This is especially important when a rejuvenator improves some asphalt properties such as viscosity but worsens other properties such as low-temperature cracking.

The economic and environmental aspects of bitumen modification are usually overlooked, while most research focuses on the experiment side of bitumen modifications. In other words, a modifier may be desirable from an experimental point of view, but its cost of production and environmental impact make it economically

infeasible. The use of life-cycle assessment (LCA) can especially help to understand the advantages of modification of bitumen from an environmental point of view, and knowing the industry's difficulties can help to optimize the product for the public need.

9.1.2 Conclusion of research

The findings of this dissertation can be grouped in five categories:

- **Wax as a warm-mix additive:** The study of wax as a warm-mix additive showed that paraffin wax has a lowering effect on the viscosity of asphalt at high temperature and can lower the mixing and compaction temperatures significantly. This effect is present at temperatures above the melting point of wax. Under the melting temperature of the wax, the binder starts to become stiffer as wax crystals start to form. This causes the complex modulus of modified bitumen to become higher than that of virgin binder. At sub-zero temperatures, wax-modified bitumen becomes highly brittle, which is evident by the stiffness and m-value measured from a bending beam rheometer (BBR) test. The direct tension test (DTT) also showed that the tensile strength of bitumen is greatly compromised after modification with wax. The results of molecular simulation showed that straight-chain wax could reduce the size of nanoaggregates of asphaltene molecules. This can be the reason behind the softening effect of wax at high temperatures, where wax molecules have higher mobility.
- **Wax as a part of rejuvenators:** The effect of wax on the properties of aged bitumen was studied by doping aged binder with wax at different concentrations.

The experiments showed that wax can reduce viscosity of aged bitumen at high temperature similar to that of virgin bitumen. Furthermore, wax increased the elasticity of aged bitumen, as illustrated by a multiple-stress creep-recovery (MSCR) test. At low temperatures, wax caused the bitumen to become stiffer and more brittle, which can increase the chance of fatigue cracking. At the nano-scale, using gel permeation chromatography, it was shown that the average molecular size of aged bitumen decreases after the introduction of wax. The same effect was observed in molecular simulation results, where wax molecules could prevent the formation of oxidized asphaltene agglomerates. This phenomenon was shown to be due to CH-pi interaction between the aliphatic chain of a wax molecule and the aromatic core of an asphaltene molecule. The molecular simulations showed that wax molecules could disperse asphaltene molecules in a medium of solvent while being mobile (not crystallized).

- **Wax as an inherent component of bitumen:** Paraffin wax is an inherent component of many kinds of bitumen, especially those from the Middle East, which are known as waxy asphalt or heavy-crude asphalt. The addition of polyphosphoric acid to soft bitumen is an old practice to overcome the softness of asphalt. Polyphosphoric acid has been shown to enhance high-temperature properties without negatively impacting the low-temperature performance of asphalt pavement. However, due to the interplay between wax and polyphosphoric acid, it is hypothesized that the presence of wax may moderate

polyphosphoric acid-bitumen interactions. The results of the molecular dynamics simulation showed that polyphosphoric acid has a strong interaction with fused aromatics such as those classified as resins in bitumen; such interactions lead to the reduced solubility of resins in heptane, causing them to precipitate out in heptane and fall into the asphaltene category. The presence of wax appeared to reduce the efficacy of polyphosphoric acid at increasing bitumen's elasticity, as evidenced by a lower complex modulus and a higher creep compliance compared to no-wax bitumen doped with polyphosphoric acid. This was further observed in computational analysis, which showed a good interaction between resin molecules and PPA molecules. However, the interaction between resins and PPA was reduced when wax was added; the wax caused resins to become more scattered, as evidenced by a significant reduction in the radial distribution function of resin molecules.

- **Using nanozeolite as a carrier for wax:** At high temperatures, the effect of wax on bitumen's rheological properties was found to be independent of using nanozeolite as a carrier for wax or adding wax and nanozeolite to bitumen separately. This was expected, due to wax being liquid above its melting point. However, at low temperatures, bitumen containing wax-impregnated nanozeolite (Winz) showed an improved resistance to low-temperature cracking, which can be attributed to reduced wax crystallization when wax is dispersed via nanozeolite. In addition, wax-impregnated nanozeolite was found to adsorb the acidic

compounds of bitumen while releasing the wax. Computational analysis showed that even though wax interacts with nanozeolite, acid molecules have preferential adsorption and easily replace wax on the nanozeolite surface. Adsorption of acids to the nanozeolite surface was also evidenced by a laboratory experiment showing a significant change in the shear-thinning behavior of bitumen doped with wax-impregnated nanozeolite when exposed to water. Hydrolysis of acidic compounds at the surface of nanozeolite caused a 42% reduction in the shear-thinning rate after water conditioning. Nanozeolite was shown to effectively adsorb acids from bitumen and release wax to bitumen. Therefore, it can be a promising candidate to facilitate the introduction of wax-based additives to bitumen to alleviate wax crystallization while adsorbing acids, thereby reducing the quantity of acids at the interface of bitumen and stone aggregates. This, in turn, can improve bitumen's resistance to both low-temperature cracking and moisture damage. The results of this paper facilitate the use of wax-based additives to reduce energy consumption during construction while enhancing the performance of the resulting pavements.

- **Environmental assessment and cost analysis of a bio-modifier from swine manure:** The use of a bio-binder obtained from a hydrothermal liquefaction process of swine manure as a partial replacement for bitumen was found to be effective to reduce the environmental impact of asphalt pavements. The results of the analysis show an improvement in the environmental impact of the asphalt binder after replacing 10 wt% of it with bio-binder from swine manure. Both the

global warming potential (GWP) and the energy consumption of the cradle-to-gate life-cycle assessment (LCA) showed a lower impact of the bio-modified binder. There was a reduction of over 50% in the mixing and compaction energy needed to maintain the proper workability of asphalt. The emission results showed that the production of conventional bitumen emitted over five times more carbon dioxide and approximately three times more methane to the environment compared to the production of bio-binder. The index of global warming potential of bio-modified bitumen was improved by 7.8% compared to that of conventional bitumen. Furthermore, a comparative analysis of the gas emissions from storing 139 kg of manure in a lagoon versus using it to produce 5 kg of bio-binder showed a decrease of over 80% in the index of global warming potential.

9.2 Recommendation for Future Research

This research showed that the effect of a modifier on bitumen could be advantageous or disadvantageous, depending on factors such as the chemical compositions of the modifier and the bitumen, the molecular structures involved, and the temperature. Further research is recommended to extend the findings of this study:

- This study focused on binder-level characterization. We showed that wax crystallizes in bitumen at intermediate temperature; this may affect the bitumen's binding to stone aggregates. Therefore, the effect of wax on the adhesion of bitumen to stone aggregates should be investigated.

- Considering the significant interplay between wax and acidic compounds, it is recommended that bitumen with various concentrations of acids be used to study adhesion and moisture susceptibility.
- Considering that we showed that the presence of wax facilitates the mobility of asphalt molecules, and that healing is highly affected by molecular diffusivity, the effect of wax on the healing process of asphalt pavement should be investigated.
- In this study, it was shown that wax crystallization could lead to unwanted effects such as promoting low-temperature cracking. Inhibitors are used in the oil industry to prevent wax crystallization. The study of inhibitors such as polyacrylates and polymethacrylates in bitumen containing wax is recommended.
- In this research it was shown that PPA can reduce the moisture susceptibility of bitumen. It is recommended to research on the interaction of PPA-silica and the mechanism of effect of water molecules on PPA modified bitumen adhesion with aggregate surface.
- The merits of using nanozeolite impregnated with wax was evaluated in this study. However, it needs further research to evaluate where in the supply chain of asphalt pavement we need to add this modifier for the best results.
- Our life-cycle assessment study showed that Bio-binder from swine manure is a promising replacement for asphalt. It is recommended to develop a

deterioration model based on operational factors (such as traffic volume) for bio-modified asphalt pavement to extend the evaluation beyond the current boundary of cradle-to-gate.

9.3 List of Publications

1. Samieadel, Alireza, and Elham H. Fini. "Interplay between wax and polyphosphoric acid and its effect on bitumen thermomechanical properties." *Construction and Building Materials* 243 (2020): 118194. https://www.sciencedirect.com/science/article/abs/pii/S0950061820301999
2. Samieadel, Alireza, Bjarke Høgsaa, and Elham H. Fini. "Examining the Implications of Wax-Based Additives on the Sustainability of Construction Practices: Multiscale Characterization of Wax-Doped Aged Asphalt Binder." *ACS Sustainable Chemistry & Engineering* 7, no. 3 (2018): 2943-2954. https://pubs.acs.org/doi/10.1021/acssuschemeng.8b03842
3. Samieadel, Alireza, Daniel Oldham, and Elham H. Fini. "Investigating molecular conformation and packing of oxidized asphaltene molecules in presence of paraffin wax." *Fuel* 220 (2018): 503-512. https://www.sciencedirect.com/science/article/pii/S001623611830190X
4. Samieadel, Alireza, Keith Schimmel, and Ellie H. Fini. "Comparative life cycle assessment (LCA) of bio-modified binder and conventional asphalt

binder." *Clean Technologies and Environmental Policy* 20, no. 1 (2018): 191-200. https://link.springer.com/article/10.1007/s10098-017-1467-1

5. Samieadel, Alireza, Daniel Oldham, and Elham H. Fini. "Multi-scale characterization of the effect of wax on intermolecular interactions in asphalt binder." *Construction and Building Materials* 157 (2017): 1163-1172. https://www.sciencedirect.com/science/article/pii/S0950061817320202
6. Pahlavan, Farideh, Shahrzad Hosseinnezhad, Alireza Samieadel, Albert Hung, and Elham Fini. "Fused Aromatics To Restore Molecular Packing of Aged Bituminous Materials." *Industrial & Engineering Chemistry Research* 58, no. 27 (2019): 11939-11953. https://pubs.acs.org/doi/10.1021/acs.iecr.9b01397
7. Pahlavan, Farideh, Alireza Samieadel, Shuguang Deng, and Elham Fini. "Exploiting Synergistic Effects of Intermolecular Interactions to Synthesize Hybrid Rejuvenators To Revitalize Aged Asphalt." *ACS Sustainable Chemistry & Engineering* 7, no. 18 (2019): 15514-15525. https://pubs.acs.org/doi/abs/10.1021/acssuschemeng.9b03263

REFERENCES

AASHTO, T. (1998). "245-97,"." *Resistance to Plastic Flow of Bituminous Mixtures Using Marshall Apparatus," American Association of State Highway and Transportation Officials, Standard Specifications for Transportation Materials and Methods of Sampling And Testing Part II Tests*, 19.

AASHTO, T. (2004). "312." *Standard Method of Test for Preparing and Determining the Density of Hot Mix Asphalt (HMA) Specimens by Means of the Superpave Gyratory Compactor.‖ American Association of State Highway and Transportation Officials*.

AASHTO T 350-14 (2014). "Standard Method of Test for Multiple Stress Creep Recovery (MSCR) Test of Asphalt Binder Using a Dynamic Shear Rheometer (DSR)." American Association of State and Highway Transportation Officials.

Ajienka, J., and Ikoku, C. (1990). "Waxy crude oil handling in Nigeria: practices, problems, and prospects." *Energy sources*, 12(4), 463-478.

Akisetty, C. K., Lee, S.-J., and Amirkhanian, S. N. (2009). "High temperature properties of rubberized binders containing warm asphalt additives." *Construction and Building Materials*, 23(1), 565-573.

Akiya, N., and Savage, P. E. (2002). "Roles of water for chemical reactions in high-temperature water." *Chemical Reviews*, 102(8), 2725-2750.

Al-Adham, K., and Wahhab, H. A.-A. (2015). "Effect of polymer type on improving rheological parameters related to rutting resistance of asphalt binders." *Bitum. Mixtures Pavements VI*, 89.

Allen, R. G., Little, D. N., Bhasin, A., and Glover, C. J. (2014). "The effects of chemical composition on asphalt microstructure and their association to pavement performance." *International Journal of Pavement Engineering*, 15(1), 9-22.

Amon, B., Kryvoruchko, V., Amon, T., and Zechmeister-Boltenstern, S. (2006). "Methane, nitrous oxide and ammonia emissions during storage and after application of dairy cattle slurry and influence of slurry treatment." *Agriculture, ecosystems & environment*, 112(2), 153-162.

Anderson, G., Smith, R., Bundy, D., and Hammond, E. (1987). "Model to predict gaseous contaminants in swine confinement buildings." *Journal of Agricultural Engineering Research*, 37(3), 235-253.

Anderson, R. M., King, G. N., Hanson, D. I., and Blankenship, P. B. (2011). "Evaluation of the relationship between asphalt binder properties and non-load related cracking." *Journal of the Association of Asphalt Paving Technologists*, 80.

Anderson, R. M., King, G. N., Hanson, D. I., and Blankenship, P. B. (2011). "Evaluation of the relationship between asphalt binder properties and non-load related cracking." *Journal of the Association of Asphalt Paving Technologists*, 80, 615-664.

Anderson, R. M., King, G. N., Hanson, D. I., and Blankenship, P. B. (2011). "Evaluation of the relationship between asphalt binder properties and non-load related cracking." *Journal of the Association of Asphalt Paving Technologists*.

Arega, Z., Bhasin, A., Motamed, A., and Turner, F. (2011). "Influence of warm-mix additives and reduced aging on the rheology of asphalt binders with different natural wax contents." *Journal of Materials in Civil Engineering*, 23(10), 1453-1459.

Asphalt Pavement Environmental Council, and Association, N. A. P. (2000). *Best Management Practices to Minimize Emissions During HMA Construction*, Asphalt Pavement Environmental Council.

ASTM D1946-90 (2015). "Standard Practice for Analysis of Reformed Gas by Gas Chromatography." *e1*, ASTM International, West Conshohocken, PA.

ASTM D2872-12e1 (2012). "Standard Test Method for Effect of Heat and Air on a Moving Film of Asphalt (Rolling Thin-Film Oven Test)." ASTM International, West Conshohocken, PA.

ASTM D3279-07 (2007). "ASTM International." *Standard Test Method for n-Heptane Insolubles*West Conshohocken, PA.

ASTM D4402 (2015). "Standard Test Method for Viscosity Determination of Asphalt at Elevated Temperatures Using a Rotational Viscometer." ASTM International.

ASTM D6373 - 16 (2016). "Standard Specification for Performance Graded Asphalt Binder." ASTM International, West Conshohocken, PA.

ASTM D6521-13 (2013). "Standard Practice for Accelerated Aging of Asphalt Binder Using a Pressurized Aging Vessel (PAV)." ASTM International, Wes Conshohocken, PA.

ASTM D6648 (2016). " Standard Test Method for Determining the Flexural Creep Stiffness of Asphalt Binder Using the Bending Beam Rheometer (BBR)." ASTM International, West Conshohocken, PA.

ASTM D6723-12 (2012). "ASTM International." *Standard Test Method for Determining the Fracture Properties of Asphalt Binder in Direct Tension (DT),* ASTM International, West Conshohocken, PA.

ASTM D7552-09 (2014). "Standard Test Method for Determining the Complex Shear Modulus (G*) Of Bituminous Mixtures Using Dynamic Shear Rheometer." ASTM International, West Conshohocken, PA.

ASTM E1269-11 (2018). "Standard Test Method for Determining Specific Heat Capacity by Differential Scanning Calorimetry." ASTM International, West Conshohocken, PA.

Athena Research Institute (2006). "A life cycle perspective on concrete and asphalt roadways: embodied primary energy and global warming potential."Ottawa, Canada: Cement Association of Canada.

Baldino, N., Gabriele, D., Rossi, C. O., Seta, L., Lupi, F. R., and Caputo, P. (2012). "Low temperature rheology of polyphosphoric acid (PPA) added bitumen." *Construction and Building Materials*, 36, 592-596.

Banerjee, A., de Fortier Smit, A., and Prozzi, J. A. (2012). "The effect of long-term aging on the rheology of warm mix asphalt binders." *Fuel*, 97, 603-611.

Baumgardner, G. L., Masson, J., Hardee, J. R., Menapace, A. M., and Williams, A. G. (2005). "Polyphosphoric acid modified asphalt: proposed mechanisms." *Journal of the Association of Asphalt Paving Technologists*, 74, 283-305.

Bennert, T., Pezeshki, D., Shaarbafan, N., and Euler, C. (2016). "Warm-mix asphalt trials in New York State: Laboratory and field performance." *Transportation Research Record: Journal of the Transportation Research Board*(2575), 175-186.

Bissada, K. A., Tan, J., Szymczyk, E., Darnell, M., and Mei, M. (2016). "Group-type characterization of crude oil and bitumen. Part I: Enhanced separation and quantification of saturates, aromatics, resins and asphaltenes (SARA)." *Organic Geochemistry*, 95, 21-28.

Bowers, B. F., Huang, B., and Shu, X. (2014). "Refining laboratory procedure for artificial RAP: A comparative study." *Construction and Building Materials*, 52, 385-390.

Brasileiro, L., Moreno-Navarro, F., Tauste-Martínez, R., Matos, J., and Rubio-Gámez, M. d. C. (2019). "Reclaimed polymers as asphalt binder modifiers for more sustainable roads: A Review." *Sustainability*, 11(3), 646.

Brown-Brandl, T., Nienaber, J. A., Xin, H., and Gates, R. S. (2004). "A literature review of swine heat production." *TRANSACTIONS-AMERICAN SOCIETY OF AGRICULTURAL ENGINEERS*, 47(1), 259-270.

Brownridge, J. "The role of an asphalt rejuvenator in pavement preservation: use and need for asphalt rejuvenation." *Proc., Compendium of papers from the first international conference on pavement preservation*, Newport Beach, Federal Highway Administration, 351-364.

Butz, T., Rahimian, I., and Hildebrand, G. (2000). "Modifikation von Straßenbaubitumen mit Fischer-Tropsch-Paraffin." *Transportation Research Board*.

Butz, T., Rahimian, I., and Hildebrand, G. (2000). "Modifikation von Straßenbaubitumen mit Fischer-Tropsch-Paraffin." *Bitumen*, 62(3).

Canestrari, F., Graziani, A., Pannunzio, V., and Bahia, H. U. (2013). "Rheological properties of bituminous binders with synthetic wax." *International Journal of Pavement Research and Technology*, 6(1), 15.

Cantrell, K. B., Ducey, T., Ro, K. S., and Hunt, P. G. (2008). "Livestock waste-to-bioenergy generation opportunities." *Bioresource technology*, 99(17), 7941-7953.

Chae, K., Jang, A., Yim, S., and Kim, I. S. (2008). "The effects of digestion temperature and temperature shock on the biogas yields from the mesophilic anaerobic digestion of swine manure." *Bioresource Technology*, 99(1), 1-6.

Chen, M., Xiao, F., Putman, B., Leng, B., and Wu, S. (2014). "High temperature properties of rejuvenating recovered binder with rejuvenator, waste cooking and cotton seed oils." *Construction and Building Materials*, 59, 10-16.

Chen, S., Popovich, J., Iannuzo, N., Haydel, S. E., and Seo, D.-K. (2017). "Silver-Ion-Exchanged Nanostructured Zeolite X as Antibacterial Agent with Superior Ion Release Kinetics and Efficacy against Methicillin-Resistant Staphylococcus aureus." *ACS applied materials & interfaces*, 9(45), 39271-39282.

Chen, S., Zhang, W., Sorge, L. P., and Seo, D.-K. (2019). "Exploratory Synthesis of Low-Silica Nanozeolites through Geopolymer Chemistry." *Crystal Growth & Design*.

Chhabra, R. P. (2010). "Non-Newtonian fluids: an introduction." *Rheology of complex fluids*, Springer, 3-34.

Chitra, R., and Yashonath, S. (1997). "Estimation of error in the diffusion coefficient from molecular dynamics simulations." *The Journal of Physical Chemistry B*, 101(27), 5437-5445.

Choi, M., Na, K., Kim, J., Sakamoto, Y., Terasaki, O., and Ryoo, R. (2009). "Stable single-unit-cell nanosheets of zeolite MFI as active and long-lived catalysts." *Nature*, 461(7261), 246.

Chowdhury, A., and Button, J. W. (2008). "A review of warm mix asphalt." Texas Transportation Institute, the Texas A & M University System.

Corbett, L. W. (1969). "Composition of asphalt based on generic fractionation, using solvent deasphaltening, elution-adsorption chromatography, and densimetric characterization." *Analytical Chemistry*, 41(4), 576-579.

Corbridge, D. E. C. (1980). *Phosphorus. An outline of its chemistry, biochemistry, and technology*, Elsevier Scientific Co.

Croteau, J.-M., and Tessier, B. "Warm mix asphalt paving technologies: a road builder's perspective." *Proc., Annual Conference of the Transportation Association of Canada, Toronto*.

Dämmgen, U., Schulz, J., Klausing, H. K., Hutchings, N. J., Haenel, H.-D., and Rösemann, C. (2012). "Enteric methane emissions from German pigs." *Landbauforschung*, 62(3), 83-96.

De Filippis, P., Giavarini, C., and Scarsella, M. (1995). "Improving the ageing resistance of straight-run bitumens by addition of phosphorus compounds." *Fuel*, 74(6), 836-841.

De Moraes, M., Pereira, R., Simão, R., and Leite, L. (2010). "High temperature AFM study of CAP 30/45 pen grade bitumen." *Journal of Microscopy*, 239(1), 46-53.

Departments of the Army and the Air Force (1988). "STANDARD PRACTICE FOR PAVEMENT RECYCLING."

Dickie, J. P., and Yen, T. F. (1967). "Macrostructures of the asphaltic fractions by various instrumental methods." *Analytical chemistry*, 39(14), 1847-1852.

Dong, H., Zhu, Z., Shang, B., Kang, G., Zhu, H., and Xin, H. (2007). "Greenhouse gas emissions from swine barns of various production stages in suburban Beijing, China." *Atmospheric Environment*, 41(11), 2391-2399.

Durrieu, F., Farcas, F., and Mouillet, V. (2007). "The influence of UV aging of a styrene/butadiene/styrene modified bitumen: comparison between laboratory and on site aging." *Fuel*, 86(10), 1446-1451.

EAPA (2016). "The Use of Warm Mix Asphalt. European Asphalt Pavement Association, EAPA position paper." <http://www.eapa.org/>. (July 12, 2018).

Eberhardsteiner, L., Füssl, J., Hofko, B., Handle, F., Hospodka, M., Blab, R., and Grothe, H. (2015). "Influence of asphaltene content on mechanical bitumen behavior: experimental investigation and micromechanical modeling." *Materials and Structures*, 48(10), 3099-3112.

Edwards, Y., and Redelius, P. (2003). "Rheological effects of waxes in bitumen." *Energy & Fuels*, 17(3), 511-520.

Edwards, Y., Tasdemir, Y., and Isacsson, U. (2006). "Rheological effects of commercial waxes and polyphosphoric acid in bitumen 160/220—low temperature performance." *Fuel*, 85(7-8), 989-997.

Edwards, Y., Tasdemir, Y., and Isacsson, U. (2007). "Rheological effects of commercial waxes and polyphosphoric acid in bitumen 160/220–high and medium temperature performance." *Construction and Building Materials*, 21(10), 1899-1908.

Einstein, A. (1905). "Über die von der molekularkinetischen Theorie der Wärme geforderte Bewegung von in ruhenden Flüssigkeiten suspendierten Teilchen." *Annalen der physik*, 322(8), 549-560.

Epps Martin, A., Zhou, F., Arambula, E., Park, E., Chowdhury, A., Kaseer, F., Yin, F., Munoz, J. C., Rose, A., and Hajj, E. (2016). "The Effects of Recycling Agents On Asphalt Mixtures with High RAS and RAP Binder Ratios." NCHRP Project.

Fini, E. H., Al-Qadi, I. L., You, Z., Zada, B., and Mills-Beale, J. (2012). "Partial replacement of asphalt binder with bio-binder: characterisation and modification." *International Journal of Pavement Engineering*, 13(6), 515-522.

Fini, E. H., Kalberer, E. W., Shahbazi, A., Basti, M., You, Z., Ozer, H., and Aurangzeb, Q. (2011). "Chemical characterization of biobinder from swine manure: Sustainable modifier for asphalt binder." *Journal of Materials in Civil Engineering*, 23(11), 1506-1513.

Fini, E. H., Yang, S.-H., and Xiu, S. "Characterization and application of manure-based bio-binder in asphalt industry." *Proc., Transportation Research Board 89th Annual Meeting*.

Finkbeiner, M., Inaba, A., Tan, R., Christiansen, K., and Klüppel, H.-J. (2006). "The new international standards for life cycle assessment: ISO 14040 and ISO 14044." *The international journal of life cycle assessment*, 11(2), 80-85.

Firoozifar, S. H., Foroutan, S., and Foroutan, S. (2011). "The effect of asphaltene on thermal properties of bitumen." *Chemical Engineering Research and Design*, 89(10), 2044-2048.

Fischer, H. R., Dillingh, E., and Hermse, C. (2014). "On the microstructure of bituminous binders." *Road Materials and Pavement Design*, 15(1), 1-15.

Franklin Associates (2011). "Cradle-to-Gate Life Cycle Inventory of Nine Plastic Resins and Four Polyurethane Precursors." The Plastics Division of the American Chemistry Council Prairie Village, KS, USA.

Gama, D. A., Yan, Y., Rodrigues, J. K. G., and Roque, R. (2018). "Optimizing the use of reactive terpolymer, polyphosphoric acid and high-density polyethylene to achieve asphalt binders with superior performance." *Construction and Building Materials*, 169, 522-529.

Gawel, I., and Czechowski, F. (1998). "Wax content of bitumens and its composition." *Erdoel, Erdgas, Kohle*, 114(10), 507-509.

Ge, D., Yan, K., You, L., and Wang, Z. (2017). "Modification mechanism of asphalt modified with Sasobit and Polyphosphoric acid (PPA)." *Construction and Building Materials*, 143, 419-428.

Giavarini, C., Mastrofini, D., Scarsella, M., Barré, L., and Espinat, D. (2000). "Macrostructure and rheological properties of chemically modified residues and bitumens." *Energy & fuels*, 14(2), 495-502.

Gibbs, M., Jun, P., and Gaffney, K. "N2O and CH4 emissions from livestock manure." *Proc., Background paper for IPCC expert meeting on Good Practice in Inventory Preparation: Agricultural Sources of Methane and Nitrous Oxide*, 24-26.

Goual, L., Sedghi, M., Wang, X., and Zhu, Z. (2014). "Asphaltene aggregation and impact of alkylphenols." *Langmuir*, 30(19), 5394-5403.

Goudriaan, F., Van de Beld, B., Boerefijn, F., Bos, G., Naber, J., Van der Wal, S., and Zeevalkink, J. (2000). "Thermal efficiency of the HTU process for biomass liquefaction." *Progress in thermochemical biomass conversion*, 2.

Häkkinen, T., and Mäkelä, K. (1996). "Environmental impact of concrete and asphalt pavements in environmental adaption of concrete." *Research Notes*.

Hanz, A., Faheem, A., Mahmoud, E., and Bahia, H. (2010). "Measuring effects of warm-mix additives: Use of newly developed asphalt binder lubricity test for the dynamic shear rheometer." *Transportation Research Record: Journal of the Transportation Research Board*(2180), 85-92.

Harwood, L. M., Moody, C. J., and Harwood, L. M. (1989). *Experimental organic chemistry: principles and practice*, Blackwell Scientific Oxford, United Kingdom.

Headen, T., Boek, E., Jackson, G., Totton, T., and Müller, E. (2017). "Simulation of asphaltene aggregation through molecular dynamics: Insights and limitations." *Energy & Fuels*, 31(2), 1108-1125.

Hellmann, B., Zelles, L., Palojarvi, A., and Bai, Q. (1997). "Emission of Climate-Relevant Trace Gases and Succession of Microbial Communities during Open-Windrow Composting." *Applied and environmental microbiology*, 63(3), 1011-1018.

Hofko, B., Eberhardsteiner, L., Füssl, J., Grothe, H., Handle, F., Hospodka, M., Grossegger, D., Nahar, S., Schmets, A., and Scarpas, A. (2016). "Impact of maltene and asphaltene fraction on mechanical behavior and microstructure of bitumen." *Materials and Structures*, 49(3), 829-841.

Hosseinnezhad, S., Johnson, C., Oldham, D., and Fini, E. H. "Investigating the Effect of Processing Parameters on Bio-binder Characteristics." *Proc., Transportation Research Board 95th Annual Meeting*.

Hosseinnezhad, S., Shakiba, S., Mousavi, M., Louie, S. M., Karnati, S. R., and Fini, E. H. (2019). "Multiscale Evaluation of Moisture Susceptibility of Biomodified Bitumen." *ACS Applied Bio Materials*, 2(12), 5779-5789.

Houston, W., Mirza, M., Zapata, C., and Raghavendra, S. (2007). "Simulating the effects of hot mix asphalt aging for performance testing and pavement structural design." *NCHR Research Results Digest*, 324.

Huang, S., Chang, C., Cheng, P., Hsiao, C., Soong, Y., and Duan, T. (2014). "First-trimester combined screening is effective for the detection of unbalanced chromosomal translocations at 11 to 12 weeks of gestation." *Reproductive Sciences*, 21(5), 594-600.

Hung, A. M., Goodwin, A., and Fini, E. H. (2017). "Effects of water exposure on bitumen surface microstructure." *Construction and Building Materials*, 135, 682-688.

Hung, A. M., Mousavi, M., Pahlavan, F., and Fini, E. H. (2017). "Intermolecular interactions of isolated bio-oil compounds and their effect on bitumen interfaces." *ACS Sustainable Chemistry & Engineering*, 5(9), 7920-7931.

Hung, A. M., Pahlavan, F., Shakiba, S., Chang, S. L., Louie, S. M., and Fini, E. H. (2019). "Preventing Assembly and Crystallization of Alkane Acids at the Silica–Bitumen Interface To Enhance Interfacial Resistance to Moisture Damage." *Industrial & Engineering Chemistry Research*, 58(47), 21542-21552.

Hunter, C. A., and Sanders, J. K. (1990). "The nature of. pi.-. pi. interactions." *Journal of the American Chemical Society*, 112(14), 5525-5534.

Intergovernmental Panel on Climate Change (1995). *IPCC guidelines for national greenhouse gas inventories*, IPCC WGI Technical Support Unit.

IPCC Intergovernmental Panel On Climate Change (2006). "Guidelines for national greenhouse gas inventories." *CD ou no site: www. ipcc. ch. Guia de Boas Práticas*.

ISO14040 (2006). "14040: Environmental management–life cycle assessment–principles and framework." *London: British Standards Institution*.

Jackson, N., Mahoney, J. P., and Puccinelli, J. "SHRP 2 Project R23-Development of Guidelines for the Design and Construction of Long Life Pavements Using Existing Pavements." *Proc., First Congress of Transportation and Development Institute (TDI) American Society of Civil Engineers*.

Jarret, G., Martinez, J., and Dourmad, J.-Y. (2011). "Pig feeding strategy coupled with effluent management–fresh or stored slurry, solid phase separation–on methane potential and methane conversion factors during storage." *Atmospheric Environment*, 45(34), 6204-6209.

Jennings, P., Desando, M., Raub, M., Moats, R., Mendez, T., Stewart, F., Hoberg, J., Pribanic, J., and Smith, J. (1992). "NMR spectroscopy in the characterization of eight selected asphalts." *Fuel science & technology international*, 10(4-6), 887-907.

Jeppsson, K.-H. (2000). "SE—Structure and Environment: Carbon Dioxide Emission and Water Evaporation from Deep Litter Systems." *Journal of agricultural engineering research*, 77(4), 429-440.

Kane, M., Djabourov, M., Volle, J.-L., Lechaire, J.-P., and Frebourg, G. (2003). "Morphology of paraffin crystals in waxy crude oils cooled in quiescent conditions and under flow." *Fuel*, 82(2), 127-135.

Kebreab, E., Clark, K., Wagner-Riddle, C., and France, J. (2006). "Methane and nitrous oxide emissions from Canadian animal agriculture: A review." *Canadian Journal of Animal Science*, 86(2), 135-157.

Kim, Y., Lee, J., Baek, C., Kwon, S., Suh, Y., and Son, J. (2013). "Evaluation of warm-mix asphalt mixtures using leadcap additive." *International Journal on Pavemnet Engineering & Asphalt Technology*, 14(2), 67-74.

Kristjánsdóttir, Ó., Muench, S. T., Michael, L., and Burke, G. (2007). "Assessing potential for warm-mix asphalt technology adoption." *Transportation Research Record*, 2040(1), 91-99.

Kriz, P., Stastna, J., and Zanzotto, L. (2008). "Glass transition and phase stability in asphalt binders." *Road Materials and Pavement Design*, 9(sup1), 37-65.

Król, J., Kowalski, K., Radziszewski, P., Piłat, J., Sarnowski, M., and Świeżewski, P. "Influence of WMA wax modifier melting point on bitumen viscosity." *Proc., 5th European asphalt technology association conference-EATA, Braunschweig*.

Krol, J. B., Kowalski, K. J., Radziszewski, P., and Sarnowski, M. (2015). "Rheological behaviour of n-alkane modified bitumen in aspect of Warm Mix Asphalt technology." *Construction and Building Materials*, 93, 703-710.

Lamarre, A., Fini, E. H., and Abu-Lebdeh, T. (2016). "Investigating Effects of Water Conditioning on the Adhesion Properties of Crack Sealant." *Am. J. Eng. Appl. Sci*, 9, 178-186.

Lashof, D. A., and Ahuja, D. R. (1990). "Relative contributions of greenhouse gas emissions to global warming."

Laukkanen, O.-V. (2017). "Small-diameter parallel plate rheometry: a simple technique for measuring rheological properties of glass-forming liquids in shear." *Rheologica Acta*, 56(7-8), 661-671.

Le Guern, M., Chailleux, E., Farcas, F., Dreessen, S., and Mabille, I. (2010). "Physico-chemical analysis of five hard bitumens: Identification of chemical species and molecular organization before and after artificial aging." *Fuel*, 89(11), 3330-3339.

Lesueur, D. (2009). "The colloidal structure of bitumen: Consequences on the rheology and on the mechanisms of bitumen modification." *Advances in colloid and interface science*, 145(1-2), 42-82.

Levine, B. G., Stone, J. E., and Kohlmeyer, A. (2011). "Fast analysis of molecular dynamics trajectories with graphics processing units—Radial distribution function histogramming." *Journal of Computational Physics*, 230(9), 3556-3569.

Li, B., Liu, T., Hu, L., Wang, Y., and Gao, L. (2013). "Fabrication and properties of microencapsulated paraffin@ SiO2 phase change composite for thermal energy storage." *ACS Sustainable Chemistry & Engineering*, 1(3), 374-380.

Li, D. D., and Greenfield, M. L. (2014). "Chemical compositions of improved model asphalt systems for molecular simulations." *Fuel*, 115, 347-356.

Li, Y., Samad, Y. A., Polychronopoulou, K., Alhassan, S. M., and Liao, K. (2014). "From biomass to high performance solar–thermal and electric–thermal energy conversion and storage materials." *Journal of Materials Chemistry A*, 2(21), 7759-7765.

Liu, J., Yan, K., You, L., Ge, D., and Wang, Z. (2016). "Laboratory performance of warm mix asphalt binder containing polyphosphoric acid." *Construction and Building Materials*, 106, 218-227.

Liu, J., Zhao, Y., and Ren, S. (2015). "Molecular dynamics simulation of self-aggregation of asphaltenes at an oil/water interface: formation and destruction of the asphaltene protective film." *Energy & Fuels*, 29(2), 1233-1242.

Lowry, E., Sedghi, M., and Goual, L. (2017). "Polymers for asphaltene dispersion: Interaction mechanisms and molecular design considerations." *Journal of Molecular Liquids*, 230, 589-599.

Lu, X., Kalman, B., and Redelius, P. "A simple test method for determination of waxes in crude oils and bitumens." *Proc., Proceedings of 4th Euroasphalt and Eurobitume Congress, Copenhagen, Denmark*.

Lu, X., and Redelius, P. (2007). "Effect of bitumen wax on asphalt mixture performance." *Construction and building materials*, 21(11), 1961-1970.

Luyt, A., and Krupa, I. (2008). "Thermal behaviour of low and high molecular weight paraffin waxes used for designing phase change materials." *Thermochimica Acta*, 467(1-2), 117-120.

Maresca, M., Derghal, A., Carravagna, C., Dudin, S., and Fantini, J. (2008). "Controlled aggregation of adenine by sugars: physicochemical studies, molecular modelling simulations of sugar–aromatic CH–π stacking interactions, and biological significance." *Physical Chemistry Chemical Physics*, 10(19), 2792-2800.

Martín-Martínez, F. J., Fini, E. H., and Buehler, M. J. (2015). "Molecular asphaltene models based on Clar sextet theory." *RSC Advances*, 5(1), 753-759.

Masson, J. (2008). "Brief review of the chemistry of polyphosphoric acid (PPA) and bitumen." *Energy & Fuels*, 22(4), 2637-2640.

Masson, J., and Collins, P. (2008). "FTIR study of the reaction of polyphosphoric acid and model bitumen sulfur compounds." *Energy & Fuels*, 23(1), 440-442.

Menapace, I., Cucalon, L. G., Kaseer, F., Arámbula-Mercado, E., Martin, A. E., Masad, E., and King, G. (2018). "Effect of recycling agents in recycled asphalt binders observed with microstructural and rheological tests." *Construction and Building Materials*, 158, 61-74.

Merino-Garcia, D., Shaw, J., Carrier, H., Yarranton, H., and Goual, L. (2009). "Petrophase 2009 panel discussion on standardization of petroleum fractions." ACS Publications.

Mills-Beale, J., You, Z., Fini, E., Zada, B., Lee, C. H., and Yap, Y. K. (2014). "Aging influence on rheology properties of petroleum-based asphalt modified with biobinder." *Journal of Materials in Civil Engineering*, 26(2), 358-366.

Mintova, S., Jaber, M., and Valtchev, V. (2015). "Nanosized microporous crystals: emerging applications." *Chemical Society Reviews*, 44(20), 7207-7233.

Mogawer, W. S., Austerman, A., Roque, R., Underwood, S., Mohammad, L., and Zou, J. (2015). "Ageing and rejuvenators: evaluating their impact on high RAP mixtures fatigue cracking characteristics using advanced mechanistic models and testing methods." *Road Materials and Pavement Design*, 16(sup2), 1-28.

Mogawer, W. S., Fini, E. H., Austerman, A. J., Booshehrian, A., and Zada, B. "Performance characteristics of high RAP bio-modified asphalt mixtures." *Proc., Transportation Research Board 91st Annual Meeting*.

Moghaddam, T. B., and Baaj, H. (2016). "The use of rejuvenating agents in production of recycled hot mix asphalt: A systematic review." *Construction and Building Materials*, 114, 805-816.

Møller, H. B., Sommer, S. G., and Ahring, B. K. (2004). "Biological degradation and greenhouse gas emissions during pre-storage of liquid animal manure." *Journal of Environmental Quality*, 33(1), 27-36.

Monteny, G.-J., Bannink, A., and Chadwick, D. (2006). "Greenhouse gas abatement strategies for animal husbandry." *Agriculture, Ecosystems & Environment*, 112(2), 163-170.

Morea, F., Marcozzi, R., and Castaño, G. (2012). "Rheological properties of asphalt binders with chemical tensoactive additives used in warm mix asphalts (WMAs)." *Construction and Building Materials*, 29, 135-141.

Morgan, T., Alvarez-Rodriguez, P., George, A., Herod, A., and Kandiyoti, R. (2010). "Characterization of Maya crude oil maltenes and asphaltenes in terms of structural parameters calculated from nuclear magnetic resonance (NMR) spectroscopy and laser desorption− mass spectroscopy (LD− MS)." *Energy & Fuels*, 24(7), 3977-3989.

Mousavi, M., Fini, E. H., and Hung, A. M. (2019). "Underlying Molecular Interactions between Sodium Montmorillonite Clay and Acidic Bitumen." *The Journal of Physical Chemistry C*.

Mousavi, M., Pahlavan, F., Oldham, D., Hosseinnezhad, S., and Fini, E. H. (2016). "Multiscale investigation of oxidative aging in biomodified asphalt binder." *The Journal of Physical Chemistry C*, 120(31), 17224-17233.

Mullins, O. C. (2010). "The modified Yen model." *Energy & Fuels*, 24(4), 2179-2207.

Musser, B. J., and Kilpatrick, P. K. (1998). "Molecular characterization of wax isolated from a variety of crude oils." *Energy & Fuels*, 12(4), 715-725.

Nagarajan, R. (1994). "On interpreting fluorescence measurements: what does thermodynamics have to say about change in micellar aggregation number versus change in size distribution induced by increasing concentration of the surfactant in solution?" *Langmuir*, 10(6), 2028-2034.

National Crushed Stone Association (1977). *Flexible Pavement Cost Estimating Guide: Inflation/Energy Effects, Worksheets, SPEC Data, Featuring the Economy of Crushed Stone Bases*, National Crushed Stone Association.

Naveed, H., ur Rehman, Z., Khan, A. H., Qamar, S., and Akhtar, M. N. (2019). "Effect of mineral fillers on the performance, rheological and dynamic viscosity measurements of asphalt mastic." *Construction and Building Materials*, 222, 390-399.

Ni, J., Vinckier, C., Coenegrachts, J., and Hendriks, J. (1999). "Effect of manure on ammonia emission from a fattening pig house with partly slatted floor." *Livestock Production Science*, 59(1), 25-31.

Nisbet, M., Marceau, M., VanGeem, M., and Gajda, J. (2001). "Environmental life cycle inventory of Portland cement concrete and asphalt concrete pavements." *Portland Cement Association. PCA R&D Serial*(2489).

Ocfemia, K., Zhang, Y., and Funk, T. (2006). "Hydrothermal processing of swine manure into oil using a continuous reactor system: Development and testing." *Transactions of the ASABE*, 49(2), 533-541.

Ogawa, A., Yamada, H., Matsuda, S., Okajima, K., and Doi, M. (1997). "Viscosity equation for concentrated suspensions of charged colloidal particles." *Journal of Rheology*, 41(3), 769-785.

Oklahoma department of transportation "Monthly asphalt binder price index." <http://www.okladot.state.ok.us/contractadmin/pdfs/binder-index.pdf>. (January 2, 2018).

Oldham, D., Fini, E. H., and Abu-Lebdeh, T. (2014). "Investigating the rejuvenating effect of bio-binder on recycled asphalt shingles."

Oldham, D. J. (2015). "The feasibility of rejuvenating aged asphalt with bio-oil from swine manure." North Carolina Agricultural and Technical State University.

Oldham, D. J., Rajib, A. I., Onochie, A., and Fini, E. H. (2019). "Durability of bio-modified recycled asphalt shingles exposed to oxidation aging and extended sub-zero conditioning." *Construction and Building Materials*, 208, 543-553.

Pacheco-Sánchez, J., Zaragoza, I., and Martínez-Magadán, J. (2003). "Asphaltene aggregation under vacuum at different temperatures by molecular dynamics." *Energy & fuels*, 17(5), 1346-1355.

Pahlavan, F., Hung, A., and Fini, E. H. (2018). "Evolution of molecular packing and rheology in asphalt binder during rejuvenation." *Fuel*, 222, 457-464.

Pahlavan, F., Hung, A. M., Zadshir, M., Hosseinnezhad, S., and Fini, E. H. (2018). "Alteration of π-Electron Distribution To Induce Deagglomeration in Oxidized Polar Aromatics and Asphaltenes in an Aged Asphalt Binder." *ACS Sustainable Chemistry & Engineering*, 6(5), 6554-6569.

Pahlavan, F., Mousavi, M., Hung, A., and Fini, E. (2017). "Characterization of Oxidized Asphaltenes and the Restorative Effect of a Bio-Modifier (Accepted with revision)." *RSC Advances*.

Pahlavan, F., Mousavi, M., Hung, A., and Fini, E. H. (2016). "Investigating molecular interactions and surface morphology of wax-doped asphaltenes." *Physical Chemistry Chemical Physics*, 18(13), 8840-8854.

Pahlavan, F., Mousavi, M., Hung, A. M., and Fini, E. H. (2018). "Characterization of oxidized asphaltenes and the restorative effect of a bio-modifier." *Fuel*, 212, 593-604.

Painter, P., Veytsman, B., and Youtcheff, J. (2015). "Guide to asphaltene solubility." *Energy & Fuels*, 29(5), 2951-2961.

Pauli, A., Grimes, R., Beemer, A., Turner, T., and Branthaver, J. (2011). "Morphology of asphalts, asphalt fractions and model wax-doped asphalts studied by atomic force microscopy." *International Journal of Pavement Engineering*, 12(4), 291-309.

Pavement interactive, <http://www.pavementinteractive.org/asphalt-modifiers/ >. (February 27, 2018).

Pedersen, S., Blanes-Vidal, V., Jørgensen, H., Chwalibog, A., Haeussermann, A., Heetkamp, M., and Aarnink, A. (2008). "Carbon dioxide production in animal houses: a literature review." *Agricultural Engineering International: CIGR Journal*.

Pedersen, S., and Sällvik, K. (2002). *Heat and moisture production at animal and house levels*, Aarhus Universitet, Det Jordbrugsvidenskabelige Fakultet.

Petersen, J. C. (2009). "A review of the fundamentals of asphalt oxidation: chemical, physicochemical, physical property, and durability relationships." *Transportation Research E-Circular*(E-C140).

Philippe, F.-X., Laitat, M., Canart, B., Vandenheede, M., and Nicks, B. (2007). "Comparison of ammonia and greenhouse gas emissions during the fattening of pigs, kept either on fully slatted floor or on deep litter." *Livestock Science*, 111(1), 144-152.

Philippe, F.-X., Laitat, M., Canart, B., Vandenheede, M., and Nicks, B. (2007). "Gaseous emissions during the fattening of pigs kept either on fully slatted floors or on straw flow."

Philippe, F.-X., Laitat, M., Nicks, B., and Cabaraux, J.-F. (2012). "Ammonia and greenhouse gas emissions during the fattening of pigs kept on two types of straw floor." *Agriculture, ecosystems & environment*, 150, 45-53.

Philippe, F.-X., and Nicks, B. (2015). "Review on greenhouse gas emissions from pig houses: Production of carbon dioxide, methane and nitrous oxide by animals and manure." *Agriculture, Ecosystems & Environment*, 199, 10-25.

Pilař, R., Honcová, P., Koštál, P., Sádovská, G., and Svoboda, L. (2014). "Modified stepwise method for determining heat capacity by DSC." *Journal of Thermal Analysis and Calorimetry*, 118(1), 485-491.

Plimpton, S. (1995). "Fast parallel algorithms for short-range molecular dynamics." *Journal of computational physics*, 117(1), 1-19.

Pomerantz, A. E., Wu, Q., Mullins, O. C., and Zare, R. N. (2015). "Laser-based mass spectrometric assessment of asphaltene molecular weight, molecular architecture, and nanoaggregate number." *Energy & Fuels*, 29(5), 2833-2842.

Qin, Q., Farrar, M. J., Pauli, A. T., and Adams, J. J. (2014). "Morphology, thermal analysis and rheology of Sasobit modified warm mix asphalt binders." *Fuel*, 115, 416-425.

Qin, Q., Schabron, J. F., Boysen, R. B., and Farrar, M. J. (2014). "Field aging effect on chemistry and rheology of asphalt binders and rheological predictions for field aging." *Fuel*, 121, 86-94.

r se Averbuch-Pouchot, M.-T., and Durif, A. (1996). *Topics in phosphate chemistry*, World Scientific.

Rao, Z., and Zhang, G. (2011). "Thermal properties of paraffin wax-based composites containing graphite." *Energy Sources, Part A: Recovery, Utilization, and Environmental Effects*, 33(7), 587-593.

Rassamdana, H., Dabir, B., Nematy, M., Farhani, M., and Sahimi, M. (1996). "Asphalt flocculation and deposition: I. The onset of precipitation." *AIChE Journal*, 42(1), 10-22.

Rathod, M., and Banerjee, J. (2014). "Experimental investigations on latent heat storage unit using paraffin wax as phase change material." *Experimental Heat Transfer*, 27(1), 40-55.

Rebitzer, G., Ekvall, T., Frischknecht, R., Hunkeler, D., Norris, G., Rydberg, T., Schmidt, W.-P., Suh, S., Weidema, B. P., and Pennington, D. W. (2004). "Life cycle assessment: Part 1: Framework, goal and scope definition, inventory analysis, and applications." *Environment international*, 30(5), 701-720.

Redelius, P. (2004). "Bitumen solubility model using Hansen solubility parameter." *Energy & fuels*, 18(4), 1087-1092.

Redelius, P., and Soenen, H. (2015). "Relation between bitumen chemistry and performance." *Fuel*, 140, 34-43.

Richter, F. (2002). "Asphalt Stability Improved by Using Synthetic Wax Additives." *Better Roads*, 72(10).

Richter, F. (2002). "Effect of waxes on bitumen quality." *Oil Gas European Magazine*, 35-38.

Rodhe, L. K., Abubaker, J., Ascue, J., Pell, M., and Nordberg, Å. (2012). "Greenhouse gas emissions from pig slurry during storage and after field application in northern European conditions." *Biosystems engineering*, 113(4), 379-394.

Rossi, D., Filippi, S., Merusi, F., Giuliani, F., and Polacco, G. (2013). "Internal structure of bitumen/polymer/wax ternary mixtures for warm mix asphalts." *Journal of Applied Polymer Science*, 129(6), 3341-3354.

Ruan, Y., Davison, R. R., and Glover, C. J. (2003). "The effect of long-term oxidation on the rheological properties of polymer modified asphalts☆." *Fuel*, 82(14), 1763-1773.

Rubio, M. C., Martínez, G., Baena, L., and Moreno, F. (2012). "Warm mix asphalt: an overview." *Journal of Cleaner Production*, 24, 76-84.

Sahimi, M., Rassamdana, H., and Dabir, B. (1997). "Asphalt formation and precipitation: Experimental studies and theoretical modelling." *SPE Journal*, 2(02), 157-169.

Samieadel, A., Høgsaa, B., and Fini, E. H. (2018). "Examining the Implications of Wax-Based Additives on the Sustainability of Construction Practices: Multiscale Characterization of Wax-Doped Aged Asphalt Binder." *ACS Sustainable Chemistry & Engineering*, 7(3), 2943-2954.

Samieadel, A., Oldham, D., and Fini, E. H. (2017). "Multi-scale characterization of the effect of wax on intermolecular interactions in asphalt binder." *Construction and Building Materials*, 157, 1163-1172.

Samieadel, A., Oldham, D., and Fini, E. H. (2018). "Investigating molecular conformation and packing of oxidized asphaltene molecules in presence of paraffin wax." *Fuel*, 220, 503-512.

Sanchez-Alonso, E., Castro-Fresno, D., Vega-Zamanillo, A., and Rodriguez-Hernandez, J. (2011). "SUSTAINABLE ASPHALT MIXES: USE OF ADDITIVES AND RECYCLED MATERIALS." *Baltic Journal of Road & Bridge Engineering*, 6(4).

Sanchez-Alonso, E., Castro-Fresno, D., Vega-Zamanillo, A., and Rodriguez-Hernandez, J. (2011). "Sustainable asphalt mixes: use of additives and recycled materials/Suderinti asfalto misiniai: priedu ir kartotinis medziagu naudojimas/Ilgtspejigs asfalta maisijums: piedevu un recikleto materialu lietojums/Kestvad asfaltsegud: lisandite ja taaskasutatava materjali kasutamine." *The Baltic Journal of Road and Bridge Engineering*, 6(4), 249-249.

Santero, N. J., Masanet, E., and Horvath, A. (2011). "Life-cycle assessment of pavements. Part I: Critical review." *Resources, Conservation and Recycling*, 55(9), 801-809.

Schmets, A., Kringos, N., Pauli, T., Redelius, P., and Scarpas, T. (2010). "On the existence of wax-induced phase separation in bitumen." *International Journal of Pavement Engineering*, 11(6), 555-563.

Sengers, J. V., Kayser, R., Peters, C., and White, H. (2000). *Equations of state for fluids and fluid mixtures*, Elsevier.

Setz, L. F., Silva, A. C., Santos, S. C., Mello-Castanho, S. R., and Morelli, M. R. (2013). "A viscoelastic approach from α-Al2O3 suspensions with high solids content." *Journal of the European Ceramic Society*, 33(15-16), 3211-3219.

Sharma, B. K., Ma, J., Kunwar, B., Singhvi, P., Ozer, H., and Rajagopalan, N. (2017). "Modeling the Performance Properties of RAS and RAP Blended Asphalt Mixes Using Chemical Compositional Information." Illinois Center for Transportation/Illinois Department of Transportation.

Siddiqui, M. N., and Ali, M. F. (1999). "Studies on the aging behavior of the Arabian asphalts." *Fuel*, 78(9), 1005-1015.

Silva, H. S., Sodero, A. C., Bouyssiere, B., Carrier, H., Korb, J.-P., Alfarra, A., Vallverdu, G., Bégué, D., and Baraille, I. (2016). "Molecular Dynamics Study of Nanoaggregation in Asphaltene Mixtures: Effects of the N, O, and S Heteroatoms." *Energy & Fuels*, 30(7), 5656-5664.

Slough, C. G., and Hesse, N. D. "High precision heat capacity measurements of metals by modulated DSC." *Proc., Proc NATAS Annu Conf Therm Anal Appl*, 160.

Soenen, H., Besamusca, J., Fischer, H. R., Poulikakos, L. D., Planche, J.-P., Das, P. K., Kringos, N., Grenfell, J. R., Lu, X., and Chailleux, E. (2014). "Laboratory investigation of bitumen based on round robin DSC and AFM tests." *Materials and structures*, 47(7), 1205-1220.

Sousa, P. d., and Pedersen, S. (2004). "Ammonia emission from fattening pig houses in relation to animal activity and carbon dioxide production."

Speight, J. G. (1999). "The chemical and physical structure of petroleum: effects on recovery operations." *Journal of Petroleum Science and Engineering*, 22(1), 3-15.

Stammer Jr, R., and Stodolsky, F. (1995). "Assessment of the energy impacts of improving highway-infrastructure materials." Argonne National Lab., IL (United States).

Stripple, H. (2001). "Life cycle assessment of road." *A pilot study for inventory analysis. 2nd revised Edition. Report from the IVL Swedish Environmental Research Institute*, 96.

Su, K., Maekawa, R., and Hachiya, Y. (2009). "Laboratory evaluation of WMA mixture for use in airport pavement rehabilitation." *Construction and Building Materials*, 23(7), 2709-2714.

Sun, H., Mumby, S. J., Maple, J. R., and Hagler, A. T. (1994). "An ab initio CFF93 all-atom force field for polycarbonates." *Journal of the American Chemical Society*, 116(7), 2978-2987.

Traxler, R. "Relation between asphalt composition and hardening by volatilization and oxidation." *Proc., Assoc Asphalt Paving Technol Proc*.

U.S. energy information administration, <https://www.eia.gov/dnav/pet/hist/LeafHandler.ashx?n=PET&s=MAPRY3E3&f=A>. (February 27, 2018).

Ungerer, P., Rigby, D., Leblanc, B., and Yiannourakou, M. (2014). "Sensitivity of the aggregation behaviour of asphaltenes to molecular weight and structure using molecular dynamics." *Molecular Simulation*, 40(1-3), 115-122.

Vaitkus, A., Čygas, D., Laurinavičius, A., and Perveneckas, Z. (2009). "Analysis And Evaluation Of Possibilities For The Use Of Warm Mix Asphalt In Lithuania." *Baltic Journal of Road & Bridge Engineering*, 4(2).

Van't Klooster, C., and Heitlager, B. (1994). "Determination of minimum ventilation rate in pig houses with natural ventilation based on carbon dioxide balance." *Journal of agricultural engineering research*, 57(4), 279-287.s

Vargas, X., Afanasjeva, N., Álvarez, M., Marchal, P., and Choplin, L. (2008). "Asphalt rheology evolution through thermo-oxidation (aging) in a rheo-reactor." *Fuel*, 87(13), 3018-3023.

Vedrenne, F., Béline, F., Dabert, P., and Bernet, N. (2008). "The effect of incubation conditions on the laboratory measurement of the methane producing capacity of livestock wastes." *Bioresource technology*, 99(1), 146-155.

Waldman, M., and Hagler, A. T. (1993). "New combining rules for rare gas van der Waals parameters." *Journal of Computational Chemistry*, 14(9), 1077-1084.

Wang, P. Y., Zhao, K., Glover, C., Chen, L., Wen, Y., Chong, D., and Hu, C. (2015). "Effects of aging on the properties of asphalt at the nanoscale." *Construction and Building Materials*, 80, 244-254.

Wang, W., Chen, J., Sun, Y., Xu, B., Li, J., and Liu, J. (2017). "Laboratory performance analysis of high percentage artificial RAP binder with WMA additives." *Construction and Building Materials*, 147, 58-65.

WCED (1987). "Our common future." *World Commission on Environment and Development (WCED)*, Oxford: Oxford University Press.

West, R. C., Watson, D. E., Turner, P. A., and Casola, J. R. (2010). *Mixing and compaction temperatures of asphalt binders in hot-mix asphalt*.

Wiehe, I. A. (2008). *Process chemistry of petroleum macromolecules*, CRC press.

Williams, M. L., Landel, R. F., and Ferry, J. D. (1955). "The temperature dependence of relaxation mechanisms in amorphous polymers and other glass-forming liquids." *Journal of the American Chemical society*, 77(14), 3701-3707.

Xiao, F., Amirkhanian, S., Wang, H., and Hao, P. (2014). "Rheological property investigations for polymer and polyphosphoric acid modified asphalt binders at high temperatures." *Construction and Building Materials*, 64, 316-323.

Xiu, S., and Shahbazi, A. (2012). "Bio-oil production and upgrading research: A review." *Renewable and Sustainable Energy Reviews*, 16(7), 4406-4414.

Xiu, S., Shahbazi, A., Shirley, V., and Cheng, D. (2010). "Hydrothermal pyrolysis of swine manure to bio-oil: effects of operating parameters on products yield and characterization of bio-oil." *Journal of analytical and applied pyrolysis*, 88(1), 73-79.

Xu, G., and Wang, H. (2017). "Molecular dynamics study of oxidative aging effect on asphalt binder properties." *Fuel*, 188, 1-10.

Xu, M., Chen, S., Seo, D.-K., and Deng, S. (2019). "Evaluation and optimization of VPSA processes with nanostructured zeolite NaX for post-combustion CO2 capture." *Chemical Engineering Journal*.

Yan, K., Zhang, H., and Xu, H. (2013). "Effect of polyphosphoric acid on physical properties, chemical composition and morphology of bitumen." *Construction and Building Materials*, 47, 92-98.

Yaseen, S., and Mansoori, G. A. (2018). "Asphaltenes aggregation due to waterflooding (A molecular dynamics simulation study)." *Journal of Petroleum Science and Engineering*.

You, Z.-P., and Goh, S.-W. (2008). "Laboratory evaluation of warm mix asphalt: a preliminary study." *International Journal of Pavement Research and Technology*, 1(1), 34-40.

You, Z., Mills-Beale, J., Fini, E., Goh, S. W., and Colbert, B. (2011). "Evaluation of low-temperature binder properties of warm-mix asphalt, extracted and recovered RAP and RAS, and bioasphalt." *Journal of materials in Civil Engineering*, 23(11), 1569-1574.

Yu, B., and Lu, Q. (2012). "Life cycle assessment of pavement: Methodology and case study." *Transportation Research Part D: Transport and Environment*, 17(5), 380-388.

Yu, X., Zaumanis, M., Dos Santos, S., and Poulikakos, L. D. (2014). "Rheological, microscopic, and chemical characterization of the rejuvenating effect on asphalt binders." *Fuel*, 135, 162-171.

Yusoff, N. I. M., Chailleux, E., and Airey, G. D. (2011). "A comparative study of the influence of shift factor equations on master curve construction." *International Journal of Pavement Research and Technology*, 4(6), 324.

Zadshir, M., Hosseinnezhad, S., and Fini, E. H. (2019). "Deagglomeration of oxidized asphaltenes as a measure of true rejuvenation for severely aged asphalt binder." *Construction and Building Materials*, 209, 416-424.

Zaumanis, M., Mallick, R., and Frank, R. (2013). "Evaluation of Rejuvenator's Effectiveness with Conventional Mix Testing for 100% Reclaimed Asphalt Pavement Mixtures." *Transportation Research Record: Journal of the Transportation Research Board*(2370), 17-25.

Żbik, M., Horn, R. G., and Shaw, N. (2006). "AFM study of paraffin wax surfaces." *Colloids and Surfaces A: Physicochemical and Engineering Aspects*, 287(1-3), 139-146.

Zhang, F., Yu, J., and Han, J. (2011). "Effects of thermal oxidative ageing on dynamic viscosity, TG/DTG, DTA and FTIR of SBS-and SBS/sulfur-modified asphalts." *Construction and Building Materials*, 25(1), 129-137.

APPENDIX A

SCANNING ELECTRON MICROSCOPY RESULTS OF NANO ZEOLITE IMPREGNATED WITH WAX

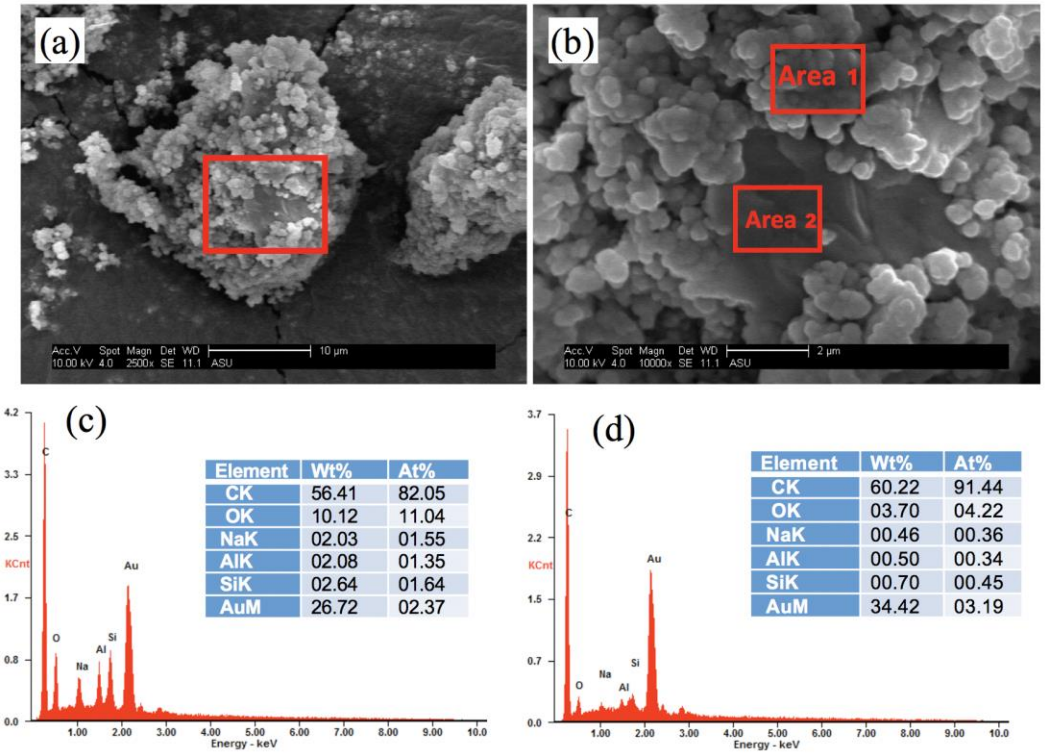

Figure A1 (a) Scanning electron microscopy (SEM) image of 5% wax Winz sample and (b) zoomed-in image of the area in (a). Energy dispersive spectra (EDS) and quantitative elemental results of area 1 (c) and area 2 (d) in (b). Area 1 shows a significant amount of Na, Al and Si, indicating the presence of nano-zeolites. In contrast, no obvious Na, Al and Si EDS signal was observed for area 2, suggesting the sole presence of waxes. (The Au signal is due to the coating for imaging, and carbon signal is due to the presence of paraffin wax and the carbon tape used for loading sample).

BIOGRAPHICAL SKETCH

Alireza finished his PhD of civil engineering at the school of sustainable engineering and the built environment at Arizona State University in 2020. He received his MSc from Amirkabir University of Technology (Tehran Polytechnic) in 2014, and he received his bachelor's degree from Isfahan University of Technology in 2012. During his Ph.D. studies, Alireza has authored and co-authored twelve technical articles in prestigious journals such as Fuel and ACS Sustainable Chemistry and Engineering and Construction and Building Materials. His work has received attention, and it was presented at transportation research board (TRB) conferences in Washington, D.C, in four consecutive years. Being a former student at North Carolina A&T state university, he was selected as an outstanding senior research assistant by the college of science and technology and received an award for outstanding contribution to research enterprise by the department of energy and environmental systems.

During his Ph.D. studies, he received the NSF Internship Award in 2019 and received funding from a CAREER award granted to Dr. Elham Fini. He successfully co-invented a new technology titled "Development of wax-impregnated zeolite for use in asphalt", Patent application 63/004,243 filed on April 2, 2020.